Genetics and genomics of prickles on rose stem

Ning-Ning Zhou

UNIVERSITE ECOLOGIE
BRETAGNE GEOSCIENCES
LOIRE AGRONOMIE ALIMENTATION

université angers

THESE DE DOCTORAT DE

L'UNIVERSITE D'ANGERS
COMUE UNIVERSITE BRETAGNE LOIRE

ECOLE DOCTORALE N° 600
Ecole doctorale Ecologie, Géosciences, Agronomie et Alimentation
Spécialité : Biochimie et Biologie Moléculaire;
Génétique, génomique et bio-informatique

Par
Ning-ning ZHOU

« Genetics and genomics of prickles on rose stem »

« Génétique et génomique des aiguillons de la tige du rosier »

Thèse présentée et soutenue à Angers, le 25 Février
Unité de recherche : UMR 1345 Institut de Recherche en Horticulture et Semences
Thèse N° : 190392

Rapporteurs avant soutenance :

Sylvie BAUDINO, Professeur, Université Jean Monnet (Saint-Etienne)
Patrick LAUFS, Directeur de Recherche, INRAE, Institut Jean-Pierre Bourgin (Versailles)

Composition du Jury :

Rapporteurs : Sylvie BAUDINO, Professeur, Université Jean Monnet (Saint-Etienne)
Patrick LAUFS, Directeur de Recherche INRAE, Institut Jean-Pierre Bourgin (Versailles)

Examinateurs : Béatrice DESNOYES-ROTHAN, Ingénieure de Recherche, INRAE, Biologie du Fruit et Pathogènes (Bordeaux)
Nathalie LEDUC, Professeur, Université d'Angers, Angers

Dir. de thèse : Fabrice FOUCHER, Directeur de recherche INRAE, UMR 1345 Institut de Recherche en Horticulture et Semences

Co-dir. de thèse : Laurence HIBRAND-SAINT OYANT, Ingénieure de Recherche INRAE, UMR 1345 Institut de Recherche en Horticulture et Semences

Genetics and genomics of prickle on rose stem

Ning-ning ZHOU

December 31, 2020

This dissertation is submitted for the degree of Doctor of biochemistry and molecular biology, genetic, genomic and bioinformatic

Université d'Angers

FRANCE

Copyrights

Non-plagiarism declaration

I, the undersigned Ning-ning ZHOU, declare that I am fully aware that plagiarism of documents or part of a document published on any medium, including the internet, constitutes copyright infringement and manifest fraud.

Consequently, I commit to cite all the sources I used to write this dissertation.

December 31, 2020

Signature : 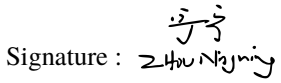

Je, soussignée Ning-ning ZHOU, déclare être pleinement conscient que le plagiat de documents ou d'une partie d'un document publiée sur toutes formes de support, y compris l'internet, constitue une violation des droits d'auteur ainsi qu'une fraude caractérisée.

En conséquence, je méngage à citer toutes les sources que j'ai utilisées pourécrire ce manuscrit de thése.

December 31, 2020

Signature : 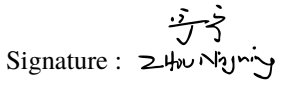

Abstract

Prickle is an undesirable trait in many crops as it makes crops difficult to handle, harvest, and can injure workers. Roses are among the most important ornamental plants, and most roses present prickles on their stems. There is a strong demand from producers and breeders for glabrous rose cultivars, particularly in cut roses. The genetic and molecular mechanisms underlying prickle initiation and development remain still largely unknown. Our objectives are to decipher the genetic and molecular control of prickle initiation and development in rose using anatomic, genetic and genomic approaches. By a survey of the different types of prickle within the genus Rosa, we classified them in two types : non-glandular (NGP) and glandular prickles (GP), with the NGP being the most common. We demonstrated that NGP are originated from a cell layer below the protoderm contrary to what was previously described. Using a F1 progeny, we detected four QTLs controlling the presence and density of stem prickle. We characterized rose gene homologues known in Arabidopsis that involved in trichome initiation. Minor different expression of the homologues in prickle (P) and prickless (NP) samples, suggesting different gene pathway between prickles and trichomes. Molecular bases of prickle initiation and development were explored using an RNA-Seq strategy by comparing the transcriptome i) of glabrous and prickle shoots and ii) during prickle development. We have identified key genes and regulatory networks controlling prickle initiation and development, with interesting genes below the QTLs. Through this project, we have built a genetic model system for studying prickles and open new research areas in the plant sciences.

Keywords : Glandular and non-glandular structure ; Trichome ; Prickle anatomy ; QTL ; RNA sequencing ; Transcriptomics

Acknowledgments

Time flies so quickly. The adventure of this thesis was not done alone and here I would like to thank all of them who have been part of this journey and making this thesis possible.

Firstly, I would like to express my appreciation to Chinese Government Scholarships (China Scholarship Council), for supporting me to do my Ph.D project in France. Thank the National Natural Science Foundation of China for supporting the research funding of this project.

Further, I express my warmest gratitude to my supervisors Dr. Fabrice FOUCHER and Dr. Laurence HIBRAND-SAINT OYANT for their continued support, patience, motivation throughout this project. Their immense knowledge and guidance helped me in all the time of research and writing of this thesis. Besides work, I would also like to thank them for their responsive help in my daily life.

I would like to extend my gratitude to Dr. Jean-Claude CAISSARD and Dr. Michel HERNOULT for being my individual monitoring committee. Their insightful comments and encouragement incented me to improve my research from various perspectives.

I'm extremely grateful to the members of my thesis juries : Dr. Sylvie BAUDINO (Jean Monnet University, Saint-Etienne) and Dr. Patrick LAUFS (INRAE, Jean-Pierre Bourgin Institute, Versailles) for accepting to be the rapporteurs of my thesis and Dr. Beatrice DESNOYES-ROTHAN (INRAE, Fruit Biology and Pathogens, Bordeaux) and Dr. Nathalie LEDUC (University of Angers, Angers) to be the examiners.

I also wish to thanks the UMR IRHS (Institute for Research in Horticulture and Seeds, INRAE, Agrocampus west, University of Angers) and all its member's staff for providing a great platform that let me perform my research in the best condition.

Many thanks to all the members of the GDO team for the welcome to me. Thank in particular Julien Jeauffre for the guidance of molecular biology experiments and qPCR data analysis. Thank Tatiana Thouroude for her contribution to manage my materials in the greenhouse and for the good times spent together. A great thank Jordan Marie Magdelaine for helping me to pass my Python course on MOOC and ignited my interest in bioinformatics. Thank Sophie Paillard for her serval key tips to solve the bug I met during the transcriptome data analyses, and also for her enthusiasm and humor brings to me much happiness. Thank Jérome Chameau for sampling with me. He was so meticulous which left a deep impression on me. Thank Laurent Ogé for

his helping in the lab and for his kindness and warm smiles. Thanks Alix, Jérémy, Agnès, Valéry, Latifa, Gilles… for all your kindness.

Many thanks also to the Loubert Rose Gardens (Rosiers sur Loire, France) for providing the experimental materials. Thank madam Loubert and her family for preparing the annual rose pruning activity and for the great lunch we spend together (all the members of GDO).

Special thanks to the leadership of Yunnan Academy of Agricultural Sciences for encouraging young researchers to pursue doctoral degrees while retaining their positions. Particularly, I'm deeply indebted to my master director Dr. Kai-Xue TANG who directly influenced my academic and work journey. I would also like to thank Prof. Hao ZHANG and Dr. Ji-Hua WANG of Yunnan Academy of Agricultural Sciences (YAAS) for accepting to be the recommenders for applying for the project funding. I would like to thank my colleagues in FRI for their help in all aspects. Especially, I am grateful to thank Dr. Hong-Ying JIAN for her contribution to revising the manuscript of the funding project and doing the oral presentations of the project acceptance defense for me, and for her responsive help for many kinds of stuff. Thank Prof. Qi-Gang WANG for sharing his experience in the rose breeding program and guide me to participate in corporate services in the rose company. Thank Dr. Xian-Qin QIU and Prof. Hui-Jun YAN for sharing their experience in performing the research projects. Thank all the term members of Woody ornamental plants R & D, FRI for the happiness or even conflict moments we spend together in years.

Thank the IMAC technical platforms (Fabienne Simonneau, Aurelia Rolland) of SFR Quasav for supervising the histological experiment and the good times spent together. Thank Muriel Bahut of the PTM ANAN of the SFR Quasav for designing the program and guide me to use the Pipetting Robot for qPCR. Thank Sandrine Balzergue of VALEMA team for participates in the discussion of experimental design and the RNA data analysis. Thank the experimental unit (UE Horti) for their technical assistance in plant management and the ImHorPhen team (Dominique Besnard, Rémi Gardet) of IRHS for taking care of the plant cuttings in the greenhouse.

Thank Eric Montaudon, Sylvain Gaillard of the BIDEFI term for helping fix several problems in install the bioinformatics tools and thanks to the bioinformatics platform (Angers, IRHS) for providing computing and storage resources. Thank the IRHS doctoral students Ming (graduated), Diana, Kevin (graduated), Aliex (graduated), and postdoctorate Deepika for the support that we have given to each other during our respective journeys. Thank Xue-Wu Dou (doctoral student of Angers university) for helping me to reproduce the structure figures which were presented in Chapter 1.

Finally, my deepest and sincere gratitude to my parents and young brother for their support and unconditional love throughout my life. I am grateful to my cousins for taking care of my parents when I and my brother were not there. Thanks also to my sister-in-law who brought a babe to our life. I also would like to thank my little nephew for bringing much happiness to us as well as for saving me from mom's attention about my aging without a child. And now that I will have time to tent to relationships, I want to thank my two unborn children for being patient.

The more I learn, the more I realize how much I don't know.

- Albert Einstein

Dedication

À mes parents et mon frère qui m'ont soutenu dans la poursuite de mes rêves.
(谨以此文献给我的父母和兄弟)

Abreviations list

ASFIM	Anatomical Structure Formation Involved In Morphogenesis
BLAST	Basic Local Alignment Search Tools
CFC	Cell Fate Commitment
DNA	Deoxyribo-Nucleic Acid
FAMP	Fatty Acid Metabolic Process
FDR	False Discovery Rate
GDR	Genome Database for *Rosaceae*
GO	Gene Ontology
GP/NGP	Glandular/Non-glandular Prickle
GT/NGT	Glandular/Non-glandular Trichome
GWAS	Genome-Wide Association Study
LG	Linkage Group
LOD	Logarithm of the Odds
MABP	Monocarboxylic Acid Biosynthetic Process
MBW	A trimeric activator complex consisting of MYB-bHLH-WDR
OB	*Rosa chinensis* 'Old Blush'
ORA	Over-Representation Analysis
PCA	Principal Component Analysis
PCR	Polymerase Chain Reaction
PEPM	Post-Embryonic Plant Morphogenesis
PSP	Pattern Specification Process
QTL	Quantitative Trait Locus
RT	Transcription Inverse
RT-qPCR	Real-Time Quantitative Reverse Transcription PCR
RW	*R.* × *wichurana*
SDE	Significantly differential expression
SMP	Secondary Metabolic Process
SSE-GO	Statistically Significant-Enriched Gene Ontology
TPM	Transcripts Per Million
UV	Ultraviolet

Glossaries list

Bark	(botany) It refers to all tissues exterior to the vascular cambium, including a number of tissue types that are periderm (composed of the cork, cork cambium, and the phelloderm), cortex (comprised of ground tissues), and phloem, and epidermis
Biseriate	(botany) Arranged in two whorls, cycles, rows, or series
Chimera	(genetics) A single organism composed of cells with more than one distinct genotype
Downy plant	(botany) The plants that organ(s) covered with fine, soft hair
Emergences	(botany) Any of various superficial outgrowths of plant tissue usually formed from both epidermis and immediately underlying tissues
Epidermis	(botany) A single layer of cells that covers the organs of plants.
Genetic redundancy	(genetics) Two or more genes are performing the same function and inactivation of one of these genes has little or no effect on the phenotype
Ground meristem	(botany) The primary meristematic tissue from where the ground tissues (i.e. non-dermal or non-vascular tissues) develop from. It directly come from the apical meristem.
Hair	(botany) Hair like structure, they refers to trichomes
Hypomorphic mutation	A type of mutation wherein the change in gene leads to the partial loss of the normal (wild-type) gene function, such as by reduced expression of the RNA or reduced activity of the protein

Meristem	(botany) A meristem (meristematic tissue) is a plant tissue that is made up of undifferentiated, actively dividing cells. Its fundamental function is growth. Some of the cells continue to give rise to new cells by cell division while others develop into differentiated cells comprising a particular permanent tissue.
Multiseriate	(botany) Arranged in rows or composed of more than one cell layer
Prickles	(botany) Sharp appendages of plant that originate from ground meristem (just under protoderm), they do not have vascular bundles and generally easy to be removed at mature stage due to the formation of abscission layer structure-like.
Prickle meristem	(botany) Derive from the ground meristem, associate with the growth of prickle in early stage
Protoderm	(botany) The primary meristem from where the epidermis of the plant are derived
Pubescent	(botany) Covered with short soft hair
Uniseriate	(botany) Arranged in a single row, layer, or serie
Thorns	(botany) Thorns are modified from stem or shoot, have vascular bundles
Trichomes	(botany) Trichomes from the Greek $\tau\rho\iota\chi\omega\mu\alpha$ (trich*ô*ma) meaning "hair", are epidermal appendages of diverse form, structures, and functions. They originate from the protoderm (or epidermis) only.
Spines	(botany) Spines are modified from leaves or part of leaves (leaflet, stipules, petiolars), have vascular bundles
Spinescence	(botany) A general designation for the sharp appendages, such as prickle, thorn and spine

Contexte de l'étude

Le projet de thése a été initié le 1er Octobre 2017 pour un peu plus de trois années de recherche sur la 'génétique et la génomique des aiguillons de la tige de rosier'. Ce projet a été soutenu financièrement par une bourse du China Scholarship Council ([2017] 3109) et de la National Natural Science Foundation of China (31760585). Le projet a été mené au sein de l'UMR IRHS (Institut de Recherche en Horticulture et Semences, INRAE, Institut Agro et Univestité d'Angers), un acteur important de la recherche dans le domaine du végétal en France, basée à Angers et dirigée par le Dr. Jean-Pierre Renou (Directeur de Recherche, INRAE). Ce projet a été proposé et supervisé par le Dr Fabrice FOUCHER (Team leader GDO, Directeur de recherche, INRAE) et Dr Laurence HIBRAND-SAINT-OYANT (Ingénieure de Recherche, INRAE) au sein de l'équipe GDO (Génétique et Diversité des plantes Ornementales). Les principales études de l'équique GDO sont réalisées sur le genre *Rosa* avec transfert vers d'autres plantes ornementales dans le cadre de projets collaboratifs. L'équipe regroupe principalement des généticiens, des biologistes moléculaires, des biologistes cellulaires avec des compétences en génomique, en génétique évolutive, en génétique quantitative, en sélection, en biologie cellulaire et en botanique.

Study context

This project was initiated on October 1st, 2017 for more than three years of research on the genetics and genomics of prickles on rose stem. The work was financially supported by the China Scholarship Council ([2017]3109) and the National Natural Science Foundation of China (31760585). The research was carried out within the UMR IRHS (Institute for Research in Horticulture and Seeds, INRAE, Institut Agro, University of Angers), a major player in plant research in France, based in Angers and directed by Dr. Jean-Pierre Renou (Research Director, INRAE). This project was supervised by Dr. Fabrice FOUCHER (Team leader GDO, Research Director, INRAE) and Dr. Laurence HIBRAND-SAINT OYANT (Research Engineer, INRAE) initially within the GDO team (Genetic and Diversity of Ornamental plants). The major studies of GDO team are carried out on the genus *Rosa* with transfer to other ornamental plants in the context of collaborative projects. The team mainly brings together geneticists, molecular biologists, cell biologists with skills in genomics, evolutionary genetics, quantitative genetics, selection, cell biology and botany.

Contents

List of Figures

List of Tables

List of Supplementary Figures

List of Supplementary Tables

Introduction and literature review

1 Introduction and literature review

1.1 Trichomes, prickles, thorns and spines

1.1.1 Distinctions and definitions based on anatomical studies

The basic terminology describe appendages on plants (trichomes, prickles, thorns and spines) is frequently inaccurately cited in scientific reports, making it even more difficult for most researchers to understand how to distinguish between the different terms. For example, commonly confused words include trichomes, emergences and prickles, since their definitions are not consistent in the literature. Some authors have described emergences as prickles, e.g., prickles on the stems or leaves of plants such as *Solatium torvium, Aiphanes acanthophylla*, roses, etc. (Bell, 1991), and and some have referred to trichomes as emergences, e.g. grape emergences (Ma et al., 2016b). Another common confusion is between prickles, thorns and spines. Many plants described as having thorns or spines (McPheeters and Skirvin, 1983; Hall et al., 1986; Canli, 2003; Coyner et al., 2005; Castro et al., 2013; Kariyat et al., 2017), actually have prickles. For instance, *Rosa* and *Rubus* have the most representative prickles. Thus, before conducting any molecular research on this subject, an essential step is to clearly describe their anatomy and to understand their origin. In this paper, we have reviewed the anatomical structure and development of those tissues in order to guide subsequent research by more effectively understanding the difference and connection between them. In this Chapter, the sharp appendages (prickles, thorns and spines) are collectively referred to as 'spinescences'.

Generally, depending on the presence or absence of vascular bundles, we can divide these structures into two categories: (i) trichomes (Figure 1a and b) and prickles (Figure 1c and d)), which are not vascularized and are generally easy to remove; and (ii) thorns (Figure 1e and f) and spines (Figure 1g)), which have vascular bundles and cannot be easily separated from the organs that have vascular tissues (spines, usually from leaves, and thorns from stems or shoots) (Figure 1h).

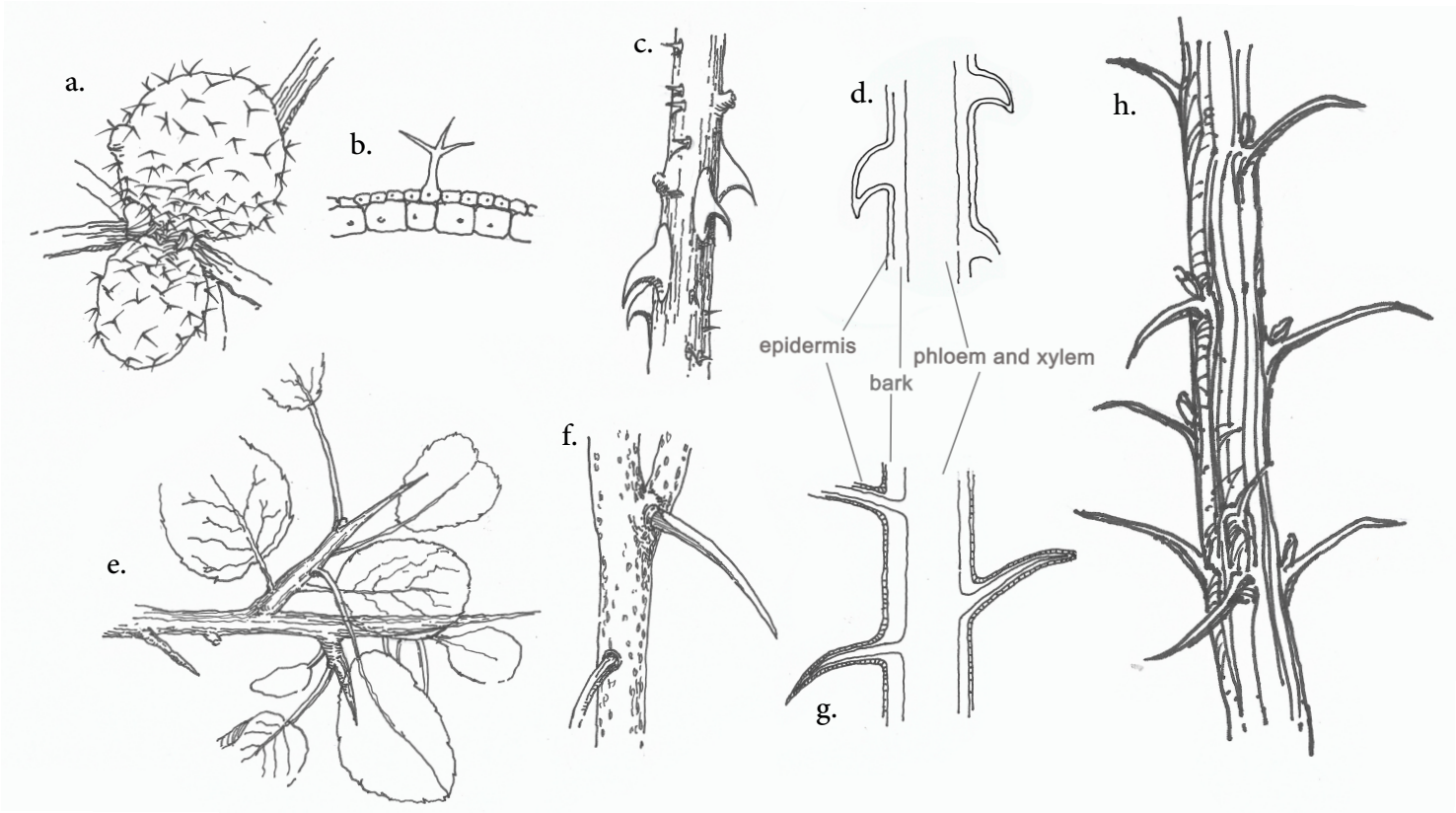

Figure 1: General methods to distinguish trichomes, prickles, thorns and spines. (a) trichomes on *Arabidopsis* leaves; (b) the anatomy of an *Arabidopsis* trichome; (c) prickles on a rose stem; (d) an anatomical illustration of prickles; (e) a shoot thorn of *Pyrus cordata*; (f) a citrus thorn; and (g) an anatomical illustration of thorns and spines. Produced by NN ZHOU and XW DOU.

1.1.1.1 Trichomes

Esau (1953) has defined trichomes as "epidermal appendages of diverse form, structure and functions ..... represented by protective, supporting, and glandular hair, by scales, by various papillae, and by absorbing hairs of roots." The major feature that indicates that these structures are trichomes is that trichomes are epidermal appendages that originate in the protoderm (or epidermis) only. Thus, they are usually distinguished from emergences, which are formed from both epidermal cells and sub-epidermal tissues (Werker et al., 1985). However, the boundary between trichomes and emergences is not always clear due to some intermediate forms. In some cases, no sub-epidermal cells take part in the development of a trichome but they are locally differentiated below the trichome (Werker, 2000). Coupled with a lack of understanding of anatomy, some authors use "trichome" as a general term for both trichomes and emergences. For instance, Payne (1978) created hundreds of terminology glossaries and described their morphological characteristics in order to distinguish different types of trichomes. This extraordinary undertaking was expected to serve as a reference for researchers concerning the description of trichomes. However, a precise definition of a type of terminology is impossible without ontogenetic studies. Many definitions on his list should be revised according to their anatomical structure. Thus, researchers need to be careful to cite these terms in their reports in order to prevent inappropriate references from creating more confusion. A developmental study is necessary to determine whether some outgrowths are solely epidermal in origin or both epidermal and sub-epidermal in origin. However, such studies are often ignored before assigning a classification.

Trichome diversity

Trichomes vary widely in their final forms and structures, locations, functions, etc. Although no classification method is totally satisfactory, some categories are remarkably uniform in a given taxon and have been used for a long time (Metcalfe and Chalk, 1957; Netolitzky and Uphof, 1962; Leelavathi and Ramayya, 1983; Wagner, 1991; Werker, 2000; Evert and Eichhorn, 2006; Osman, 2012).

Depending on their morphology and secretion ability, trichomes are mainly divided into two general categories: "non-glandular" and "glandular". Non-glandular trichomes (NGT) are diverse in their morphology, anatomy and microstructure. They may be unicellular (Figure 2 a and b) or multicellular (Figure 2 c, d and e), and both types can be branched or unbranched. Unbranched multicellular trichomes and the stalk of branched multicellular trichomes can be uniseriate (Figure 2 c), biseriate or multiseriate (Figure 2 d). Within these categories, they may differ in size, shape, length, and may be jagged or smooth. They may also be soft, sinuous or stiff because of variations in cell wall thickness and substances in the cell. Branched multicellular trichomes may have unicellular or multicellular branches, constituting a variety of tufted appearances. Glandular trichomes (GTs) are defined by the presence of cells that have the ability to secrete or store large quantities of secretions (Fahn, 1979; Fahn and Shimony, 1996; Huchelmann et al., 2017). They also can be unicellular (rarely, Figure 2 f) or multicellular (commonly, Figure 2 g, h, i, j and k), branched or unbranched, and have various shapes. Depending on the location of the gland cell or "collecting cell" and the morphology

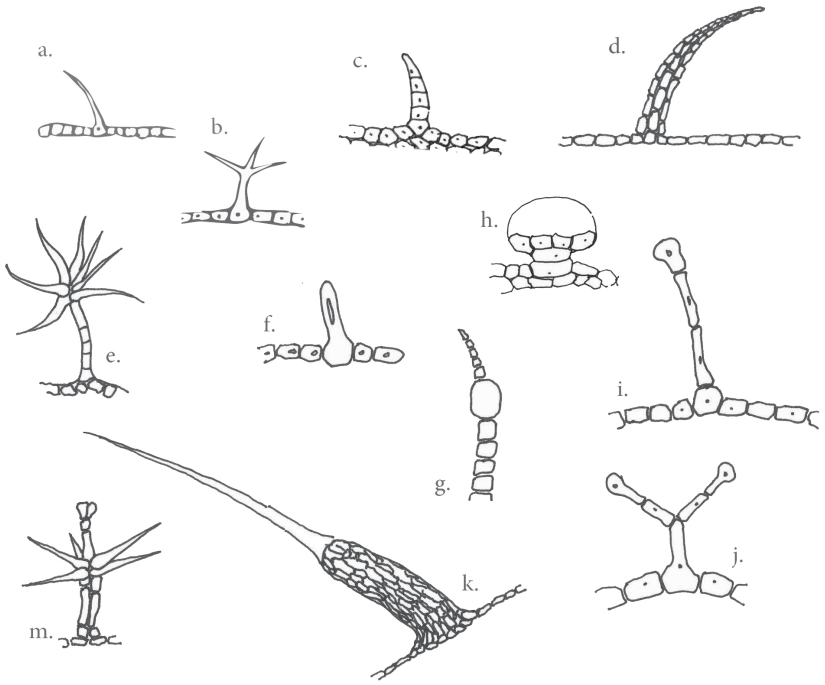

Figure 2: Diversity in trichomes. Non-glandular trichomes: unicellular (a) unbranched and (b) branched trichomes; multicellular (c) uniseriate unbranched, (d) multiseriate unbranched, and (e) uniseriate branched trichomes. Glandular trichomes: (f) unicellular unbranched; multicellular (g, h, i, and k) unbranched and (j) branched. (m) Trichome with non-glandular and glandular branches. Reproduced by NN ZHOU and XW DOU.

properties, some GTs have been classified as capitate (Figure 2 i and j) and peltate (Figure 2 h) (Ascensão et al., 1995; Corsi and S., 1999; Turner et al., 2000), or as stinging hairs (MacFarlane, 1963; Thurston and Lersten, 1969) (Figure 2 k). Some exceptional cases cannot be simply classified in GT or NGT. For example, some trichomes have both non-glandular and glandular branches (Figure 2 m).

Origin and development of the different trichomes

Trichome development starts at a very early stage of leaf development, often prior to stomatal development, and sometimes even before the leaf primordium can be distinguished. Werker (2000) extensively studied and distinguished the seven different types of trichome development: “(1) One protoderm cell that gives rise to a unicellular (Figure 3 a) or multicellular trichome (Figure 3 b and 3 c); (2) One protoderm cell that gives rise to a uniseriate or multiseriate trichome, but neighboring epidermal cells give rise to the pedestal of the trichome; (3) "Twin hairs" that were classified by Metcalfe and Chalk (1965) as two armed hairs; (4) More than one epidermal cell that gives rise to a multiseriate trichome; (5) Hair development by splitting of cells; (6) Subepidermal cells, in which one to all the local tissues subtending the epidermis may take part in the formation of a trichome/emergence; (7)"False hairs" that develop by partial disintegration of cell walls.”

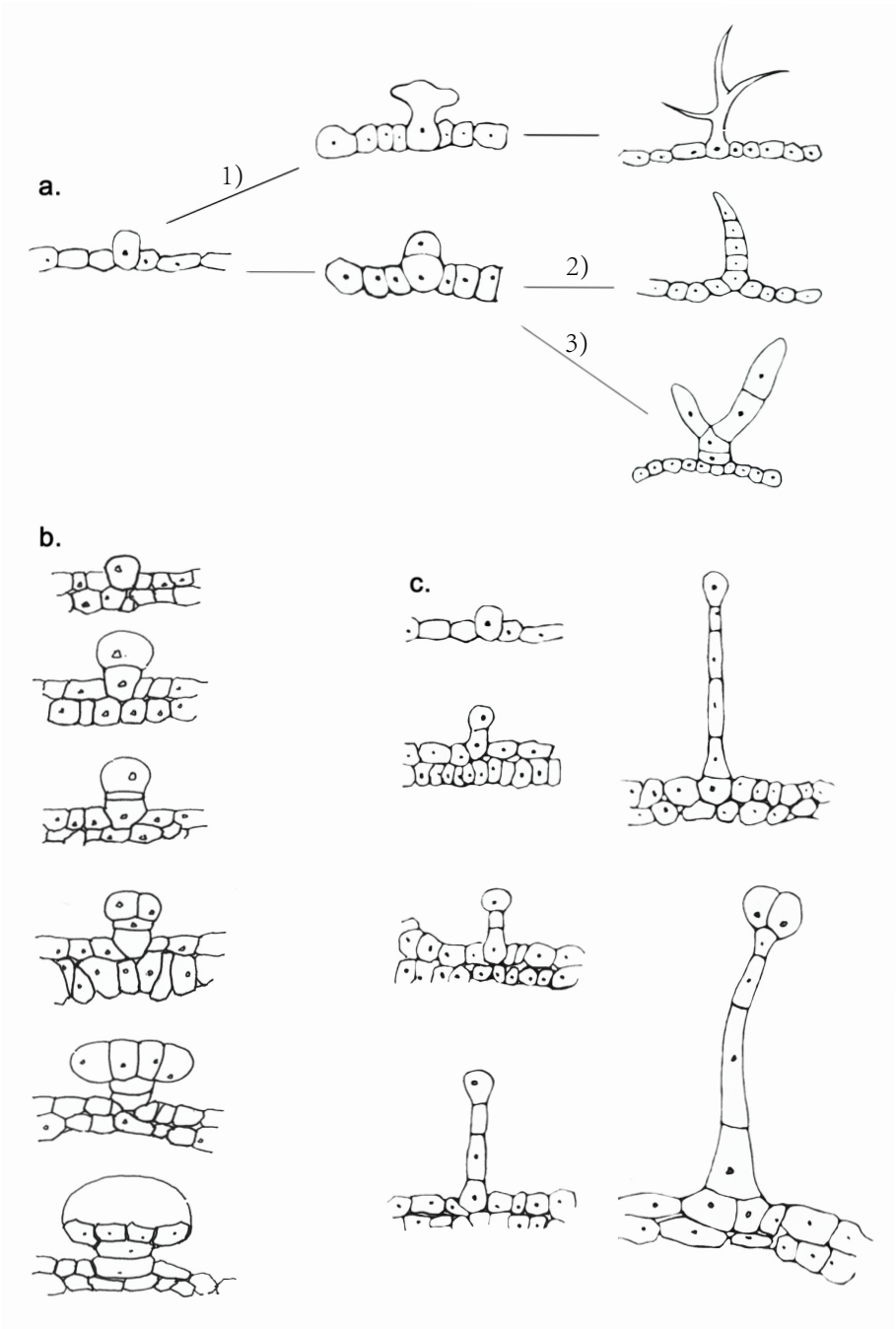

Figure 3: The origin and development of different types of trichomes. (a1) non-glandular trichome (unicellular and branched) development in wild type of *Arabidopsis* (Hülskamp 2004). (a2) non-glandular unbranched and branched; (a3) trichome development in *Origanum vulgare* (Kintzios, 2002). Glandular trichome development on leaves in (b) *Origanum dictamnus* L (Bosabalidis and Tsekos, 1982). and (c) *Sideritis syriaca* (Karousou et al., 1992). Reproduced by NN ZHOU and XW DOU.

1.1.1.2 Prickles

In a glossary of plant hair terminology list, Payne (1978) defined a prickle as "a sharp, rigid, epidermal outgrowth, often relatively massive, as for Rosa; frequently and erroneously termed spine.". In blackberries and raspberries, prickles were described as a stiffer structure, morphologically similar to glandular trichomes and originnating from multiple cellular divisions of the epidermis and a lack of internal vascular material that later became cutinized as hard sharp appendages (Peitersen, 1921; Esau, 1960; Coyner et al., 2005), whereas there was no evidence to support the fact that the origin of prickles is from epidermal cells. Later, a few reports described the prickle's anatomical structure (Asano et al., 2008; Kellogg et al., 2011; Li et al., 2012; Angyalossy et al., 2016) and suggested that prickles may develop from sub-epidermal or/and epidermal cell layers (regularly confused with trichomes). The conclusion based on microscopic pictures of young prickles is regularly subject to controversy and confusion.

Concerning rose, Asano et al. (2008) described prickles as sharply pointed spines, lacking vascular tissue and growig from tissue under the outer layer of the plant. By analyzing the sections of a tender-soft prickle and a mature-hard one, he observed a cell layer in the young and mature prickles but not in the very early stages of development. This cell layer resembles the abscission layer of deciduous leaves. Considering that the mature prickles are easy to peel off with the fingers, and based on previous observations, the authors suggested that the rose prickles were spines or modified leaves (see section of spines and thorns). This conclusion is not supported by strong evidence. Later, Li et al. (2012) suggested that cells in the prickle abscission region were different from cells in the petiole abscission zone by studying the anatomical structure and chemical composition of tender prickles. Then, based on examination of the longitudinal sections of immature prickles and microscopic observations of prickle development, Kellogg et al. (2011) defined rose and raspberry prickles as "epidermal tissue, and modified from glandular trichomes by continuing to grow and hardening into the prickle structure". This conclusion is based on the observation of the glandular head on the tip of a prickle, that falls off during prickle development. They added: "if these glandular structures were absent or reduced in size, the resulting cultivars were prickless or almost prickless, respectively". Based on this, they further hypothesized that secondary metabolites produced in the glandular trichome may play a role in prickle development. Although this argument was supported by other researchers (Ma et al., 2016b; Pandey et al., 2018; Khadgi and Weber, 2020a), the questions remain: firstly, do prickles originate from epidermal tissues like trichomes? Secondly, why is the origin of prickles is closer to that of glandular trichomes but not non-glandular trichomes? Later, Angyalossy et al. (2016) defined prickles as "sharp outgrowths from the bark, without vascular tissue", based on examination of longitudinal sections of the young prickles of *Polyscias mollis*, *Piptadenia gonoacantha* and *Oplopanax horridus*. However, there is still no anatomical evidence to support the prickle origin. Moreover, "bark" is an imprecise term that refers to all tissues exterior to the vascular cambium including a number of tissue types that are periderm (composed of the cork, cork cambium, and the phelloderm), cortex (comprised of ground tissues), phloem and epidermis (Dickison, 2000; Evert and Eichhorn, 2006). These tissues are formed at a relatively later stage of stem development, while prickle formation normally takes place earlier (almost simultaneously with leaf primordia) (Asano et al., 2008). Therefore, the definition of prickles needs to be defined in relation

to their origin.

Do prickles originate from which tissue(s) or cell layer(s)? Are epidermal cells involved in the differentiation of parts? To answer these questions, we need to provide anatomical evidence of prickle development, including initiation and later developmental stages, which are still absent.

1.1.1.3 Thorns and spines

Thorns and spines are usually distinguished based on the modified organ from which they come. Thorns are defined as a sharp-pointed stems or shoots (Delbrouck, 1875; Blaser, 1956; Michael G., 2010). They can sometimes bear leaves (Figure 1 e, *Prunus spinosa*, *Crataegus laevigata* L.), flowers (*Ulex europaeus*), or be bare (Figure 1 f), and can be unbranched (*Crataegus monogyna*, *Ccrataegus crus-galli*) or branched (*Gleditsia triacanthos*). By comparing the non-thorny and thorny branches of *Crataegus laevigata* L., *Prunus spinosa* L. and *Pyrus communis* L, *Pyrus Matus* L, *Mespilus germanica* L, Aubertot (1910) described the thorny branches as being shorter than the ordinary ones, growing in all directions (*Prunus spinosa*), with smaller leaves(*Pyrus, Prunus*), and more indented lobes (*Crataegus*). The stipules were often reduced in *Crataegus*. Based on anatomical study, one remarkable trait of thorny was the woody conductive tissue (Aubertot, 1910), which consist of a considerable reduction in the vascular network, a reduction that may affect the number of vessels only (*Pynus*) or their diameter (which decreased from an average of 50% in *Crataegus*,).

Delbrouck (1875) classified numerous spinescences and noted that thorns may be produced from normal axillary buds, from supernumerary buds, or from terminal buds. In *Gleditsia*, thorns are usually branched and bare, represented by the typical three-parted thorn that arises from one axillary meristem. This meristem gives a shoot that will become a thorn. This shoot also bears two additional axillary meristems that can grow later and give rise to two new thorns, leading to the branched thorn (Blaser, 1956).

Spines are variously described as leaves or leaflet spines (as in *Cactaceae*, *Ulex europaeus*, *Phoenix*), stipule spines (as in *Vachellia xanthophloea*), petiolar spines (as in *Fouquieria*), or parts of leaves (as in *Ilex aquifolium*) (Michael G., 2010). Some authors prefer not to distinguish between thorns and spines because, unlike prickles, they are both usually vascularized (Bell, 1991). For instance, *Cacti* have evolved succulent stems (in order to store water) with specialized buds called areoles. Areoles produce a cluster of spines where the spines are vestigial leaves, sometimes with no vascular tissue visible. Most cacti spines are diverse in terms of form: 'long or short', 'hairlike, papery, hooked, corrugated, or flattened', 'heavy or thin', 'barbed, smooth, or glandular'. Even though some have none as adults (e.g. *Ariocarpus*, *Lophophora*, *Rhipsalis*), they usually have them at the juvenile stage (Boke, 1980). In *Bartschella* or *Opuntia*, spine primordia arose in the same manner as leaf primordia, but they both lack lamina and vascular tissue. The spine appears in the spine-leaf transition forms that usually occur on expanding areoles (Boke, 1944, 1956). Apical maturation of spine primordia is both precocious and covers the entire structure. Further growth is restricted to a well-defined basal intercalary meristem in which continuation of growth activity and planes of cell division determine the length, breadth and cross-sectional configuration of the mature structure (Boke,

1980). In non-cacti plants, spines are mostly described at the macroscopic level, and anatomical evidences is rarely. Gallenmüller et al. (2015) examined the cross and longitudinal sections of young spines in *Asparagus setaceus* and *Asparagus falcatus*. They are both composed of different types of tissues, including leaf, stem, axillary bud or lateral shoot. The scale of the different tissues differs between species, with a higher contribution of leaf and lateral shoot tissue in *A. setaceus*, where a cork layer is formed between leaf and stem tissues of the spines. The cork layer was not observed in spines of *A. falcatus*.

Many structures cannot clearly be classified in these categories (thorns, prickles or spines). The most important point for biologists is to understand the initiation and development of this structure (origin). The same or similar developmental patterns of organs and tissues may be controlled by similar genetics pathways. Good knowledge of its structure and development patterns will be an assist for reverse genetics research.

1.1.2 An efficient adaptive strategy to response to biotic and abiotic stress

Superficial tissues (epidermis) and appendages structures (trichomes, spinescences) of plant organs are the first line of plant defense. They play a crucial role against multiple abiotic and biotic stresses. Since they comprise the outermost boundary between the plant and its environment, they mediate a plethora of plant-environment interactions, plant-pathogen interactions and plant-herbivorous interactions, as well as plant-plant interactions. In this section, I will review the protective and defensive role of these appendage structures in plant-environment and plant-herbivorous interactions.

1.1.2.1 Adaptation to extreme environments

A wide range of hypotheses concerning trichome functions in plant-environment interactions have been reported, but have not always been experimentally tested. Hundreds of different forms of trichomes are found on different organs in different plants and may have a great variety of functions, whereas a number of trichome functions have only been either hypothesized or are totally unknown (Werker, 2000). Investigation of the morphological characteristics of plants in extreme environments shows how trichomes play an important role in protecting plants against increasing solar radiation, extreme temperatures, drought and windy environments. The most typical representative examples are alpine plants (Körner, 2003) and cacti (Nobel, 1988, 2002), whose younger organs are always covered with high-density trichomes or spinescences, which may remain over the lifetime of the plant.

Plant adaptation to the light environment

In plants, radiation absorptance is a major driver of both carbon and energy balance, two important aspects of plant survival and reproduction in any ecosystem. Regulating the absorptance and reflection of radiation is important for plants living in a variety of light environments (Shull, 1929; Billings and Morris, 1951; Ehleringer, 1981; Körner, 2003). Apine plants, in particular, are under heightened selective pressure to

structurally and physiologically adapt to their unusual light environment. Trichomes are one of the essential adaptation structures to control absorptance and reflection radiation (Johnson, 1975). In desert and subalpine plants, Billings and Morris (1951) observed consistently higher reflectance in the pubescent leaf exposed to visible spectrum radiation, whereas in soybean lines (varying from glabrous to pubescent), leaf trichomes increase their absorptance and decrease their reflectance through diffuse radiation, and entrap incoming near-IR light (Gausman and Cardenas, 1973). The optical properties of trichomes in plants vary greatly in response to visible spectrum radiation. For dynamic lights adaptation, the variation in trichomes response is explained by trichome density (Ehleringer et al., 1976; Ehleringer, 1981), and as well as their forms and structures (Pierce, 2007; Mershon et al., 2015). Ultraviolet (UV)-mediated induction of trichome density has been demonstrated using genetic approaches. In *A. thaliana*, using wild type and several trichome-related mutants (*gl1, gis, gis2, zfp8, try82,* and *gl3*), and overexpressing trichome positive regulator lines (35S::GIS and 35S::GIS2), Yan et al. (2012) demonstrated that trichome density significantly increased under UV-B enhanced radiation conditions, suggesting a clear induction of trichome formation by UV-B.

Considering that trichomes absorb UV-B radiation, some authors have suggested that trichomes covering different organs play a protective role against damage from UV radiation (Karabourniotis and Fasseas, 1996; Karabourniotis et al., 2020; Skaltsa et al., 1994; Ntefidou and Manetas, 1996; Liakoura et al., 1997; Agati et al., 2012), although no direct evidence has shown that genotypes that lack trichome protection suffer from increased injury by UV-B. Plants have very effective systems of UV-protection and repair because plants in the natural environment rarely show any signs of UV damage (Jenkins, 2009). The benefits of UV-B to plants may far outweigh the damage. UV-B makes up just a small fraction of the total solar radiation, but it represents a crucial signal that initiates several responses in plants that affect metabolism, development, and viability (Jenkins, 2009). It has been shown that UV-B-mediated induced morphological and physiological changes in plants as a reinforcement of plant defense in some cases (reviewed by Robson et al. (2015) and Escobar-Bravo et al. (2017)). For example, in an experiment, where no pesticides were applied, Mazza et al. (1999, 2013) found that solar UV-B significantly indirectly reduced insect herbivory. This indirect benefit of UV-absorbtance by plants is mainly due to increased phenolic compounds and trichome density (Mewis et al., 2012; Đinh et al., 2013; Jeschke et al., 2015; Zavala et al., 2015; Escobar-Bravo et al., 2017). Use of the UV-B light component of solar radiation to enhance crop defense against pests and pathogens, as well as crop production, has aroused increasing interest (Wargent and Jordan, 2013).

Trichome may protect plants from extreme temperatures

Alpine plants that grow in the high alpine zone at high altitudes, always have a high density of trichomes. This may indicate that these hairs play a certain role in adaptation to extreme conditions and particularly low temperatures. For example, Himalayan snowball plants (Figure 4) are considered to be an extreme form of downy plants. Tsukaya et al. (2002) examined the downy inflorescences of *Saussurea medusa* and analyzed the temperature within inflorescences after the absorbance of light energy. They found that the downy bracts of *S. medusa* have two major functions thermal insulation to protect the inside of flowers against cold and

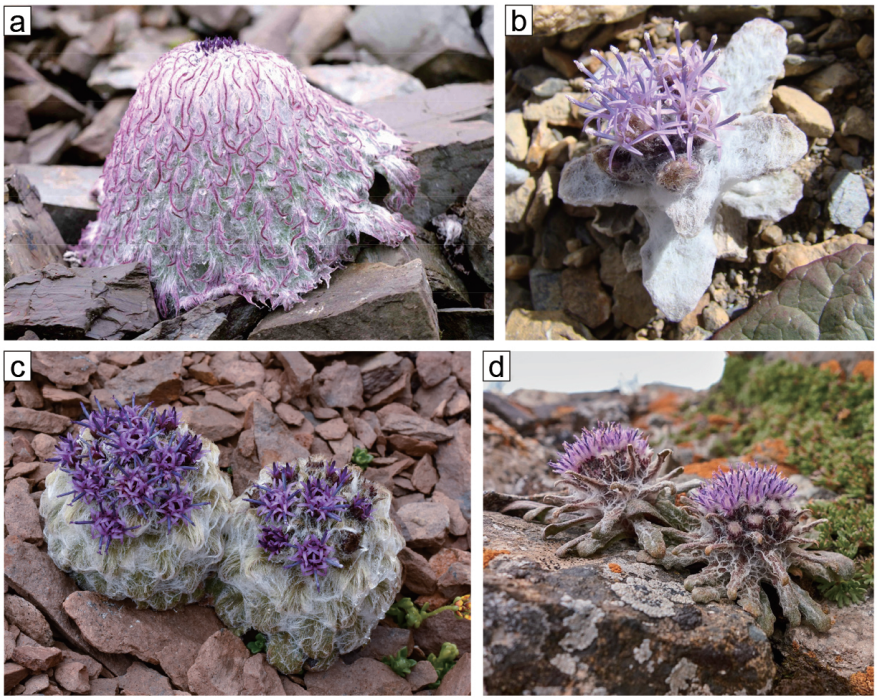

Figure 4: Himalayan snowball plants. (a) *Saussurea medusa*. (b) *Saussurea gnaphalodes*. (c) *Saussurea aster*. (d) *Saussurea glacialis*. Credits: CGIN nature film crew (a); iNaturalist (Kulbhushansingh Suryawanshi (b); Harry Jans (c); Ruslan (d)).

the accumulation of heat on the upper surfaces of the inflorescence.

Some trichomes and spinescences may be adapted to drought conditions

Plants growing in arid habitats had higher-density trichomes than similar plants in mesic habitats (Ehleringer et al., 1976; Ehleringer, 1981; Fahn, 1986; Nobel, 1988, 2002). Evert and Eichhorn (2006) reviewed the studies on plants growing in aird regions and concluded that "an increase in leaf pubescence (hairiness) reduces the transpiration rate by (1) increasing the reflection of solar radiation, which lowers leaf temperatures; and (2) increasing the boundary layer (the layer of still air through which water vapor must diffuse).". In addition, naturally arid conditions always corresponded to a higher frequency of spinescent plants distribution, indicating that spinescence may be adapted to arid conditions (Shmida, 1981; Nobel, 1988).

1.1.2.2 Adaptive defense responses to herbivores

The defense system against herbivores is a large and changeable network and may involve the cooperation among of multiple strategies. To ward off an attack by different types of organisms, plants possess a surveillance system to perceive who attacked them and to thus introduce specific defenses (Crawley, 1983; Van loon et al., 2009; Futuyma and Agrawal, 2009; Kant et al., 2015; Lev-Yadun, 2016). For instance, wounding can be chemically identified (Van loon et al., 2009; Karban, 2015), plants can then recognize

herbivore attacks for a long time (Gagliano et al., 2014; Karban, 2015). Plants can employ bodyguards such as ants (Jolivet, 1998) and use volatiles to attract the natural enemies of invertebrates to attack herbivores (Kessler and Baldwin, 2001; LoPresti and Karban, 2016). Different strategies include the production of large and strong fruits, reducing damage to other vital organs of herbivores (Janzen, 1976), visual or chemical intimidation of herbivores (Lev-Yadun, 2009), use of colors to pretend to be inedible (Givnish, 1990; Lev-Yadun, 2009), ect. Plants have many types of mechanical defenses (Lucas et al., 2000), even anisotropic structural defense arrangements, which may cause invertebrate herbivores to leave the plant (Vermeij, 2015). Spinous plants can inject pathogens into the herbivores, causing injury or death (Halpern et al., 2007, 2011). Of course, no single species can possess all of these defenses at the same time. However, the plant kingdom as a whole has a large weapon arsenal. In the following section, I briefly review the role of trichomes and spinescence as a defense against herbivores, including insects and large mammals.

Trichomes

From an evolutionary perspective, trichomes may have appeared much earlier than herbivores. This hypothesis is supported by evolutionary genealogy studies. Thus, non-glandular trichomes (NGTs) are normally thought to have evolved primarily as physiological barriers against extreme environmental conditions, as we discussed in a previous section. However, many types of trichomes may also have co-evolved with herbivores (especially insects), and perhaps the most widespread function of plant trichomes (especially GTs) today is to protect plants from herbivores (Levin, 1973; Johnson, 1975; Fahn, 1979; Howe and Westley, 1988). The earliest evidence for the occurrence of modified trichomes comes from fossils of the late Carboniferous (Stephanian stage, $\sim$ 290 Mya) and these modified multicellular hairs were glandular trichomes (GTs) (Krings et al., 2003; Lange, 2015). Krings et al. (2003) proposed that these GTs possessed a touch-sensitive mechanism that opened the secretory cell when touched. Compared to the plant trichomes of today, they further support the implications of GTs in plant-insect interactions in the Late Carboniferous. Indeed, many insect herbivores, including leaf beetles, leafhoppers, and caterpillars, have been shown to be physically-deterred or incapacitated by trichomes (Levin, 1973; Johnson, 1975; Ribeiro et al., 1994; Webster et al., 1994; Eisner et al., 1998; Smith, 1999; Andres and Connor, 2003). NGTs may form physical barriers that can reduce or prevent insects from moving on the plant or from feeding, whereas GTs may release various forms of chemical repellents or traps. Numerous studies have reported the negative relationship between trichome density and the rates of herbivore damage (Pullin and Gilbert, 1989; Valverde et al., 2001; Handley et al., 2005), and an induced resistance has been widely observed in plants following damage by insect herbivores (Gibson, 1971; Harvell, 1990; Karban and Baldwin, 1997; Traw and Dawson, 2002; Tian et al., 2012). In *Brassica nigra* (L.), for instance, leaf trichomes are induced differently in response to different herbivores attacks(Traw and Dawson, 2002). Leaves of plants damaged by *Pieris rapae* had 76% more trichomes per unit area than control plants, and leaves of plants damaged by *Trichoplusia ni* had 113% more trichomes. It has been suggested that specialized defense mechanisms in response to herbivores usually involve glandular trichomes (Tingey, 1991), and some GTs secret antibiotic compounds that directly intoxicate arthropod

herbivores (Wang et al., 2004; Ranger et al., 2004; Hare, 2005). Molecular engineering of GT biochemistry has been successfully targeted as a measure to promote pest resistance (Haudenschild and Croteau, 1998; Wang et al., 2004; Calo et al., 2006), and some plant genes responsible for the antibiotic compounds have been used to engineer microbes that produce specific compounds (Ro et al., 2006). In some cases, very small insects such as spider mites and aphids use trichomes to protect themselves against their natural enemies like coccinellid beetles (Eisner et al., 1998), which means that some insects may be specifically adapted to glandular trichomes (Dam and Hare, 1998; Hare and Elle, 2002). Some insects may utilize specific terpenes to locate their host (Roda et al., 2003). Based on this hypothesis, there has been increasing interest in incorporating trichome-based resistance in plant breeding programs (Simmons et al., 2004, 2006; Glas et al., 2012; Simmons and Gurr, 2006). Except for their well-recognized roles in entrapping or impeding small insects, Peiffer et al. (2009) supposed that GTs also function as an early detection system against herbivores. Following insect movement, GTs release plant defense signals that quickly activate the expression of defense genes' in response to insect movement. Other studies have reported that herbivore feeding induces local and systemic changes in gene expression. For example, van de Wilhelmina et al. (2000) identified squash genes (SLW1 and SLW3) that were systemically induced after silverleaf whitefly feeding. Yoshida et al. (2009) suggested GL3 is a key transcription factor of wound-induced trichome formation acting downstream of JA signaling in *Arabidopsis*.

Spinescence

Spinescence has been proposed as a defense against herbivory. It has been the working assumption of scientists who study ecological interactions between plants and animals (Cooper and Owen-Smith, 1986; Belovsky et al., 1991; Burns, 2014; Wilcox, 2017). A study of paleontological fossils offered evidence that spinescent structures may have appeared in the late Silurian ($\sim$ 400 million years ago), which is before the advent of large herbivores (Chaloner, 1970). This evidence assumed that the evolution of prickles may be a response to the pressure of herbivorous insects. Kariyat et al. (2017) later reported that prickles may play a role in deterring insects by restricting caterpillar movement. In the process of co-evolution with herbivores (especially mammals), plants have evolved an impressive diversity of defenses. Many types of spinescence have been produced (or modified) from the shoots, leaves, fruits, pedicels and even roots. They specifically react against vertebrates rather than against invertebrates or insects, especially thorn and spines (**?**). After secondary compounds, spinescence has been proposed as the most successful defense strategy against herbivory (Belovsky et al., 1991). Those spinescent structures frequently team up with predatory pathogenic bacteria, fungi, toxic chemicals, volatiles, and coloration, to enhance their attack or defense ability (Lev-Yadun, 2003; Halpern et al., 2007; Hartmann, 2008; Halpern et al., 2011). A number of diseases caused by injecting pathogenic bacteria and fungi into predators have been reported. Halpern et al. (2007) identified 58 bacterial isolates from the thorns of *Phoenix dactylifera* and *Crataegus aronia*, belonging to 22 different bacterial species, 13 of them known to be pathogenic for animals or humans, such as *Bacillus anthracis, Clostridium perfringens and Clostridium tetani*. *Bacillus anthracis* is the causative

agent of anthrax, primarily a disease in mammals, including humans (Jensen et al., 2003). *Clostridium perfringens* is a ubiquitous pathogen that produces many toxins and hydrolytic enzymes (Petit et al., 1999). *Clostridium tetani* is the causative agent of tetanus, and injuries caused by spinescences have been reported to cause tetanus in humans in several countries (Hodes and B., 1990; Pascual et al., 2003; Ergonul et al., 2003; Campbell et al., 2009; Tadele, 2017). Mycetoma caused by *Eumycetoma* (fungi) or *Actinomycetoma* (filamentous bacteria), and sporotrichosis diseases caused by Sporothrix schenckii (fungi) are also referred to as "plant thorn synovitis" and "rose-thorn or rose-gardeners' disease" , respectively. The most common route of infection is the introduction of spores to the subcutaneous cellular tissue through a skin wound (Fahal, 2004; Barros et al., 2011; Vásquez-del-Mercado et al., 2012; Mahajan, 2014; Kieselova et al., 2017). Dermatophytes that cause subcutaneous mycoses are unable to penetrate the skin and must be introduced into the subcutaneous tissue by a puncture wound (Willey et al., 2008). Thus, the physical defense provided by thorns, spines and prickles against herbivores might be only the tip of the iceberg in a much more complicated story (Halpern et al., 2007, 2011). These sharp plant structures inject bacteria into herbivores by wounding them, enabling the microorganisms to pass the animal's first line of defense (the skin), and in so doing, may cause severe infections that are much more dangerous and painful than the mechanical wounding itself (Lev-Yadun, 2016).

Understanding the evolutionary process of these defense strategies and their potential joint relationship will help biological scientists to better understand the genetic collaboration network hidden behind them.

1.2 The genetic and molecular bases of trichome and prickle initiation and development

Concerning the genetic basis of trichome and prickle development, the main results were obtained on trichomes in model plants such as *Arabidopsis*. In this section, I will review what is known about molecular networks that control trichome initiation and development.

1.2.1 Trichomes have been one of the models for studying plant differentiation and cell factories

As mentioned in the first section, trichomes are mainly divided into two general categories, glandular (GT) and non-glandular (NGT), depending on their morphology and secretion ability. Among all the appendages structures, the studies of NGT are the most systematic and comprehensive, and are mainly done on the unicellular branched trichome of *A. thaliana*, which has been considered as a model system to study the structure initiation and development at the single-cell level (Hülskamp, 2004). Over 30 genes involved in the initiation and development of NGTs have been identified and have been used to generate a developmental framework, whereas GTs have been chiefly studied to reveal the biochemical pathways of the compounds they secrete and to advance our understanding of secondary metabolism in plants (Champagne and Boutry,

2013; Lange and Turner, 2013; Huchelmann et al., 2017; Hao et al., 2019; Pradhan and Maradi, 2020).

1.2.1.1 Non-glandular trichomes

Depending on the cell's position, each cell perceives different signaling, responds to signaling pathways, and adopts a specific cell fate (Larkin et al., 2003; Schiefelbein, 2003). The subsequent differentiation of the cell often involves complex changes, e.g., cells may exit the mitotic cycle or enter an endoreplication cycle. Cellular architecture is modified to meet the functional requirements of the respective cell type, and cell metabolism changes according to its function (Hülskamp, 2004). A branched unicellular NGT originates from one cell of the protodermal epideris (Hülskamp et al., 1994; Werker, 2000; Hülskamp, 2004). This cell only initiates endoreduplication cycles but no mitotic cell division, which causes the cell to increase in size and to branch to form the mature structure (Melaragno et al., 1993; Hülskamp et al., 1994; Folkers et al., 1997). In *A. thaliana*, leaf trichome nuclei have elevated ploidy levels, reaching 4C, 8C, 16C, 32C, and 64C (1C is the nuclear DNA content of the unreplicated haploid genome) (Melaragno et al., 1993). The molecular network was deciphered using mutants impaired in NGT initiation and development (Marks, 1997; Hülskamp et al., 1998). The genetic of NGT in *A. thaliana* is well understood as this time and numerous genes have been identified. Hülskamp (2004) assumed that only very few genes are trichome-specific and that most genes are related to many cell types and are involved in more general cellular processes.

Gene network controlling unicellular NGT initiation and differentiation

A development framework for unicellular NGT formation has been extensively studied (Folkers et al., 1997; Hülskamp, 2004; Balkunde et al., 2010; Yang and Ye, 2013; Pattanaik et al., 2014). We will recall here the main transcription factors that control unicellular NGT initiation in *A. thaliana*, and show how they work together (Figure 5). They generally belong to MYB, bHLH, WD40, WRKY and C2H2 zinc finger proteins families.

A trimeric activator complex (MBW) consisting of MYB (GLABRA1, GL1)-bHLH (GLABROUS3/ ENHANCER OF GL3, GL3/EGL3)-WDR (TRANSPARENT TESTA GL1, TTG1) plays a key role in trichome initiation (Schiefelbein, 2003; Zhang, 2003; Hülskamp, 2004; Kirik et al., 2005; Pattanaik et al., 2014). Mutations in both the *GL1* and *TTG1* genes both lead to the complete absence of trichomes (Koornneeff, 1981; Koornneeff et al., 1982), while the *gl3* mutant still exhibits fewer trichomes compared to wild-type plants, probably caused by a close homologue, *EGL3*, that may be able to rescue the failed function of *GL3*. In fact, *gl3 egl3* double mutants are devoid of trichomes (Zhang, 2003). Downstream, the MBW trimeric complex finely regulates the temporal and spatial expression of *GLABRA2 (GL2)* and *TRANSPARENT TESTA GL2 (TTG2)*, determining the fate and pattern of trichome precursor cells (Rerie et al., 1994; Ishida et al., 2007, 2008). The MBW complex is a hub that integrates different signals that controls trichome initiation. The R3MYB subfamily genes, *TRY, CPC, TCL1, ECT1, ETC2* and *ETC3*, act as negative regulators by competing with *GL1* for binding to *GL3* (Schnittger et al., 1999; Scheres, 2002; Esch et al., 2003; Wang

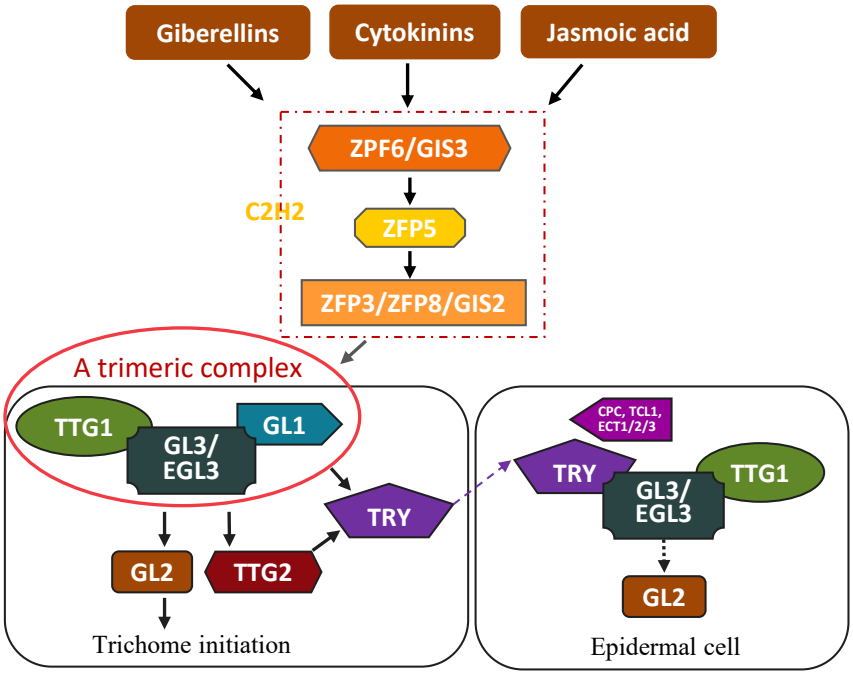

Figure 5: Summary the genes network of non-glandular trichome initiation.

et al., 2008; Wester et al., 2009; Wang and Chen, 2014). *try* mutants produce trichome clusters whereas all other inhibitors are involved in trichome density regulation (Pesch and Hülskamp, 2011). The active *TTG1* complex, in interaction with *TTG2*, regulates the expression of the R3 MYB inhibitors that move to the neighboring cells where they repress trichome initiation (Pesch and Hülskamp, 2004; Hülskamp, 2004). Upstream, plant growth regulators, such as gibberellin (GA), iasmonic acid (JA) and cytokinin (CK) regulate trichome initiation by regulating transcription upstream of the MBW complex. Different C2H2 zinc finger proteins such as GLABROUS INFLORESCENCE STEM (GIS), GIS2, GIS3, ZINC FINGER PROTEIN5, 6 and 8 (Gan et al., 2006, 2007) include GA and cytokinin signaling pathways (Zhou et al., 2013). The novel transcription factor *TRP* interacts with *ZFP5* and negatively regulates trichome initiation through the gibberellic acid pathway (Kim et al., 2018). In addition, Ultraviolet-B-mediated induction can increase trichome density and *GL3* expression in the *zfp8* and *gis* mutants (Yan et al., 2012). JASMONATE ZIM DOMAIN1 (JAZ1) protein, an important repressor in the JA signalling pathway is degraded by JA. This degradation releases MBW activity and promotes trichome initiation (Qi et al., 2011).

Cell-cycle control during unicellular NGT development

The cell cycle is the indispensable process required for organ or tissue development. It consists of four phases: Gap 1 (G1), DNA synthesis (S) and Gap 2 (G2) and Mitosis (M) (Figure 6). Endoreplication (or endoreduplication), is a common cell cycle variant in which cells increase their genomic DNA content without dividing (Edgar and Orr-Weaver, 2001). A survey of *Arabidopsis* revealed polyploidy in unicellular NGT (uNGT) (Melaragno et al., 1993), and the number of endoreplication cycles determines the ploidy level

and trichome growth; mutants with reduced endoreplication cycles result in smaller trichomes with fewer branches, while increased endoreplication cycles have larger trichomes with more branches (Hülskamp et al., 1994). As in other eukaryotic organisms, cyclin-dependent kinases (CDKs) control progression of the plant cell cycles (Morgan, 1997). Different CDK-cyclin complexes phosphorylate a plethora of substrates at the key 'G1 to S' and 'G2 to M' transitions, triggering the onset of DNA replication and mitosis, respectively. All eukaryotic organisms studied to date possess at least one CDK with the PSTAIRE hallmark in their cyclin-binding domain. In plants as well, a bona fide PSTAIRE CDK, designated CDKA plays a pivotal role at both the 'G1 to S' and 'G2 to M' transitions. Plants possess a unique class of CDKs, the so-called B-type CDKs (CDKB) that have not been described for any other organism (Joubès et al., 2000; Boudolf et al., 2001). *Arabidopsis* harbors two CDKB1 (CDKB1;1 and CDKB1;2) and two CDKB2 (CDKB2;1 and CDKB2;2) family members. *CDKB1* transcripts are accumulatef during the S, G2 and M phases, whereas *CDKB2* expression is specific to the G2 and M phases (Segers et al., 1996; Porceddu et al., 2001; Breyne et al., 2002; Corellou et al., 2005). CDK activity is regulated by phosphorylation and associated with their binding activators and inhibitors (Inzé and Veylder, 2006). Cyclins, as the activators of CDKs, exist extensively in plants and are classified into many distinct types, regulating the transition between different phases of the cell cycle. B-type cyclins mainly control the transition of G2 to M (reviewed by Ishida et al. (2008);Yang and Ye (2013)). Ectopic expression of B-Type Cyclin *CYCB1;2* and D-Type Cyclin *CYCD3:1* in the uNGT genotype induces normal cell divisions resulting in multicellular trichomes (Schnittger et al., 2002a,b), and the latter also increase the DNA content in trichomes. Interestingly, *CYCB1;2* is not expressed during wild-type unicellular trichome development whereas it was detected in pGL2::CYCD3;1 and *sim* mutant trichomes (multicellular type) (Schnittger et al., 2002b), suggesting that the expression of *CYCB1;2* is inhibited by SIM. The *SIAMESE (SIM)* gene encodes a putative CDK inhibitor with a key function in the switch from mitosis cycle to endoreplication cycles (Churchman et al., 2006). The *CCS52A1* gene, which encodes a CDH1/FZR-like protein, is a genetic modifier of the multicellular trichome phenotype of *sim* mutants. Overexpression of *CCS52A1* completely suppresses the *sim* mutant phenotype, while the *ccs52A1* mutation enhances the multicellularity of *sim* mutant trichomes, supporting the hypothesis that *CCS52A1* and *SIM* cooperate in repressing the accumulation of B-type cyclins to switch the trichome cell from mitotic to endoreplication (no M phase) (Kasili et al., 2010).

Two of the cell fate genes described above, *GL3* and *TRY*, also act as positive and negative regulators of endoreplication cycles. Different *gl3* mutant alleles showed an astonishingly contrasting function in endoreplication, one that reduced DNA content (smaller NGTs with fewer branches) (Koornneeff et al., 1982; Hülskamp et al., 1994) and another one that increased it (oddly shaped NGT with a striking nuclear morphology) (Esch et al., 2003). The *try* mutants have NGTs with more branches and increased DNA contents (64C). These pleiotropic effects raise the hypothesis that trichome cell-fate choice is functionally linked to cell-cycle regulation (Hülskamp, 2004). Cell-cycle control is usually thought to act downstream of the regulatory complex of trichome cell fate. Strikingly, a reduction of endoreplication leads to fewer trichomes, whereas promoting endoreplication in glabrous patterning mutants could restore the initiation of trichomes. Therefore, the endoreplication cycle plays a role in trichome cell fate (Bramsiepe et al., 2010).

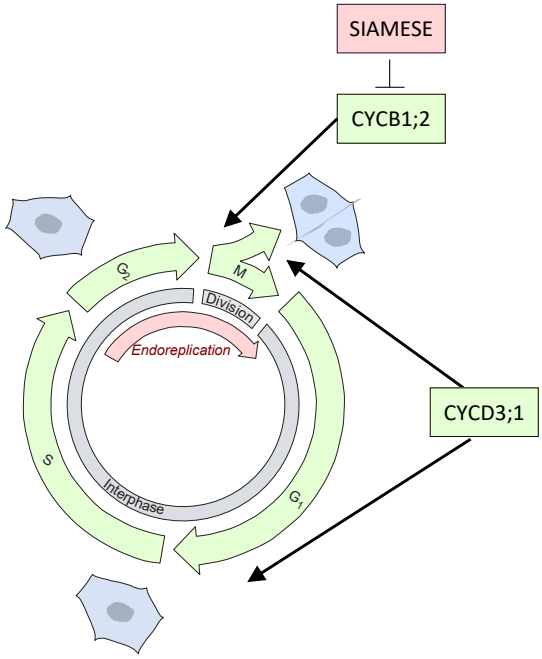

Figure 6: Regulation of the cell cycle during trichome development (Evert and Eichhorn, 2006). G1 phase refers to cell size increases and cellular contents duplicated, S phase to DNA and chromosomes replication, G2 refers to cell enlargement and organelles development and proteins synthesis in preparation for cell division. M phase refers to mitosis followed by cytokinesis (cell separation). Reproduced by NN ZHOU.

SIM is most probably a direct target for *GL3* for controlling endoreplication during the maintenance of trichome cell fate (Morohashi and Grotewold, 2009).

In addition, gibberellin (GA) signaling may also control endoreplication cycles by regulation of *GL1* or its homolog (Ishida et al., 2008). In *spindly* (*spy*) mutants, which exhibit a constitutive GA response, trichomes have eight branches and a high level of endoreplication (64C). In *kaktus* (*kak*), *rastafari* (*rfi*), *polychome* (*poc*) and *hirsute* (*hir*) mutants, trichomes all show a very similar phenotype and ploidy level, like in the *spy* mutant (reviewed by Hülskamp (2004)). The *KAK* gene encodes a member of the HECT ubiquitin-protein ligase family, suggesting that ubiquitin-regulated protein degradation negatively controls the progression of endoreplication and thereby reduces trichome branching (Downes et al., 2003; El Refy et al., 2004).

A regulatory link exists between the progression of endoreplication cycles (or cell proliferation), programed cell death, and resistance to pathogens. The *cpr5* mutant was reported to be constitutively resistant to virulent pathogens. (Bowling et al., 1997). In *cpr5* mutant trichomes, endoreplication cycles stop after two rounds instead of four, and the trichomes then die, the nucleus disintegrates, and the cell collapses. It is therefore suggested that *CPR5* is also involved in programmed cell death control and endoreplication cycles (Kirik et al., 2001). A similar relationship between cell death and endoreplication cycles is found in transgenic plants that misexpress CDK inhibitor (*ICK1/KRP1*). *ICK1/KRP1* expression in uNGTs reduces endoreplications and induces cell death (Schnittger et al., 2003).

1.2.1.2 Glandular trichomes

A key and unique characteristic of GTs is their ability to synthesize and secrete large compounds, mainly terpenoids, but also phenylpropanoids, flavonoids, methylketones and acyl sugars (Huchelmann et al., 2017). Since no GTs are found in *A. thaliana*, research on GT has been carried out on various other plant species, but most researchers are committed to elucidating the biosynthetic pathway of the compounds, and the molecular genetic aspects of GTs development are still unclear (see Huchelmann et al. (2017) and Chalvin et al. (2020)). In *Nicotiana tabacum*, *GL1* homologue overexpression did not alter the glandular trichome phenotype of the tobacco plants (Payne et al., 1999), perhaps indicating a different pathway between GT and NGT. Several studies have recently reported genes and protein complexes that regulate glandular trichome development in *A. annua* (Yan et al., 2017, 2018; Shi et al., 2018; Hao et al., 2019) and tomato (Yang et al., 2011; Nadakuduti et al., 2012; Ewas et al., 2016; Vendemiatti et al., 2017; Gao et al., 2017; Chang et al., 2018; Xu et al., 2018). The majority of regulators belong to the R2R3-MYB and HD-ZIP IV transcription factor subfamilies, and may play essential roles in glandular trichome initiation (Chalvin et al., 2020). In *A. annua*, for example, two members of the R2R3-MYB factors have been characterized as positive regulators of glandular trichome initiation: *AaMYB1* (Matías-Hernández et al., 2017) and *AaMIXTA1* (Shi et al., 2018). A homeodomain-leucine zipper (HD-ZIP) IV transcription factor, AaHD8, interactes with a MIXTA-like protein AaMIXTA1 forming a regulatory complex. This complex activates AaHD1 to induce glandular trichome initiation (Yan et al., 2018).

1.2.2 Genetic and molecular studies in prickles

A few studies on the quantitative trait locus (QTL) of prickles have been reported, mainly in the genus *Rosa* and a few in *Rubus* (Table 1). In the diploid rose population (with a predominance of the *Rosa multiflora* genotype), the presence of prickles on the stem was assumed to be controlled by a single dominant gene (Debener, 1999; Shupert et al., 2007) located on linkage group 3 (LG3) (Linde et al., 2006), whereas two QTLs were detected on LG3 with the scoring of prickle density (Crespel et al., 2002) using an F1 population from a cross with a hybrid of *Rosa wichurana* as the paternal parent. Using two F1 progenies (including a genetic background of *Rosa wichurana*), we also identified a large QTL (or two neighboring QTLs) on LG3 (between positions 31 Mb and 46.5 Mb, corresponding to the end of chromosome 3) which was further supported by a GWAS analysis on a diversity panel showing a significant association in positions 31 and 32.4 Mb (Hibrand-Saint Oyant et al., 2018). In a tetraploid F1 roses population (referred to as K5), three QTLs were identified in relation to the number of prickles on the stem: two located on LG2 and one on LG3 (Koning-Boucoiran et al., 2009). Using the same K5 population with the same phenotype data but a new SNP dense genetic map, different QTLs were detected on LG3, 4 and 6 and on LG2 (one year) (Bourke et al., 2018a). In *Rubus idaeus*, two QTLs were detected on LG4 and 6 (Molina-Bravo et al., 2014).

In roses, the gene network of prickle initiation and development are still largely unknown. No gene has been identified to control prickle formation. Only a WRKY transcription factor (RcTTG2), homologous to *Arabidopsis* TTG2, was found to be located close to the major QTL of the prickle trait in rose and

Table 1: Overview of previous genetic studies for prickle in rose and *Rubus*

	Population					
Species	Parents	Ploidy	Size	Counting method	Genetic determinism	Reference
Rose	93\1-117 × 93\1-119	2n	60	\	Prickles are controlled by a single dominant gene	Debener (1999)
Rose	OW	2n	563	\	Prickles dominant to no prickle	Shupert et al. (2007)
Rose	HW	2n	91	5th-7th nodes	A major and a minor QTL located on the same linkage group of the single seasonal-blooming gene	Crespel et al. (2002)
Rose	OW, YW	2n	151, 174	Over 4 internodes in the middle of the floral stem	a major QTL on LG3	Hibrand-Saint Oyant et al. (2018)
Rose	K5	4n	184	4th-6th nodes on the main stem	A2-2@Rh91-135, A2-3@P11M55-237, A3-1@H3-16	(Koning-Boucoiran et al., 2012)
Rose	K5	4n	151	4th-6th nodes on the main stem	LG3@K7826_576, LG4@K5629_995, LG6	Bourke et al. (2018a)
Rubus idaeus	NC497	2n	\	Scored visually on a scale of 0-5, where 0 is no prickle and 5 is densely covered in prickles	LG4@Rub116a, LG6@Rub103a	Molina-Bravo et al. (2014)

the gene transcripts are differentially accumulated between roses with prickles and roses without prickles (Hibrand-Saint Oyant et al., 2018).

1.3 Rose as a model to study the genetic mechanism of prickles

1.3.1 Rose: a complex genus

Wild roses belong to the genus *Rosa* in the family *Rosaceae*, a medium-sized family of flowering plants, including 2825 ∼ 4900 species in 95 ∼ 125 genera, although these numbers should be seen as estimates since much taxonomic work remains to be done (Yu, 1974; Gu et al., 2003; Royal Botanic Gardens and Kew and Missouri Botanic Garden, 2013; Christenhusz and Byng, 2016). The name *Rosaceae* is derived from the genus type *Rosa*. Up to 90 species of the *Rosaceae* family are of economic importance and include the following fruit trees (e.g. apple, pear, plum, cherry, peach, apricot, hawthorn, strawberry, raspberryand blackberry) and ornamental plants (e.g., rose) (Longhi et al., 2014).

Several fossils of wild roses have been found in the North America (Becker, 1963), Europe (Edelman,

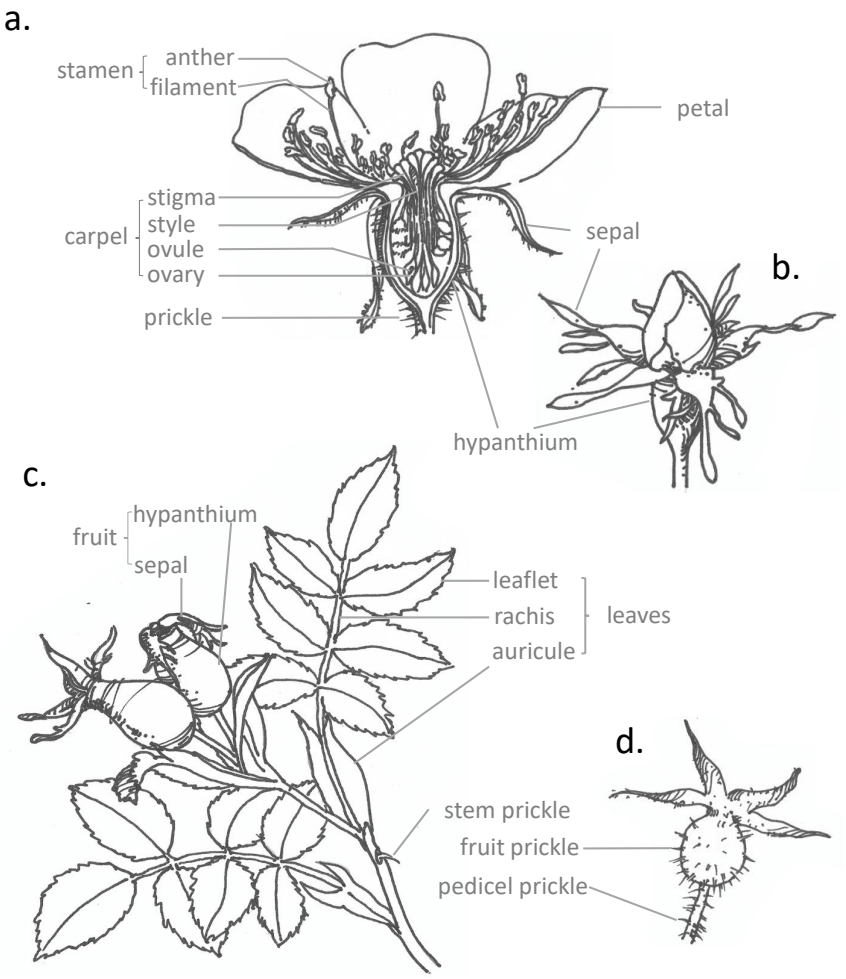

Figure 7: Morphology and anatomy of wild rose. (a) Terms used for the position of the flower (cross-section of a flower), (b) bud, (c) leaves and fruit, (d) fruit and pedicel prickles. Produced by NN ZHOU and XW DOU.

1975) and China (Su et al., 2016). Using time calibration based on fossil records, Fougère-Danezan et al. (2015) estimated that an early lineage of wild roses evolved during the Eocene-Oligocene 24 MY ago (54 Mya - 30 Mya). Today, the genus *Rosa* is composed of $\sim$ 200 species (or variants), widely distributed from cold temperate to subtropical regions (Rehder, 1940). A total of 95 species (65 endemic) are distributed in China (Gu and Robertson, 2003).

1.3.1.1 Rose characteristics and classification

As a member of the genus *Rosa*, roses have their own characteristics that distinguish them from other genera of the family *Rosaceae*. In particular, carpels are usually numerous (Figure 7 a), rarely few; the fruit is an achene, rarely drupaceous (Figure 7 b); sepals are persistent (Figure 7 c); leaves are alternate, odd-pinnate (Figure 7 d), and very rarely simple (except in *R. persica*) (Yu, 1974; Gu and Robertson, 2003).

Based on the phenotypic variations, several attempts to classify wild roses have been reported, and

taxonomy needs to be updated. In Europe (led by France), Rehder (1940) divided the genus into four subgenera (*Eurosa*, 69 species; *Platyrhodon*, one species; *Hulthemia*, one species; *Hesperhodos*, one species), and the subgenus *Eurosa* contains ten sections (*Banksianae, Bracteatae, Caninae, Carolinae, Cinnamomae, Gallicanae, Indicae, Pimpinellifoliae, Laevigatae*, and *Synstylae*). Later on, Wissemann (2003) further divided the section *Caninae* into six subsections (*Caninae, Vestitae, Rubrifoliae, Rubiginae, Trachyphyllae, Tomentellae*) based on the works of Christ (1873) and Crépin (1889).

In China, Yu (1974) divided the genus into two subgenera (*Hulthemia* (Dumort.) *Focke*, one species; *Rosa*, other species) based on the leaves (simple or compound) and stipule (with or without); the subgenera *Rosa* was divided into nine sections (*Pimpinellifoliae* DC., *Rosa*, *Cinnamomeae* DC., *Chinenses* DC. ex Ser., *Synstylae*, *Banksianae* DC., *Laevigatae* DC., *Braeteatae* Lindl., *Mierophyllae* Crép); the section *Pimpinellifoliae* was divided into two Series (*Spinosissimae* Yu et Ku, *Sericeae* (Crép) Yu et Ku) based on the number of petals (five or four); and the section *Cinnamomeae* was divided into three series (*Beggerianae* Yu et Ku, *Cinnamomeae* Yu et Ku, *Webbianae* Yu et Ku) based on the sepal, carpel and leaflet size; and the section *Synstylae* was divided into two series (*Multiflorae* Yu et Ku, *Brunoaianae* Yu et Ku) based on stipule (dentate, irregularly serrate or smooth at margin).

On the basis of previous researches, Masure (2013) reported on 500 roses (including species, varieties and modern hybrid) and classified them into four subgenera *Hulthemia* (Dumort.) Focke, *Platyrhodon* (Hurst) Rehd., *Hesperhodos* Cockerell, *Rosa* (Yu et Ku); *subgenera* Rosa includes nearly 150 species and is subdivided into ten sections, including *Banksianae* Lindl, *Bracteatae* Thory, *Caninae* DC., *Carolinae* Crép., *Chinenses* DC. (syn. *Indicae* Thory), Rosa (syn. *Cinnamomeae* DC). *Gallicanae* DC, *Laevigatae* Thory, *Pimpinellifoliae* DC., *Synstylae* DC. For a more in-depth description and a recent review on *Rosa* taxonomy, please refer to Tomljenovic and Pejić (2018); Debray (2020).

Based on molecular and genomic data, it was confirmed that *R. subg. Rosa* is not *monophyletic* and that other subgenera do not branch at the base of the phylogeny, suggesting that the subgenera of *Platyrhodon*, *Hulthemia* and *Hesperhodos* can be considered as the sectional level (Fougère-Danezan et al., 2015; Debray, 2020). In the subgenera *Rosa*, the section *Carolinae* can be merged with the section *Rosa*, and the section *Chinenses* can be merged with the section *Synstylae* (Fougère-Danezan et al., 2015; Debray, 2020). *R. praelucens* is mostly derived from a cross between section *Rosa* lineages and no relationship between *R. praelucens* and *R. roxburghii* was detected. This supported the hypothesis that *R. praelucens* is a full member of the section *Rosa*, making it possible for *R. roxburghii* to be the representative species of the subgenera *Platyrhodon* (Debray, 2020).

1.3.1.2 Prickle and other trait diversity in rose

Rose growth habits

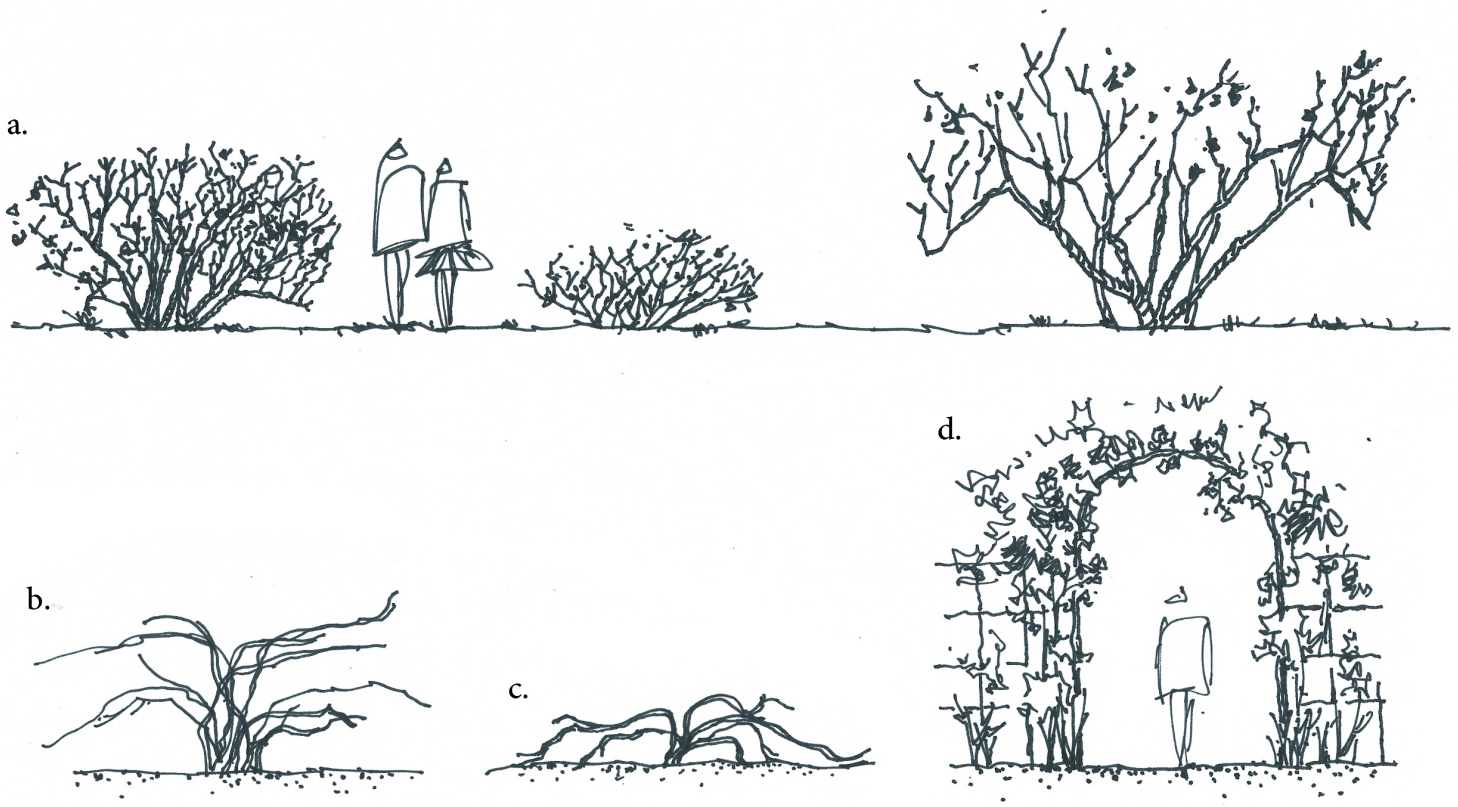

Figure 8: Rose growth habits: (a) Erect type of roses in a variety of crown widths and heights; (b) Semi-erect rose; (c) Trailing rose; (d) Climbing rose. Reproduced by NN ZHOU and XW DOU.

Rose species as woody perennial shrubs can be climbing, erect or diffuse (Yu, 1974; Gu and Robertson, 2003) (Figure 8). They are distinguished from trees by their multiple stems without clear trunks and their shorter height, usually less than 10 m tall (Allaby, 1999). Roses grow in all different shapes and sizes, from tiny miniatures only 30 cm high to climbers that can sprawl over a house. A few climbing species can exceed 10 m if they find a support nearby. For example, *Rosa banksiae* 'Albo Plena' (Lady Banksia Rose) is a native species in China. Unlike most roses, it is prickless or almost prickless. This species can climb to the top of the tree and occupy the entire canopy.

Stems and stem prickles

Rose stems are terete and usually green or red during the first years of growth, and then turn gray/brown when older. Many young stems secrete a thin waxy film that disappears on older stems. Stems are mostly prickly, glabrous or puberulous, and the prickles and bark in some cases peel off from old stems, which can be frequently observed in the platyrhodon subgenus, represented by *R. roxburghii* and *R. minutifolia*. Here, we selected some representative genotypes in four subgenera and a few of the sections under subgenus *Rosa* to show the prickle diversity on stems (Figure 9). Their distribution can be paired at leaf bases (Figure 9 p, q, s and t), unpaired but regularly distributed (Figure 9 g, h and i), randomly scattered (Figure 9 e, l and o), or densely bristly (Figure 9 b, c, d, j and m). Their shapes present a large diversity; they can be straight, slightly curved or curved, thin-soft or thick-hard, acicular (soft or hard), gradually tapering off to an elliptic base or abruptly flaring into a broad base, glabrous or hairy. These prickle shapes are also varied in size and color. Young prickle colors are normally green, sometimes slight red, bright red, ruby red, and some may even be white (Figure 9 i and j), and the colors usually change to rust, gray, or white when the prickles mature and dry. Some species can be reliably recognized by their prickles' characteristics.

Leaves

The alternating leaves are generally odd pinnate (Figure 9 p, s and t), 5 $\sim$ 15cm long (except for extreme cases), and the stipules are adnate or inserted at the petiole (Figure 7 c), except for the leaves of *R. persica* that are simple, sessile and lack stipules (Figure 9 r). They are composed of 5 $\sim$ 9 leaflets on average with a range that varies from 3 $\sim$ 17 between species, which is considered as an important character for rose classification. A variation of serrated patterns can often be observed on the leaflet and stipule margins. Leaflets can be glabrous, or bear pubescence on both surfaces or only on the abaxial surface, and some have glandular emergences. Glandular emergences can often be observed on both sides of the rachis, while prickles are normally only present underneath.

Inflorescences and flowers

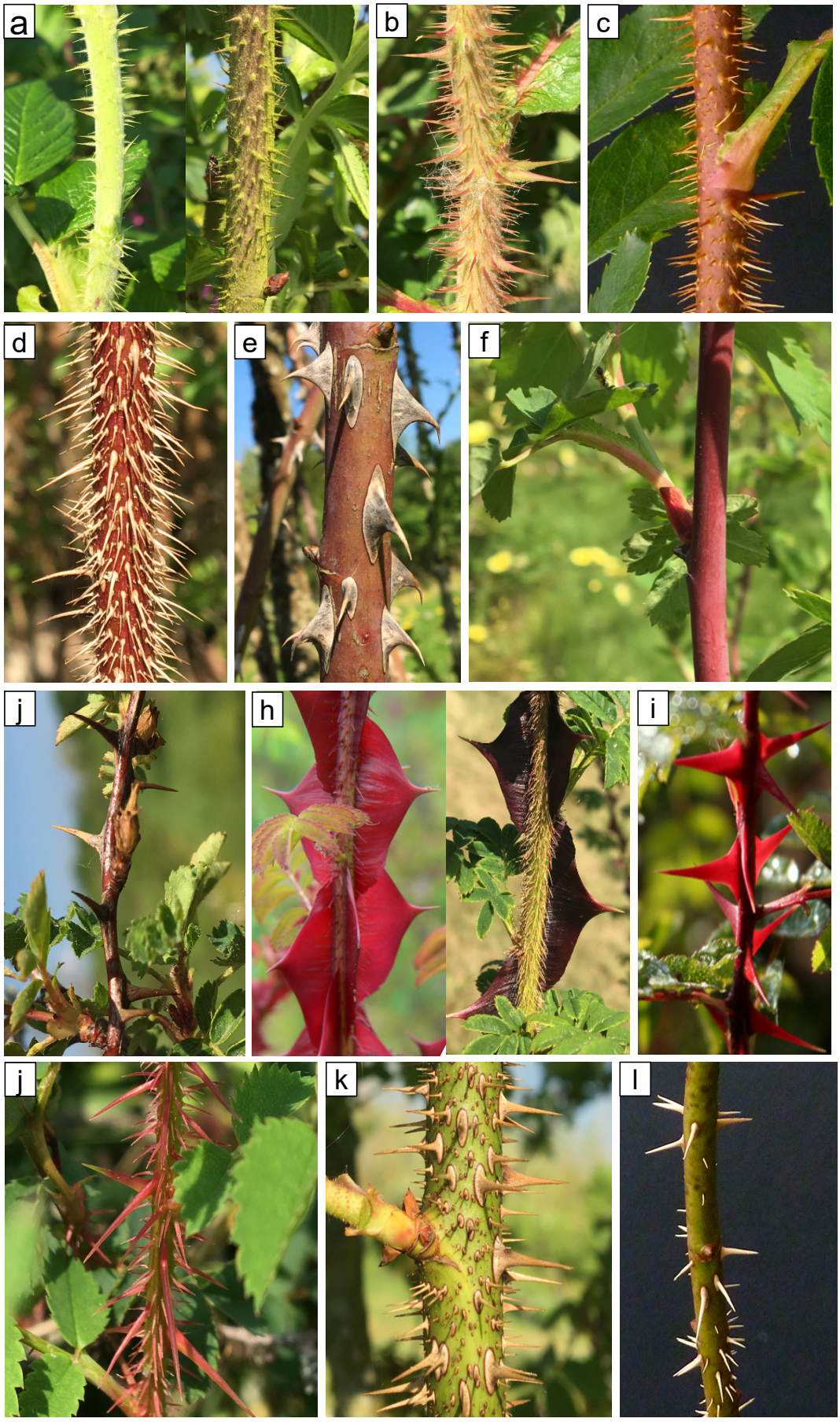

Figure 9: Continued on the next page

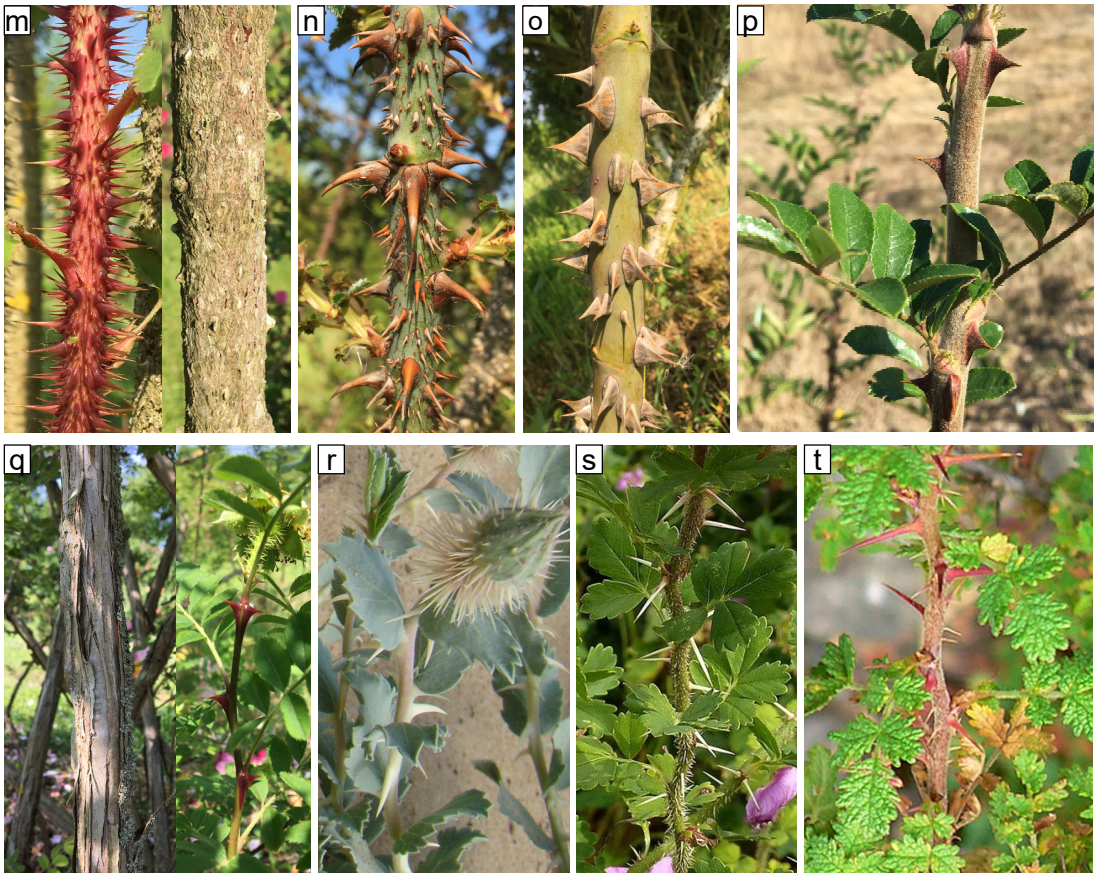

Figure 9: Prickle diversity on rose stem. **Subg. *Rosa***: **section *Cinnamomeae***. (a) *R. rugosa scabrosa*, (b) 'Marie Bugnet' (Hybrid *Rugosa*.), (c) *R. acicularis*, (d) *R. Rubella*, (e) *R. laxa retzius*, (f) *R. fraxinifolia*; **section *Pimpinellifoliae*** (g) *R. ecae*, (h) *R. omeiensis*, (i) *Rosa primula* (Les racines du vent), (g) *R. pimpinellifolia* King of the Scots, (k) *R. pimpinellifolia aïcha*, (l) *R. foetida*. **section *Bracteate* Theory** (m) *R. sherardi*, (n) *R. horrida*, (o) *R. scabriuscula*, (p) *R. bracteate*; **Subg. *Hesperhodos***: (q) *R. roxburghii hirtula*. **Subg. *Hulthemia*** (r) *R. hultemia persica*. **Subg. *Platyrhodon*** : (s) *R. stellata,* (t)*R. minutifolia*. Credits: NN ZHOU, except r (Yuriy Danilevsky), s (Dave's Garden), t (Stan Shebs).

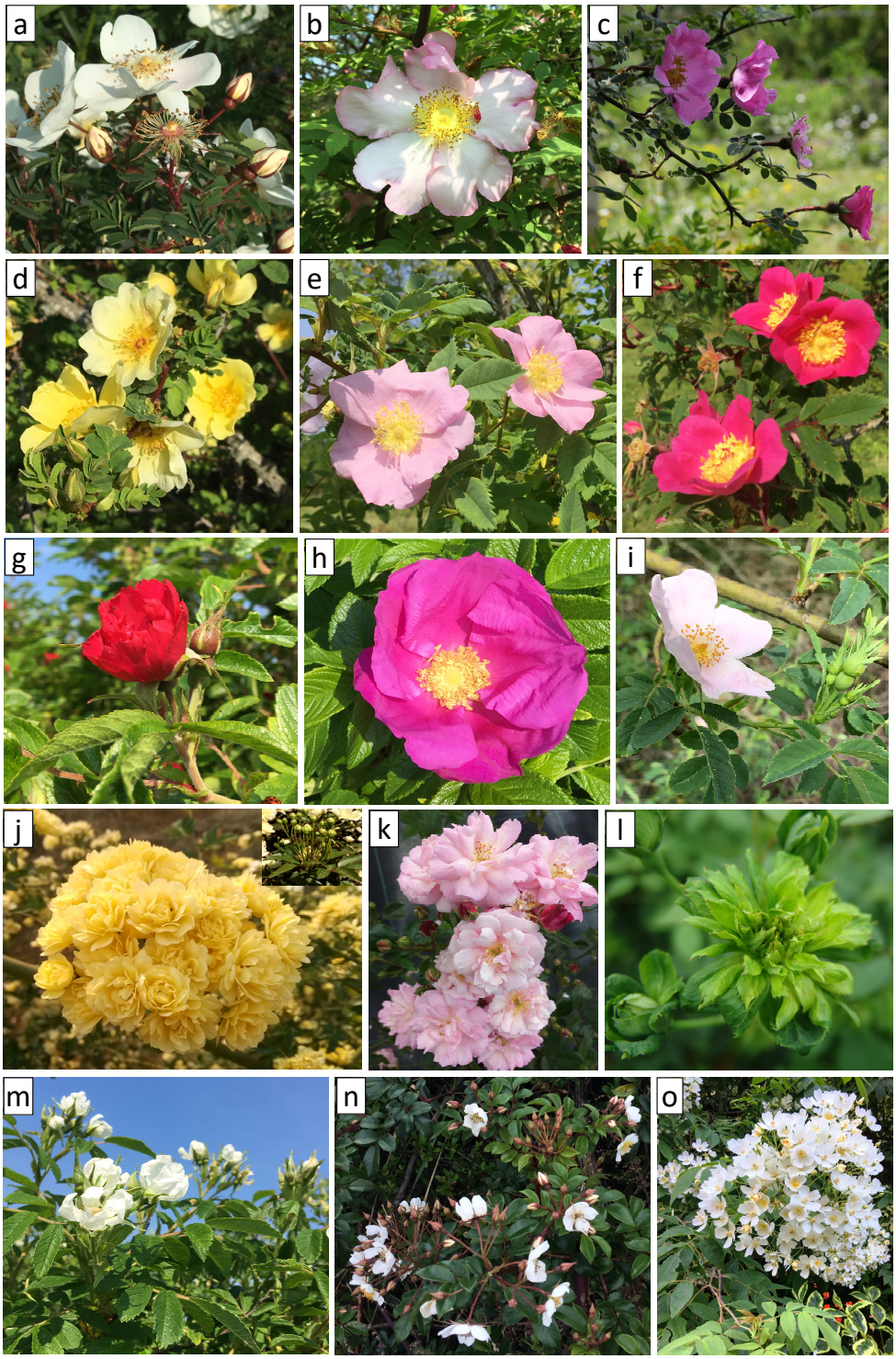

Figure 10: Diversity of Inflorescences and flowers in roses. (a) *R. pimpinellifolia* 'King of the Scots'; (b) *R. roxburghii hirtula*; (c) *R.praelucens* Byhouwer (d) *R. pimpinellifolia* lutea; (e) *R. laxa* Microcarpa; (f) *R. sherardi*; (g) *R. iwara*; (h) *R.* × 'Grootendorst Supreme'; (i) *R. rugosa scabrosa*; (j) *R. macrantha*; (k) *R. chinensis* 'Old blush'; (l) *R. chinensis* f. viridiflora'; (m) *R. longicuspis*; (n) *R. banksiae* 'alba plena'; (o) *R. filipes* 'kiftsgate'. Credits: NN ZHOU, except o (floraekspres).

Flowers are generally solitary (Figure 10 a-f) or in a corymb (commonly consisting of flowers 2 $\sim$ 3 flowers (Figure 10 g-i and j), a few contain more than 10, e.g., *R. banksiae* 'Alba Piena' (Figure 10 j)), and a few in form a compound corymb (Figure 10 k-n) or panicle inflorescence (Figure 10 o). Wild rose flowers usually have five petals and five sepals, are imbricate, except for *R. mairei, R. morrisonensis, R. omeiensis, R. sericea, R. sikangensis and R. taronensis*, that only has four (Yu, 1974). Some wild variants have multiple petals, such as *R. praeluceus* and *R. banksiae*. Petal colors may be white, pink, red, yellow, and rarely green (eg. *R. chinensis* f.viridiflora, Figure 10 l), and the frequently observed gradient varies from white to pink or white to yellow, depending on the species. Sepals are arranged into two outer, two inner, and one middle sepal, with a the margin that is entirely or variously pinnately lobed, and they sepals usually bear high-density hairs and glandular trichomes or emergences. The understructure that carries petals and sepals is called the hypanthium (Figure 7 a and b), and may be globose, urceolate, or cupular and constricted at the neck. A disc is inserted at mouth of the hypanthium, and there are numerous stamens in several whorls inserted in the disc (Figure 7 a). The numerous carpels (there are rarely few) are free (i.e., not fused together in a single ovary), inserted at the margin or base of the hypanthium. Styles are terminal or lateral, exserted or not, free or connate in the upper part (Figure 7 a) (Yu, 1974; Gu and Robertson, 2003).

1.3.2 The history of rose breeding and application in human society

Roses have always been greatly appreciated at different periods of history and in many different civilizations. Rose domestication is usually related to the most prosperous periods of history. As of this time, more than 33,000 roses have been created (Young et al., 2007) and roses have been the most economic important ornamental plant in the world.

1.3.2.1 Ancient rose domestication and human selection

Little archaeological evidence of rose cultivation has been found. Rose seeds along with other fruits and nuts, including Corylus, Pyrus, Crataegus, and *Rubus* were found at a formally inhabited site of the early Neolithic (5000 B.P.) near Swifterbant in the Netherlands (Zeist and Palfenier-Vegter, 1981). Humans may have intentionally gathered rose fruit for food. Possible rose seeds have also been described at sites in Switzerland (3500 B.P) and in Britain (Renfrew, 1973; Widrlechner, 1981).

The origin and domestication of rose are always topics of debate for scientists (Hurst, 1941; Widrlechner, 1981; Tucker, 2004; Wang, 2005; Chwalkowski, 2016; Bombarely, 2018; Debray, 2020). Although it is reported that the oldest known historical evidence of rose dates back to the Minoan civilization (Hurst, 1941; Widrlechner, 1981; Tucker, 2004; Ministry of Culture and Sports, 2007; Debray, 2020), this assumption is extremely weak if we carefully analyze the evidence, the restoration of "The Bluebird Fresco" ($\sim$ 1450 B.C.) by Émile Gilliéron (Figure 11). In the photo, the flower, described as a rose, has six petals, whereas roses have usually five and rarely four petals. Even if there is a debate concerning the number of petals since Tucker (2004) mentioned that the 6th petal was added during the restoration, we can still deny that hypothesis on the basis of the characteristics of the bud or fruit (not clear from the photo), the plant posture and the leaves.

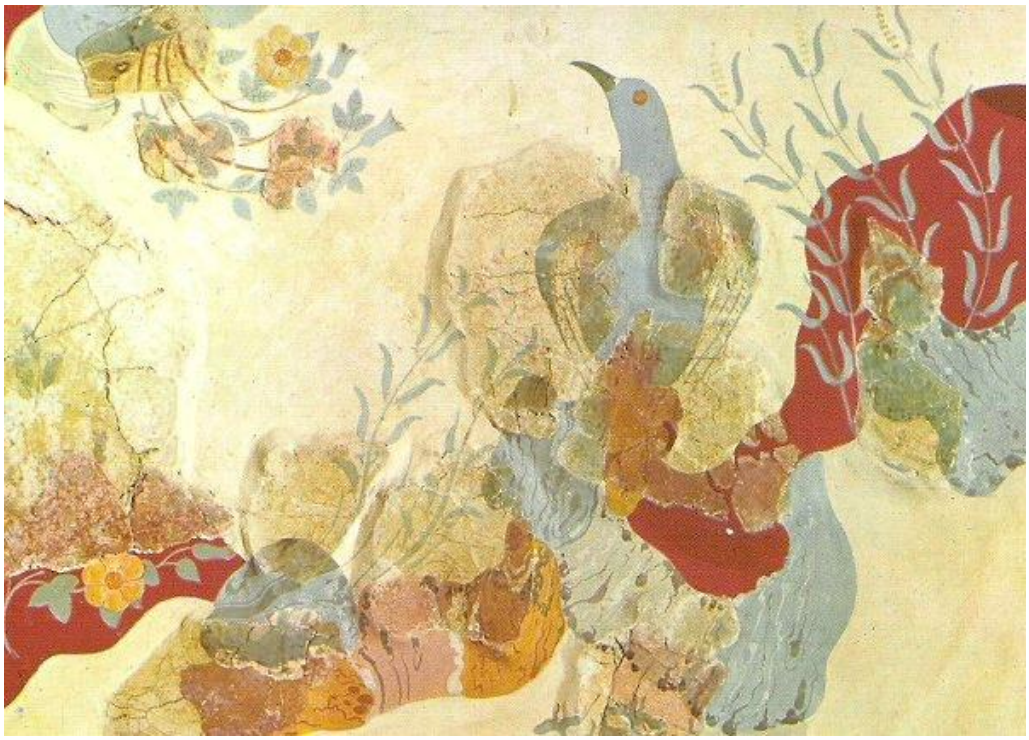

Figure 11: The blue bird fresco (detail from a modern reproduction by Émile Gilliéron fils) from the House of Frescoes at Knossos, Late Bronze Age (∼ 1450 B.C.); Paintings on wet lime plaster, H. 60cm, Heraklion Museum of Crete, Greece.

As we described in the previous section, rose flower buds have a hypanthium structure that holds the petals and sepals during the flowering period and from which the fruit develops at the end (Figure 7), but it is clear that the flower in the photo does not have a hypanthium like roses. The number of leaflets of the compound rose leaf is rarely three and the leaves are usually alternating (Figure 9), not opposite (Figure 11). Taking a step back, five-petals is not a specific characteristic for the genus *Rosa*, since many other plants have five petals, including roses. Hurst (1941) suggested that the painted flower is a natural *R.* × *richardii* hybrid between *R. phoenicia* Boiss and *R. gallica* L., whereas these species are much too different compared to the painted flowers. Tucker (2004) argues that it is more similar to *R. pulverulenta* (syn. *R. glutinosa*) based on the 3-leaflets leaves on flowering shoots and the distribution of its current cultivation, but this species also has five-leaflets and major differences with the flower in the photo. In conclusion, the nature of this painted flower is still a source of debate.

In China, roses were bred for ornamental purposes, with a history that goes back more than 1500 years. According to the records, there are three names for roses in Chinese, 'Qiángwēi', 'Méigui', and 'Yuèjì', and these names are still used today. 'Qiángwēi' generally refers to wild roses; except for *R. rugosa*, *rugosa* varieties and hybrids, which referred to as 'Méigui'. 'Yuèjì' refers to the roses that can bloom every month. Many poems have highly praised the roses because of their scent, different colors, beautiful posture, and blooming in four seasons. A rose with bright-red petals and a light fragrance was described in the poem 'Yǒng Qiángwēi shī' by Xiè Tiǎo (464 - 499). He described the gradient of colors from purple-red to bright red from bud and bloom, with new flowers that bloom at the same time as the old ones (may fruit) on the

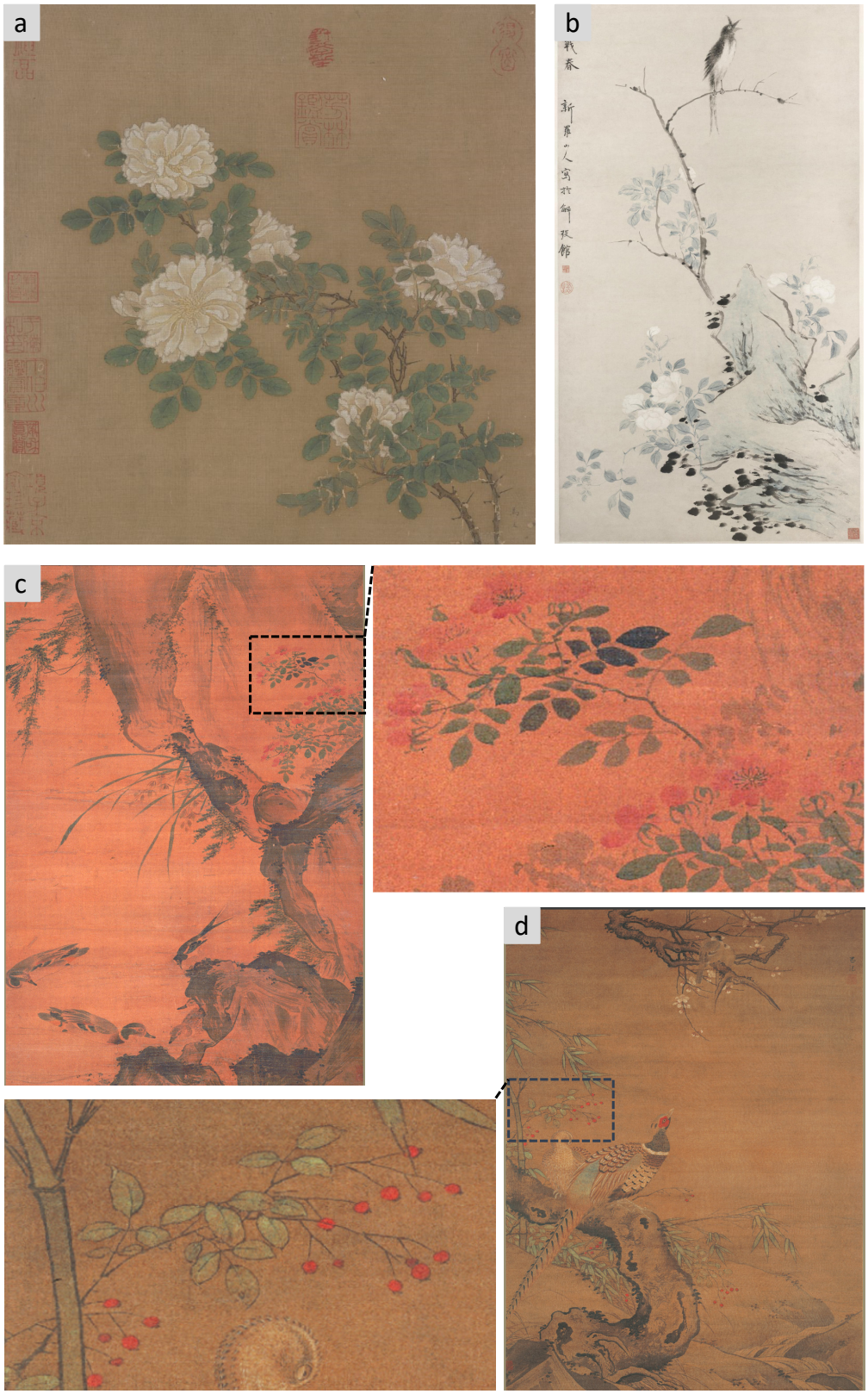

Figure 12: Continued on the next page

Figure 12: Chinese old garden rose paintings throughout history. (a) 'Bái qiángwéi tú', Chinese Silk Painting; Painter: Mǎ Yuǎn (1160-1225 BC), Song Dynasty; Texture: Silk; Size: 26.2cm x 25.8cm; Collecting of the Palace Museum in Bejing, China. (b) Qiángwēi shān niǎo zhóu, Chinese Handscrolls; Painter: huá yán (1682-1756 BC), Qing Dynasty, Kangxi mark; Size: 127.1cm x 55.5cm; Texture: paper; Collection of the Palace Museum in Bejing, China. (c) Yùfú túzhóu and Shuāngzhì Túzhóu (d) Chinese Silk Painting; Painter: Lü Jì (1477-unknown), Ming Dynasty; Size: 153.4 cm x 98.3 cm (c); 128.4 cm x 84.9 cm (d); Texture: Silk; Collection of the Shanghai Museum. (e,f,g) Falangcai ('foreign color') vase, Chinese porcelain, Qing Dynasty, Qian long enamel mark and period (1736-1795 BC); Collecting in the Shanghai Museum. (h) Wucai shieryue huā huì wenbēi - Yuèjì, Chinese porcelain, Qing Dynasty Kangxi mark and period (662-1722 BC); Size: 4.9 cm x 6.7 cm; Collection of the Shanghai Museum. Description: Twelve flowers correspond to twelve months, and the Rose cup to November: 'Unlike a thousand other species that die out, this one alone blazes in red throughout the year.'

same plant. The habit of continuous flowering in rose (wirh red petals and prickles) was clearly described in the poem 'Yuèjì huā' by the poet Liú Huì (458-502). A number of poems about roses were written during the Tang Dynasty (618 - 907) and Song Dynasty (960 - 1279) and were passed on to later generations. To capture the fragrance, we know that people in the Song Dynasty made sachets from roses and carried to cover up body odors, based on the description in the poem 'Yù Méigui', by the poet Sòng Qí (998 - 1061). In the poem 'Yǐng zhōu dào zhōng xiàn cì Méigui huā', Xiàng An-shí (1129 - 1208) described an fragrance that belonged to a prickly rose that accompanied him passing the Yǐng-zhōu road on a snowy day in early spring. The Yǐngzhōu road may be in the Yǐngzhōu county of the Song Dynasty since the Xiàng An-shi lived nearby, and Yǐngzhōu is currently located in Zhongxiang county in Hubei province. The above poems were obtained by searching for the keyword 'Qiángwēi', 'Méigui', or 'Yuèjì' in the ancient Chinese poems included in the online "Han Dian" (`http://sc.zdic.net/`) and "Gu shi wen wang" (`https://so.gushiwen.org/`) sites. There are still many records describing roses in ancient Chinese books. The 'earliest records' and 'impact of human participation on the rose domestication' questions need to be studied with the participation of historians, linguists and botanists. The Ming (1368 – 1644) and Qing (1636-1912) dynasties was a heyday for porcelain development, and many flowers were painted on brightly colored porcelain, including roses (Figure 12). The paintings will help botanists, as a source for classification and tracing of the origin of rose traits based on ancient records. These records are useful information to speculate about the genetic background of ancient Chinese roses which are one of the most important ancestors of modern roses. From the late Qing Dynasty (1840) to Chairman Mao Zedong proclaiming the foundation of the People's Republic of China (1949), invasion and civil war never ceased in China, and rose breeding entered a period of stagnation. It was in this period that rose breeding in Europe was entering in the golden age (Liorzou et al., 2016). In Europe, roses were once integrated into the religious culture, and the prosperity and decline of rose planting are always associated with different religious cultures in different periods (Joret, 1892; Touw, 1982; Debray, 2020). A recent review of the history of rose culture in Europe was recently published by Debray (2020).

1.3.2.2 Modern rose selection

In the 18th century, the introduction of Chinese cultivars into Europe was a major landmark in rose breeding history. It changed the history of ancient European roses that can only bloom once or occasionally twice (Hurst, 1941; Joyaux, 2015). According to Joyaux (2015), *R. chinensis* may be the first Chinese rose brought into Europe. The evidence is based on a specimen under the name "Chineeshe Eglantier Roosen", which was grown by the Dutch botanist Gronovius in 1733, and probably brought back to Europe through the Dutch East India Company. This specimen looks like the *R. chinensis* var. spontanea (Rehd. Wils.) Yu Ku. Another Chinese cultivar probably originating from a nursery in Guangdong (Canton), was introduced into England in the late 18th century. This cultivar is called 'Yuè yuè fěn' in Chinese (which means 'blooming monthly with pink petals'), renamed *R. chinensis* 'Old Blush' or 'Parson's Pink China' in 1793 by the Colville Nursery. Concurrently, a red cultivar, called 'Yuè yuè hóng', meaning 'blooming monthly with red petals' in Chinese, was planted in Calcutta in 1789, and renamed *Rosa chinensis* var. semperflorens Koehne in Europe (Joyaux, 2015).

At the beginning of the 19th century, these Chinese roses were crossed with old European cultivated roses, and led to the creation of thousands of hybrids (1st generation of hybrids like the Bourbon or Noisette roses and 2nd generation like the recurrent blooming hybrid). In 1867, Jean-Baptiste André Guillot created the first hybrid tea rose, named *Rosa* 'La France', by crossing Chinese tea-type roses with a hybrid of unknown parentage, but 'Madame Falcot' is considered as a possible parent (Beales, 2002). The 'La France' ushered in a new era of modern roses. From that year on, several thousand of rose cultivars were created and the industry flourished worldwide (Joyaux, 2015). Genetic analysis reveals that during this important breeding period in Europe, the genetic background of cultivated roses has shifted from an old European genetic background to a Chinese genetic background (Liorzou et al., 2016).

Rose breeding objectives depending on the markets

Currently, roses are major ornamental plants with an important economic value, a wide diversity and diverse application forms, including cut roses, garden roses, roses for urban beautification, house roses in small pots, roses for essential oil, rose teas and roses for culinary purposes. The breeding target of roses is different depending on their application form, and breeding requires different environments for varietal testing.

Cut roses The global market for cut flowers was estimated at 29.2 billion USD in the year 2020, and is projected to reach a revised size of 41.1 billion USD by 2027, growing at a CAGR of 5% over the analysis period 2020-2027. The rose industry is projected to reach 14.3 billion USD by the end of the analysis period (5.8% growth annually) (ReportLinker, 2020). The cut rose industry involves multiple processes, including rose breeding, variety field testing, propagation, promotion, efficient cultivation, post-harvest processing, transportation logistics, wholesale and retail marketing, etc. For breeding, the main companies are historically located in European countries, especially in France and the Netherlands, and still occupy an important share of the market today. From planting to sales, the Netherlands currently has the most complete production system and the world's largest action market. However, due to costly labor and energy requirements in Europe, European companies are gradually shifting their production bases to areas with low-cost labor and favorable climates (temperature and photoperiod) such as Africa (Kenya), South America (Ecuador, Colombia) and Asia (China, India) (Leus et al., 2018). Production centers are far away from the trading centers and the products earmarked for the consumer require more transfer and packaging, which greatly promotes the development of cold chain transportation. The tolerance of cut roses to storage and transportation is one of the most important factors to assess the market recognition of cut rose cultivars. Tolerance of rose to transportation helps the product maintain freshness and avoid premature withering during the marketing process. Therefore, vase life has become an important trait to assess the quality of cultivars and for breeding, and many factors affect vase life, such as genetic factors, pre-harvest and post-harvest conditions, storage and transportation, etc. (Mortensen and Fjeld, 1998; Marissen, 1999; Dahal, 2013). The number of prickles will undoubtedly largely affect transportation capacity and vase life since

removing prickles is an essential step before packaging. This process will inevitably cause branch injuries, with an impact on vase life. Moreover, the injured branches will decrease the ornamental value. Therefore, even if the market requires roses with exceptional ornamental characteristics (form, color, scent), and producers require roses with disease resistance, good yield and long vase life, the presence of too many prickles is not acceptable for cut roses (personal communication Arnaud Delbard, "Société nouvelle des Pépinières Georges Delbard").

Changes in the production area also promote the development of local breeding. For instance, the rapid development of cut flower production in Yunnan province (China) in recent years is remarkable. Benefiting from favorable climatic conditions and cheap labor, China's Yunnan is now one of the largest production areas for cut roses, and has developed the world's second largest flower auction market (Kunming International Flower Auction Exchange Center) (Xu and Wu, 2019). With the improvement of the laws protecting Plant Variety Rights (PVR), more and more companies and applied research institutes have begun to focus on cultivating new varieties of independent intellectual property rights and strive to carry out market promotion. The promotion and planting of new cultivars in Yunnan are mainly through the "company + production base + farmers" model. Using the radiation effect of the business management model, it was possible to convince growers in the region to adjust the product structure, thereby improving agricultural production efficiency and ensuring increased income for rose farmers. The new cultivars rapidly reach the market and provide substantial economic benefits for enterprises and farmers. The opinion of growers concerning the planting new cultivars has changed from passive acceptance to active demand. The gradual regulation of the payment of PVR fees has attracted international breeders to contribute new outstanding roses to China's market. The production of cut roses in Yunnan has developed from traditional, classic cultivars (single-head and cup-shaped flower buds) to more diverse ones (single or multiple-head buds, rich colors and diversity shaped flower buds). For rose breeders, the market is full of challenges and opportunities and constitutes new area for rose breeding in China (personal communication with Prof. Qi-Gang Wang (FRI, Yunnan Academy of Agricultural Sciences, Kunming, China)).

Garden roses Garden roses have the most abundant application form, but their market is much smaller than that of cut roses. The garden rose market still has much room in which to expand. Floribundas and flowers (color, type, perfume) are important selection traits. However, disease resistance and the absence of prickles are definitely the most important traits that require improvement. Black spot disease (BSD), caused by the hemibiotrophic fungus, *D. rosae*, is responsible for the presence of round dark spots on leaves, followed by chlorosis and premature defoliation of the host, thus reducing the aesthetics of the host (Blechert and Debener, 2005; Gachomo et al., 2006). Prickles and other spinescent structures make the plants difficult to plant in gardens or urban greening areas because of their safety risks. Indeed, prickles may cause diseases by infection resulting from stabbing injuries, (Vincent and Szabo, 1988; Fahal, 2004; Halpern et al., 2007; Cruz et al., 2007; Barros et al., 2011; Vásquez-del-Mercado et al., 2012; Kieselova et al., 2017; Frothingham, 2019). Thus, for cultivars with the same ornamental value, those with no or only very few prickles may be more popular for using in public urban greening areas. Garden roses with no prickles will provide growers

with more choices.

Indoor roses Roses used as houseplants are mainly miniature type of roses. Miniature roses have become more and more popular in recent years especially in cities, since people have progressively less room (or even room at all) to cultivate plants. Thus, the first breeding target of indoor roses is to change them into smaller than usual species by selecting miniature plants or plants that respond to regularly used plant growth retardants (such as paclobutrazol and chlorocholine chloride). The producers require rose varieties with many flowering branches and a good level of resistance to diseases. Due to insufficient sunlight and ventilation in the room, and because the root system is trapped in the flowerpot, the maintenance of indoor roses is much more difficult than that of garden roses. Spider mites and powdery mildew are always the biggest problems for growers. Benefiting from the high productivity of automated modern greenhouses, a new form of miniature rose was created for consumption in recent years. As for cut flowers, these miniature roses are produced quickly, $4 \sim 6$ cuttings that are assembled into a plastic flowerpot and sold after buds growth. These products are usually eliminated by the consumer after their first blooming.

Oils roses The cultivation of essential oil roses has a long history with applications that include cultural rituals, aromatherapy, perfumery, body care, ayurveda, flavoring and spiritual traditions (Apothecary, 2020). Rose oil is extracted from petals. It is an expensive, labor-intensive procedure that takes more than 4000 kg (around 1,600,000 rose blossoms) of rose petals to produce 1kg of 100% pure distilled rose essential oil (Lubbe and Verpoorte, 2011). Consequently, rose oil is one of the most expensive essential oils, and a kilo of good quality oil will fetch around 5000-7000 USD. Only a few species (mainly *R.damascena* and *R. centifolia*) are used to produce rose oil and rose absolute. *R. rugosa*, *R. alba*, *R. bourbonia* and *R. moschata* are also used to produce rose otto and rose absolute, but in limited quantities. The aroma of *R. damascena* is very rich, deep, sweet-floral, slightly spicy and honey-like. These roses are mainly grown in Bulgaria's Rose Valley and in Turkey. On the other hand, *R. centifolia* has an aroma that is rich, sweet, deeply floral, spicy, slightly honey, intensely rosy and somewhat woody, and is mainly grown in Morocco. The chemical compounds present in rose oils are different (Apothecary, 2020). The key fragrance compounds that contribute to the distinctive scent of rose oil, are *beta-damascenone, beta-damascone, beta-ionone*, and rose oxide, and the presence of a proportion of *beta-damascenone* is an important criterion for the quality of rose oil (Leffingwell, 1999; Khan and Abourashed, 2011). Even though these compounds make up less than 1% of rose oil, they contribute to more than 90% of the odor due to their low odor detection thresholds (Leffingwell, 1999). What should be mentioned here is that *beta-damascenone* does not naturally exists in roses. It is formed during distillation from precursors present in the petals. Therefore, the breeding targets for the rose oil industry are the scent components and the increase in plant productivity (number of petals, rose blossoms per plant, compound content, ability to emit scents etc.).

1.3.3 The high quality of rose genome sequences supports the study of roses at the omics level

1.3.3.1 Roses have a complex genome with different levels of ploidy and high heterozygosity

The genus *Rosa* (*Rosaceae*) has a base chromosome number of 7 (x = 7) (Täckholm, 1920; Hurst, 1925; Roberts et al., 2009; Jian et al., 2010b). The ploidy level of wild rose species ranges from diploid (2n =2x = 14) to decaploid (2n = 10x = 70) with almost all levels of even and odd ploidy with around half of the species being diploid. The highest level of ploidy (decaploid) were only found in *R. praelucens* , a critically endangered alpine rose with an extremely narrow geographic distribution in Northwestern Yunnan, China (Jian et al., 2010a, 2018). Its high level of ploidy may be due to inter-specific hybridization, but not directly to auto polyploidization (Jian et al., 2010a). Several intersectional hybridizations reveal the need to consider the genus *Rosa* as a hybrid system (Debray, 2020). For instance, the hybrid origin of *R. spinosissima* (syn. *R. pimpinellifolia*) is derived from a cross between *R. sect. Rosa* and *R. sect. Pimpinellifoliae*. Some individuals of the *Caninae* section are derived from *R. sect. Synstylae* and *R. sect. Rosa*. *R. marginata* is an intersectional hybrid between *R. sect. Rosa* and *R.sect. Caninae* (Debray, 2020).

1.3.3.2 Genetic resources: development of genetic maps from F1 crosses

Molecular markers are useful tools for assessing genetic diversity and for mapping studies. In roses, several genetic maps have been built with microsatellites or simple sequence repeats (SSR), amplified fragment length polymorphism (AFLP) markers, restriction fragment length polymorphism (RFLP) markers, sequence specific amplified region (SCAR) markers and nucleotide binding site (NBS) markers, mostly in diploid crosses (Debener and Mattiesch, 1999; Crespel et al., 2002; Yan et al., 2005; Dugo et al., 2005; Linde et al., 2006; Hibrand-Saint Oyant et al., 2008; Terefe and Debener, 2011). Genetic maps from four different populations (Yan et al., 2005; Linde et al., 2006; Shupert et al., 2007; Remay et al., 2009) were firstly integrated into a consensus map by Spiller et al. (2011), based on four diploid populations and more than 1000 initial markers. This integrated consensus map comprises 597 markers that are distributed over a length of 530 cM on seven linkage groups (LGs). Then later, high-density SNP (single-nucleotide polymorphism) maps were developed and used for anchoring and ordering the rose genome sequences (Hibrand-Saint Oyant et al., 2018). These genetic maps were used for genetic mapping and QTL studies in rose stem prickles (Zhou et al., 2020) and black spot disease (Lopez-Arias et al., 2020).

Next-generation sequencing facilitated the creation of transcriptomes and large numbers of SNP markers. Using the 68K WagRhSNP array, ultra-dense genetic maps have been produced in diploid (Hibrand-Saint Oyant et al., 2018) and tetraploid rose (Vukosavljev et al., 2016; Bourke et al., 2017) populations. In diploid rose, two genetic maps, female and male, were built using 151 hybrids obtained from a cross between *R. chinensis* 'Old Blush' and a hybrid of *R. wichurana* (OW). There were 5635 and 2331 SNPs for seven LGs of the female and male genetic maps, respectively, which contained 556 and 427 unique loci with a map density of 0.87 and 0.9 markers/cM, respectively (Hibrand-Saint Oyant et al., 2018). In tetraploids, SNP array data

currently provides the clearest information on the allele dose of markers. Using the dosage of SNP markers, tetraploid SNP genotypes can be used for linkage analysis with dedicated polyploid mapping software such as TetraploidSNPMap (Hackett et al., 2017) or polyMapR (Bourke et al., 2018c,b). One genetic map was developed using 151 hybrids of the K5 rose population (a cross between the cut roses cultivars 'P540' and 'P867') (Bourke et al., 2018b), including 25,695 SNP markers (not unique positions). Another map was built using 177 hybrids obtained from a cross between garden rose cultivars 'Red New Dawn' and 'Morden Centennial' (Hackett et al., 2017). In addition, 96 diverse tetraploid garden rose genotypes were using for the genome-wide association study (GWAS) of certain traits in roses, such as of the anthocyanin and carotenoid contents of rose petals (Schulz et al., 2016), the number of rose petals and prickle density (Hibrand-Saint Oyant et al., 2018), root formation in vivo and in vitro (Nguyen et al., 2020a) and callus formation (Nguyen et al., 2020b).

1.3.3.3 Rose has now entered the area of genomics studies

The first rose genome was released from wild and heterozygous *Rosa multiflora* (Nakamura et al., 2018). However, the quality of the genome was low, with 83,189 scaffolds. Soon afterward, two high-quality genome sequences were published both by sequencing a doubled haploid line from *R. chinensis* 'Old Blush' (Hibrand-Saint Oyant et al., 2018; Raymond et al., 2018) .

Hibrand-Saint Oyant et al. (2018) used PacBio long-read sequencing, and obtained a total genome length of 512 Mb haploids. These sequences were corrected with Illumine short-read sequencing technologies and anchoring to a high-density genetic female and male maps, which was developed from a diploid OW population, as mentioned in the previous sub-section. Finally, the doubled haploid rose genome assembly was anchored to seven pseudo-chromosomes containing 512 Mb with N50 of 3.4 Mb and 551 contigs (the N50 is defined as the sequence length of the shortest contig at 50% of the total genome length). A total of 95% of the sequence is contained in only 196 contigs. The length of 512 Mb represents 90.1 $\sim$ 96.1% of the estimated haploid genome size of rose. The genome includes 39,669 protein-coding genes and 4,812 non-coding genes. Evidence of transcription was found for 87.8% of a total 44,481 predicted genes. The predicted non-coding genes included 99 microRNA, 170 small nuclear RNA, 186 ribosomal RNA, 384 small nuclear RNA, 751 transfer RNA, and 3,222 unclassified genes (annotated as non-coding RNA) with evidence of transcription but no consistent coding sequence.

Raymond et al. (2018) also used PacBio long-read sequencing and assembled a total length of 515 Mb with 82 contigs for an N50 of 24 Mb. The seven pseudo chromosomes were built by integrating 86.4% of the 25,695 markers (not all unique positions) of a tetraploid K5 high-density SNP genetic map (Bourke et al., 2017), which was developed from a cross between the cut roses cultivars (Koning-Boucoiran et al., 2012). From an evolutionary point of view, rose is a very interesting model species as it includes species at several ploidy levels as well as having a rich phenotype and a broad genetic diversity. However, owing to the highly heterozygous character, the assembly of a rose genome is always a challenging task, which has greatly limited the progress of related research in rose. The completion of these two high-quality genomes

is a starting point that has propelled rose into the area of genomic (Smulders et al., 2019). Both are publicly available at the GDR (Jung et al., 2019) website.

1.4 Rationale/issues and thesis objectives

Economic issues

In the agricultural production process, prickles are an undesirable trait, not only in rose but in most crops in general. Roses are among the most popular and economically important horticultural crops, especially cut rose cultivars. Cut roses with prickles are more difficult to handle, harvest and transport, and also constitute safety hazards for consumers and workers. In addition, the tolerance of rose cultivars to storage and transportation is one of the most important factors to assess the market recognition of cut rose cultivars since they are important factors that affect vase life. Prickles on the stem will undoubtedly considerably affect transportation capacity and vase life since removing them is an essential step before packaging. This process will inevitably cause branch injuries, with an impact on vase life and a decrease in ornamental value. Thus, cultivars with no or very few prickles are in high demand from producers and breeders. Further studies are necessary to develop markers for breeding selection and to identify the molecular bases. In the General Discussion, I will elaborate on how the availability of markers can be used in rose breeding in general and to obtain dedicated roses without prickles.

Scientific issues

Prickles are sharp appendages of plants that was thought to be a defense against insect and mammalian herbivores. Many studies have been carried out concerning on their ecological, evolutionary and biogeographic implications, but the histological origin, genetic and molecular mechanisms underlying prickle initiation and development remain largely unknown. A wide diversity of prickles is present in roses. With the recent development of genetic and genomic resources, rose can be a good model to study the molecular and genetic bases of prickle initiation and development. Our objectives are to decipher the genetic and molecular control of prickle initiation by studying the morphology, genetic determinism, and gene network (at the transcriptomic level) of stem prickles in roses. Through this project, we expect to build a genetic model system for studying prickles and to open new research areas in the plant sciences. We have developed histological, genetic and genomic approaches.

In Chapter 2, we investigated prickle types in wild species and 'Old Blush' × *R.* × *wichurana* F1 progeny, and carried out a comprehensive anatomical study for two representative types of prickles. We hope to answer the following questions: What types of prickles exist in roses? Where do the prickles originate from? How do they develop? Which stage leads to prickle absence in glabrous plants?

In Chapter 3, we performed QTL analysis and anchored the SNP markers on the reference genome to determine the credible interval of prickle loci that control the presence and density of prickle on the 'Old Blush' genome. We studied the interaction of the QTL alleles to further discover the genetic background of prickles in the OW population. We used a candidate-gene approach to characterize rose gene homologues known in *Arabidopsis*, involved in trichome initiation to test the relationship between prickles and trichomes. Through those studies, we expect to address the following issues: Which loci control the absence/presence of prickles on the rose stem? Which loci impact the prickle density? Do rose prickles share a similar gene network with trichomes?

In Chapter 4, we used a transcriptomic approach to decipher the gene network that controls prickle initiation and later development. We compare the transcriptome of glabrous and prickle shoots at different stages (from initiation and late developmental stages). We explore potential good candidate-genes that are involved in cell fate, cell proliferation, cell differentiation, cell division and cell cycle that are highly associated with prickle initiation. We highlight the best potential regulators of prickle formation by combining the transcriptomic results with genetic studies (Chapter 3). Through these studies, we hope to answer the following questions: Which genes are involved in prickle initiation? and which genes are involved in prickle development?

Experimental design and Results

The materials, methods, experimental design, and results will be displayed in details in each article of this thesis. The results part is divided in 3 Chapters corresponding to 3 articles. The second one has been accepted for publication in Theoritical and Applied Genetics.

2 Morphological studies for rose prickles provided new insights

Zhou N N[1,2], Simonneau F[1], Thouroude T[1], Hibrand Saint-Oyant L[1*] & Foucher F [1*]

1 Univ Angers, Institut Agro, INRAE, IRHS, SFR QUASAV, F-49000 Angers, France.

2 National Engineering Research Center for Ornamental Horticulture; Flower Research Institute (FRI), Yunnan Academy of Agricultural Sciences, Kunming 650231, China.

* both authors contributed equally to the work.

Corresponding author: zhouning1116@aliyun.com

Key message: Rose prickles originate from multiple cells of the ground meristem under the protoderm. It gave in majority non-glandular prickles (NGP) and some glandular prickles (GP). For GP, the glands come from the epidermis (or protoderm).

2.1 Introduction

Prickles are common in plants (Bagella et al., 2019), with mainly knowledge of their function in defense against insects and large mammalian herbivores. The morphogenetic and molecular mechanisms underlying prickle formation and development remain still largely unknown. Although a few reports have described prickle's anatomical structure (Asano et al., 2008; Kellogg et al., 2011; Li et al., 2012; Angyalossy et al., 2016), their conclusions based on microscopic analysis of prickles in late developmental stages are regularly controversial and confused. The most common assumption is that prickles are originated from multiple cellular division of the epidermis (Peitersen, 1921; Esau, 1960; Canli and Skirvin, 2003). Prickles were considered as modified glandular trichomes, with lignification leading to a hard-sharp appendage (Coyner et al., 2005; Kellogg et al., 2011; Ma et al., 2016b; Khadgi and Weber, 2020a), because glandular and non-glandular prickles were considered as different developmental stages of the same prickle. Based on this hypothesis, in rose F1 genotypes with no-, low- and high-density of prickles, (Hibrand-Saint Oyant

et al., 2018) identified and studied the expression of candidate-genes presenting homology with genes from Regulatory Genes Networks, described for the initiation and development of trichomes in *Arabidopsis*. In addition, in *Rubus*, using a transcriptomic approach, a genetic mechanisms of prickles initiation was proposed with similarity with the one described for trichome initiation in *Arabidopsis* (Zhou et al., 2020). However, the origin tissues of prickle are not clearly identified in these studies, no anatomical evidence was provided to support the 'epidermis' origin. In a rose F1 progeny, glandular and non-glandular prickles were demonstrated to have their own developmental processes (Zhou et al., 2020). Therefore, in the absence of strong evidence concerning the relationship between prickles and trichomes, cautions should be taken regarding the conclusions.

Another hypothesis was that the rose prickles are spines, defined as modified leaves and lack internal vascular tissues (Asano et al., 2008). The authors proposed that the abscission cell layer of prickle resembles the abscission layer of deciduous leaves, with mature prickles easy to peel off with fingers. This conclusion was not supported by strong evidences. Li et al. (2012) suggested that cells in the prickle abscission region were different from cells of the petiole abscission zone by studying the anatomical structure and chemical composition of tender prickles.

Later, Angyalossy et al. (2016) defined prickles as "sharp outgrowths from the bark, without vascular tissue", based on longitudinal sections through the developed prickle of *Polyscias mollis*, *Piptadenia gonoacantha* and *Oplopanax horridus*. However, the "bark" term is unprecise as it refers to all tissues exterior to the vascular cambium, including a number of tissue types like periderm (composed of the cork, cork cambium, and the phelloderm), cortex (comprised of ground tissues), phloem and epidermis (Dickison, 2000; Evert and Eichhorn, 2006). In vascular plants, the apical meristem give rise to the protoderm, the ground meristem, and the procambium. The protoderm differentiates into the epidermis. Beneath it, the ground meristem and procambium differentiates into the ground tissue (the pith and cortex) and the vascular tissues (the xylem, phloem, and vascular cambium), respectively (Evert and Eichhorn, 2006). Therefore, the origin of prickles requires further investigations.

Wild roses belong to the genus *Rosa* in the family *Rosaceae*. The genus *Rosa* is composed of $\sim$ 200 species, widely distributed in cold temperate to subtropical regions (Rehder, 1940). Roses were always popular at different periods and in many civilizations. Today, rose is one of the most economically important ornamental plant in the world. Most roses have prickles on their stems. For cut roses production, removing prickle is an essential step before packaging. This process causes wounding on the stem, largely affect transportation tolerance and vase life, and also reduces the ornamental value. Rose cultivars with a lot of prickles are not accepted for cut roses even if they have other outstanding ornamental traits.

Roses will become a good model plant to study the molecular and genetic bases of prickle initiation and development. Prickles in rose are very diverse with different types, shapes, sizes, density, and colors. Several high-density SNP-based genetic maps from rose F1 populations (Vukosavljev et al., 2016; Bourke et al., 2017; Lopez-Arias et al., 2020; Zhou et al., 2020) and GWAS panels (Schulz et al., 2016; Nguyen et al., 2017; Hibrand-Saint Oyant et al., 2018; unpublished data from GDO team) have been used for genetic

studies. The recent production of two high-quality genome sequences (Hibrand-Saint Oyant et al., 2018; Raymond et al., 2018) allows genomics approaches.

For precise genetic and genomic studies, histological approaches are necessary to clearly differentiate the rose shoot structures and identify the tissue of origin of the rose prickle. In this study, our main objectives were to characterize histologically in detail the initiation and development of prickles in roses and to investigate their diversity in terms of form. The major questions are: (i) which types of prickles do exist in roses? (ii) which tissue do prickles originate from? and (iii) how do the prickles develop? A thorough understanding of prickle morphology and anatomical histology in roses will help us to well organize the experiment design for subsequent genetic and genomic studies, and will help to complete the limited data on prickles in roses.

2.2 Materials and methods

2.2.1 Plant materials

A diploid OW population, obtained from a cross between the female *Rosa chinensis* 'Old Blush' (OB) and the male *Rosa* × *wichurana* (RW), was grown in a field and managed by the Horticulture Experimental Unit (INRAE, Angers, France). We have selected three once-flowering individuals, OW9068, OW9137 and OW9106, to have vegetative branches. Those genotypes were cut and managed in IRHS greenhouses in November 2017.

Rosa resources were planted in Loubert Rose Gardens (Rosiers sur Loire, France), INRAE (Angers, France) and Flower Research Institute (FRI, Kunming, China). We have selected twelve representative genotypes to perform details analyses of the type and developmental stages of prickles: *Rosa ecae, Rosa laxa, Rosa sherardi, Rosa moschata, Rosa omeiensis, Rosa damascena*, *Rosa rugosa* scabrosa, *Rosa iwara,* 'Grootendorst Supreme', *Rosa rubella*, 'General Kleber' and 'Parkzauber'. For 110 genotypes (Table 2), we scored the type of prickles on the stems.

2.2.2 Macroscopy and microscopy

The experiments were performed at Plateform IMAC (SFR QuaSav, Angers). Fresh rose stems were photographed with STEREO-MICROSCOPE M205FA-LEICA.

2.2.3 Histology study

Sample dissection was done under microscope to remove the leaves. Various steps were performed:

• *Fixation at 4°C*: The samples were immersed in the 4% (v/v) glutaraldehyde solution mixed with 0.2 mol/L phosphate buffer at pH 7.2. The volume of the solution must be equal to 50 times the volume of the

sample. The sample were put under vacuum to remove air. The vacuum was broken every 4 minutes. After 2h of vacuum, the glutaraldehyde solution (4% v/v) is changed, the tubes are left 12h at 4 °C, then rinsed twice with phosphate buffer pH 7.2 and stored at 4 °C.

• *Dehydration at room temperature*: Samples are rinsed 3 times with distilled water, immersed in 50% (v/v) alcohol 10min, 70% (v/v) alcohol 10min, 90% (v/v) alcohol 10min, and 100% alcohol 15min, successively.

• *Pre-infiltration*: Sample are transferred in pre-infiltration solution (100° alcohol /Technovit® 7100 resin ((Heraeus Kulzer, Wehrhrim, Germany) (v/v)) at 4°C and under vacuum for 2h, then samples are stored for 12h at 4 °C.

• *Infiltration*: Samples are transferred to infiltration solution (dissolve 1 sachet of hardener I in 100 mL (Heraeus Kulzer, Wehrhrim, Germany) of Technovit® 7100 resin) under vacuum for 20 minutes minimum at 4 °C, and the tubes are placed for 12h at 4 °C.

• *Inclusion*: The samples are included using an inclusion solution (1ml of hardener II® (Heraeus Kulzer, Wehrhrim, Germany) and 15 ml of infiltration solution) and stored at 37 °C. The sections can be made after a week at 37 °C.

The samples were cut in 3 μm sections for anatomical observation using LEICA RM2165 Rotary Microtome. After staining with toluidine blue 1% (O'Brien et al., 1964), they are observed and photographed using an ergonomic system microscope LEICA DM1000.

2.2.4 Score the type of prickle on the 110 roses

Taxonomical nomenclature followed the one described in Yu (1974), Gu and Robertson (2003) and Masure (2013). Each species or hybrids was associated with the types of prickles that were previously determinate on the OW population and on the twelve representative roses

To characterize the prickle types on each species were collected based on photographs which are mainly taken from Loubert Rose Gardens (Rosiers sur Loire, France) and Flower Research Institute (FRI, Kunming, China). For some species, the conclusion is based on professional knowledge and experience, and the photographs online. All the roses and their origin are presented in Table 2.

2.3 Results

For the anatomical study, first, we performed a detailed analysis on individuals of the OW progeny (photography and histological studies) as the OW progeny will be studied in details in subsequent genetic and transcriptomic studies. Then, based on these observations, we performed a survey of prickle diversity on the genus *Rosa*, with a more precise observation on twelve representative genotypes.

2.3.1 Prickles types determination and anatomical study in OW population

2.3.1.1 Prickle types determination

In the OW population, both parents present prickles on their stems. A very clear separation of prickle traits (type and density) on stem was observed in the F1 hybrids. Based on the macroscopic analysis, we have previously determined three types of prickle on the stems of the OW progeny: (i) the "prickless" referred to the glabrous stems, (ii) the "non-glandular prickle (NGP)" without glands and (iii) the "glandular prickle (GP)" referred to the prickles with glandular head (Figure 13).

We selected three representative genotypes of each type of prickle for the morphological and anatomical studies (Figure 13):

* OW9068 is a genotype with glabrous stems.

* OW9137 has the most common type of prickles which are non-glandular, unbranched, slightly curved, gradually tapering to a broad base.

* OW9106 bears a mixture of prickles, NGPs and GPs.

Based on the macroscopic analysis, we determined three types of prickle on stem for the OW progeny: (i) the "prickless" referred to the glabrous stems, (ii) the "non-glandular prickle (NGP)" with non-glandular head and (iii) the "glandular prickle (GP)" referred to the prickles with glandular head (Figure 13).

2.3.1.2 Prickles development and anatomy

In OW9137 and OW9106, we observed that the prickle development is associated with the stem development, it means that the prickle appears early during stem development and prickles develop in parallel with the stem. No new prickle appears on developed stems. According to the specific morphogenetic events during its development, we defined different stages for the development of NGP and GP on rose stem (Figure 13).

Stage I is defined as the prickle initiation and the first outgrowth. The initiation appeares at the very early stage of internode development (probably simultaneously with the first internode, under the petiole (Figure 14 a, white dotted frame)). It appears later than the formation of leaf primordium. The first visible sign of NGP is the cell proliferation of multiple cells of the ground meristem (Figure 14 d). The rapid division of those cells causes an oblique rise to triangular (100$\sim$ 500 μm) which can be observed by macroscope (Figure 13a - stage PI and Figure 14 a). This process was absent in stems of the prickless genotype OW9068: no appendage was observed (Figure 13 c and Figure 15). For GP, 2$\sim$4 cells located at the first (and/or second) layers of the ground meristem firstly appeared to differentiate and to divide (Figure 14 m), they gave rise to a cylindrical bump (around 50 μm) (Figure 14 n; Figure 13 b - stage PI). Subsequently, on the upper part of this new structure, multiple cells of the protoderm (meristem that will give the epidermis) gave

the precursor gland cells (Figure 14 o). This is the main feature to distinguish GP from NGP: in GP, the protoderm (or maybe the epidermis) differentiated into glands cells; this differentiation is absent in NGP, where the protoderm (or the epidermis) only continues to grow by cell division.

In Stage II, both NGP and GP are continuously growing, coloring, and shaping, but the tissue remains juvenile (Figure 13 a and 13 b - Stage PII). The difference between GP and NGP is that the precursor gland cells of GP formed a new structure - glandular head, whereas no such a structure was observed at the tip of the NGP. We have divided stage II into three sub-stages:

For NGP, epidermal cells maintain normal cell proliferation during prickle development (Figure 14 g-l). In stage IIa, prickles are keeping upwards growth (Figure 13 a) due to covered under the unopened leaves. The anatomical analysis showed that the upper part cells (from up to down) of the prickle begin to enlarge (elongation process), suggesting that the cells gradually lose their division ability, while the cells of the lower part may still keep division (small cells) (Figure 14 g). These cell proliferation ability and cell division orientation may determine the prickle shape and the width of the prickle base in the later stages. In stage IIb, as the leaves open, the prickles are growing outwards (Figure 13 a - stage PIIb). The cells (from up to down) of the lower part of the prickle are gradually stopping proliferation and begin to enlarge and elongate, except the bottom part (Figure 14 h and i). In stage IIc, after the leaves are fully opened, prickles are almost fully developed and forming downward curved hooks (only for curved prickle) (Figure 13 a - stage PIIc). All the cells continue to elongate, and most cells gradually stop dividing at the end (Figure 14 j-l).

For GPs, their developmental stages are similar to NGP, except the development of the gland head (Figure 13 b; Figure 14 p and 14 r). The gland is usually surrounding by one cell layer and occasionally two cell layers (Figure 13), and occasionally two cell layers (Figure 14 o and 14 p). The division stopped at early stage IIa and then the cells only enlarge, thereby forming a glandular head (Figure 14 p and 14 r). The size of the glandular head only slightly increases during GP development ($100 \sim 150$ µm).

The NGP and GP enter stage III when they begin to lignify and gradually hardening (Figure 13 a and 13 b - stage PIII). An abscission layer structure-like is also formed (Figure 14 q). Thus, they are easy to be separate from the stem. At the end of this stage, the cells are full-enlarged and lignified. Stage IV is defined as death stage, the NGP and GP completely hardened, lose moisture and cell might die gradually (Figure 13 a - Stage PIV).

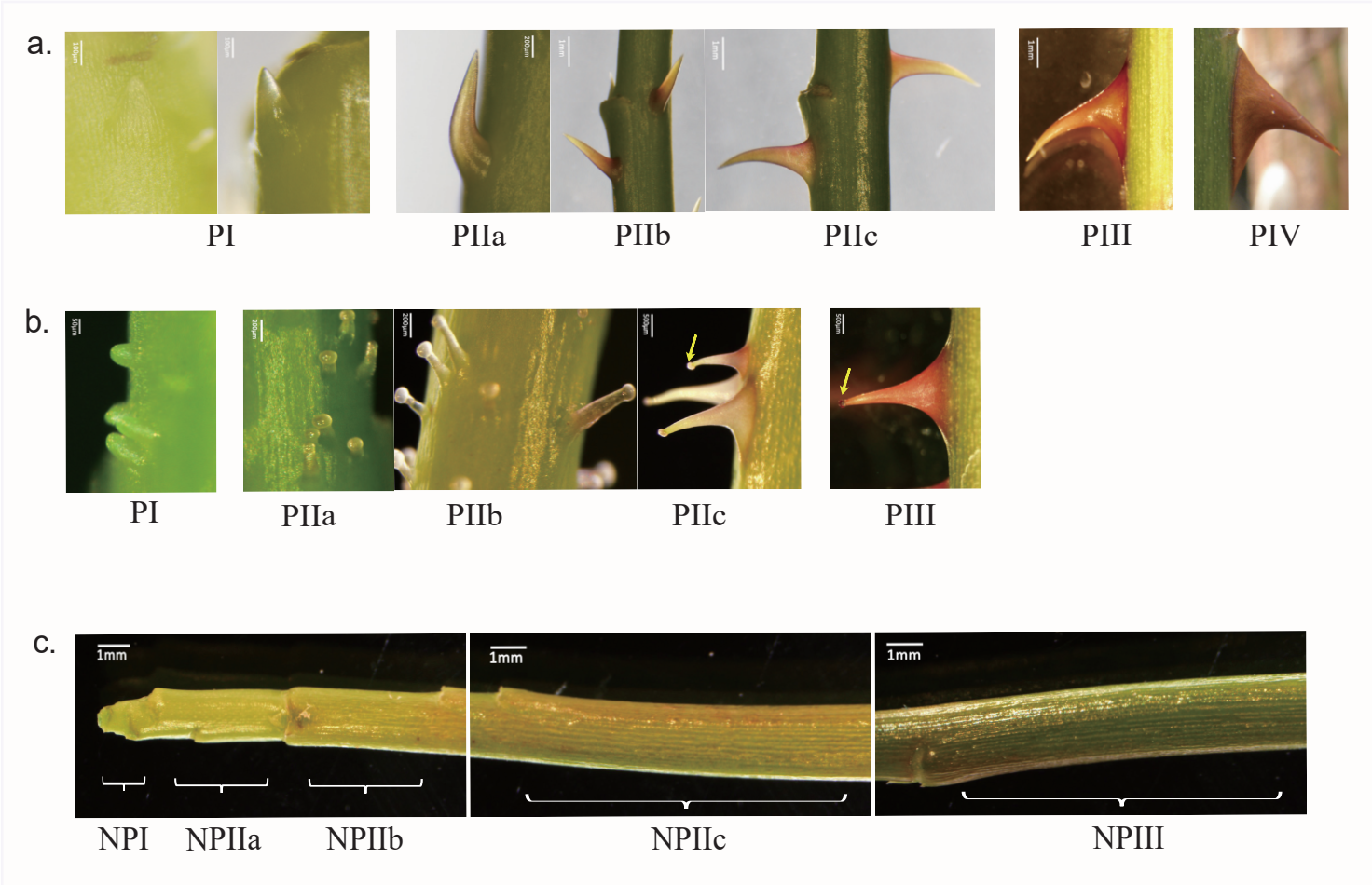

Figure 13: Developmental stages of non-glandular and glandular prickles in OW individuals. (a) non-glandular prickles (NGP, OW9137), (b) glandular prickles (GP, OW9106), and (c) glabrous stems (NP, OW9068). For the glabrous stems, the developmental stages correspond to the same developmental stages for the stem with prickles.

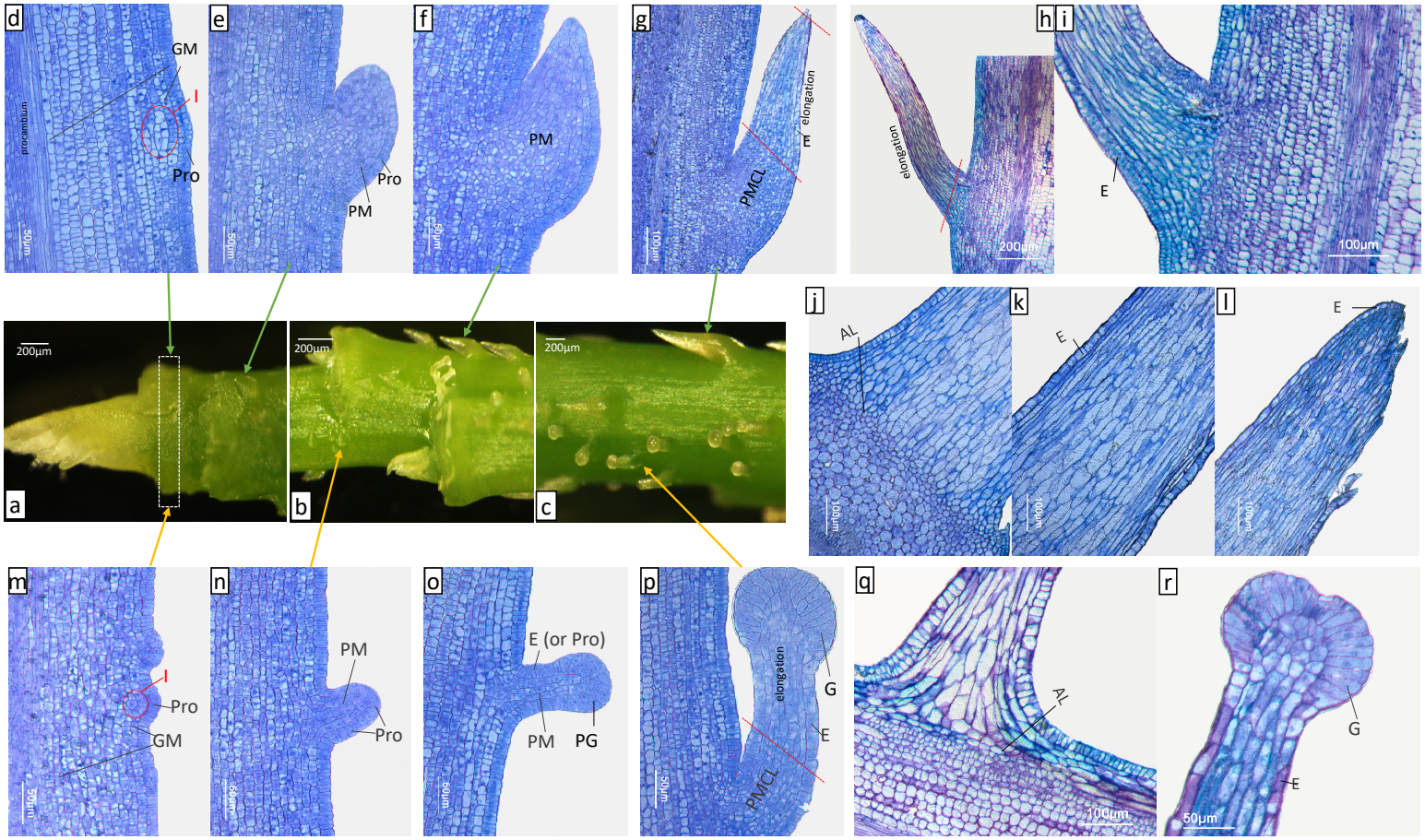

Figure 14: Anatomy of Non-glandular and glandular prickles in OW9106. (a-c) Macroscopic pictures of the different stages of GP and NGP on the stem; Anatomy of stage I (d-f), IIa (g), IIb (h and i) and IIc (j-l) of non-glandular prickle; Anatomy of stage I (m-o), IIa (p) and III (q and r) of glandular prickle. White dotted frame: the first internode; I: prickle initiation; Pro: protoderm; GM: ground meristem; PM: prickle meristem; PMCL: prickle meristematic cell like; E: epidermis; PG: precursor gland; G: gland; AL: abscission layer structure-like.

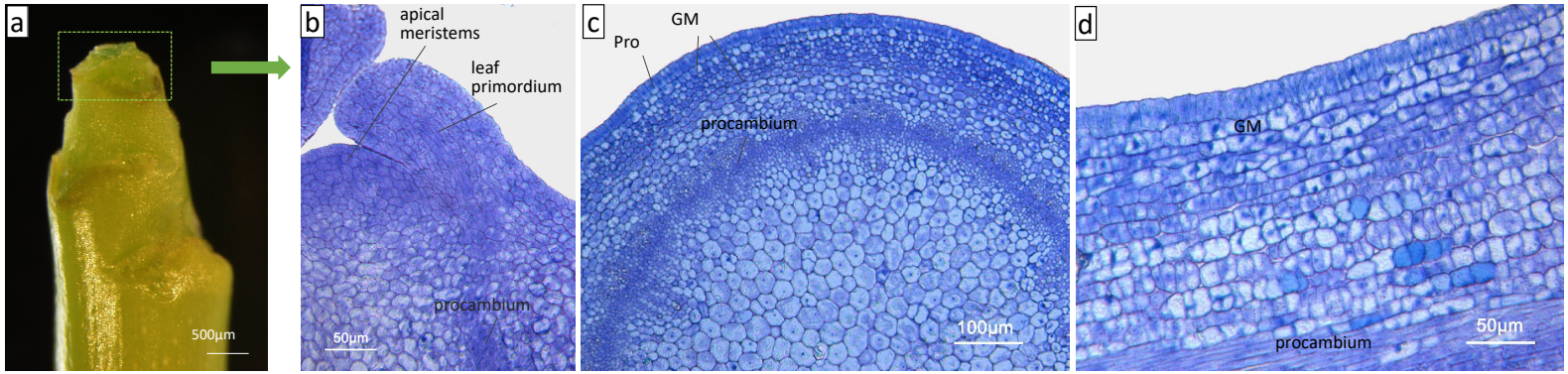

Figure 15: Anatomy of a prickless stem in OW9068. (a) Macroscopic pictures for prickless shoot tip; (b) Longitudinal sections of shoot tips; (b, c) Cross and longitudinal sections below the apical meristems, respectively. GM: ground meristem; Pro: protoderm; E: epidermis.

2.3.2 Discover different types of prickles in rose resources

To identify and describe the different types of prickles present in the *Rosa* genus, we conducted a statistical survey of prickle types in 110 wild rose species, varieties or ancient hybrids (Table 2, Figure 16). Twelve representative individuals (highlighted in pink in Table 2), which represent different sections of *Rosa* classification, were selected for morphological studies. According to the macroscopic observations, we classified the prickles into two general categories: glandular prickles (GP) and non-glandular prickles (NGP), as we previously did for OW individuals. The majority of roses present NGPs (98 out of 110), and all these NGPs are unbranched (Figure 16). Few unbranched NGPs are covering with hairs ("hairy") whereas the majority (91 out of 98) do not have ("naked"). Among the 98 wild roses with NGPs, 17 present unbranched GPs simultaneously which includes 13 naked and 4 hairy. 5 genotypes present only GPs which are branched and naked. 7 roses are glabrous but can sometimes be described with rare NGP (as we mentioned above in NGP categories). Now, I will describe the developmental process of different types of prickles through examples in rose resources.

2.3.2.1 Unbranched NGPs

For all the 98 wild roses that present NGPs, all these NGPs are unbranched.

Naked

No other appendage grows on the surface of the unbranched NGPs. They are the most common type which were observed in 91 roses out of 110. In the five representative genotypes (*R. ecae, R. sherardii, R. moschata synstylae*, and *R. omeiensis*, Figure 17, 18 and 19), the mature prickles have a large diversity in shapes, colors, sizes, and densities. We found that the early stage of development of the prickles in those species (except the bristles prickle, Figure 19 i-n) are similar to the one previous described for NGP (Figure 13 a - stage I and IIa). The primordial cells give rise to an oblique triangular structure (100 $\sim$ 500 μm) that keeps upwards growth. Then a large difference in shapes appears at the later stages. The size of the triangular structure in stage I is one of the important factors that decides the size of mature prickle. Prickle density is determined by the number of prickle initiation at early stage of shoot development and normally no prickle initiates at later stages (stage IIb and later). But there are slightly differences for prickle initiation in different genotypes. In *R. ecae* (Figure 17 a-e), *R. laxa* (Figure 17 f-i) and *R. omeiensis* (large winglike prickle, Figure 19 a-h), prickle initiation only happened at shoot tip; therefore, all the prickles are at the same stage on the same location of the stem. Their developmental stages are quite similar to the one previously described for the prickle of OW9137 (previous section). While in *R. sherardi* and *R. moschata*, prickle initiation happened not only at the shoot tip, but also appears on stages PIIa or PIIb in different parts of stem (Figure 18 b and 18 i). Prickle initiation can take place during a longer period, and the prickles that initiate later are relatively smaller at maturity (Figure 18 a-f, 18 h-k). Thus, location of initiation is other important factors that impact the density and the size of prickles present on the mature stem.

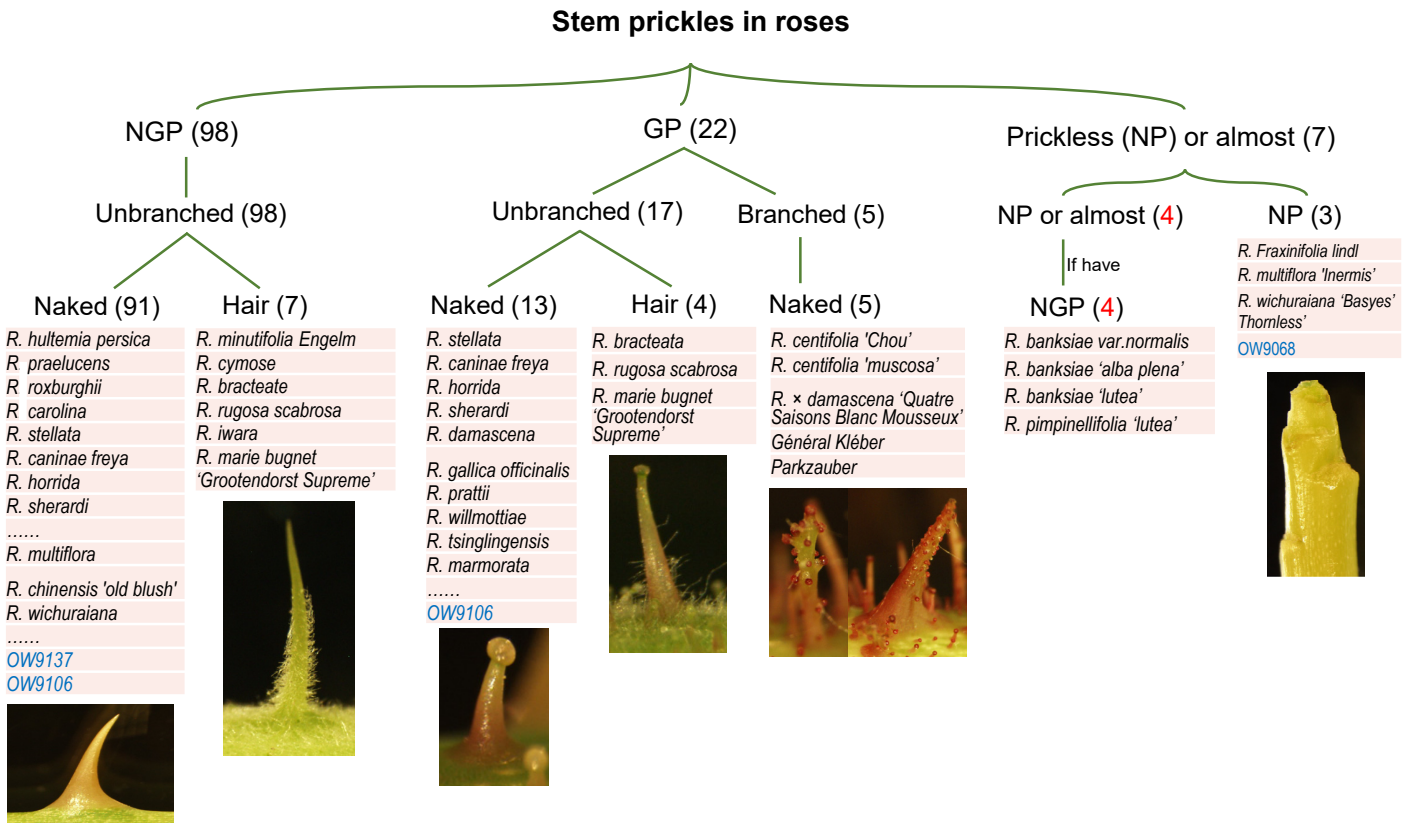

Figure 16: Different types of prickles in rose resources. The number of roses is presented in the brackets. The '4' in red means that 4 genotypes were sometimes prickless or sometimes have a few NGPs (*R. banksiae var.normalis* , *R. banksiae* 'alba plena', *R. banksiae* 'lutea', *R. pimpinellifolia* 'lutea'). OW individuals (showed in blue) didn't count in the number.

Hairy

Some unbranched NGPs are covered with hairs (non-glandular trichomes). Among the 110 genotypes, only seven have this type of prickles (Figure 16). These are *R. minutifolia* Engelm, *R. cymosa, R. bracteata, R. rugosa scabrosa* (Figure 20 a-g) and three hybrids of *R. rugosa* (*R. iwara* (Figure 20 h-q), 'Grootendorst Supreme' (Figure 20 r-v), 'Marie bugnet'). In *R. rugosa* scabrosa, hairs are present on the stem and on the prickles. On stem, a great density of hairs is present from shoot tip to developed part of the stem. The hair initiation is earlier than prickle's one, and they only appear on stems and not on the stage I of prickles (Figure 20 a). Later, during the prickle development, the lower part of the prickle present hairs, and the upper part is naked during all the stages. In R. iwara, the hairs appeared latter and at relatively lower density. Prickles and stems during stage I to IIb have no hair (Figure 20 h, 20 i and 20m) and clearly hairs appear at stages IIc (Figure 20 k and l).

2.3.2.2 Unbranched GPs

22 of 110 roses present GPs. 17 have unbranched with 13 "naked" and 4 "hairy" GPs. Five roses have branched and "naked" GPs (Figure 16).

Naked

No other appendage grows outside of the unbranched GPs surface. The developmental process and the origin of these prickles have been described in the previous section. We found that these prickles are generally not present alone in roses but always appear with NGPs (Table 2), as in the following species or varieties: *R. iwara* (Figure 20 n and 20 o), *R. stellate*, *R. caninae* 'freya', *R. horrida*, *R. rubella* (Figure 21 a-f), *R. damascena* (Figure 21 g-j), *R. gallica officinalis*, *R. prattii, R. willmottiae, R. tsinglingensis, R. marmorata, R. pimpinellifolia* 'king of the scots', *R. pimpinellifolia* 'aïcha' and *R. anemoniflora*.

Hairy

Unbranched GPs are covering with hairs (or trichomes). Very rare species (4) have this type of prickles. They are *R. bracteata*, *R. rugosa* 'scabrosa', 'Marie Bugnet' and 'Grootendorst Supreme' (two hybrids of *R. rugosa*) (Figure 20 t and 20 u).

2.3.2.3 Branched GPs

Branched GPs were only found only in five roses, *R. centifolia* 'chou', *R. centifolia* 'muscosa', *R.* × *damascena* 'Quatre Saisons Blanc Mousseux', and two hybrids 'Général Kléber' (Figure 22 a-f) and

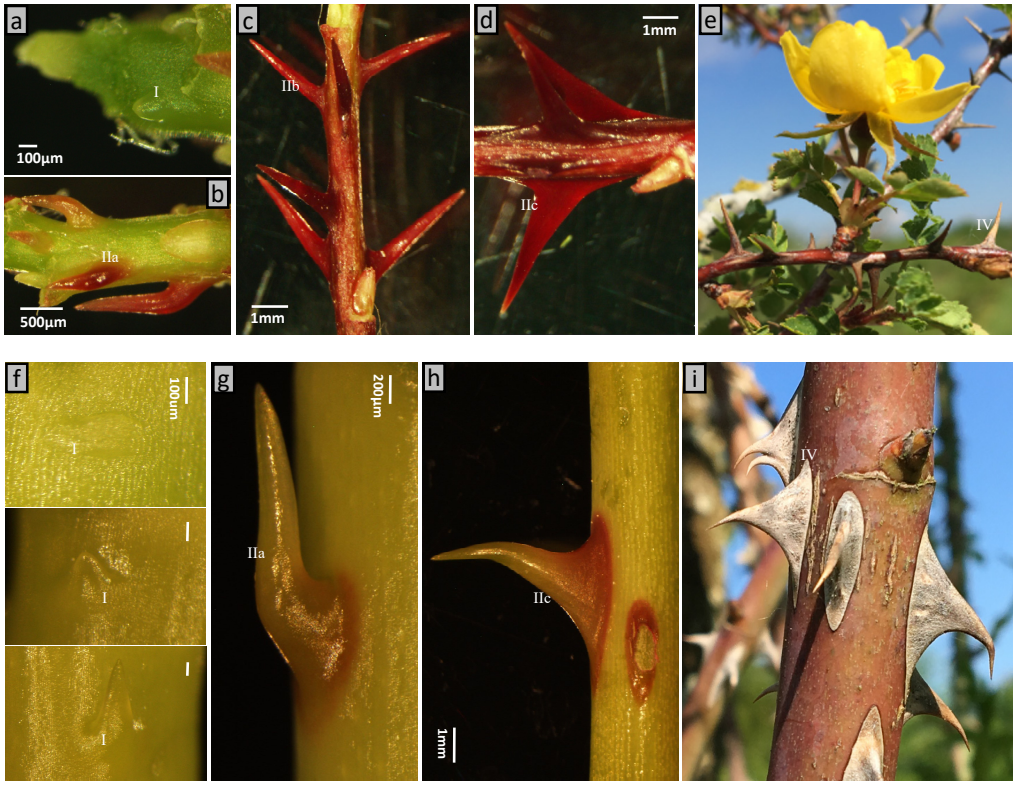

Figure 17: Non-glandular prickle development process in (a-e) *R. ecae* and (f-i) *R. laxa*

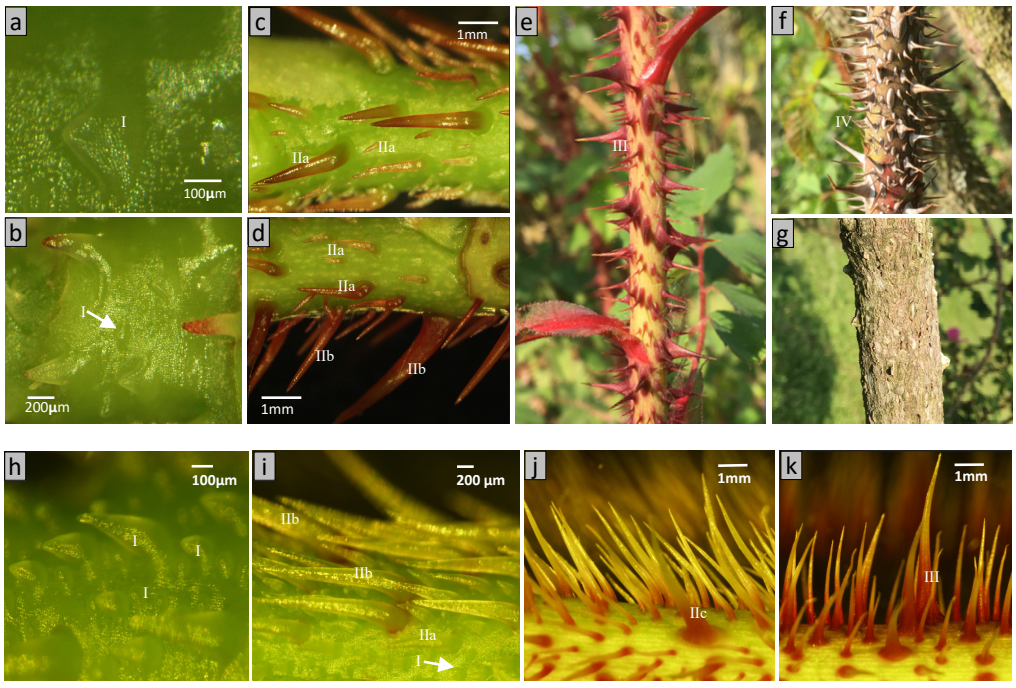

Figure 18: Non-glandular prickle development process in (a-g) *R. sherardi* and (h-k) *R. moschata* synstylae

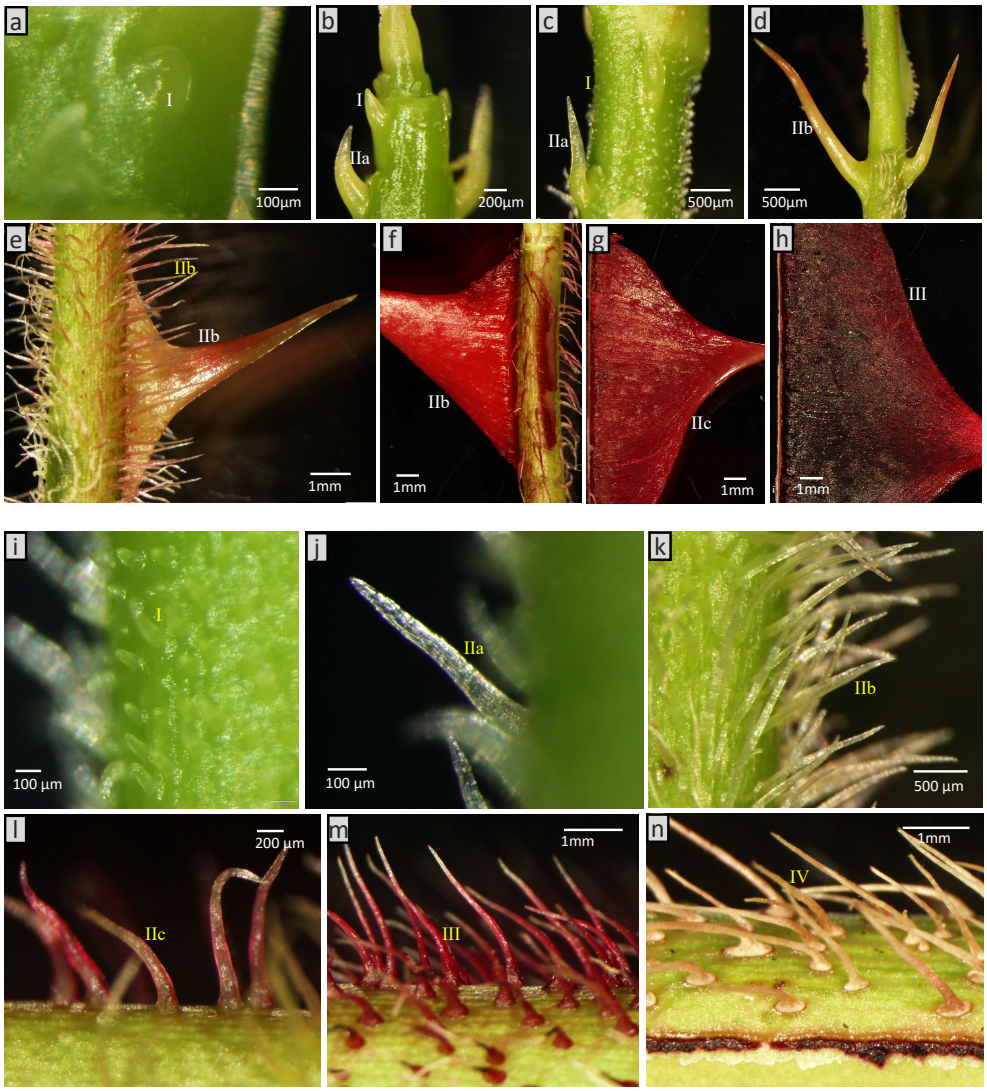

Figure 19: Non-glandular prickle development in *R. omeiensis*. The initiation of needle-like prickles (i-n) (bristles) is later than wing-like prickle (a-h).

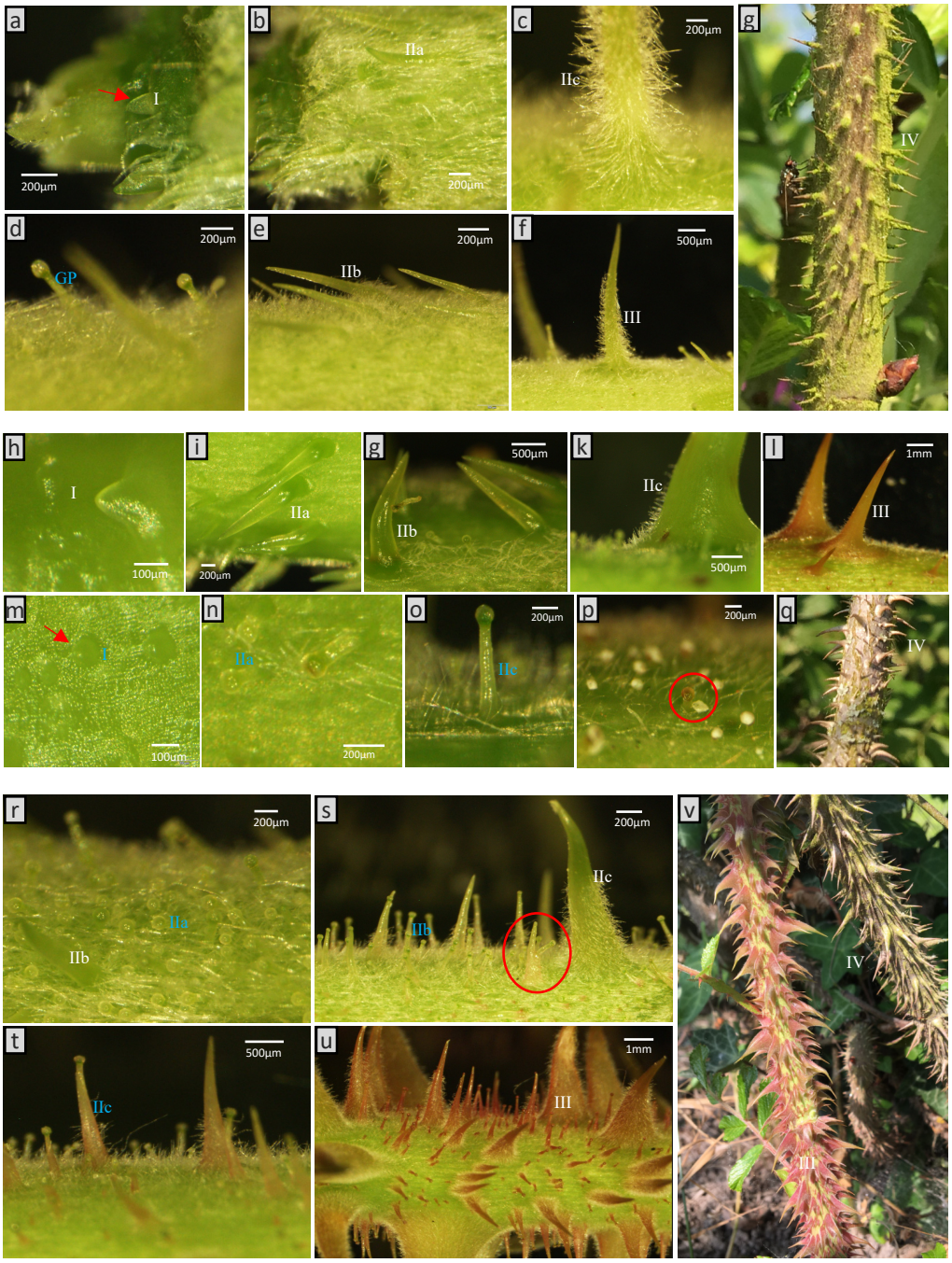

Figure 20: Non-glandular and glandular prickles development in (a-g) *R. rugosa* 'scabrosa', (h-q) *R. iwara* and (r-v) 'Grootendorst Supreme'

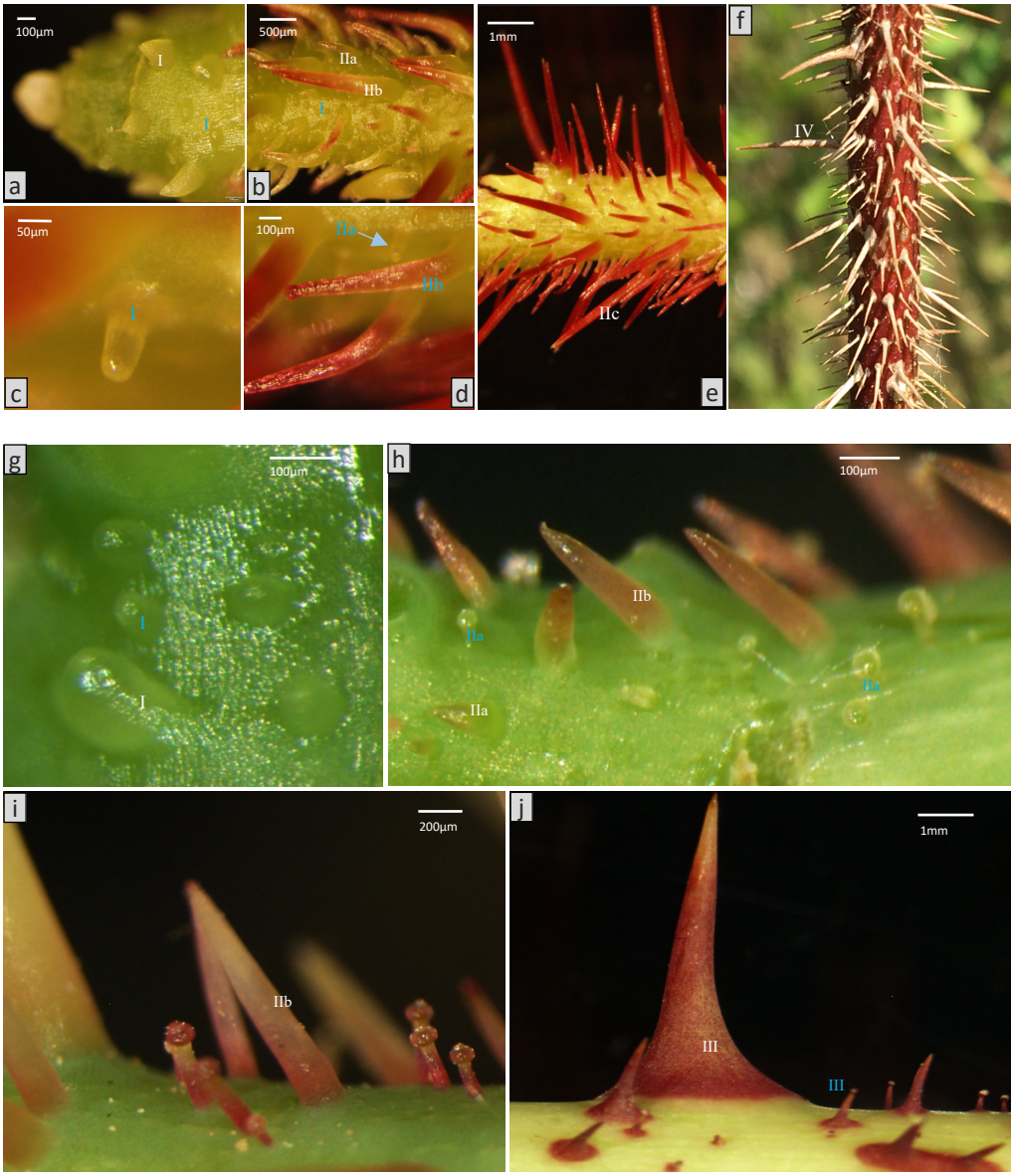

Figure 21: Non-glandular and glandular prickle development in (a-f) *R. rubella* and (g-j) *R. damascena*

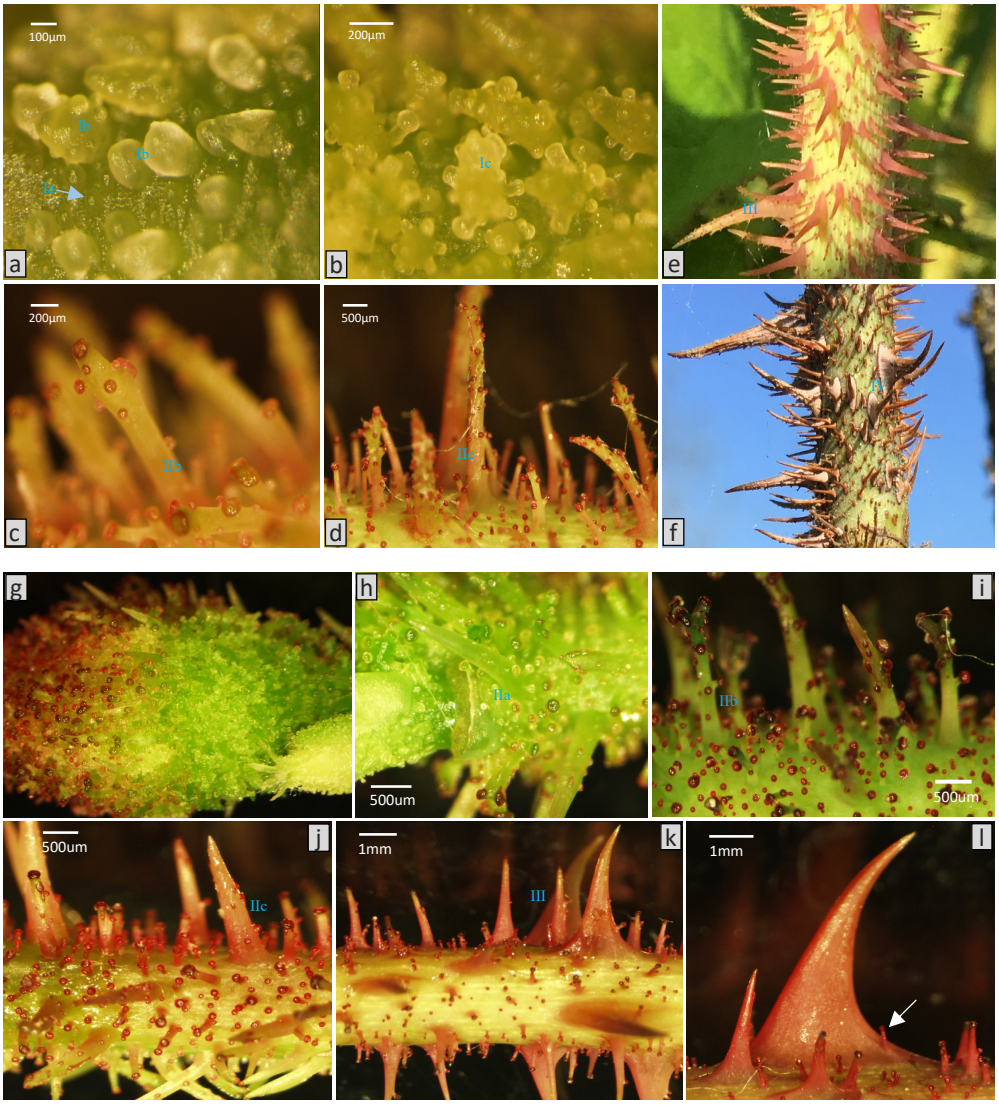

Figure 22: Branched and naked glandular prickles development in (a-f) 'General Kleber' and (g-l) 'Parkzauber'.

'Parkzauber' (Figure 22 g-l). The prickles are naked, no hairy type was found in this sub-category. Interestingly these roses are belonging to a particular type of roses, the moss roses (see discussion).

The development of branched GPs is more complicated than unbranched ones at stage I. Thus, we divided three sub-stages for the stage I. In stage Ia, multiple divisions give rise to a near round protuberance (Figure 22 a). Appearing branch bumps is a sign of entering the stage Ib (Figure 22 a). In stage Ic, the bumps continue to grow and to differentiate into glands and stalk (Figure 22b). The following stages are similar to the unbranched GPs (Figure 22 c-f).

2.3.2.4 Others

Other cases that are not easy to be classified in the previous categories: One or several small GP(s) can develop on a large NGP (Figure 22 l); A prickle has a similar size of non-glandular and glandular branches

(Figure 20 s).

All types of prickle formation will go through the process of initiation, development, and senescence. Most of prickle do not fall off from stem, but few does (Figure 18 g).

2.4 Discussion

2.4.1 New insight in the type of prickles and their origin

The major objectives of this project were to understand prickle morphology, anatomy, and define the developmental stages to serve as the foundation for genetic and molecular studies.

We have found several types of prickles in roses, they can be glandular or non-glandular, branched or unbranched, naked or covering with hairs. We suggested to classify them into two general categories: glandular prickles (GPs) and non-glandular prickles (NGPs), depending on their morphology that presence and absence of glandular structures, respectively. The GPs which are observed in roses, have a glandular head or several glands positioned along the prickle that accompanies them throughout their lifetime, in contrast, NGP have no glandular structures at all. This conclusion is different from previous studies in raspberry and roses: prickles were extensions or modifications of glandular trichomes since the cell mass of glandular fall off the stalk when they reached a certain height in *Rubus* and *Rosa* habrid (Kellogg et al., 2011), and in other species (Ma et al., 2016b).

We also provide anatomical evidence for the very early stages. We revealed that the NGPs and GP are initiated from the ground meristem below the protoderm. For GPs, the main structure (stalk) of prickle originates from the ground meristem, the glandular head originates the protoderm (or epidermis) cells. These conclusions are also different from previous studies, which reported that prickles were origin from epidermal cells (Peitersen, 1921; Esau, 1960; Coyner et al., 2005) and modified from glandular trichomes (Kellogg et al., 2011; Khadgi and Weber, 2020a), or including from glandular trichomes (Pandey et al., 2018), or from bark tissue (Angyalossy et al., 2016).

Furthermore, the glandular head was not produced at the prickle initiation but during the prickle's development (Figure 14 m-r), which may suggest that GPs might be modified from NGPs. A similar situation is present in the trichome: the earliest glandular trichomes are modified from the non-glandular trichome. The earliest evidence for the occurrence of modified trichomes (glandular) comes from fossils of the late Carboniferous (Stephanian stage, $\sim$ 290 Mya) (Krings et al., 2003; Lange, 2015). GTs possessed a touch-sensitive mechanism that opened the secretory cell when touched. This mechanism of GT may be important for plant-insect interactions in the late Carboniferous (Krings et al., 2003). The glands of prickle may also play an important role for plant-insect interactions. The GTs on the stem are relatively fewer in rose and found in different species presented large divergence time suggesting that GTs on stem appear several times during rose speciation (data not shown).

2.4.2 Suggestions for the genetic and genomic studies in rose prickles

The difference between GPs and NGPs is also related to their segregation in the OW population, demonstrating that different genetic determinisms are involved (Zhou et al., 2020). Therefore, we suggested that they should be studied separately in genetic and molecular studies. Here we focused only on prickle present on the stem. Prickle on petiole, pedicel, and fruit may have different patterns, especially at the initiation stage (see discussion for moss roses).

For reverse genetics and RNAseq approach

According to the specific morphogenetic events during its maturity, we divided NGP and GP development into four stages, and three sub-stages for the stage II. These stages of NGPs have been used for reverse genetics (Zhou et al., 2020) and RNAseq approach (Chapter 4) to discovery the genes involved in prickle initiation and development.

For forward genetics approach

Quantitative trait locus (QTL) analysis and genome-wide association study (GWAS) are the most popular methods used to reveal the genetic base of quantitative traits. Both methods are achieved by looking for correlation between the phenotype and the genotype. Therefore, how to evaluate the phenotype is an important question for starting these two forward genetic approaches. Here we proposed a rapid way to phenotype the different prickles in rose according to few characteristics (Figure 16). First the presence of glandular head (GP vs NGP), then the presence of branched (unbranched vs branched trichomes) and the presence of hairs on the trichome (‘naked’ vs ‘hairy’).

In OW population, both parents only have NGPs, but a few individuals present NGPs and GPs. Coupled with the segregation of GP and NGP showed in different genetic determinisms, suggesting that they should be studied separately (see Zhou et al., 2020, Chapter 3).

Wild rose species or varieties have more diversity of phenotypes than the F1 hybrids such as OW population. This made it more complicated for this trait phenotyping in genome-wide association study (GWAS). Presently, we do not know whether the different types of prickles have the same genetic pathway for initiation or not, or perhaps they are sharing part of the pathway. Thus, the methods of phenotyping must be used by paying attention to the different types of prickles and their anatomy.

2.4.3 Prickless may be more adapted from human selection

We notice that glabrous roses are rare, in our 110 samples, we found only 7 glabrous roses (no GP or NGP). Among them, four were sometimes observed with few prickles, one (*R. fraxinifolia* Lindl) was described with few prickles occasionally (even by our scoring, no prickle was observed) (Masure, 2013).

The majority of glabrous roses are in fact cultivars selected from wild species: *R. multiflora* 'inermis', *R. wichurana* 'Bayses' Thornless', *R. pimpinellifolia* 'lutea', *R. banksiae* 'alba plena' and *R. banksiae* 'lutea'. Only two wild species (*R. banksiae var. normalis*, *R. fraxinifolia* Lindl) were glabrous. It suggests that the glabrous is not adapted for roses in wild, and again highlight that prickle is a beneficial and important trait in rose domestication. Perhaps the absence of prickle is due to a mutation like the selection for the recurrent blooming. So, the hypothesis is that the mutant has been selected and rescue by humans. It could explain the rare genotypes without prickles found in the wild. Those glabrous roses are interesting material for genetic and genomic studies.

2.4.4 Branched GPs in moss roses

The branched GPs are also rare, only presented in 5 roses among the 110: *R. centifolia* (*Rosa* Chou) (Inconnu, < 1595), *R. centifolia* 'muscosa' (< 1700), *R.* × *damascena* 'Quatre Saisons Blanc Mousseux', 'Général Kléber' and 'Parkzauber' (1956) (Nédelec, 2018). Interestingly these roses are all moss roses. Moss roses are covered with a mossy growth on flower pedicel and calyx. They are old garden roses belonging to the subgenus *Rosa* sect. *Caninae* DC (Masure, 2013). *R.* × *centifolia* 'muscosa' may be obtained by bud-mutation. *R.* × *damascena* 'Quatre Saisons Blanc Mousseux' may be a sport or bud-mutation of *R.* × *damascena* 'bifera' which is a repeat-blooming hybrid of *R.* × *damascene* (Caissard et al., 2006). *R.* × *damascena* 'Quatre Saisons Blanc Mousseux' was the first repeat-blooming cultivar in moss roses (Caissard et al., 2006). The exact genetic relationship between *R.* × *damascena* and *R. centifolia* are still unclear. The origin of the moss roses is also unknown. *R.* × *damascena* (< 1245) only presented unbranched GPs and NGPs on stem and leaves, suggesting that the branched GPs on the stem may obtain from *R.* × *centifolia* but not *R.* × *damascena*.

Table 2: Types of stem prickle in the list of rose resources.

			Stem prickles						
Subgen	Section	Species	NGP	GP	Branched	Unbranched	Hairy	Naked	Plant in
Hulthemia		*R. hultemia* persica (*R. berberifolia*)	+	-	-	+	-	+	LRG
Platyrhodon		*R. roxburghii var hirtula*	+	-	-	+	-	+	LRG
		R. praelucens	+	-	-	+	-	+	FRI
		R. kweichowensis	+	-	-	+	-	+	FRI
Hesperhodos		*R. minutifolia Engelm*	+	-	-	+	+	-	WS1
		R. stellata	+	+	-	+	-	+	LRG
Rosa	Banksianae	*R. banksiae* var.normalis	-/+	-	-	-/+	-	-/+	FRI
	Lindl.	*R. banksiae* 'alba plena'	-/+	-	-	-/+	-	-/+	FRI
		R. banksiae 'lutea'	-/+	-	-	-/+	-	-/+	FRI
		R. cymosa	+	-	-	+	+	-	LRG
	Carolinae	*R. palustris*	+	-	-	+	-	+	LRG
	Crép.	*R. carolina*	+	-	-	+	-	+	LRG

Continued.....

Table 2–*Continued from previous page..*

Subgen	Section	Species	Stem prickles						Plant in
			NGP	GP	Branched	Unbranched	Hairy	Naked	
	Bracteate	*R. bracteata*	+	+	-	+	+	-	FRI
	Theory								
	Caninae	*R. caninae* freya	+	+	-	+	-	+	LRG
	DC.	*R. corymbifera*	+	-	-	+	-	+	LRG
		R. horrida	+	+	-	+	-	+	LRG
		R. foliolosa	+	-	-	+	-	+	LRG
		R. sherardi	+	-	-	+	-	+	LRG
		R. scabriuscula	+	-	-	+	-	+	LRG
		R. centifolia 'Chou'	-	+	+	-	-	+	LRG
		R. centifolia 'muscosa'	-	+	+	-	-	+	LRG
		R. damascena	+	+	-	+	-	+	LRG
		R. × *damascena* 'Quatre Saisons Blanc Mousseux'	-	+	+	-	-	+	LRG
		R. gallica officinalis	+	+	-	+	-	+	LRG
	Cinnamomeae	*R. acicularis*	+	-	-	+	-	+	INRAE
	DC.	*R. albertii*	+	-	-	+	-	+	FRI
		R. beggeriana	+	-	-	+	-	+	FRI
		R. bella	+	-	-	+	-	+	FRI
		R. caudata	+	-	-	+	-	+	FRI
		R. chengkouensis	+	-	-	+	-	+	FRI
		R. corymbulosa	+	-	-	+	-	+	FRI
		R. davidii	+	-	-	+	-	+	FRI
		R. davurica	+	-	-	+	-	+	FRI
		R. fedtschenkoana	+	-	-	+	-	+	FRI
		R. forrestiana	+	-	-	+	-	+	FRI
		R. fraxinifolia lindl	-	-	-	-	-	-	LRG
		R. giraldii	+	-	-	+	-	+	LRG
		R. laxa retzius	+	-	-	+	-	+	LRG
		R. macrophylla	+	-	-	+	-	+	FRI
		R. majalis plena	+	-	-	+	-	+	LRG
		R. marretii	+	-	-	+	-	+	LRG
		R. moyesii	+	-	-	+	-	+	LRG
		R. multibracteata	+	-	-	+	-	+	FRI
		R. murielae	+	-	-	+	-	+	FRI
		R. oxyacantha	+	-	-	+	-	+	FRI
		R. pendulina	+F	-	-	+F	-	+F	LRG
		R. pinetorum	+	-	-	+	-	+	WS2
		R. prattii	+	+	-	+	-	+	FOC
		R. pseudobanksiae	+	-	-	+	-	+	FRI
		R. rubella	+	-	-	+	-	+	LRG
		R. rugosa 'scabrosa'	+	+	-	+	+	-	LRG
		R. sertata	+	-	-	+	-	+	FRI
		R. sweginzowii	+	-	-	+	-	+	LRG

Continued.....

Table 2–*Continued from previous page..*

Subgen	Section	Species	Stem prickles						Plant in
			NGP	GP	Branched	Unbranched	Hairy	Naked	
		R. tibetica	+	-	-	+	-	+	FOC
		R. webbiana	+	-	-	+	-	+	FOC
		R. willmottiae	+	+F	-	+	-	+	FRI
	Chinenses DC.	*R. chinensis* 'old blush'	+	-	-	+	-	+	INRAE
		R. lucidissima	+	-	-	+	-	+	FRI
		R. odorata var. gigantea	+	-	-	+	-	+	FRI
		R. chinensis var. spontanea	+	-	-	+	-	+	FRI
	Pimpinellifoliae DC.	*R. mairei*	+	-	-	+	-	+	FRI
		R. omeiensis	+	-	-	+	-	+	LRG
		R. sericea	+	-	-	+	-	+	FRI
		R. sikangensis	+	-	-	+	-	+	FRI
		R. taronensis	+	-	-	+	-	+	FRI
		R. farreri	+	-	-	+	-	+	FOC
		R. foetida	+	-	-	+	-	+	LRG
		R. graciliflora	+	-	-	+	-	+	FRI
		R. hugonis	+	-	-	+	-	+	LRG
		R. kokanica	+	-	-	+	-	+	FRI
		R. koreana	+	-	-	+	-	+	FOC
		R. platyacantha	+	-	-	+	-	+	FRI
		R. primula	+	-	-	+	-	+	LRG
		R. spinosissima	+	-	-	+	-	+	FRI
		R. transmorrisonensis	+	-	-	+	-	+	FRI
		R. tsinglingensis	+	+	-	+	-	+	FOC
		R. xanthina	+	-	-	+	-	+	LRG
		R. ecae	+	-	-	+	-	+	LRG
		R. marmorata	+	+	-	+	-	+	LRG
		R. pimpinellifolia (*R. oxyacantha*)	+	-	-	+	-	+	WS3
		R. pimpinellifolia 'king of the scots'	+	+	-	+	-	+	LRG
		"*R. pimpinellifolia* 'aïcha' (*R. spinulifolia aïcha*)"	+	+	-	+	-	+	LRG
		R. pimpinellifolia 'lutea'	-/+	-	-	-/+	-	-/+	LRG
	Laevigatae Thory	*R. laevigata*	+	-	-	+	-	+	FRI
		R. cooperi burmese	+	-	-	+	-	+	LRG
	Synstylae DC.	*R. anemoniflora*	+	+	-	+	-	+	FRI
		R. arvensis	+	-	-	+	-	+	LRG
		R. brunonii	+	-	-	+	-	+	FRI
		R. filipes	+	-	-	+	-	+	LRG
		R. glomerata	+	-	-	+	-	+	FRI
		R. helenae	+	-	-	+	-	+	FRI
		R. henryi	+	-	-	+	-	+	FRI

Continued.....

Table 2–*Continued from previous page.*.

Subgen	Section	Species	Stem prickles						Plant in
			NGP	GP	Branched	Unbranched	Hairy	Naked	
		R. kwangtungensis	+	-	-	+	-	+	FOC
		R. lichiangensis	+	-	-	+	-	+	FRI
		R. longicuspis	+	-	-	+	-	+	FRI
		R. maximowicziana	+	-	-	+	-	+	FRI
		R. moschata	+	-	-	+	-	+	LRG
		R. multiflora	+	-	-	+	-	+	FRI
		R. multiflora 'Inermis'	-	-	-	-	-	-	FRI
		R. rubus	+	-	-	+	-	+	FRI
		R. soulieana	+	-	-	+	-	+	FRI
		R. wichuraiana	+	-	-	+	-	+	INRAE
		R. wichuraiana 'Basyes' Thornless'	-	-	-	-	-	-	FRI
	Hybrids	*R. iwara* (Hybrid *Rugosa*)	+	+	-	+	+(NGP)	+(GP)	LRG
		Marie Bugnet (Hybrid Rugosa)	+	+	-	+	+	-	LRG
		Général Kléber	-	+	+	-	-	+	LRG
		Parkzauber	-	+	+	-	-	+	LRG
		Grootendorst Supreme (Hybrid Rugosa)	+	+	-	+	+	-	LRG
		Werner dirks	+	-	-	+	-	+	LRG
		La France	+	-	-	+	-	+	INRAE

$^{-/+}$ means the genotype is prickless or almost and if have few prickles, it's NGPs.

$^{+F}$ means the genotype have this type of prickle, but only few.

^{Pink} shows the twelve representative species we used in the macroscopy study.

^{Green} shows the glabours or almost glabours genotypes.

^{LRG} Loubert Rose Gardens (Rosiers sur Loire, France).

^{INRAE} Institut de Recherche en Horticulture Et Semences, Angers, France.

^{FRI} Flower Research Institute, Yunnan Academy of Agricultural Sciences, Kunming, China.

^{FOC} Flora of China (http://www.iplant.cn/foc).

^{WS1} web sources - https://fr.wikipedia.org/wiki/Rosa_minutifolia.

^{WS2} web sources - http://www.elkhornsloughctp.org/factsheet/factsheet.php?SPECIES_ID=97.

^{WS3} web sources - https://www.wikiwand.com/en/Rosa_pimpinellifolia.

Author's contributions

Zhou NN, Foucher F, Hibrand Saint-Oyant L conceived and designed the study. Zhou NN performed experiments, collected and analyzed data, and drafted the manuscript. Foucher F and Hibrand-Saint Oyant L were responsible for supervising the project and for revising the manuscript. Simonneau F provided full technical knowledge for performing the histological experiments. Thouroude T was contributed to the F1 cutting plant management in the greenhouse and to record planting information on wild rose resources.

Acknowledgements

We gratefully thank the IMAC technical platforms of SFR Quasav for supporting the histological experiments, especially Aurelia Rolland for participating in the discussion during the histological experiments. We gratefully thank the Loubert Rose Gardens and especially Thérèse Loubert (Rosiers sur Loire, France) for providing the experimental materials. We would also like to thank Jian Hong-Ying and Shu-Fa Li (FRI, Kunming, China) for the wild roses collection and for identifying the species. We thank Latifa Hamama (IRHS, Agrocampus-ouest, Angers, France) for the discussion and advice on anatomical terms. We thank the PHENOTIC platform (IRHS, Angers, France) to manage the plants.

Funding

This work was supported by funding from the China Scholarship Council ([2017]3109) and the National Natural Science Foundation of China (31760585).

3 Genetic determinism of prickles in rose

This work was published in Theoretical and Applied Genetics, and is presented in the second part of the results. The authors who contributed to this work are:

Zhou NN[1,2], Tang KX[2], Jeauffre J[1], Thouroude T[1], Lopez Arias D[1], Foucher F[1*], & Hibrand-Saint Oyant L[1*]

1 Université d'Angers, Agrocampus-Ouest, INRAE, GDO-IRHS (Genetics and Diversity of Ornamental Plants, Institut de Recherche en Horticulture et Semences), SFR 4207 QUASAV, 49071 Angers, France. 2 National Engineering Research Center for Ornamental Horticulture; Flower Research Institute, Yunnan Academy of Agricultural Sciences, Kunming 650231, China.

* both authors contributed equally to the work.

Corresponding author: ningning.zhou@aliyun.com

Key message: The genetic determinism of prickle in rose is complex, with a major locus on LG3 that controls the absence/presence of prickles on the rose stem.

Abstract Rose is one of the major ornamental plants. The selection of glabrous cultivars is an important breeding target but remains a difficult task due to our limited genetic knowledge. Our objective was to understand the genetic and molecular determinism of prickles. Using a segregating diploid rose F1 population, we detected two types of prickles (glandular and non-glandular) in the progeny. We scored the number of non-glandular prickles on the floral and main stems for three years. We performed QTL analysis and detected four prickle loci on LG1, 3, 4 and 6. We determined the credible interval on the reference genome. The QTL on LG3 is a major locus that controls the presence of prickles, and three QTLs (LG3, 4 and 1) may be responsible for prickle density. We further revealed that glabrous hybrids are caused by the combination of the two recessive alleles from both parents. In order to test if rose prickles could originate from a 'trichome-like structure', we used a candidate approach to characterize rose gene homologues known in *Arabidopsis*, involved in trichome initiation. Four of these homologues were located within the overlapping

credible interval of the detected QTLs. Transcript accumulation analysis weakly supports the involvement of trichome homologous genes, in the molecular control of prickle initiation. Our studies provide strong evidence for a complex genetic determinism of stem prickle and could help to establish guidelines for glabrous rose breeding. New insights into the relationship between prickles and trichomes constitute valuable information for reverse genetic research on prickles.

Keywords Trichome, QTL, *ZFP5*, *GIS2*, *MYB61*, *MYC1*

3.1 Introduction

Rose is the major ornamental plant worldwide with a wide diversity, diverse application forms and an extensive cultivated area. Roses are sold as cut flowers, garden plants, in pots, for essential oil, flower tea and culinary purposes. In past centuries, with the continuous efforts of breeders, more than 33,000 varieties of roses were created (Young et al., 2007). However, most of these varieties have persistent prickles on the stem. Prickles can protect against herbivores by deterring them from eating the stem (Ronel and Lev-Yadun, 2012; Burns, 2014). Furthermore, prickles can be desirable in roses when they are used in hedges to protect properties (as was the case in Reunion Island during the 19th century). However, garden roses without prickles are often desirable. Cut roses with prickles are more difficult to handle, harvest and transport and also constitute safety hazards for consumers and workers. Retailers commonly remove prickles from stems prior to sale. Removing the prickles increases labor costs and causes mechanical damage to the stems, which affects vase life and ornamental value. Although a strong market demand to develop roses without prickles exists (Nobbs, 1984; Debener, 1999; Canli, 2003; Canli and Skirvin, 2003, 2008), relatively little is known about the genetic and molecular bases of prickle initiation and development.

In plants, prickles are described as outgrowths of the epidermis and subjacent layers that lack vasculature, and mainly consist of lignin, suberin, cellulose and hemicellulose (Asano et al., 2008; Li et al., 2012). In rose and raspberry, it was thought that prickles were modified glandular trichomes that differentiate at the time of lignification into their final prickle morphologies (Kellogg et al., 2011).

Until recently, only a few studies had been published about the molecular regulation of prickle development, but great progress has been made in trichome initiation and development, especially in *Arabidopsis*. Several transcription factors (TFs) such as MYB, bHLH, WD40, WRKY and C2H2 zinc finger families' proteins have been identified as being involved in trichome initiation and development (reviewed in Balkunde et al. (2010); Pattanaik et al. (2014); Ma et al. (2016a); Huchelmann et al. (2017); Chopra et al. (2019)). A trimeric activator complex consisting of MYB (GLABRA1) - bHLH (GLABROUS3/ENHANCER OF GL3) - WDR (TRANSPARENT TESTA GL1) plays a key role in trichome development (Zhang, 2003; Kirik et al., 2005; Patra et al., 2013). This trimeric complex finely regulates the temporal and spatial expression of GLABRA2 (GL2) and TRANSPARENT TESTA GL2 (TTG2), determining the fate and pattern of trichome precursor cells (Rerie et al., 1994; Ishida et al., 2008). The bHLH family genes, MYC1 and TT8, belong to the

same clade as GL3. AtMYC1 acts as a positive regulator of trichome initiation (Symonds et al., 2011; Zhao et al., 2012), and AtTT8 controls trichome development on leaf margins (Maes et al., 2008). AaMYB1 and its orthologue AtMYB61, belonging to the R2R3MYB subfamily, were thought to affect terpene metabolism and trichome development in *A. annua* and *A. thaliana*, respectively (Matías-Hernández et al., 2017).

The active TTG1 trimeric complex can be repressed by R3 MYB subfamily genes: TRY/CPC/TCL1 act as negative regulars by competing with GL1 for binding to GL3 (Wang et al., 2008; Wester et al., 2009; Wang and Chen, 2014). The active TTG1 complex, in interaction with TTG2, regulates the expression of the R3 MYB inhibitors that move to the neighboring cells where they repress trichome initiation (Pesch and Hülskamp, 2004; Pesch et al., 2014).

Different growth regulators positively affect trichome initiation, such as GA3, cytokinin and jasmonic acid (Traw and Bergelson, 2003), through the activation of GL1 (Gan et al., 2006). Different C2H2 zinc-finger proteins such as GLABROUS INFLORESCENCE STEM (GIS), GIS2, GIS3, ZINC FINGER PROTEIN5, 6 and 8 (Gan et al., 2006, 2007) include GA and cytokinin signaling pathways (Zhou et al., 2013). The novel transcription factor TRP interacts with ZFP5 and negatively regulates trichome initiation through the gibberellic acid pathway (Kim et al., 2018).

In diploid rose, the presence of prickles on the stem was assumed to be controlled by a single dominant gene (Debener, 1999; Shupert et al., 2007) located on linkage group 3, LG3 (Linde et al., 2006). Furthermore, two QTLs were detected on LG3 with the scoring of prickle density (Crespel et al., 2002). Using two F1 progenies,Hibrand-Saint Oyant et al. (2018) also identified a large QTL (or two neighboring QTLs) on LG3 (between position 31 Mb - 46.5 MB corresponding to the end of the chromosome 3) and a significant association between position 31 and 32.4 Mb using a GWAS approach. In tetraploid roses, three QTLs were identified in relation to the number of prickles on the stem: two located on LG2 and one on LG3 (Koning-Boucoiran et al., 2009). Using the same K5 population with the same phenotype data but a new genetic map, different QTLs were detected on LG3, 4 and 6 and on LG2 (one year) (Bourke et al., 2018a). Recently, a WRKY transcription factor, homologous to *Arabidopsis* TTG2, was located close to a QTL controlling prickle density, and the gene transcripts are differentially accumulated between prickle and prickless roses (Hibrand-Saint Oyant et al., 2018).

In this study, our objectives were to decipher the genetic determinism of stem prickles in rose and to characterize candidate genes involved in prickle initiation and development. First, we defined the different types of prickles on the stem and studied them separately. Using an F1 progeny, we detected QTLs and their position in the rose genome sequence. We further analyzed how the alleles of the major QTLs affect the presence of prickles. We identified putative candidate genes (homologues of genes involved in trichome initiation and development in*Arabidopsis*) and studied their transcript accumulation. That study suggested that prickles and trichomes may carry two different genetic pathways, providing new insights into the relationship between prickles and trichomes.

3.2 Materials and methods

3.2.1 Plant materials

A progeny of 151 diploid F1 hybrids obtained from a cross between the female *Rosa chinensis* 'Old Blush' (OB) × the male *R.* × *wichurana* (RW) was used for map construction (described in (Hibrand-Saint Oyant et al., 2018) and QTL analysis. The plants were grown in a field and managed by the Horticulture Experimental Unit (INRAE, Angers, France). The plants were pruned each December. In the following spring, new stems developed from the axillary buds from the old pruned stems, and are referred to as "floral stems" since they develop flowers. Later, new stems arise from the base of the plant and are referred to as "main stems". They remain vegetative in once-flowering individuals and may become floral in continuous-flowering individuals.

3.2.2 Phenotypic data collection and analyses

To score prickle density, we selected three independent floral and main stems for each F1 progeny and the two parents. The prickle numbers were counted for each selected stem on four internodes (located in the middle of the stem) for three years (2016, 2017 and 2018).

Statistical analysis and visualization were performed using R version 3.2.3. We visualized the frequency distribution and Q-Q plot using the *'hist'*, *'legend'*, *'qqnorm'* and *'qqline'* functions. We performed mixed--factorial ANOVA analysis with *'aov'*. A *'shapiro.test'* was used to test the normality of the original data and the ANOVA residuals. When the null hypothesis was negated, *'kruskal.test'* was used to test if there was any significant difference between the replicate shoots, years and the type of stem variance. '*pairwise.wilcox.test*' with '*p.adjust.method =BH*' was used to calculate pairwise comparisons between group levels with corrections for multiple testing. We displayed the distribution of prickle density with a boxplot to compare the difference between the variance using the *ggplot2* and *ggpubr* packages.

Variance components were estimated with the restricted maximum likelihood (REML) method using the *sommer* package. Phenotype variance components of prickle density were obtained using the following model:

$$P_{ijlr} = \mu + G_i + S_l + Y_{(l)j} + GS_{il} + GY_{ij} + \varepsilon_{ijlr} \tag{3.1}$$

Where P_{ijlr} is the phenotypic value of a trait counted on a triplicate stem *r* of the stem type *l* of the individual *i* in the year *j*, μ is the overall mean, G_i is the random effect of genotype *i*, S_I is the random effect of stem type *l*, $Y_{(l)j}$ is the random effect of year *j* nested in stem type *l*, GS_{il} is the random interaction between genotype *i* and stem type *l*, GY_{ij} is the random interaction between genotype *i* and year *j*, and ε_{ijlr} is the random residual error.

The phenotypic variance (σ^2_P) of stem prickles was divided into the variance of genotypic effect (σ^2_G) genotype × year interaction (σ^2_{GY}), genotype × stem type interaction (σ^2_{GS}), and the residual error variance (σ^2_E).

Narrow-sense heritability (h^2) was calculated as follows:

$$h^2 = \sigma^2_G/(\sigma^2_G + \sigma^2_{GY}/y + \sigma^2_{GS}/s + \sigma^2_E/ysr) \tag{3.2}$$

Where *y* is the number of years, *r* is the number of replication shoots per individual, and *s* is the number of stem types (PF and PM).

3.2.3 Genotypic data

The genetic determinism was conducted using the genetic map previously obtained by Hibrand-Saint Oyant et al. (2018) and modified by Lopez-Arias et al. (2020).

3.2.4 QTL Analysis

In this study, we performed QTL detection for prickles on the floral (PF) and main (PM) stems from data scored in 2016, 2017, 2018 (referred to as PF2016, PF2017, PF2018, PM2016, PM2017 and PM2018, respectively). QTL analyses were carried out using the R/qtl in *R version 3.2.3*. Based on the non-normal phenotype distribution data, single QTL analysis and LOD scores were calculated using the *'scanone'* function with non-parametric model (*model='np', ties.random = FALSE, method = 'em'*) and the two-part model (*model='2part', upper = FALSE*) (Boyartchuk et al., 2001).

In the non-parametric model, the genome-wide and chromosome-wide significance thresholds of LOD scores were estimated by permutations tests (*n.perm = 1000, n.cluster = 20*). The Bayesian credible interval was computed with 0.95 and 0.99 coverage probabilities. When QTLs for different traits had overlapping 0.95 credible intervals, they were declared to be a potentially "common QTL (cQTL)" (Kawamura et al., 2011). The percent of variance explained by each QTL was calculated by *'makeqtl'* and *'fitqtl'* with a *'normal'* model.

In the two-part model, the phenotype was separated into two parts: first, the trait value was considered as without (0) or with (1) prickles; if it had prickles, the trait value above zero was assumed to be normally distributed. Three LOD scores for each genomic position were calculated: LOD(p) and LOD(μ) were calculated for binary traits (0 or 1) and non-zero phenotype quantitative traits (> 0), respectively; LOD(p,μ) is simply the sum of the LOD scores from the two separate analyses (Broman, 2003). The genome-wide significance thresholds of three LOD hypotheses were also estimated by 1000 permutation tests and summarized by a 0.05 alpha threshold. The percent of variance explained was calculated by *'makeqtl'* and *'fitqtl'* with *'binary'* and *'normal'* models for binary(p) and quantitative(μ) traits.

3.2.5 Selection of rose candidate genes involved in prickle density

Proteins involved in trichome initiation and development were selected in *A. thaliana* from the TAIR database (https://www.arabidopsis.org) with searching terms *GL1, MYB82, MYB61, CPC, TRY, GL3, TT8, MYC1, TTG1, TTG2, ZFP5, ZFP1, GIS2, GIS3, GL2*. Rose homologues were searched using BLASTp in the *Rosa chinensis* Genome v1.0 (Hibrand-Saint Oyant et al., 2018). In addition, we also searched the transcription factors (TF) belonging to the bHLH, WD40, R2R3MYB, C2H2 and WRKY families in rose and which were located on the major cQTL interval of LG3. Using Geneious 9.1.7, *'Multiple Align'* was performed for the family gene sequences. Conserved domains were used to build phylogenetic trees using the *'Geneious Tree Builder'* tool with the Jukes-Cantor genetic distance model and the UPGMA tree build method. The rose candidate genes were named according to the following nomenclature corresponding to Rc (for *Rosa chinensis*) added to the corresponding gene name in *Arabidopsis*, e.g., RcTTG2 for the rose TTG2 homologue.

3.2.6 Gene expression analysis

Primers were designed using Primer Premier 5.0 software. To ensure the specificity of the primers, forward and reverse primers were designed in the last exon and in the beginning (first 100 bp) of the 3'UTR. Primer length was between 18 and 25 bp, product length was between 70 and 200 bp, GC content was between 40% and 60%, and the annealing temperature was 58 $\sim$ 65 °C. Primers are listed in Supplementary Table A.1. For the qPCR experimental design, we selected four contrasting once-flowering individuals from the OW progeny for prickle density: two with no prickle (OW9067 and OW9068) and two with prickles (OW9137 and OW9071 with means of 2.5 and 4 prickles per internode on the main stem, respectively). The materials were sampled in April 2018 in a greenhouse (three biological replicates). Stems were harvested at different stages of prickle development for roses with prickles, and stems at the same stages for roses without prickles (Chapter 2, Figure 13). Total RNA was extracted using the NucleoSpin RNA Plus-XS kit for early stages (I and IIa) and using the NucleoSpin RNA Plus-kit for later stages (IIb, IIc and III) according to the manufacturer's instructions, with minus modifications (2% PVP40 in lysis buffet). The purity of the RNA was checked on 1% agarose gel, and the concentration was measured by an UV spectrophotometer. cDNA was obtained from 500 ng of total RNA using iScriptTM Reverse Transcription Supermix for RT-qPCR (Bio-Rad, Hercules) accordant to the manufacturer's instructions. The purity and quality of the cDNA were checked by performing PCR amplification with a blank and RW's DNA sample control, and the concentration was measured with a UV spectrophotometer. RT-qPCR reactions were performed using the SsoAdvanced™ Universal SYBR® Green Supermix (Bio-Rad) on the CFX Connect Real-time PCR system (Bio-Rad). The gene efficiency was evaluated with a serial dilution of the thirty cDNAs pooling (1: 10, 25, 50, 100, 250, 500, 1000). A 1: 25 dilution of each cDNA was used to analyse the expression pattern of ten candidate genes and two reference genes *UBC* and *TCTP* (Randoux et al., 2012). Data collection was performed using the Bio-Rad CFX Maestro1.1. Amplification efficiency of the ten genes ranged from 90.5 $\sim$ 104.1%. The reference genes *UBC* and *TCTP* presented high expression stability in all the samples.

For the technical replicates, potential outliers were excluded from the analysis when the standard deviation (SD) of samples is higher than 0.5. Only seven technical replicates (seven out of 390) were excluded: CPC in PIIb (biological group A, C) and in NPIIc (group A), GIS2 in NPIIc (group C), NPIII (group B) and PIII (group B).

Normalized expression ($\triangle\triangle$Cq) was calculated using Bio-Rad Maestro1.1 software by applying the 'gene study' tool. The cluster analysis for sample and target genes with the mean value of normalized expression was performed using R software with the *'pheatmap'* package. NP samples were used as controls to compare the normalized expression of genes between P and NP samples in the different stages. | Fold change (FC) | > 2 and the Wilcoxon signed rank test (*p-value* < 0.05) as cut-off values in scatter plots were used to demonstrate the significant difference of normalized expression between P and NP samples. NPI was used as a control to visualize the relative normalized expression during stem development in prickle and glabrous stems.

3.3 Results

3.3.1 Type, distribution and genetic variability of stem prickles in OW progeny

Both parents of the F1 progeny ('Old Blush' and *R. x wichurana*) present prickles on their stems (Figure 23 a) (a mean of around ten prickles on four internodes). In the F1 progeny, hybrids without prickle can be observed (14 out of 151; no prickle on the three stems scored over three years). These hybrids with glabrous stems (Figure 23 b) are referred to as 'prickless' individuals (Figure 23 c). Out of the 137 F1 individuals with prickles (Figure 23 b), nine hybrids were nearly prickless (prickle number on four internodes < 1 for three scored years and two types of stems (Figure 23 d)), and numerous stems were glabrous for some individuals, whereas other stems presented a few prickles (variable between the genotypes with unstable states between years and types of stems). Macroscopic analysis shows that parents that present prickles originated from a 'non-glandular' structure. These prickles are referred to as Non-Glandular Prickles (NGP). All the F1 prickly individuals (137 out of 151) have NGP. However, some individuals with NGP prickles also present another type of prickle (27 out of 137). These prickles present a 'glandular head' structure and are referred to as Glandular Prickles (GP) (Figure 23 b and 23 c, Supplementary Figure A.1). Since the presence of GP in the OW progeny is rare (27 and 12 out of 151 on flowers and main stems, respectively; Figure 23 d) and very irregular, we decided to consider only NGPs in this study.

The Shapiro-Wilk normality test and the Q-Q plot of original data (W = 0.692 $\sim$ 0.936, p -value < 2.96 × 10^{-8}) (Supplementary Figure A.1) and variance residuals (W = 0.88591, p -value < $2.2e^{-16}$) showed that the NGP densities on stems in the F_1 population were not normally distributed. We tried to transform data (log10, SQRT, box-cox) to make them normal but without success. The Kruskal-Wallis test reveals a genotype effect, a year effect and a stem effect (Table 3). The high heritability ($h^2 \simeq 0.97$) demonstrated that the genetic analyses of stem prickle of this population were reliable (Table 3).

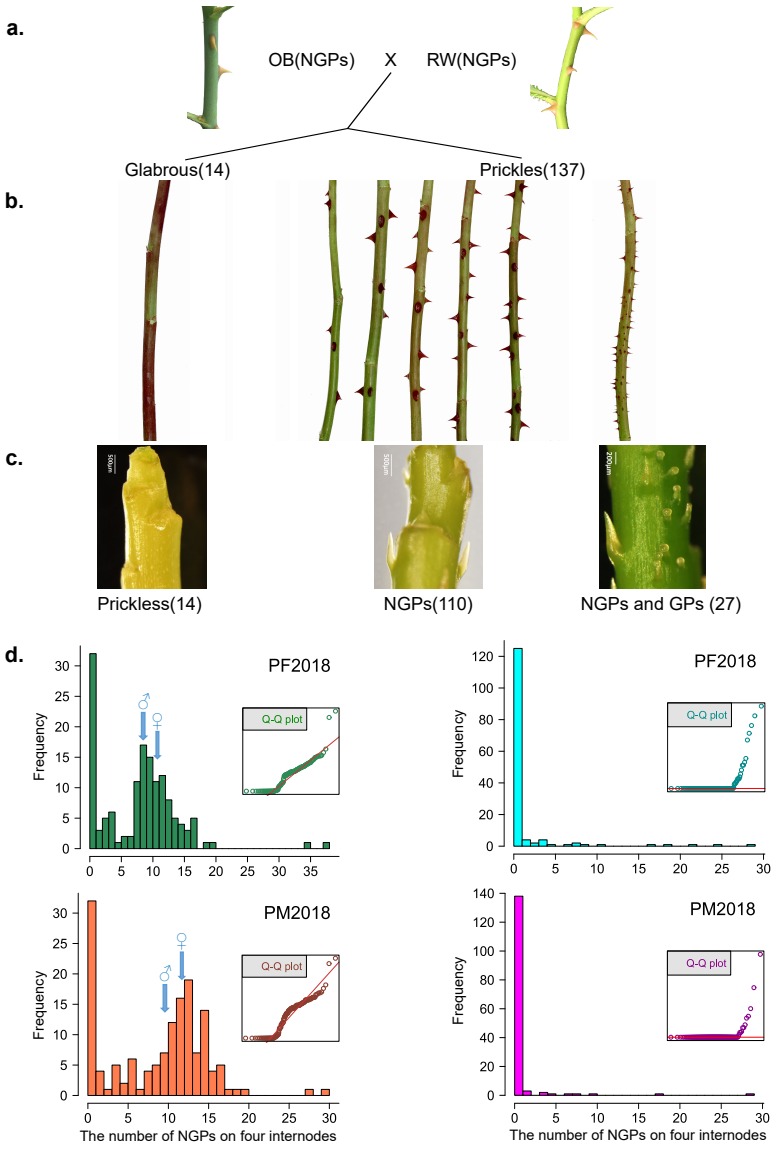

Figure 23: Different types of prickles on the OW progeny stem and their distribution. (a) Stem prickles in the female 'Old Blush' (OB) and the male *R. x wichurana* (RW); NGPs: non-glandular prickles. (b) Stem prickles in F1 progeny. Glabrous: no prickle whatsoever on the recorded stems in the three years. (c) Macroscopic photos of the terminal part of the stems with different types of prickles (number of offspring); GPs: glandular prickles. (d) The distribution and Q-Q plot of NGPs and GPs in the F1 progeny in 2018; PF: prickles on the floral stem; PM: prickles on the main stem.

Table 3: Mean, median and range values for prickle number on 4 internodes, phenotypic variance components and the trait heritability

		OB	RW	F1					Kruskal-Wallis test				Variance component in σ^2_P									
Trait	Year	Mean±SD	Mean±SD	Range	1st Qu	Mean	Median	3rd Qu	Genotype	RepS	Year	Stem type	σ^2_G	SE_G	σ^2_{GY}	SE_{GY}	σ^2_{GS}	SE_{GS}	σ^2_E	SE_E	h^2(%)	SE
PF	2016	11.3±1.3	8.9±0.8	0-43	2.4	8.5	9.8	12.7														
	2017	11.6±1.1	8.9±0.9	0-52	2.7	9.0	9.7	13.0	<2.20E-16***	0.96^N	0.06**											
	2018	10.6±1.0	8.4±0.5	0-38	2.7	7.9	9.0	11.3				4.93E-08***	41.41	4.98	1.50	0.26	1.27	0.27	9.13	0.29	96.66	0.0048
PM	2016	11.9±1.6	9.3±1.2	0-48	6.7	10.2	11.7	13.3														
	2017	11.8±1.4	9.2±1.1	0-47	3.0	10.2	11.3	14.0	<2.20E-16***	0.81^N	0.04***											
	2018	11.7±1.6	9.1±1.1	0-30	3.5	8.8	10.8	13.0														

PF prickles on the floral stem
PM prickles on the main stem
1st Qu first quartile(Q1) means 25% observations are below this quantity (approx)
3rd Qu third quartile(Q3) means 75% observations are below this quantity (approx)
σ^2_G variance components of genotype, genotype x year interaction (σ^2_{GY}), genotype x stem interaction (σ^2_{GS}), and the residual error (σ^2_E)
SE the standard error
h^2 narrow sense heritability

3.3.2 QTL analysis

3.3.2.1 Non-parametric QTL analysis

For the female and male maps, strong QTLs were detected on LG3 for the two types of stems and for the three years (Figure 24 and Table 4). The LOD scores are higher for the male map (between 8 and 11.5) and relatively lower for the female map (between 2.3 and 6.2). These QTLs explained between 6.65 to 37.4% of the phenotypic variance. The locations of these QTLs are very close. Indeed, on the female map, the marker at the peak of the QTLs is the same for both types of stems (Rh12GR_16570_782, 51.1 cM, located on the chr3 at 44,459,262 bp according to the *Rosa chinensis* Genome v1.0 (Hibrand-Saint Oyant et al., 2018)), except for PM2018 (Rh12GR_34665_95, 45.7 cM, located on chr3 at 41,401,120 bp). On the male map, for the two types of stems and for the three years, the marker with the highest LOD for the QTLs detected on LG3 is the same, Rh12GR_52506_1218 (42.6 cM on the LG3, 42,317,122 bp on Chr3), which is the terminal marker on the genetic map but not on the physical map.

Furthermore, if we consider the common 0.95 Bayesian credible interval of these QTLs on LG3 on the female and male maps, all intervals are overlapping (Table 4 and 26). For the female map, the interval on LG3 was 40.38 $\sim$ 53.75 cM, which corresponds to the interval 36,517,224 $\sim$ 46,440,369 bp on the physical map of chr3 (Figure 26 a), and for the male map, the interval on LG3 was 37.69 $\sim$ 42.55 cM, corresponding to the interval 41,648,024 $\sim$ 42,317,122 bp on the physical map (Table 4, Figure 26 b).

On LG4, QTLs were only detected on the female map for the main stem for the three years (Figure 24, Table 4). The peak marker Rh12GR_60129_183 located at 30.6 cM, which is located on chr4 at 52,239,028 bp, explained 10.35 to 13.18% of the observed variance depending on the year of the phenotypic variance in the single QTL model. The common 0.95 credible interval on LG4 was 20.53 $\sim$ 48.59 cM (Figure 26 a), which covered from 46,189,407 $\sim$ 56,107,784 bp on the physical map (Table 4).

On LG6, QTLs were only detected on the male map for three years for PM and for two years (2017 and 2018) for PF (Figure 24 and Table 4). For PM (2016, 2017 and 2018) and PF (2017), the peak marker is the same, Rh12GR_56601_1304 (29.7 cM, located on chr6 at 31,814,891 bp). For PF2018, the peak marker is Rh88_37299_454 (11.5 cM, located on chr6 at 5,410,244 bp). These QTLs explained between 5.28 and 8.45% of the observed variance. The common 0.95 credible interval was from 15.59 to 42.49 cM, which covered from 8,578,645 to 44,264,630 bp on the physical map (Figure 26 b, Table 4).

On LG1, QTLs were only detected on the male map for PF for two years (2016 and 2018), and explained 6.52 and 6.99% of phenotypic variance, respectively. The common 0.95 credible interval was at 12.78 $\sim$ 44.11 cM, which covered from 20,231,658-62,553,371 bp on the physical map (Figure 26 b, Table 4).

We checked the interaction between OB3@Rh12GR_16570_782 and OB4@Rh12GR_ 60129_183, and between RW3@Rh12GR_52506_1218 and RW6@Rh12GR_56601_1304, and no significant interaction was detected.

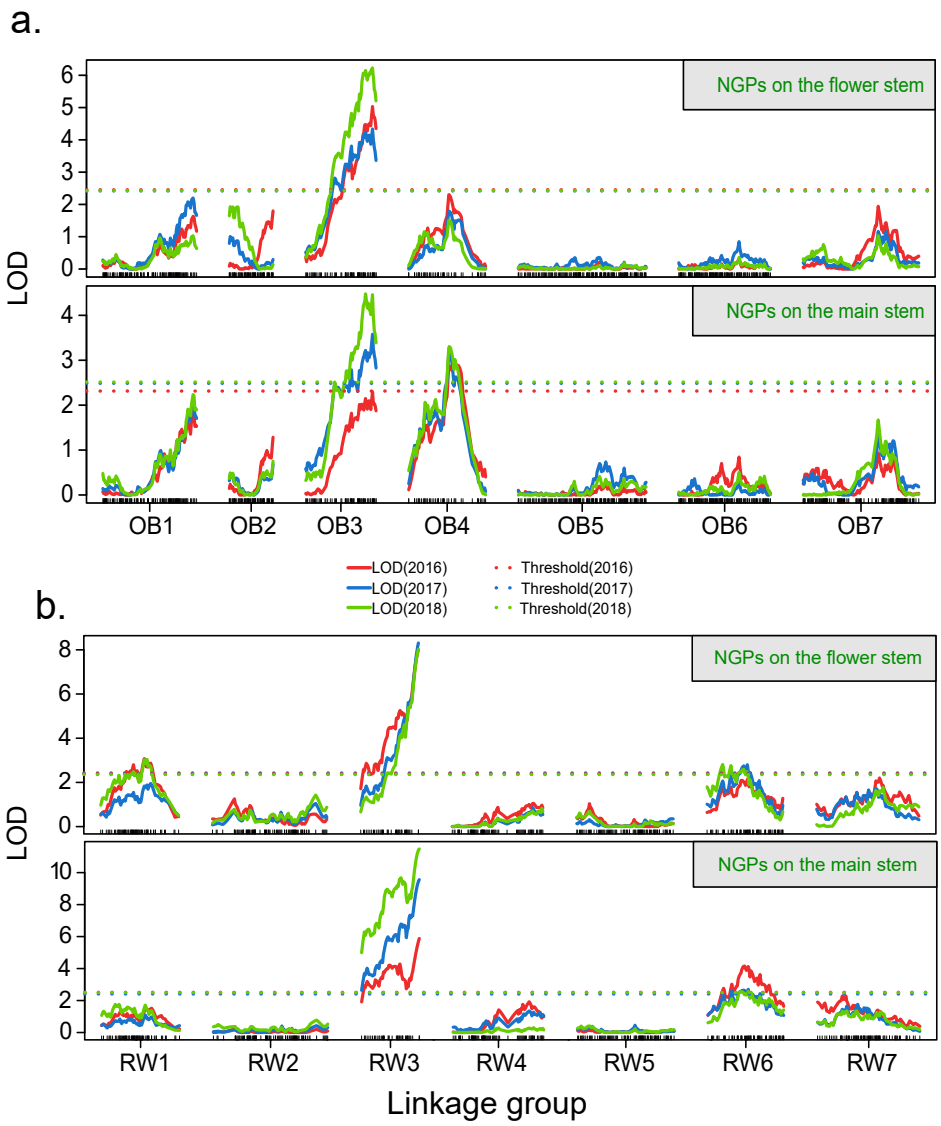

Figure 24: LOD curves of the QTL scan for the NGPs on the floral (FM) and main (PM) stems in (a) female (OB) and (b) male map (RW) calculated with a non-parametric model for the three years (2016, 2017 and 2018, with red, blue and green lines, respectively). The LOD threshold value is represented by a dotted line in red, blue and green for 2016, 2017 and 2018, respectively.

3.3.2.2 Two-part QTL analysis

In order to extend the analysis even further, we performed a two-part QTL analysis to test the penetrance (presence/absence of prickles, LOD(p) were calculated with binary traits) and the severity (density of prickles on stems with prickles, LOD(μ) were calculated with non-zero quantitative phenotype) of these QTLs.

For the hypothesis LOD(p) on the female and male maps, we obtained a significant LOD(p) on the LG3 for the two types of stem (PF and PM) and the three years (Figure 25, Supplementary Table A.2). The marker with the highest LOD score on the OB map is the same: Rw35C24 (SSR marker) located at 44.4cM (Chr03: 40,215,502 bp). This QTL explained 13.38% to 16.72% of the variation. The peak marker on the RW map is also the same for PF and PM for the three years: Rh12GR_52506_1218 located at 42.6 cM (42,317,122 bp). This QTL explained 20.69 to 33.21% of the variation. These data suggested that the QTL detected on LG3 mainly controls the presence/absence of prickles. Moreover, the LOD(p) on LG2 and LG6 for the male map were only significant in PF2016 and PM2016, respectively (Figure 25), and they showed a weak effect with an explanation of 1.80% and 2.70% of the variance, respectively (Supplementary Table A.2).

For the LOD(μ) hypothesis, we detected a significant QTL on the female map on LG4 for PM (2016 and 2017) and PF (2016) (Figure 25, Supplementary Table A.2). The QTLs explained 9.02% to 9.88% of the observed phenotypic variances. Therefore, this QTL might be involved in the control of prickle density. On LG3, a significant QTL was detected on the male map for PM (2016, 2017, 2018) and PF (2016), suggesting that a QTL on LG3 might also control prickle density. This QTL is in the same region of the QTL detected for penetrance (Figure 25, Supplementary Table A.2). On LG1, the LOD(μ) peaks in OB (PM2018) and in RW (PF2018) were higher than the genome-wild threshold (μ); these QTLs explained 6.66% and 7.80%, respectively, of prickle density variation.

3.3.2.3 The interaction of the LG3-QTL allele between OB and RW

Based on non-parametric and two-part methods, we identified QTLs for the presence of prickles on LG3 for the OB and RW maps in the same region. To further investigate how the alleles on these QTLs affect the presence of prickles, we visualized the number of prickles for each genotype in the hybrid population depending of the Mendelian distribution of the SNP markers at the LOD peak (Figure 27). The female and male alleles are referred to as *a,b* and *c,d,* respectively. The separation ratio *ac: ad: bc: cd* in offspring is *33: 54: 16: 48*, and was significantly different from the expected segregation of 1: 1: 1: 1 (37.5 for each) with a *p-value* = 0.004 estimated by a chi-squared test (Figure 27).

For PF and PM in all three years, we clearly see that the *bd* allele combination in hybrids is correlated with no-prickle individuals or individuals with only a few prickles (less than two on four internodes), whereas *ac*, *ad* and *bc* genotypes present prickles (Figure 27). These results suggest a dominant/recessive model for this QTL with the *b* and *d* alleles linked to the null or recessive alleles (prickless mutant) and the *a* and *c* alleles linked to the dominant alleles (prickles). For PM, a co-dominant effect can be detected since the phenotype for *ac* is significantly different from the one for *ad* and *bc* ($ac > ad$ and $ac > bc$, $p\text{-value} < 0.05$,

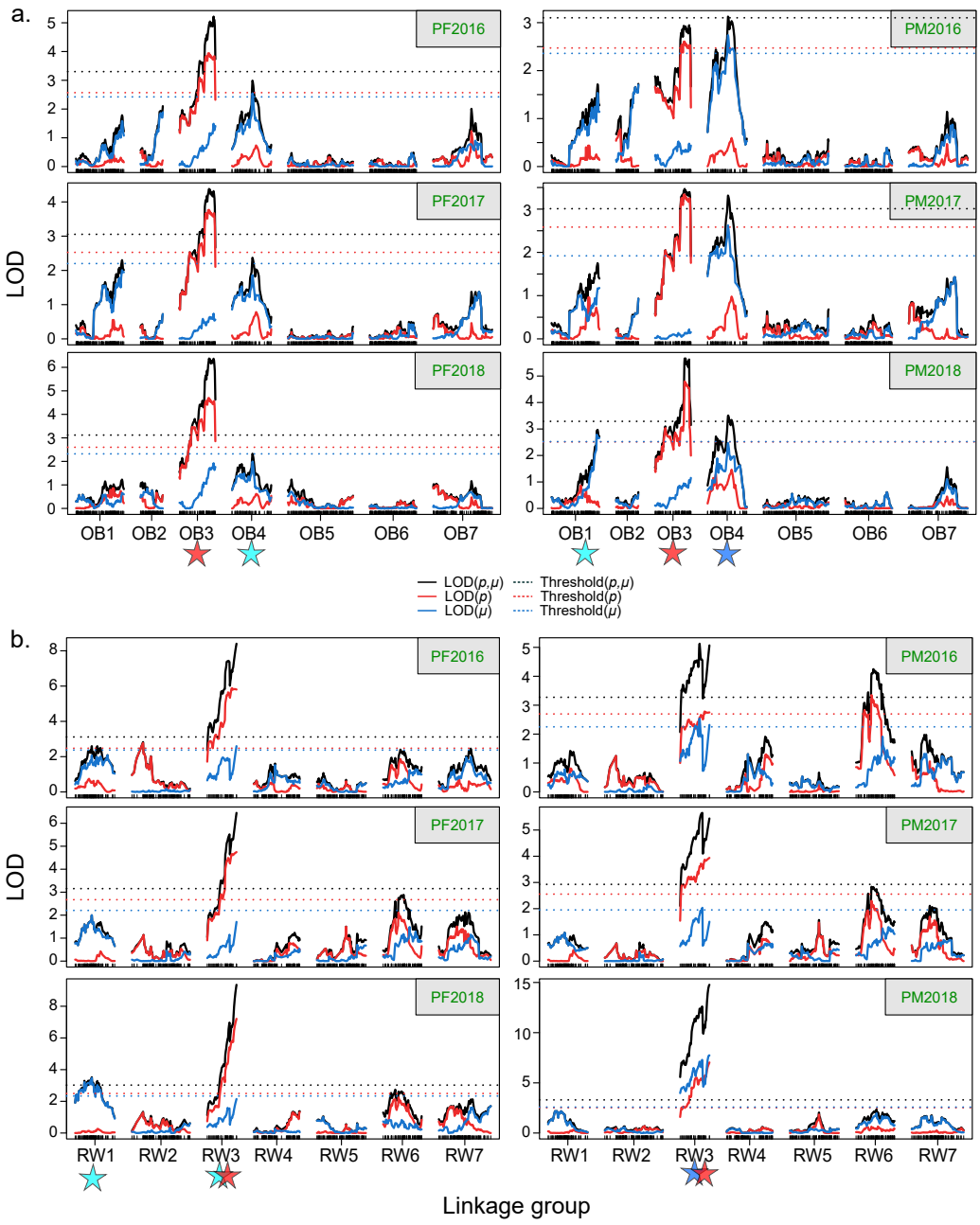

Figure 25: LOD curves of the QTL scan for the NGPs on the floral (FM) and main (PM) stems in (a) female (OB) and (b) male (RW) maps calculated using the two-part approach. The LOD (p) value (penetrance) is in red, the LOD (μ) value (severity) is in blue, and the LOD (p, μ) value is in black. The dotted line represents the LOD threshold. QTLs above threshold value are indicated by stars: red for penetrance, blue for severity.

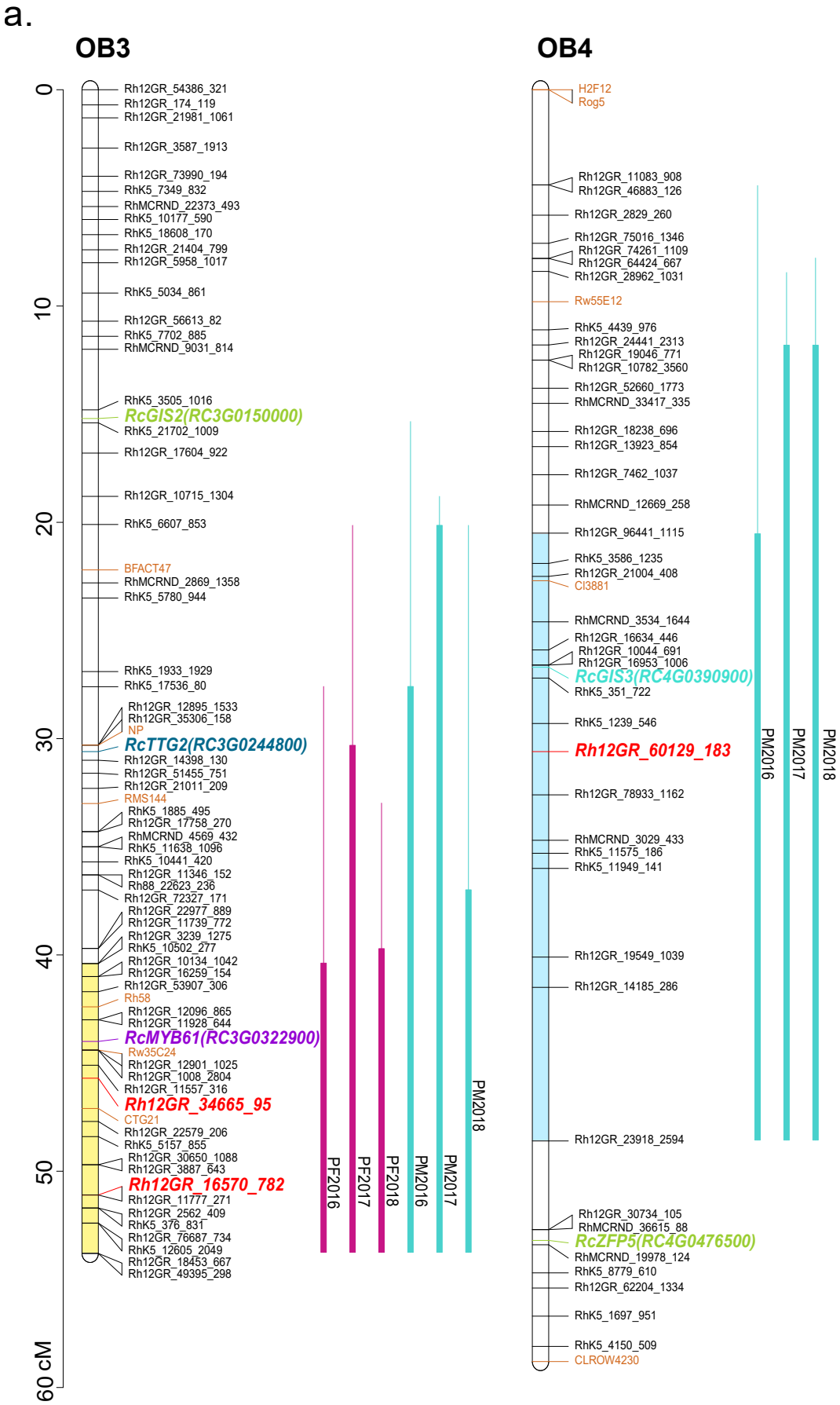

Continue to the next page....

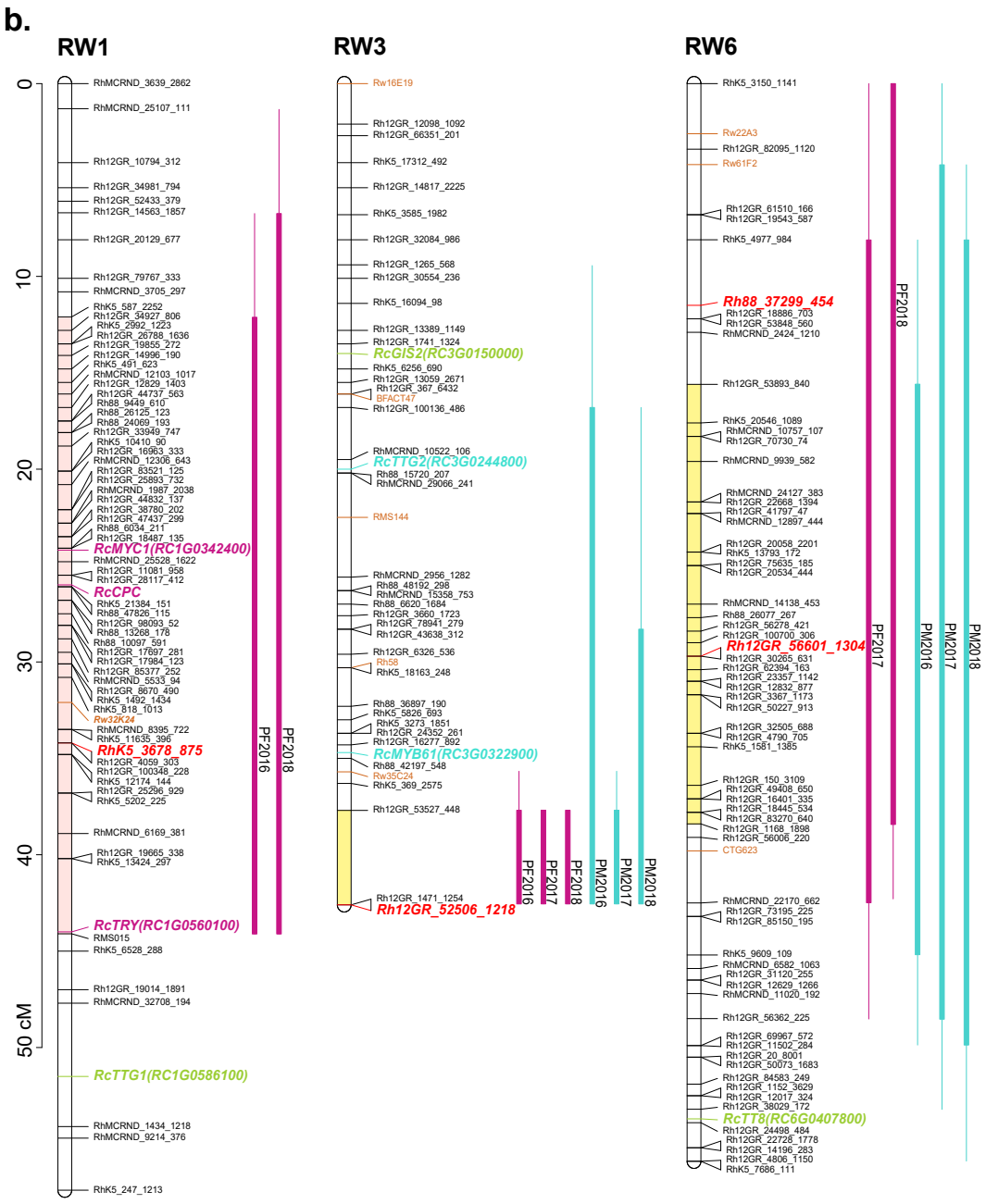

Figure 26: Common QTLs (cQTLs) and candidate genes in (a) the female linkage groups 3 and 4, and (b) the male linkage groups 1, 3 and 6. Areas highlighted in pink, blue and yellow on the linkage groups represent the 0.95 Bayesian interval of cQTL for specific PF, PM and both, respectively. Bars and lines on the right of each chromosome represent 0.95 and 0.99 Bayesian intervals of the QTL with a different color for NGPs on the floral stem and the main stem (pink and blue, respectively). The red markers are the peak of the QTL. Brown markers are SSR markers and black markers are SNP markers.

Table 4: Summary of QTLs for NGP with non-parametric model in OW progeny

			QTL Characteristics					0.95 bayes interval		0.98 bayes interval	
QTL	Phenotyping	PT[a]	LOD	LG@positon[b]	r(%)[c]	MM[d]	bp[e]	cM[f]	bp	cM	bp
1a	PF2016	2.45	5.03	OB3@51.1	11.74	Rh12GR_16570_782	44459262	40.38-53.75	36517224-46440369	27.59-53.75	27934327-46440369
	PF2017	2.42	4.33	OB3@51.1	6.92	Rh12GR_16570_782	44459262	30.31-53.75	33612066-46440369	20.14-53.75	24888779-46440369
	PF2018	2.43	6.22	OB3@51.1	14.84	Rh12GR_16570_782	44459262	39.71-53.75	36517224-46440369	32.98-53.75	33612066-46440369
	PM2016	2.31	2.31	OB3@51.1	7.29	Rh12GR_16570_782	44459262	27.59-53.75	27934327-46440369	15.43-53.75	23585838-46440369
	PM2017	2.49	3.58	OB3@51.1	6.65	Rh12GR_16570_782	44459262	20.14-53.75	24888779-46474274	18.8-53.75	24000000-46440369
	PM2018	2.51	4.48	OB3@45.7	11.78	Rh12GR_34665_95	41401120	36.99-53.75	35014990-46440369	20.14-53.75	24888779-46440369
1b	PF2016	2.42	8	RW3@42.6	20.05	Rh12GR_52506_1218	42317122	37.69-42.55	41648024-42317122	35.67-42.55	40854291-42317122
	PF2017	2.38	8.31	RW3@42.6	12.94	Rh12GR_52506_1218	42317122	37.69-42.55	41648024-42317122	37.69-42.55	41648024-42317122
	PF2018	2.36	8.03	RW3@42.6	21.45	Rh12GR_52506_1218	42317122	37.69-42.55	41648024-42317122	37.69-42.55	41648024-42317122
	PM2016	2.51	5.88	RW3@42.6	12.76	Rh12GR_52506_1218	42317122	16.8-42.55	32557591-42317122	9.44-42.55	16767733-42317122
	PM2017	2.41	9.56	RW3@42.6	12.12	Rh12GR_52506_1218	42317122	37.69-42.55	41648024-42317122	35.67-42.55	40854291-42317122
	PM2018	2.5	11.48	RW3@42.6	37.40	Rh12GR_52506_1218	42317122	28.3-42.55	36807925-42317122	16.8-42.55	32557591-42317122
2	PM2016	2.31	2.89	OB4@30.6	11.64	Rh12GR_60129_183	52239028	20.53-48.59	46189407-56107784	5.77-48.59	33319795-56107784
	PM2017	2.49	3.15	OB4@30.6	13.18	Rh12GR_60129_183	52239028	11.81-48.59	36731337-56107784	4.43-48.59	30431277-56107784
	PM2018	2.51	3.3	OB4@30.6	10.35	Rh12GR_60129_183	52239028	11.81-48.59	36731337-56107784	7.78-48.59	34803638-56107784
3	PF2017	2.38	2.8	RW6@29.7	6.73	Rh12GR_56601_1304	31814891	8.11-42.49	4339433-44264630	0-48.52	1518964-48810479
	PF2018	2.36	2.81	RW6@11.5	6.67	Rh88_37299_454	5410244	6.74-44.11	7764439-62612495	1.34-54.05	1461254-64122872
	PM2016	2.51	4.16	RW6@29.7	8.45	Rh12GR_56601_1304	31814891	0-38.43	1518964-48896977	0-42.49	1518964-44264630
	PM2017	2.41	2.7	RW6@29.7	7.07	Rh12GR_56601_1304	31814891	15.59-45.19	8578645-45439915	8.11-49.9	4339433-41715319
	PM2018	2.5	2.58	RW6@29.7	5.28	Rh12GR_56601_1304	31814891	4.21-48.53	3340353-48180089	0-53.21	1518964-52689670
4	PF2016	2.42	3.08	RW1@34.2	6.52	RhK5_3678_875	59006755	12.78-44.11	20231658-62553371	6.74-54.05	7764439-64122872
	PF2018	2.36	3.04	RW1@34.2	6.99	RhK5_3678_875	59006755	6.74-44.11	7764439 -62553371	1.34-54.05	3670420-64122872

[a] PT Genome-wild LOD significance threshold was defined by a permutation test.

[b] LG@positon Chromosomal linkage group, using the separate map (OB and RW) numbering of (Hibrand-Saint Oyant et al., 2018) @ peak location in cM.

[c] r(%) Percentage of explanation.

[d] MM Closest molecular marker (MM) associated.

[e] bp Location in base pair (bp) on the Rosa chinesis Genome v1.0 (Hibrand-Saint Oyant et al., 2018).

[f] cM CentiMorgan position of QTL peak.

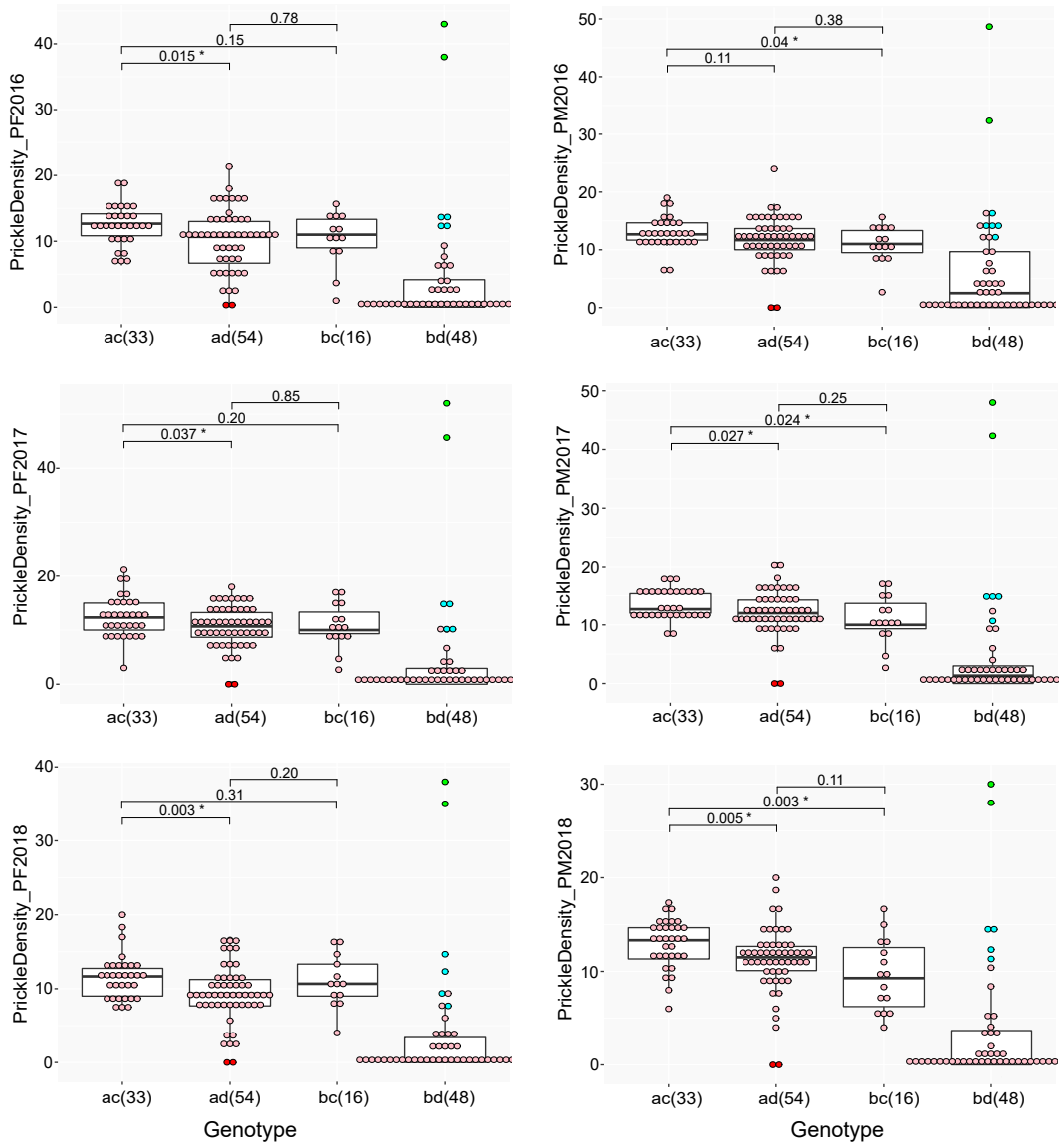

Figure 27: The interaction of the different alleles of the LG3 QTL between OB and RW. Genotype: *ac, ad, bc, bd* (number of individuals), *a/b* and *c/d* alleles belong to females and males, respectively. For the phenotype, the mean values of prickle density for PF and PM for the three years are presented. Some individuals are highlighted with green dots (OW9106 and OW9107), blue dots (OW9062, OW9021, OW9052 and OW9109) and red dots (OW9067 and OW9068). The asterisk indicates that the difference is significant with a p-value of less than 0.05

except for PM2016 between *ac* and *ab*; Figure 27), even if the effect is weak (no large difference between the mean for *ac* and *ad/bc*). For PF, no co-dominant effect was detected.

We also observed some odd phenotypes. For instance, OW9067 and OW9068 (red dots) had no prickle and were grouped in the *ad* genotype, perhaps due to recombination between the marker and the prickle locus (Figure 27). For individuals with the *bd* genotype, six individuals (blue and green dots) always have prickles: OW9062, OW9021, OW9052 and OW9109 (blue dots) look like the usual prickle genotypes and are probably caused by recombination, but the two extreme exceptions, OW9106 and OW9107 (green dots) with the highest prickle density are not that easy to clarify. Moreover, some individuals exist with both prickly and glabrous stems in the same plant.

3.3.3 Candidate genes in the QTL interval region and gene expression analysis

3.3.3.1 Candidate gene characterization and location in rose

Since it was proposed that prickles originate from a deformation of glandular trichomes in rose (Kellogg et al., 2011), we looked for rose homologues of transcription factors (TF) known to be involved in the molecular control of trichome initiation and development in *Arabidopsis*. The information from 15 TFs such as the bHLH (basic helix-loop-helix), C2H2 Zinc-Finger, MYB, WD40 repeat and WRKY families are presented in Supplementary Table A.3. For a more detailed annotation, we performed phylogenetic analyses on these protein families (Supplementary Figure A.2).

Concerning the bHLH family (Supplementary Figure A.2 a), RC7G0190300, RC1G0342400 and RC6G-0407800 showed strong similarity with GLABROUS3, MYC1 and TT8, respectively, where all of the proteins are in the same clade. They are referred to as RcGL3, RcMYC1 and RcTT8, respectively.

For the C2H2 family, RC3G0150000, RC4G0390900 and RC4G0476500 are closely related to GLABROUS INFLORESCENCE STEMS proteins (GIS, GIS2 and GIS3) and ZINC FINGER PROTEIN (ZFP5, 6 and 8). RC3G0150000 seems to be more closely related to GIS2, RC4G0390900 to GIS3 and RC4G0476500 to ZFP5. RC2G0415300 and RC6G0454700 are related to ZFP1 and ZFP3 and AT5G10970. They are referred to as RcZFP1-like1 and RcZFP1-like2, considering that they are closer to ZFP1 (Supplementary Figure A.2 b).

R2R3 MYB and R3 MYB belong to the MYB family (Supplementary Figure A.2 c). In the R2R3 MYB sub-family (blue sub-tree), RC7G0156100 is in the same clade as GLABROUS1, whereas RC2G0033100 and RC7G0261400 are more closely related to MYB82 and TT2, respectively. RC3G0322900 is in the same clade as MYB61, MYB50 and MYB86. In the R3 MYB sub-family (red sub-tree), RC2G0548400, RC1G0560100 and Chr1g0359121 (Raymond et al., 2018) are in the same clade of CPC, TRY, ETC1 and ETC3. RC1G0560100 and Chr1g0359121 are more closely related to TRY and CPC, and are referred to as RcTRY and RcCPC, respectively. (Supplementary Figure A.2 d).

In the WD40 family, RC1G0586100 showed a strong similarity to TRANSPARENT TESTA GLABRA 1(TTG1), and RC3G0186600 and RC2G0693200 also belong to this clade. In the WRKY family, as previously shown by (Hibrand-Saint Oyant et al., 2018), RC3G0244800 shows a strong similarity with AtTTG2 (TESTA-TRANSPARENT GLABRA2), whereas RC3G0309600 and RC3G0309700 seem to be more closely related to WRKY54 and WRKY70, RC3G0392200 to WRKY74, and RC3G0414600 appears to be related to WRKY34 and WRKY2. We then located these rose homologue genes on the rose genome and looked for co-location between these genes and the QTLs previously described (Figure 26 a and b). Concerning the QTLs on LG3 (male and female map, Figure 26 a and b), the most interesting TF among the detected genes was RcMYB61 (RC3G0322900, at Chr03: 39,896,892 - 39,899,077bp) located in the cQTL interval (36.517-46.440 Mb) for the female map (Figure 26 a). As previously described (Hibrand-Saint Oyant et al. 2018), a homologue of TTG2, a WRKY transcription factor (RC3G0244800), is also located in the credible interval. RcGIS2 (RC3G015000), a GIS2 homologue is also located on LG3 but not in the cQTL interval. In addition to the candidate TFs, we also scanned the other TFs co-located in the cQTL interval on LG3 of the female map. There are four bHLH, two C2H2, three R2R3MYB and seven WD40 transcription factors (Supplementary Figure A.2, in blue) located under the cQTL.

Concerning the cQTL interval on LG4, RcGIS3 is positioned at Chr04: 50,315,805 - 50,317,009 (1.21 Kb), and near the peak marker Rh12GR_55601_1304 (52,239,028 kb) on the female map (Figure 26 a). RC4G0476500, a ZFP5 homologue, is also located on the female LG4 but not in the QTL interval.

Concerning the QTL on the male LG1, RcMYC1, RcTRY and RcCPC, which are positioned at 44,468,298 - 44,473,643 bp, 47,708,966- 47,709,896 bp and 62,070,383 -62,072,848 bp, respectively, are located in the cQTL region (20.232Mb-62.553Mb) of PF (2016, 2018) on the male LG1. The gene RC1G0586100 (RcTTG1) is also located on LG1 but outside this interval. For the male LG6, RC6G0407800, a homologue of TT8, is not located in the cQTL credible interval, and no studied gene was detected below this QTL.

3.3.3.2 Candidate gene expression in glabrous and prickle roses

Based on the positional approach, we identified ten interesting candidate genes, six within the QTL interval and the other four outside of QTL but near the credible interval (Figure 26). In order to obtain more information about these genes, we studied their transcript accumulation by RT-qPCR in tissues from prickle (P) and prickless (NP) stems at different developmental stages: I, IIa, IIb, IIc, III (Chapter 2, Figure 13).

The cluster analysis of gene expression clearly showed that all the samples can be divided into two main groups: PI, NPI, PIIa, NPIIa, PIIb, NPIIb were gathered into one group, and PIIc, NPIIc, PIII, NPIII into another group (Figure 28 a). At the sup-group level, PI and NPI, PIIa and NPIIa, PIIb and NPIIb, PIIc and NPIIc were clustered together, respectively. At the same stem developmental stage, prickle and glabrous samples (P and NP) behave similarly, suggesting no major difference of transcript accumulation between prickle and glabrous samples; the observed differences are more closely related to stem development.

To extend the analysis even further, we used NP as a control to compare the normalized expression of

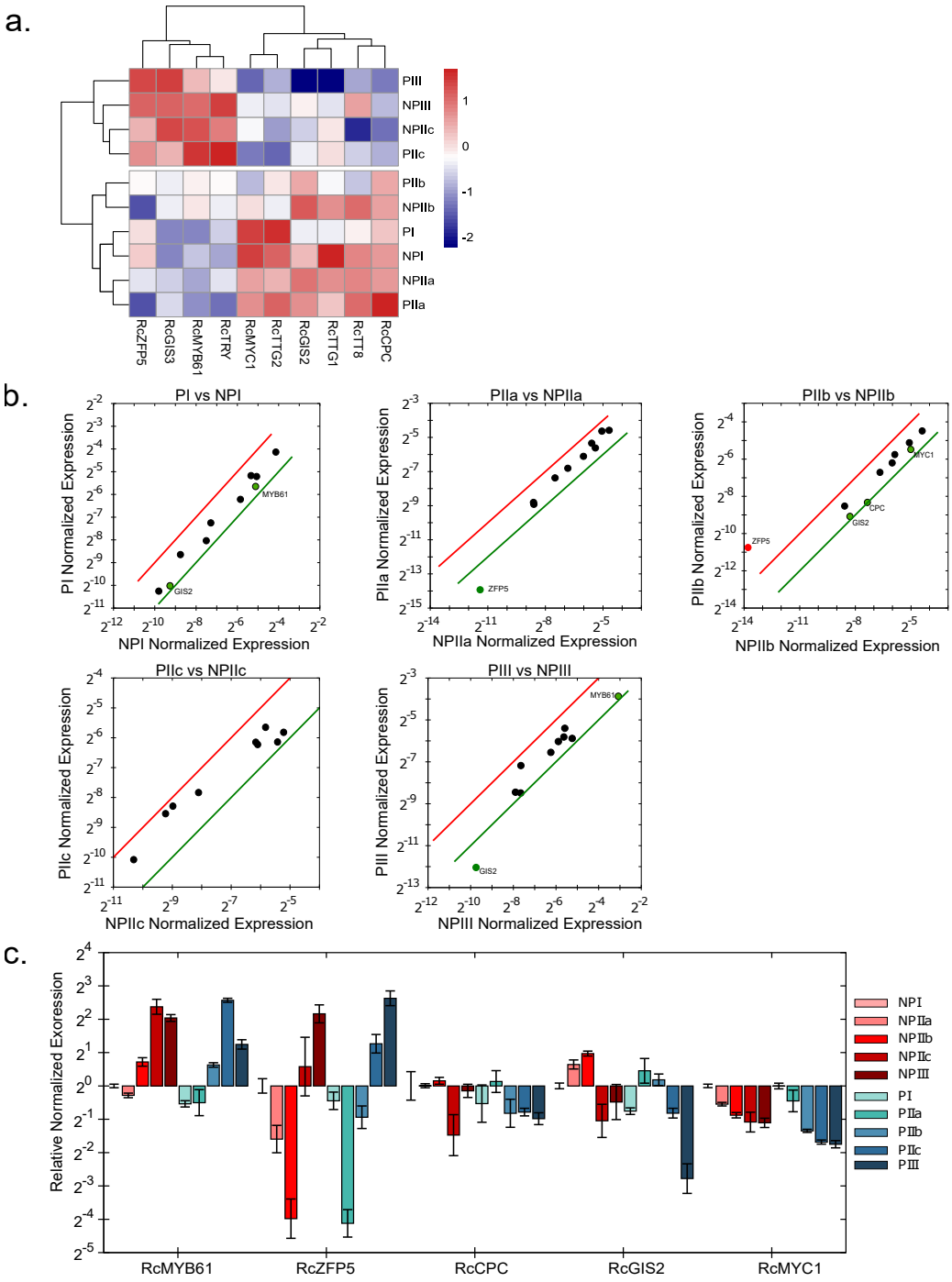

Figure 28: Transcript accumulation of candidate genes followed by qPCR during prickle development. (a) A heatmap of samples and genes. (b) The scatter plot of the candidate genes' normalized expression in prickle and glabrous individuals in different stages (as defined in Chapter 2, Figure 13). The red and green lines represent a two-fold change in the accumulation with an increase or a decrease, respectively. Gene transcripts differentially accumulated (p-value < 0.05) are represented by red or green dots for up- or down-accumulation, respectively. (c) Transcript accumulation in the different stages of prickle (P) and glabrous (NP) stems with NPI as a control.

genes between P and NP samples in the different stages (Figure 28 b). In stage I, two genes are differentially expressed: RcMYB61 and RcGIS2 were down-regulated in prickly stems, with a significant *p-value* = 4.1^{e-5} and 2.9^{e-4} (Figure 28 b), respectively. In stage IIa, only RcZFP5 was significantly differentially expressed between P and NP, with a *p-value* = 0.0056 and FC = -5.7606 (Figure 28 b). A different pattern is observed in stage IIb where RcZFP5 expression was up-regulated with FC = 8.2240 and a *p-value* = 0.0025. In addition, the transcripts of RcMYC1, RcCPC and RcGIS2 were also significantly accumulated (*p-value* = 4.1^{e-5}, 0.0048, 0.0012, respectively) in stage IIb. In stage IIc, no significant change in gene expression was detected. In stage III, the RcGIS2 transcript is differentially accumulated with FC = -4.908 and a *p-value* = 0.043. The same pattern is observed for RcMYB61 with a *p-value* = 4.9^{e-4}.

We followed the transcript accumulation during stem development in prickly and glabrous stems (NPI as a control; Figure 28 c). All the studied genes are regulated between the different samples. For instance, RcMYB61 is up-regulated and RcMYC1 is down-regulated between the different stages. For RcZFP5, we observed a delay in the decrease of transcript accumulation, with a decrease in stage IIa for glabrous stems and in stage IIb for stems with prickles (Figure 28 c).

3.4 Discussion

3.4.1 Two types of prickles are present in the OW progeny, originating from different structures

A good understanding of prickle morphology is required to serve as the foundation for genetic and molecular studies. We identified two different types of prickles in our population: it appears that GP and NGP originate from glandular and non-glandular structures, respectively. This conclusion is different from previous studies in rose, which reported that prickles were extensions or modifications of glandular trichomes (Kellogg et al., 2011), and in other species (Ma et al., 2016b; Pandey et al., 2018). Asano et al. (2008) observed two types of prickles in the cultivated rose 'Laura', described as large size and small size prickles. The large size prickles look similar to NGPs in our study. The small size prickles, referred to as acicles (Asano et al., 2008), are more closely related to the glandular prickles (GP) we observed since they have a glandular head that accompanies them throughout their lifetime. The difference between these two types of prickles is also related to their segregation in the OW population (Figure 23 d), demonstrating that different genetic determinisms are involved. In this study, since only a few F_1 individuals had GPs, we cannot perform a genetic analysis on GPs, we concentrated our analysis on NGPs.

3.4.2 A complex genetic determinism for prickles in rose

Prickles on stems exhibited transgressive segregation in diploid OW, the same as for the tetraploid K5 population (Koning-Boucoiran et al., 2012; Gitonga et al., 2014; Bourke et al., 2018a), supporting the hypothesis that multiple loci may be responsible for this trait.

Using the 'non- parametric' QTL approach, we detected a stable QTL on LG3 in the three different years for both types of stems (PM and PF) on both the male and female genetic maps. We also demonstrated that this QTL mainly controls the presence/absence of prickles (Figure 24) using the 'two-part' QTL method. Interestingly, for PM in males, the QTL on LG3 may also be involved in regulating prickle density (severity in the two-part QTL analysis; Figure 24). A similar phenomenon was observed for the petal number with a locus on LG3 that controls the difference between simple and double petals, and a variance of the petal number that exists within the double petal flower is controlled by another locus (Roman et al., 2015; Hibrand-Saint Oyant et al., 2018).

We further enhanced the description of QTLs on LG3 that affect the presence/absence of prickles. A significantly distorted segregation was observed at the peak marker position. That unusual segregation ratio might be explained by the presence of a self-incompatibility locus (Hibrand-Saint Oyant et al., 2018) near the peak marker for this QTL. On the basis of the phenotype-genotype relationship (Figure 27), we proposed that the *PRICKLE* alleles on this QTL are both heterozygous (np/P) in OB and RW, and that the presence of prickles is controlled by a dominant allele (np/P or P/P), and that the glabrous stem in the progeny is due to the combination of the two recessive alleles coming from both parents (np/np). These results are important for breeders who need to combine recessive alleles to obtain glabrous roses, an allelic combination that can be difficult in tetraploid roses. Development of specific molecular markers of the recessive allele may by useful for breeders. However, it should be noted that the actual markers used (peak of the QTL) are only closely linked to the *PRICKLE* locus and few recombinants are observed in the progeny. Furthermore, the phenotype of the individuals with the two recessive alleles (*bd* phenotype; Figure 27) are not stable and some of the hybrids were regularly seen to develop some prickles on parts of the stems. Indeed, this phenomenon is widespread in roses. Rose breeders have reported that glabrous mutants have either been unstable for the prickless trait (Nobbs, 1984; Rosu et al., 1995), or reverted to the prickly character after a freezing winter or other environmental stresses (Nobbs, 1984; Oliver, 1986; Druitt and Shoup, 1991; Canli, 2003). Taken together, we assumed that a single major locus on LG3 controlled the absence/presence of stem prickles. Further investigations are necessary to more closely identify molecular markers (for molecular assisted breeding) and the mechanisms behind the instability.

In the *ac*, *ad* and *bc* genotypes, each genotype has a continuous quantitative trait, indicating that there are other loci responsible for prickle density variance. Other QTLs affecting quantitative traits were detected on LG4 in OB and on LG1 and 3 in RW (Two-part QTL analysis; Figure 24). The LG4 QTL has a strong effect on PM but a weak effect on PF. For the QTL on LG1, it only had a weak effect on PF and on PM in 2018. Those three loci are related to the density of prickles, indicating that there are multiple genes responsible for the density trait, and that those genes have a different effect on the different stems.

3.4.3 Detected QTLs are conserved in the *Rosa* genus and the *Rosideae* subfamily

Thanks to the link between genetic maps and reference genome sequences (Hibrand-Saint Oyant et al., 2018), we were able to compare our results with previous genetic studies by associating genetic map markers.

A QTL was previously detected on LG3 in different diploid and tetraploid populations (Crespel et al., 2002; Linde et al., 2006; Koning-Boucoiran et al., 2012; Hibrand-Saint Oyant et al., 2018; Bourke et al., 2018a), which is consistent with our results: a strong QTL on Chr3 with a high LOD value was detected in all of the environments (across and between years and types of stems). This demonstrated that Chr3 QTL is a robust QTL detected independently of ploidy and the environment, and is present in various genetic backgrounds.

Recently, three QTLs on LG3, 4 and 6 were detected in the tetraploid K5 population with a high density of SNPs genetic map (Bourke et al., 2018a). Interestingly, the QTLs identified from the diploid (OW) were almost identical to tetraploid (K5) populations (LG3, 4 and 6), with the slight difference that we also detected a weak QTL on LG1, which was only significant in males for two of the years. This slight difference might be due to the genetic background of the parents of the K5 and OW populations. In fact, in K5 populations, one parent is prickly and the other glabrous, whereas in OW populations, both parents have prickles. Bourke et al. (2018a) reported that two SNP markers, K7826_576 (located on the Chr3: 37,706,920 pb) and K5629_995 (located on the Chr4: 57,791,999 bp) are linked to the stem prickle trait. When compared with our results, K7826_576 is located within our Chr3 cQTL interval region (36,517,224 - 46,440,369 bp; Figure 26), and K5629_995 is very close to our Chr4 QTL interval (46,189,407 - 56,107,784 bp). These results suggest that QTLs detected on LG3 and 4 could be similar between OW and K5 progenies.

In *Rosaceae*, the genetic determinism of prickle was studied in raspberry (*Rubus idaeus*), where two QTLs were detected on LG4 and 6 (Molina-Bravo et al., 2014). Using synteny viewer tools (`https://www.rosaceae.org/synview/search`; Jung et al. (2014)), we checked the synteny. The region where the QTL is located on LG6 in *R. occidentalis* (position 6.028Mb) is syntenic with a region on rose chromosome 2 (position 42.330 Mb), where no QTL for prickle density was detected in our study. The region where the QTL 4 is located (position 0.101 Mb) is syntenic with the region on rose chromosome 4 (position 58.768 Mb), very close to the main QTL we detected on this chromosome (Table 4). These results could suggest that the two QTLs in rose and raspberry might be syntenic and share a common evolutionary history. In another publication, Graham et al. (2006) identified the gene H that controls cane pubescence. The locus is mapped on LG2, which is syntenic with the rose LG6 where one of the QTLs is located, detected in *R. x wichurana*. However, no precise location is available to allow us to assume a possible common origin.

3.4.4 Candidate gene below the QTL interval region

Prickles are assumed to originate from a 'trichome-like structure'. In order to find a putative candidate gene for the identified QTLs, we looked for homologue genes known to be involved in trichome initiation and development in *Arabidopsis*. We annotated 15 rose TFs that, based on similarity, can be involved in trichome development in rose: RcGL1, RcMYB82, RcMYB61, RcCPC, RcTRY, RcGL3, RcTT8, RcMYC1, RcTTG1, RcTTG2, RcZFP5, RcGIS3, RcGIS2, RcZFP1 and RcGL2 (Supplementary Table A.3). Among them, a few were below the detected QTLs: RcMYB61 and RcTTG2 below the QTL on LG3; RcGIS3 below the QTL on LG4; and RcCPC, RcTRY and RcMYC1 below the QTL on LG1. ZFP5 (Chr04: 57,125,905 bp) is out of

the QTL interval on LG4 in OW, but close to the peak LOD marker K5629_995 of QTL in the K5 population (Chr04: 57,791,999 bp) (Bourke et al., 2018a). These genes are good candidates for the detected QTLs.

3.4.5 Candidate genes transcript expression in glabrous and prickle F_1 individuals

We quantified ten TF gene transcripts in glabrous and prickle F_1 individuals in different developmental stages using RT-qPCR. Surprisingly, minor differences were observed between glabrous and prickle samples, with the main differences occurring between developmental stages (as demonstrated by the heatmap analysis, Figure 28 a). Based on transcript accumulation, this suggests that these homologues, known to be involved in trichome initiation and development in *Arabidopsis*, are not implicated in prickle initiation in rose, leading to the hypothesis that the two processes (trichome initiation and prickle initiation) might involve different gene pathways. The candidate gene approach may not be appropriate and a non-a priori approach such as a transcriptomic analysis could be done between individuals with and without prickles. Nevertheless, some differences in transcript accumulation are observed between candidate genes. In the early stage (stage I), only *RcMYB61* and *RcGIS2* are slightly more highly accumulated in glabrous stems. However, GIS2 and MYB61 are positive regulators of trichome initiation (Gan et al., 2006), which is difficult to reconcile with an increase in transcript accumulation in glabrous stems (Figure 28). Negative feedback regulation during prickle initiation can explain this point, as regularly observed in trichome initiation (Pattanaik et al., 2014) or, perhaps, differences are not at the transcriptional level. It could be interesting to sequence the genes in the two parents to see if a mutation can explain the phenotype.

RcZFP5 may also be an interesting candidate gene. This gene showed a different regulation between glabrous and prickly stems. At stage IIa, *RcZFP5* shows a strong down-regulation in glabrous tissue, whereas this down-regulation is observed later at stage IIc in tissues with prickles (Figure 28 c). Furthermore, this gene is close to the QTL on LG4. Its early repression in glabrous stems might explain why no prickle developed. In *A. thaliana*, *ZFP5* controls trichome initiation through GA signaling (Zhou et al., 2011). These data (concerning ZFP5 and MYB61) might suggest an implication of GA in prickle development. However, this hypothesis needs to be functionally validated in rose.

Conclusions

Prickle structure is an undesirable trait, not only in rose but in most crops in general. We identified a complex genetic determinism with a major locus on LG3 that controls the presence of prickles and a few QTLs that control prickle density. Further studies are necessary to develop markers for breeding selection and to identify the molecular bases. Using a candidate gene approach, we proposed different hypotheses concerning the gene involved in prickle initiation in rose. Approaches such as transcriptomics may help to identify new key regulators of prickle initiation and development in rose.

Author's contributions

Zhou NN designed the projects and obtained funding, planned and performed experiments, collected and analyzed data, and drafted the manuscript. Foucher F and Hibrand-Saint Oyant L were responsible for piloting and supervising the project, and for revising the manuscript. Tang KX contributed to designing the project and obtaining funding. Jeauffre J led the qPCR experiment and analyzed data. Thouroude T prepared the plant cuttings of F1 individuals in the greenhouse. Lopez Arias D modified the genetic map and helped to develop the R/qtl script.

Orcid-ID

Zhou NN: orcid.org/0000-0002-5208-6788

Tang KX: orcid.org/0000-0003-3807-784X

Jeauffre J: orcid.org/0000-0001-6770-0552

Thouroude T: orcid.org/0000-0001-7908-7353

Lopez Arias D: orcid.org/0000-0001-8129-2786

Foucher F: orcid.org/0000-0002-3693-7183

Hibrand-Saint Oyant L: orcid.org/0000-0002-4451-8798

Acknowledgments

We are grateful to the experimental unit (UE Horti) for their technical assistance in plant management, and the ImHorPhen team (Besnard D, Gardet R) of IRHS for taking care of the plant cuttings in the greenhouse. We would also like to thank the IMAC technical platforms (Simonneau F, Rolland A) of SFR Quasav for supervising the histological experiment, and the PTM ANAN (Bahut M) of the SFR Quasav for overseeing the RT-qPCR experiment. We acknowledge Chameau J of the GDO team for helping to obtain the different stages of the sample.

Funding

This work was supported by funding from the National Natural Science Foundation of China (31760585), the China Scholarship Council ([2017]3109) and the Natural Science Foundation of Yunnan (2016FB061).

4 In-depth RNA sequencing analysis provides molecular mechanism insight into prickle initiation and development in rose

Zhouu NN[1,2], Tang KX[2], Jeauffreu J[1], Thouroude T[1], Hibrand-Saint Oyant L[1*] & Foucher F[1*]

1 Univ Angers, Institut Agro, INRAE, IRHS, SFR QUASAV, F-49000 Angers, France.

2 National Engineering Research Center for Ornamental Horticulture; Flower Research Institute, Yunnan Academy of Agricultural Sciences, Kunming 650231, China.

Corresponding author: ningning.zhou@aliyun.com or fabrice.foucher@inrae.fr

4.1 Introduction

Prickles are non-vascular sharp appendages and can be easily distinguished from thorns and spines which are modified stems and leaves respectively (and therefore they are usually vascularized). Many studies have been reported on their ecological, evolutionary, and biogeographic implications. From a functional perspective, spinescences (prickles, thorns, and spines) have been proposed as an effective defensive strategy against herbivores (Janzen, 1976; Cooper and Owen-Smith, 1986; Belovsky et al., 1991; Gowda, 1996; Burns, 2014; Wilcox, 2017).

A piece of paleontological works offered evidence that spinescence structure may appear in the late Silurian ($\sim$ 400 million years ago) which is before the mammal herbivores' appearance (Chaloner, 1970). Thus, the evolution of spinescences may not be a response to the pressure of large herbivores (like mammals) but rather to other biotic or abiotic pressures (such as small herbivores like insects, reviewed by (Wilcox, 2017). While this is still a controversial topic since most researchers supported that spinescence evolved against mammalian herbivores (Cooper and Owen-Smith, 1986; Burns, 2014). Nevertheless, in the process of co-evolution with herbivores, plants have evolved an impressive defense system where spinescences play a key role. Many types of spinescence have been produced (or modified) from the shoot, leaves, fruits, pedicels, and even roots. Besides providing mechanical protection, the spinescence structures are frequently cooperating with predatory pathogenic bacteria, fungi and toxic chemicals, enhancing their attack or defense

ability (Halpern et al., 2007; Lev-Yadun, 2016). On thorns of *Phoenix dactylifera* and *Crataegus aronia*, fifty-eight bacterial isolates were found and they are belonging to 22 different bacterial species: 13 of them are known to be pathogenic for animals or humans, such as *Clostridium tetani*, a etiological agent of tetanus (Halpern et al., 2007). Spinescence injuries have been reported to cause tetanus on humans and others predators in several countries (Hodes and B., 1990; Pascual et al., 2003; Ergonul et al., 2003; Campbell et al., 2009; Tadele, 2017). Thus, rose bush prickles can cause puncture wounds that resulted in tetanus (Pascual et al., 2003). Important human diseases are caused by prickle wounding: mycetoma caused by *Eumycetoma* (fungi) or *Actinomycetoma* (filamentous bacteria) and sporotrichosis diseases caused by *Sporothrix schenckii* (fungi), are called "plant thorn synovitis" and "rose-thorn or rose-gardeners' disease" respectively. The most common route of infection is the introduction of spores to the subcutaneous cellular tissues through a wound of the skin (Fahal, 2004; Barros et al., 2011; Vásquez-del-Mercado et al., 2012; Mahajan, 2014; Kieselova et al., 2017). *Dermatophytes* that cause subcutaneous mycoses are unable to penetrate the body and must be introduced into the subcutaneous tissue by a puncture wound (Willey et al., 2008). These spinescence structures inject bacteria into herbivores (or other mammals as human) by wounding, they may cause severe infections that are much more dangerous than the mechanical wounding itself (Halpern et al., 2007; Lev-Yadun, 2016). Some bacteria species probably are adapted to live and multiply on the spinescences (hence they are present in large numbers) and not just landed on the spinescence accidentally (Halpern et al., 2007). Spinescence color is also an important aspect of the protective property. The bright color prickles and other types of sharp appendages are frequently observed, especially in the juvenile phases of development. This special character confers a selective advantage as herbivores learn to associate conspicuous coloration with unpleasant qualities (Cott, 1940; Edmunds, 1974; Ruxton et al., 2004; Speed and Ruxton, 2005).

In addition, the role of spinescences against insects is often neglected nowadays. Some species (such as *Acacia collinsii*) developed large hollow spines as a habitat for ants, which protect the plants against herbivory insects (Janzen, 1976). Prickles, such as those on roses, may play a role in reducing caterpillar feeding by restricting their movement (Kariyat et al., 2017).

In the agricultural production process, prickle is an undesirable trait in many crops as roses because it can injure workers and also damage crops (especially for cutting roses). Rose is a typical representative of prickly plants with the most important economic value in ornamental plants. In roses, prickles are distributed wildly on stems, pedicel, peduncles, leaves, or fruits, and their distribution on the organs is a source of a large diversity within the *Rosa* genus. Two major categories of prickles on stem have been described in roses: 'non-glandular (NGP)' and 'glandular (GP)' prickles (see Zhou et al., 2020, Chapter 2). NGPs are normally unbranded and can be naked on the surface or covering with hairs (hairy). GPs can be branched or unbranched, and the unbranched GPs also present the naked and hairy types (see Chapter 2, unpublished yet). Unbranched and naked NGP is the most common type of stem prickle found in wild (see Chapter 2). The genetic and molecular mechanisms underlying prickle initiation and development remain still largely unknown. Four loci on linkage group 1, 3, 4, 6 have been detected to control stem NGPs in OW population (*Rosa chinensis* 'Old Blush' × *R.* × *wichurana*) (see Zhou et al., 2020, Chapter 3). The

major locus on LG3 was shown to control the absence/presence of NGPs. Another major locus on LG4 was associated with prickle density (Zhou et al., 2020). NGP are described as modified glandular trichomes (Peitersen, 1921; Coyner et al., 2005; Kellogg et al., 2011; Ma et al., 2016b; Khadgi and Weber, 2020a). However, this hypothesis was not supported by histological study and molecular data, as prickle does not come from protoderm (or epidermis) but from ground meristem under protoderm (see Chapter 2) and the rose homologue of genes involved in *Arabidopsis* trichome initiation and development might not be controlling prickle initiation and development in rose (see Zhou et al., 2020, Chapter 3). Further studies are necessary to identify new key regulators of prickle initiation and development in rose.

Here our objectives are to decipher the gene network that controls prickle initiation and development in rose using a transcriptomic approach. Using four F1 individuals of OW population, we present the first profile of the transcriptomic changes during prickle initiation and development by comparing the transcriptome of rose stems with and without prickles and a detailed time-course transcriptomic analysis of prickle development. This detailed analysis allows us to detect important regulators of prickle initiation and development. By combine with previous genetic data (Zhou et al., 2020), we spotlight the best potential regulators of prickle initiation. We provided pieces of evidence to support our new insight of non-glandular prickles and trichomes have different gene pathways.

4.2 Materials and methods

4.2.1 Plant materials

A diploid OW population obtained from the female *Rosa chinensis* 'Old Blush' (OB) × the male *Rosa x wichurana* (RW), were grown in a field and managed by the Horticulture Experimental Unit (INRAE, Angers, France). We selected four once-flowering individuals: two presented non-glandular prickles (NGP) (OW9071 and OW9137) and two are glabrous (OW9067 and OW9068). Those genotypes were vegetatively propagated and grown in a greenhouse in November 2017. Harvesting was done in the morning from March 27th to April 5th, 2018. We mixed OW9067 and OW9068 materials as prickless samples, and OW9071 and OW9137 as prickle samples. We randomly divided 18 cuttings per genotype into three groups as three biological replicates. Under a microscope, unexpanded leaves and buds were removed, and we took samples of stages I, IIa, IIb, IIc and III strictly according to previously described stages of prickle (P) and glabrous stem (NP, stems at the same stages for P) (see Zhou et al., 2020, Chapter 2).

4.2.2 RNA isolation and experimental design

RNA was isolated according to Zhou et al. (2020). Total RNA concentration, RIN value, 28S/18S and fragment size were measured using Agilent 2100 Bioanalyzer (Agilent RNA 6000 Nano Kit). Purity of RNA was determined by agarose gel electrophoresis and ultraviolet spectrophotometer NanoDropTM.

Experiment design depending on the morphological studies of developing rose prickle (see Chapter 2). We designed two experiments to study genes involved in prickle initiation and development. 1) For prickle development, stage I, IIa, IIb, IIc, III of P samples (refers to PI, PIIa, PIIb, PIIc, PIII respectively) and I and IIa of NP samples (refers to NPI and NPIIa) were selected to search for gene expression patterns throughout the prickle initiation and development. Compare the differentially expressed genes in PIIavsPI and NPIIavsNPI to understand the specific and common genes that expressed in glabrous and prickle samples' development. We expected to answer what genes may be involved in prickle development. 2) Focus on prickle initiation, stages I and IIa of prickless (NP, control) and prickle (P, treatment) samples were selected to research genes' differential expressed in prickle and prickless. We expected to answer what genes may be involved in prickle initiation. In total, 21 samples were sent for RNA sequencing, they are NPI, NPIIa, PI, PIIa, PIIb, PIIc, PIII, each sample has three biological replications to verify the repeatability of the gene expression.

4.2.3 Generation of RNA-seq data

Library preparation and cDNA sequencing were performed at the Laboratory of the Beijing Genomics Institute (BGI), Hongkong, China. All the samples were sequenced by BGISEQ-500 platform in a Pair-End (PE)100 base pair run.

4.2.4 Bioinformatics analysis approach

We developed an RNA-seq analysis workflow that suitable for our data situation and for our project purpose (Supplementary Figure B.1). We provide details of the parameters used in each step as follows:

4.2.4.1 Quality control of data processing and genome alignment

FastQC version 0.11.2 (Andrews et al., 2010) was used to assess the quality of the raw and clean reads. RSeQC version 2.6.4 (Wang et al., 2012) was used to evaluate sequencing saturation, mapped reads distribution, coverage uniformity, strand specificity and transcript level RNA integrity. IGV (Robinson et al., 2011; Thorvaldsdóttir et al., 2013) tool was used to visualize the bam format file to check the distribution of reads alignment on the reference genome. MultiQC (Ewels et al., 2016) was used to have an overview of the results from FastQC, RSeQC, and STAR mapping.

4.2.4.2 Raw data filtering

Trimmomatic (Bolger et al., 2014) was used to trim low-quality bases and remove the shorter reads with the following parameters: *TruSeq3-PE.fa:2:30:10*, *LEADING:3*, *TRAILING:3*, *SLIDINGWINDO- W:4:15* and *MINLEN:50*. We kept the paired files as clean data for the next step analysis.

4.2.4.3 Reference genome alignment and expression analysis

Rose reference genome sequence (Hibrand-Saint Oyant et al., 2018) and annotation files were downloaded from the Genome Database for *Rosaceae* (GDR, (Jung et al., 2019)). STAR source code (Dobin et al., 2013) and binaries were used to generate genome indexes and to run mapping jobs. Parameters 'sjdbOverhang 99' and 'genomeSAindexNbases 13' were used to build rose reference genome indexes. For reference genome alignment, non-default parameters were set as follows: *'outFilterType BySJout'*, *'outFilterMultimapNmax 10'*, *'outFilterMismatchNmax 6'*, *'alignIntronMin 20'*, *'alignIntronMax 20000'*, *'alignMatesGapMax 20000'*, *'outFilterIntronMotifs RemoveNoncanonicalUnannotated'*, *'outSAMprimaryFlag AllBestScore'*, *'outFilter--MultimapScoreRange 0'*, *'outSAMtype BAM SortedByCoordinate'*, *'outSAM-unmapped Within'*.

FeatureCount source code (Liao et al., 2019) was used to count the number of sequence fragments that have been assigned to each gene and summary the assigned information of unique mapped reads. StringTie version 1.3.6 (Pertea et al., 2015) was used to calculate the normalized expression value, transcripts per million (TPM), of each gene.

4.2.4.4 Identification of differential expression genes

DESeq2 package (Love et al., 2014) was used to test for differential expression. Reads per genes calculated from FeatureCount were used for the input value. Condition formula was designed as multiple groups, then used *'coef'* argument of *'lfcshrink'* function to extract comparisons of interest after fitting the model. *'lfcShink'* function (with *lfcThreshold = 1* and *type='apeglm'* (Zhu et al., 2019)) was used to improve the previous estimator and to wrap up the result table. *'subset'* function was used to export the result table. When the svalue < 0.05 and $|log2FoldChange|$ >1, we considered that the genes were significantly differentially expressed (SDE).

4.2.4.5 Principal Component Analysis (PCA) analysis

PCA plot was carried out in R using the *calibrate* package. The input value (log transformation) is calculated by DEseq2 with *DESeqDataSetFromMatrix* and *rlogTransformation* function.

4.2.4.6 Clustering expression pattern in the prickle development stage

TCseq package was used to do clustering analysis and visualization of prickle development sequencing data (Wu et al., 2008). *'DBanalysis'* function was used to perform differential binding analysis with setting *filter.type = 'cpm'*, *filter.value = 1*, *samplePassfilter = 2*. *'timecourseTable'* function was used to constructs time course table for clustering analysis with setting *value= 'expression'*, *norm.method = 'cpm'*, *filter = TURE*. *'timeclust'* function performed clustering analysis with setting *algo = 'cm'*, *k=9*, *standardize = ture*. *'timeclustplot'* function plot clustering results.

4.2.4.7 Gene ontology and enrichment analysis

The similarity of the 44,481 annotated genes of *Rosa chinensis* 'Old Blush' was determined by pairwise sequence comparison using the blastx algorithm against various protein databases (GDR, https://www.rosaceae.org/species/rosa/chinensis/genome_v1.0) with an expectation value cutoff less than 1^{e-9} for the NCBI nr (Release 2017-07) and 1^{e-6} for the *Arabidopsis* proteins (TAIR10) (Hibrand-Saint Oyant et al., 2018). 28,760 genes that have matched uniport SwissProt ID which was set as a reference background for GO enrichment analysis. With *A. thaliana* as the organism database and Over-Representation Analysis (ORA) as the method of interest, gene ontology (Biological process nonredundant, cellular componentnonredundant, and molecular function nonredundant) functional database and Uniprot-SwissPort gene ID were used for performing functional enrichment analysis, on the webGestalt 2019 platform (Liao et al., 2019). For the SDE genes of PIvsNPI, we reported enrichment of biological process nonredundant when the false discovery rate (FDR) was ≤ 0.1. For the nine clusters of genes expressed in different patterns of the prickle developmental stages, we reported the enriched category with the FDR ≤ 0.05. With *log10* of FDR, we visualized the enriched GO in the different patterns of genes. When *FDR = 0*, we convert to *-log10 (0)* as 10.

4.2.4.8 Protein-Protein Interaction Networks

We used STRING tool (https://string-db.org/) to search protein-protein interaction networks between the candidate genes by searching SwissProt ID in *A. thaliana* dataset. The network type is full network (the edges indicate both functional and physical protein associations). Active interaction sources including text mining, experiments, databases, co-expression, neighborhood, gene fusion, and co-occurrence. Minimum required interaction score is medium confidence (0.4). Clustering method is kmeans clustering (number of clusters: 3).

4.2.4.9 Functional prediction for best candidate-genes

We first summarized the function information from the TAIR (https://www.arabidopsis.org/) by using the *A. thaliana* (AT) homologs name. Then we used the UNIPROT (https://www.uniprot.org/) to replenish the function information by searching SwissProt ID. AT homologs and SwissProt ID were obtained from automatic annotation of 'Rosa chinensis Genome v1.0' (Hibrand-Saint Oyant et al., 2018). For the most interesting genes, we performed gene family phylogenetic trees to represent evolutionary relationships among family genes as previously described in Zhou et al. (2020). Using Geneious 9.1.7, the family genes were searched in genome protein databases: *A. thaliana* (https://www.arabidopsis.org), *Rosa* species (*R. chinensis* 'Old Blush' (Hibrand-Saint Oyant et al., 2018; Raymond et al., 2018), *R. multiflora* (Nakamura et al., 2018), *R. xanthina, R. rugosa, R. persica* (Hibrand-Saint Oyant et al., 2018)), and the other woody *Rosaceae* species (*R. occidentalis* genome (Van Labeke and Dambre, 1998), M. domestica Borkh genome (Daccord et al., 2017), *P. communis* genome (Linsmith et al., 2019), *P. armeniaca* genome

(Jiang et al., 2019), *P. avium* 'Tieton' (Wang et al., 2020), *P. persica* genome (Verde et al., 2017). The genome protein databases of *Rosaceae* recourses were downloaded from the GDR databases.

4.3 Results

4.3.1 Quality control of RNA sequencing, data processing and genome alignment

All samples' raw data have robust quality (Supplementary Figure B.2 a and b), as only a few reads were trimmed and quality is equivalent between all samples. The average raw and clean database of the 21 samples is 6.65 Gb and 6.46 Gb, respectively. In clean data, the Q20 and Q30 reads account for 98.87 $\sim$ 99.01% and 93.23 $\sim$ 93.88% respectively (Supplementary Table B.1). Using '*Rosa chinensis* Genome v1.0' as reference genome (Hibrand-Saint Oyant et al., 2018), we got 91.89 $\sim$ 94.45% uniquely mapped reads, and the average of all was 93.34% (Supplementary table B.2). In addition, there are 2.11 $\sim$ 2.74% (average: 2.41%) reads mapped on multiple loci. We noticed that the percentage of unmapped reads is higher for P stages than for NP ones (4.37% versus 3.56%) (Supplementary Table B.2) and in P stage the percentage is higher for later stages (IIb, IIc and III, more than 4%). Inner Distance distribution analysis showed that most of the paired-reads in each dataset actually present high frequency overlapping each other (Supplementary Figure B.2 d); this is a desirable outcome as the consensus of the overlapping sections of R1 and R2 provides extra confidence for the bases. Junction Saturation analysis showed that the number of "known junction" reached a plateau at 40% of total reads (Supplementary Figure B.2 e), indicating that we have enough coverage depth to do downstream analyses. In addition, we found 64,578 - 73,566 novel junctions in the different datasets (Supplementary Figure B.2 f), compared with the number of annotated splice junctions (99,155 $\sim$ 103,557). The novel junction will greatly supplement the known junction's database which can be used in the alternative splicing studies. For the total of uniquely mapped reads, there are 91.39 $\sim$ 95.2% were assigned to 44,481 genes features in the annotation file, 4.52 $\sim$ 8.37% were mapped to regions of reference genome that were not annotated, and 0.23 $\sim$ 0.28% were ambiguously assigned (Supplementary table B.1). For the differential analysis, we used only the reads mapped to sequences with 'assigned feature' to analyze the differentially expressed genes. The database of 'reads per gene' of 44,481 genes in 21 samples is presented in Supplementary Datasets 1 / sheet 1.

4.3.2 RNA-Seq data highly correlate with RT-qPCR data

Using a principal component analysis (PCA), each biological triplicates of a sample were clustered together with a high correlation (Figure 29 a), indicate that they are highly reproducible. For the overall expression patterns, first principal component (PC1) has large associations with the developmental stages from I to III (from the left to right) with 72.8% variability. The second component (PC2) is more linked with the different between NP and P at the early stages (NP at the bottom and P at the top for stages I and IIa) with 18.6% variability. To evaluate the quality of the expression analysis by RNASeq (this study), we

have selected nine trichomes-candidate genes whose expression has been studied by RT-qPCR on the same samples at the same stages in a previous study to identify if the trichomes genes are controlling prickle initiation (Zhou et al., 2020). Here, we have compared the nine genes' normalized expression (TMP) by RNA sequencing and relative transcript accumulation obtained by RT-qPCR. We found similar expression pattern, indicating those two data were reliable and can support subsequent results (Figure 29 b). Since the biological triplicates are highly reproducible, we used the sum of transcripts per million (TPM) values of the triplicates as the expression level of the gene in the corresponding sample. The normalized expression value (TPM) of all genes in all the samples are presented in the Supplementary Datasets 1 / sheet 2.

4.3.3 Which genes may be involved in prickle development?

4.3.3.1 Discover SDE genes from comparing prickle developmental stages

To decipher the gene network controlling prickle development, we selected stages I, IIa, IIb, IIc, and III of prickle samples and stages I and IIa of glabrous samples. Condition design set as PIIavsPI, PIIbvsPIIa, PIIcvsPIIb, PIIIvsPIIc (as 'Treat'vs'Control'). 914 (650 up- and 264 down-regulation), 580 (509 up and 71 down), 3444 (2434 up and 1010 down), 3837 (1929 up and 1908 down) SDE genes (svalue < 0.05, $|LFC| \geq 1$) were detected from those comparisons, respectively (Supplementary Figure B.3, Supplementary Datasets 2 / sheet 1-4). The SDE genes between early stages (PI and PIIa, PIIa and PIIb) are fewer in number comparing to those differentially expressed between later stages (PIIb and PIIc, PIIc and III). There are 329, 84, 1820 and 2259 unique SDE genes between PIIa and PI, PIIb and PIIa, PIIc and PIIb, PIII and PIIc respectively; only 38 are in common between the 4 comparisons (Figure 30 a, Supplementary Figure B.3, Supplementary Datasets 2 / sheets 6-17).

As previously described (Chapter 2, Figure 13), prickles develop in parallel with stem: stage I correspond to early developmental stages of the stem after bud-outgrowth (prickle initiate just below the shoot apical meristem) and stage III corresponds to a stage where internode are fully developed (Chapter 2, Figure 13). For glabrous individuals, we have selected stages corresponding to the same stage of stem development as stages I and IIa for prickle samples (Chapter 2, Figure 13). In order to obtain more useful information, we investigated the SDE genes that were shared or not shared with prickle and stem development. We discovered 1484 (894 up and 590 down) SDE genes involved in NPIIavsNPI (Supplementary Datasets 2 / sheet 5), these genes are supposed to be involved in stem development. By comparing with the SDE genes of PIIavsPI, we discovered 363 (282 up and 81 down) SDE genes specifically involved in PIIavsPI, and 933 specifically in NPIIavsNPI (Supplementary Datasets 2 / sheets 18-19); and 551 in common (362 and 183 SDE genes were both up- and down-regulation between stage I and IIa of prickle and glabrous cultivates; 6 SDE genes were up-regulated in PIIavsPI but down in NPIIavsNPI) (Figure 30 b , Supplementary Datasets 2 / sheet 9). For those 'specific' and 'common' SDE genes, we performed the Gene Ontology (GO) and enrichment analyses to hunt their functional characteristics (Supplementary Figure B.4).

The 363 unique genes of PIIavsPI were supposed to be specifically involved in the early stage of prickle

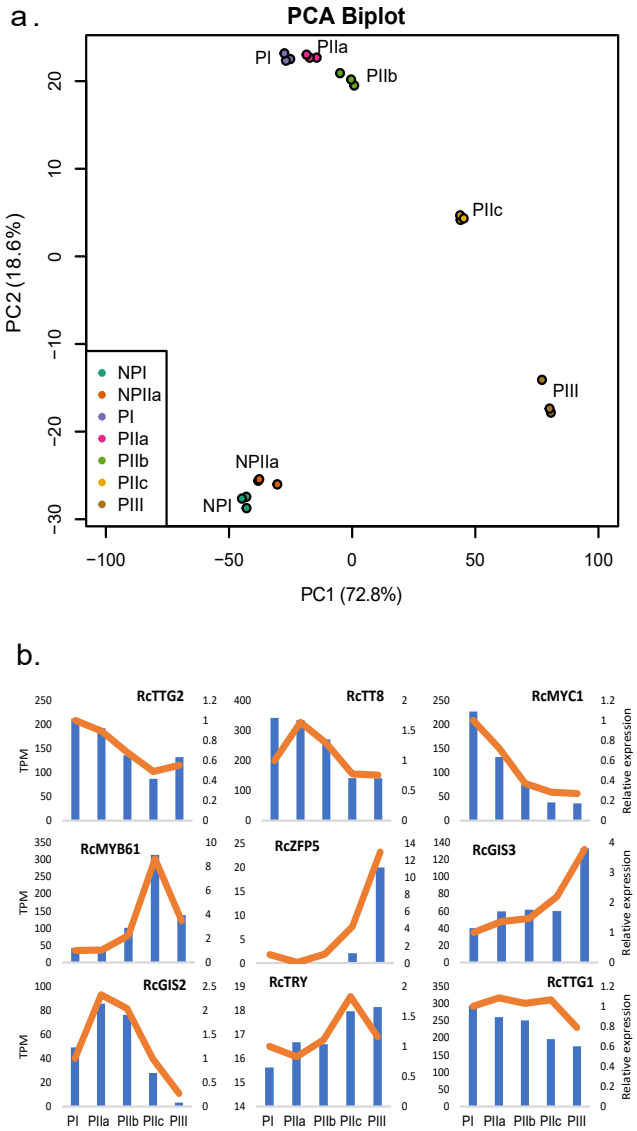

Figure 29: Verify the credibility of expression quantification of the RNAseq data. (a) a PCA Biplot showed the biological replication of all samples. (b) genes expression patterns of nine genes previously studied by RT-qPCR (line) (based on data published in Zhou et al. (2020) and by RNA-Seq (bar) (this study, using the sum of replicates' TPM)

development, not in stem. Among these genes, we found that many genes are enriched involved in 'cell recognition' and 'secondary metabolic process'. Furthermore, we observed enriched genes were for responding to gibberellin and karrikin (Supplementary Figure B.4 a).

Of the 'common' SDE genes, we noticed many genes involved in organ development, such as the top 5 enriched GO biological processes 'anatomical structure formation involved in morphogenesis (ASFIM)', 'post-embryonic plant morphogenesis', 'pattern specification process', 'floral whorl development' and 'shoot system development'. We also gained 'common' genes response to auxin, cytokinin, and nitrogen compound. We even discovered common genes that are involved in the phosphorelay signal transduction system and tropism (Supplementary Figure B.4 b). These functions are expected as these genes are supposed to be involved in the early stages of stem or/and prickle development.

Of the 'specific' SDE genes only involved in glabrous stem development from stage I to IIa (Supplementary Figure B.4 c): organ development processes were also discovered as enrichment, represented by 'plant organ morphogenesis', 'leaf development', and 'ASFIM'; We found the top significant enriched GO process involved in response to auxin, and then in 'monovalent inorganic cation transport', 'protein autophosphorylation', 'fatty acid derivative metabolic process' and 'secondary metabolic process'. These 933 SDE genes are supposed to be specifically involved in the early stages of glabrous stem development.

4.3.3.2 DE genes expression pattern in developmental stages

To well understand the genes expression patterns in the prickle developmental stages, we performed time course sequencing (Tcseq) analysis for all stages of prickle samples. A total of 6958 differential expression (DE) genes were detected and clustered in nine groups, showing different expression patterns during the prickle and stem development (Figure 30 c). The gene list and annotation information for the genes of each cluster are presented in Supplementary Datasets 3 / sheets 1-9. We exported the DE genes that 'membership value' > 0.5 of each cluster, and obtained 523, 1018, 291, 195, 424, 458, 619, 1097, 1157 DE genes involved in clusters 1, 2, 3, 4, 5, 6, 7, 8 and 9 respectively. For those DE genes of each pattern, we performed the Gene Ontology (GO) and enrichment analyses to hunt their functional characteristics. We then checked the GO enrichment biological process and cellular component process. Statistically significance enriched (SSE) categories (FDR < 0.05 set as cut-off value) were presented in Figure 30 d.

Cluster 1 genes mainly expressed in stage I (Figure 30 c). We observed several SSE-GO processes highly associated with organ formation, represented by ASFIM, cell proliferation, cell fate commitment, post-embryonic plant morphogenesis, anatomical structure arrangement, floral whorl/organ development, shoot system development, phloem or xylem histogenesis, peptidyl-amino acid modification, meristem and leaf development (Figure 30 d).

Cluster 2 genes mainly expressed in stages I and IIa, and their expression decreases as the prickle and stem develop (Figure 30 c). In this cluster, we clearly observed a large number of SSE-GO (FDR < 0.05) processes associated with cell proliferation, cell cycle, cell division, organelle fission/assembly, RNA

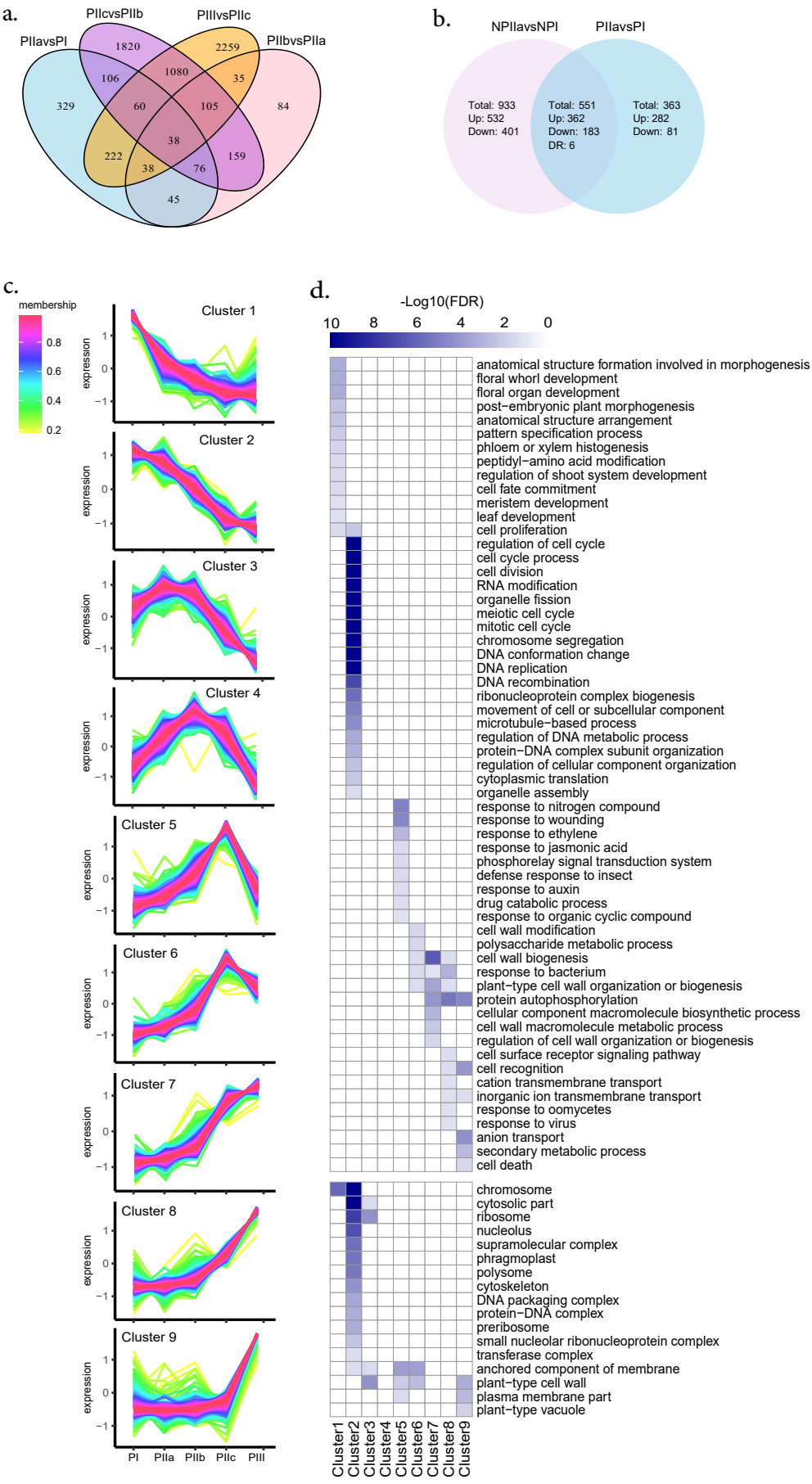

Figure 30: Caption on next page.....

Figure 30: DE gene expression patterns in the development stages and their function enrichment. Venn diagrams (a, b) show the number of SDE genes across compared conditions. Total: total number of SDE genes; Up: up-regulated genes; Down: down-regulated genes; DR: differently-regulated genes in two comparison groups. Comparison group referred to as 'Treat'vs'Control'. (c) Time course sequencing (Tcseq) analysis showed the DE gene expression patterns in all the stages of prickle tissues. (d) A heatmap presented the enriched GO processes of genes in each pattern.

modification, chromosome segregation, DNA conformation change/replication/recombination, ribonucleoprotein complex biogenesis, movement of cell or subcellular component, microtubule-based process, regulation of DNA metabolic process, protein-DNA complex subunit organization, regulation of cellular component organization, cytoplasmic translation (Figure 30 d). SSE-GO cellular component process located in chromosome, cytosolic part, ribosome, nucleolus, supramolecular complex, phragmoplast, polysome, cytoskeleton, DNA packaging complex, protein-DNA complex, pre-ribosome, small nucleolar ribonucleoprotein complex, transferase complex, anchored component of membrane (Figure 30 d). Those processes are all important and highly associated with the anatomical features of prickle development from stage I to stage IIa (14d-f).

Cluster 3 genes mainly expressed in stages IIa and IIb. Cluster 4 genes are mainly expressed in stages IIa, IIb and IIc (with highest expression in stage IIb) (Figure 30 c). No SSE-GO biological process was found in these two patterns, but we can observe some genes of cluster 3 that are involved in plant epidermis and embryo development (not shown in Figure 30 d since they are not significant), and several genes of cluster 4 that are involved in cell wall modification and different types of metabolic processes (not shown in Figure 30 d). The SSE-GO cellular component located in cytosolic part, ribosome, anchored component of membrane and plant-type cell wall.

Cluster 5 genes mainly expressed in stage IIc (Figure 30 c). In this cluster, we observed a large change of the SSE-GO terms (Figure 30 d). This cluster gathers mainly genes involved in response to different stimuli (nitrogen compound, wounding, ethylene, jasmonic acid, auxin, drug catabolic process, organic cyclic compound), defense response to insect, and phosphorelay signal transduction system. GO Cellular Component process mainly located in anchored component of membrane, plant-type cell wall and plasma membrane part.

Clusters 6 and 7 genes mainly expressed in stages IIc and III with different patterns. The transcript accumulation in stage IIc of cluster 6 is obviously higher than in stage III, but relatively higher in stage III of cluster 7 (Figure 30 c). Enriched genes are responding to bacterium were still observed in these clusters. In Cluster 6 genes, new SSE-GO processes were observed that involved in the cell wall (modification, organization, biogenesis), protein autophosphorylation and polysaccharide metabolic processes. The cell wall (biogenesis, organization) and protein autophosphorylation were also enriched in cluster 7. Except that, we observed new SSE-GO biological processes involved in cell wall macromolecule metabolic, and cellular component macromolecule biosynthetic process. GO cellular component process mainly located in the anchored component of membrane and plant-type cell wall also observed in cluster 5 (Figure 30 d).

Clusters 8 and 9 genes mainly expressed in stage III. A slight difference between the two clusters

is that the genes of cluster 8 are also relatively low expressed in stage IIc and cluster 9 genes are not (Figure 30 c). For the biological process, we still can observe cell wall (biogenesis, organization), defense genes response to bacterium and protein autophosphorylation processes in cluster 8 pattern. New and specific enriched processes appear in cluster 8 including cell surface receptor signaling pathway, cation transmembrane transport, and response to oomycetes and virus. 'cell recognition and inorganic ion transmembrane transport' as the new processes are both enriched in cluster 8 and 9. The 'anion transport, secondary metabolic process and cell death' processes were specifically enriched in cluster 9 (Figure 30 d).

4.3.4 Which genes may be involved in prickle initiation?

4.3.4.1 Genes significant differential expressed between prickle and glabrous cultivars in the early stage of prickle initiation

To decipher the gene network controlling prickle initiation, we compared the early stage of prickle development (Stage I) with the non-prickle plant at the same developmental stage (PIvsNPI). Using the DEseq2, we detected 2939 genes (1159 up- and 1780 down-regulars) are significantly differential expression (SDE, svalue < 0.05 and $|LFC| \geq 1$) between the stages I of prickle and glabrous samples (Supplementary Figure B.3 PIvsNPI, Supplementary Datasets 4 / sheet 1). Then 356 genes with low expression (corresponding to a gene whose sum TPM was below 1.5) both in PI and NPI were removed (Figure 31). Using a heatmap, we visualized the co-expression pattern of the 2583 SDE genes (z-score transformed TPM value) in all the samples (Figure 31 b, Supplementary Datasets 4 / sheet 2). A large set of genes are specifically highly expressed in NPI, or both in NPI and NPIIa (Figure 31 b). Interestingly, these kinds of genes are rarely expressed in prickle samples. We suggested those genes can be considered as a candidate gene pool which are negative regulators for prickle initiation or positive regulators for glabrous phenotype. Another set of genes are mainly expressed in prickle samples, and rarely expressed in glabrous samples, they were considered as a candidate pool of positive regulators that control prickles initiation and development.

In addition, we found that numerous genes specifically highly expressed in PIIb, PIIc, or PIII, but with relative lowly expression in PI, are also generally low expression in NPI (Figure 31 b). The expression patterns of these genes are similar to the expression pattern of genes from clusters 4, 5, 6, 7, 8 and 9 (Figure 30 c). Coupled that we have revealed those clusters' genes are mainly involved in the later stage of the cell wall (modification, organization, biogenesis) and response to different stimuli, etc (see the previous section, Figure 30 d). Hence, to identify the genes specifically involved in the prickle initiation, we removed 465 SDE genes that already presented in cluster 4, 5, 6, 7, 8 and 9 to gain insights into the function of the remained SDE genes (Figure 31 c). On the remaining 2118 SDE genes Supplementary Datasets 4 / sheet 3, 1075 genes have functional annotations (based homology search (Supplementary Datasets 4 / sheet 4)). Used their homology's UniProt-SwissProt ID, we performed gene ontology (GO) and enrichment analyses (Figure 31 h). Interestingly, the top of enriched biological process (non-redundant) is involved in post-embryonic plant morphogenesis (FDR = 0.005), then is fatty acid metabolic process (FDR = 0.01) and cell fate commitment (FDR = 0.05). In addition, we found several SSE-GO biological processes with FDR value higher than 0.05

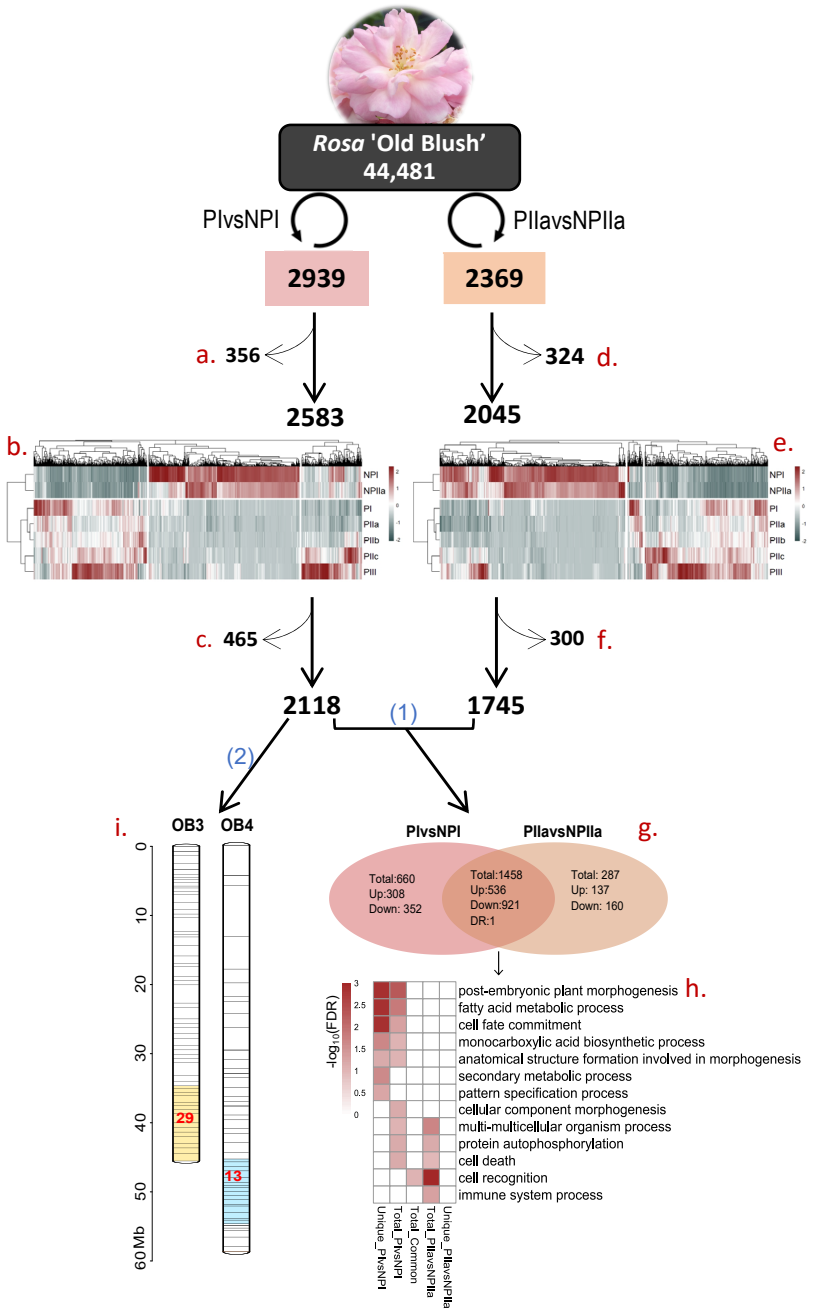

STEP 1:
Discover SDE genes between prickle and prickless samples at stage I (PIvsNPI) and IIa (PIIavsNPIIa).

STEP 2:
Filter the low expression SDE genes with the TPM (Transcripts Per Kilobase Million), and visualize the relative expression of the residual SDE genes in all the samples.

STEP 3:
Filter the genes that are mainly expressed in the later stages.

STEP 4:
Strict selection of good candidate genes for prickle initiation.

(1) Unique and common genes differentially expressed in stage I and IIa between prickle and prickless samples.

(2) Highlight the good candidates by combining transcriptomics and genetic approaches

Figure 31: Caption on next page.....

Figure 31: Data-mining workflow to identify the best candidate-genes for prickle initiation. Significant differential expression (SDE) genes identified from stages I and IIa between prickle and prickless samples using DEseq2 (step1). Low expressed SDE genes (corresponding to whose sum TPM was less than 1.5) were removed (a, d). The relative expression of the remaining SDE genes were visualized (b, e) in order to check their expression patterns in all the samples (step 2). The genes that are mainly expressed in the later stages were removed (c and f): for SDE genes of stage I and IIa, we first filtered the genes with a relatively low expression in stage PI (c) and PIIa (f). We then filtered the genes presented in clusters 4, 5, 6, 7, 8 and 9 (c) and 5, 6, 7, 8 and 9 (f), respectively (step 3). Two methods to narrow the range of the best candidate genes (promoters or inhibitors) for prickle initiation were used (step 4): (1) The two groups of SDE genes (g) are compared to each other to retrieve the specific and common SDE genes involved in stages I and IIa; (2) The genetic and transcriptomic approaches were combined to reveal the SDE genes (PIvsNPI) that are located under the confidence interval of the prickle loci on chromosome 3 (OB3) and 4 (OB4) (i), '29' and '14' refer to the number of SDE genes under the intervals. Venn diagram (g) of the number of SDE genes between the different conditions. Total: total number of SDE genes; Up: up-regulated genes; Down: down-regulated genes; DR: differentially-regulated genes between the two comparison groups. Comparison group named as 'Treat'vs'Control'. Gene Ontogeny enrichment function analyses were used to check the function of the SDE genes in each step. (h) A graph showing the GO terms enriched (FDR < 0.1) for the unique, common, and total SDE genes of stages I and IIa.

but less than 0.1 are also highly associated with the morphological characters. Such as, 'cell death', 'cellular component morphogenesis', 'multi-multicellular organism process', 'ASFIM' are all important for the organ formation. 'Protein phosphorylation' is the most basic, common and important mechanism for regulating and controlling protein vitality and function. Thus, we suggested this relatively narrow range of SDE genes (2118) can be used as the candidate genes pool for further step analysis. The co-expression pattern of the genes involved in those SSE-GO biological processes were visualized in Supplementary Figure B.5 and the supporting databases presented in Supplementary Datasets 4 / sheet 5.

4.3.4.2 Narrow the range of good candidate genes for prickle initiation

Stage I of the prickle sample included initiation and the beginning of development (grow out). Considering the development of prickle in stage I is a result of the prickle cell division (or cell proliferation) process, and this process is also observed in stage IIa (see Chapter 2, Figure 14). Therefore, we investigated the 'unique' and 'common' SDE genes for stage I and IIa between the comparisons of PIvsNPI and PIIavsNPIIa (Figure 31 g) to mine the more interesting genes which specially involved in prickle initiation. We expected to concentrate on the genes who mainly involved in initiation. First, we discovered 2369 genes (987 up- and 1382 down-regulars, Supplementary Datasets 4 / sheet 6) were significantly differential expression in PIIavsNPIIa (Supplementary Figure B.3 PIIavsNPIIa, Figure 31). Using the similar filtering methods as previously done for PIvsNPI, we first removed 324 low expression genes (Figure 31 d) and then filtered out the genes (300) that are present in clusters 5, 6, 7, 8, 9 (Figure 30 c), and 1745 SDE genes passed the filter (Figure 31 f). The normalized expression (TPM) and the functional annotation of these SED genes are presented in Supplementary Datasets 4 / sheet 7. We then compared these 1745 genes with the 2118 SDE genes of PIvsNPI (Figure 31 g, Supplementary Datasets 4 / sheet 8-15), and found that a large number of genes (1458) are in common between the two-stages comparison: 536 are up- and 921 are down-regulated and only 1 present an opposite pattern of expression (Figure 31 g). However, for genes of that large group, we only found 'cell recognition' enriched biological process (Figure 31 h), but we noticed that among the

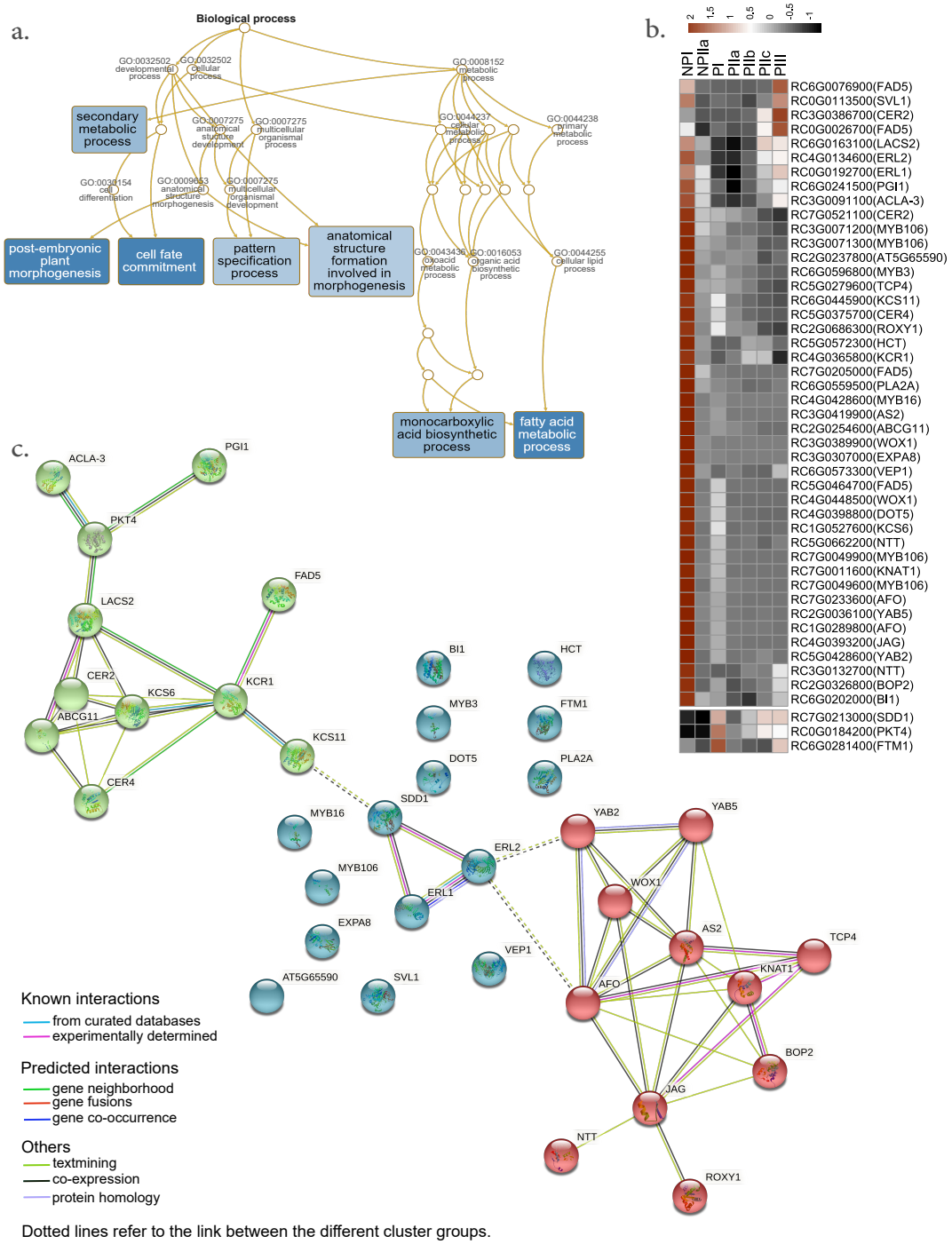

Figure 32: Caption on next page.....

Figure 32: Detailed analysis of the 660 specific SDE genes of stage I between P and NP samples. (a) GO tree view showing the enriched GO terms involved. The dark blue background with white font and the light blue background with blank font indicate that the GO terms are enriched at a significant level FDR < 0.05 and 0.05 < FDR < 0.1, respectively. (b) Heatmap showing the co-expression pattern of the SDE genes (involved in the seven enriched biological process Figure 32 a) in all the samples. *Arabidopsis* protein inside brackets refers to the homologue of rose protein, rose proteins are obtained from automatic annotation. (c) Protein-protein network between the SDE genes which are presented in Figure 32 b. Network nodes represent proteins. The network is clustered to three clusters using kmeans clustering method, and same color of node refers to one cluster. Filled and empty nodes indicate some 3D structure is known (or predicted) and unknown respectively. Edges represent protein-protein associations (associations are meant to be specific and meaningful, i.e. proteins jointly contribute to a shared function; this does not necessarily mean they are physically binding each other.). Different colors of line refer to the different types of data support, the detail have been showed on the Figure 32 c.

other enriched GO terms involved in both 'total' of PIvsNPI and PIIavsNPIIa, some genes belong to the 'common', some to the 'unique'. 660 SDE genes are unique in stage I with 308 up- and 352 down-regulated genes (Figure 31 g). Interestingly, we observed many unique SDE genes were especially involved in seven enriched (FDR>0.1) biological process which contents 'post-embryonic plant morphogenesis (PEPM)', 'fatty acid metabolic process (FAMP)', 'cell fate commitment (CFC)', 'monocarboxylic acid biosynthetic process (MABP)', 'ASFIM', 'secondary metabolic process (SMP)' and 'pattern specification process (PSP)' (Figure 31 h). 287 SDE genes are unique in stages IIa with 137 up- and 160 down-regulated genes (Figure 31 g), and no enriched biological process was identified in this group (Figure 31 h). Those results of function prediction are highly consistent with the morphological characteristics: PI stage corresponds to initiation and first development processes (see Chapter 2), and the 2118 SDE genes of PIvsNPI contain the genes special involved in prickle initiation, development or in both processes.

The 660 unique SDE genes of PIvsNPI contents the most interesting of the SSE-GO biological processes associated with prickle initiation, we suggest that they can be as the priority candidate genes for studying prickle initiation. We visualized a Gene Ontology Tree using the weighted set cover of the WebGestalt tool to intuitively display the relationship network of SSE-GO processes of these 660 unique SDE genes (Figure 32 a, Supplementary Datasets 5 / sheets 1). The FMP, MABP and SMP processes are the sub-processes of metabolic process; the PEPM, CFC, PSP and ASFIM are the sub-processes of developmental and cellular process. A heatmap (Figure 32 b) showed the co-expression pattern of the genes which belong to the seven SSE-GO terms display in Figure 32 a. Most SDE genes are highly co-expressed in prickless samples, and only a few genes in prickle samples. Different GO terms sometimes shared common genes, such as the homology of *AFO, JAG, ROXY1, DOT5, YBA5* (Supplementary Figure B.5). Some genes may be duplicated genes or genes from multifamily (same functional annotation). This is the case for the homologues of *MYB106* (Four homologue genes are co-expressed in NPI), *AFO* and *FAD5* (two homologues genes are co-expressed in NPI) (Figure 32 b). We also studied the protein-protein network between these genes (Figure 32 c, Supplementary Datasets 5 / sheet 2-3). A protein interaction networks between 25 (out of 37 in total) protein was detected with setting a minimum required interaction score (0.4 confidence). This network is clustered to three clusters using kmeans clustering method, and same color of node refers to one cluster. The green groups are associated with metabolic process. The blue and red groups are associated with

developmental and cellular process and these genes have been reported to be involved in the different organs or tissues development, the best known were: petal, floral or inflorescence development process, represented by *JAG, AFO, ROXY1, BOP2, SDD1*; leaf development process, represented by *AS2, JAG, KNAT1, BOP2, WOX1 and WOX3*; embryonic shoot apical meristem development, represented by *AFO, YAB5, YAB2, TCP4, KNAT1*; the initial decision of protodermal cells, represented by *ERL1, ERL2*; the ovary transmitting tract cells and pollen tube growth, represented by *NTT*; cutin or cuticular wax formation, represented by *CER2, CER4, KSC6, ABCG11, LACS2*. Our studies supported that those gene homologue in rose (Figure 32 b) probably have function involved in promoting or inhibiting prickle initiation.

4.3.4.3 Highlight the best candidates by combining transcriptomics and genetic approaches

Using a genetic approach, we have identified two major QTLs on Linkage group (LG) 3 and 4, controlling the presence and the density of prickles on stem (Zhou et al., 2020). By linked SNP markers with the reference *Rosa chinensis* Genome v1.0 (Hibrand-Saint Oyant et al., 2018), we obtained 95% overlapping confidence interval of cQTLs (cQTLoci): LG3 (Chr03: 36.52Mb $\sim$ 46.44Mb), LG4 (46.18Mb $\sim$ 56.11Mb) (see Zhou et al., 2020, Chapter 3). Here, we combined the genetic and transcriptomic data: among the 2118 candidate genes discovered from PIvsNPI SDE genes, 29 and 14 SDE genes were located within cQTLoci of Chr03 and Chr04 respectively (Supplementary Table 4, Figure 31 i).

With TPM normalized expression value, we studied the co-expression patterns of those 43 SDE genes in all the samples. Two main expression patterns are observed with genes mainly co-expressed in prickle and prickless samples respectively at stage I (Figure 33 a). To gain information on the potential function of those 43 genes, we summarized the functional annotation based on their homologs in *A. thaliana* (AT) (Supplementary Table B.4). 13 out of 43 genes have no similarity (E-value < 1^{e-6}) in AT, our transcriptomic study supported that they might be involved in prickle initiation (and development). For others, we presented the nomlized expression (TPM) in all the samples (Figure 33 b), and we selected the ten most promising genes based on their putative function (from AT similarity) (Figure 33 b in red) and discussed in details:

RC3G0389900 and RC4G0448500 belong to WUSCHEL-related homeobox (WOX) gene family (Supplementary Figure B.6 a). WOX members are known to be involved in different organ development, for example, in shoot meristem of *Petunia* and *Antirrhinum majus* (Stuurman et al., 2002; Kieffer et al., 2006), in root apical meristem of *A. thaliana* (Sarkar et al., 2007), in ovule development of *Arabidopsis* (Park and Luger, 2006), in petal and carpel fusion of *Petunia* and *Arabidopsis* (Vandenbussche et al., 2009), in adaxial/abaxial patterning of leaves (Nakata et al., 2012) in *Arabidopsis*, in lateral root development and root hair formation in rice (Yoo et al., 2013; Sun et al., 2017), in conferring glabrousness of rice leaves and glumes (Angeles-Shim et al., 2012). In rose, WOX genes is a large family, we found 209/381 WUSCHEL-like annotated genes in the two *Rosa chinensis* 'Old Blush' Genomes (Hibrand-Saint Oyant et al., 2018; Raymond et al., 2018). Interestingly by phylogenetic analysis, RC3G0389900 and RC4G0448500 belong to a clade with no *Arabidopsis* representatives (Supplementary Figure B.6 a), we named them as RcWOX-g1 and RcWOX-g2 respectively. We found that these two genes have a few duplicates (Supplementary Figure B.6

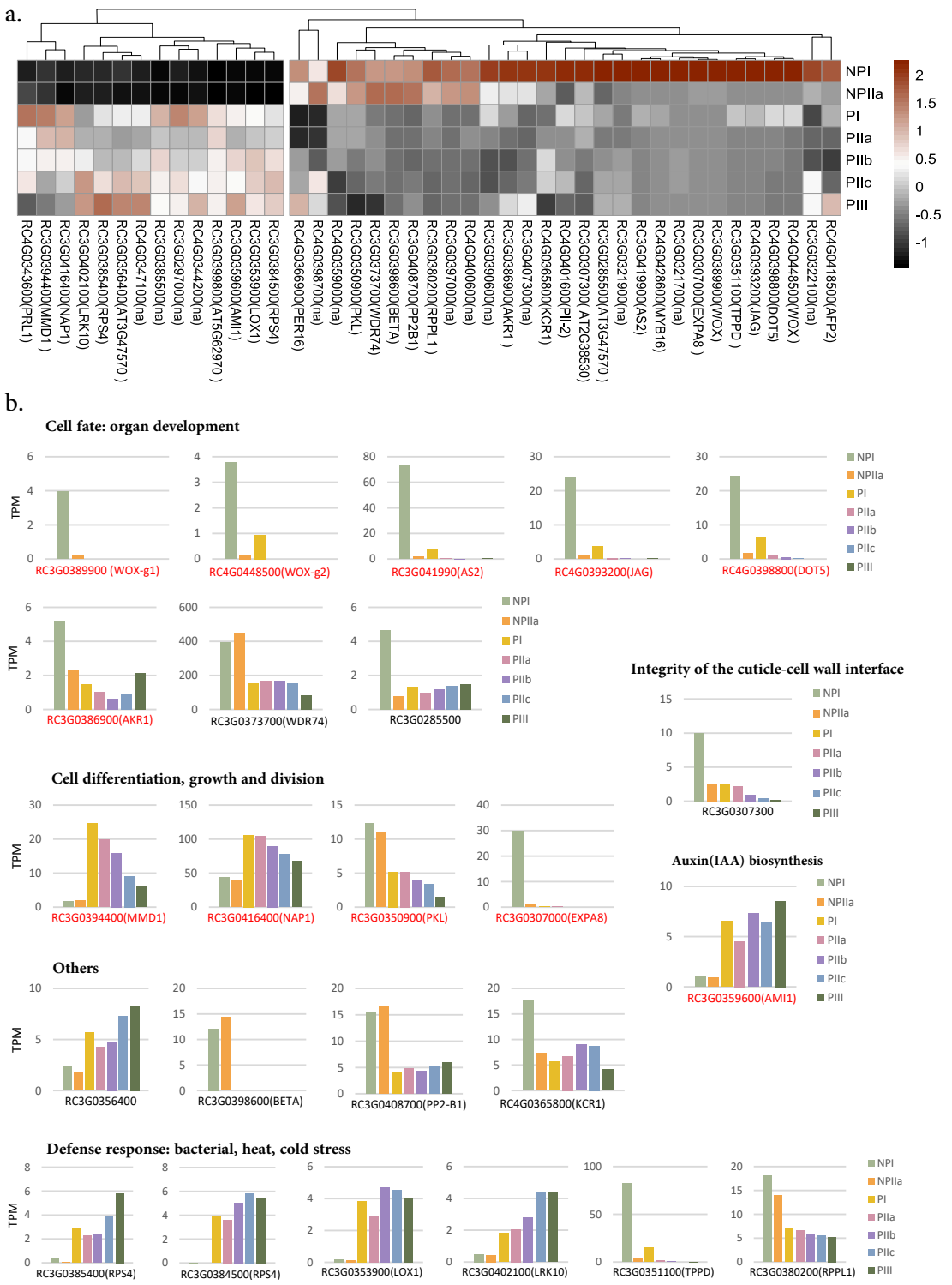

Figure 33: Best candidate-genes were selected by combining genetic and transcriptomic approaches. (a) A heatmap shows the co-expression pattern of the candidate-genes (forty-three SDE genes between PI and NPI stages) that located under the confidence intervals of prickle loci on LG 3 and 4. (b) The normalized expression (TPM) of candidate genes in the different stages of prickle (P) and glabrous (NP) samples. The best ten candidate-genes based on their potential function in prickle initiation were highlighted in the red.

a). Using the synteny tool of the GDR (https://www.rosaceae.org/synview/search), we confirmed RchiOBHm_Chr3g0450921 and RchiOBHm_Chr4g0441541 are the alleles of RC3G0389900 and RC4G04-48500, respectively. Protein alignment showed they are highly heterozygous in OB genotype. The WUS-box motif 'T-L-X-L-F-P-X-X' (van der Graaff et al., 2009) was not conserved in RC3G0389900 and deleted in RC4G0448500 (Supplementary Figure B.6 a), and lost in all the orthologs duplication in the haploid chromosome (Hibrand-Saint Oyant et al., 2018). In addition, their orthologs were only found in rose species and *R. occidentals* (prickle plants), suggesting a recent duplication in the *Rosoideae* plants. These two genes are highly expressed in stage I of prickless sample and near no expression in all the stage of prickle samples (33b), suggesting they are up-regulated in glabrous stem or down regulated in prickless genotypes and should be involved in repressing prickle initiation.

RC4G0393200 (*RcJAG*) encodes a putative C2H2 and C2HC zinc fingers superfamily protein (Supplementary Figure B.6 b). Its ortholog, AT1G68480(JAG), together with NUB/JGL function to define stamen and carpel shape, together with AS1 and AS2 define sepal and petal from their boundaries (Xu et al., 2008). RC4G0398800's ortholog, AT1g13290 (DOT5), also belong to C2H2 zinc finger protein family (Supplementary Figure B.6 b). In AT, DOT5 is required for normal shoot and root development (Petricka et al., 2008). Both rose genes have a specific high expression in the early stage of glabrous stems, suggested that they may function as prickle initiation repressors (33b).

RC3G0419900 (*RcAS2*) encodes ASYMMETRIC LEAVES 2 (AS2) like protein and belongs to LATERAL ORGAN BOUNDARIES (LOB) domain family (Supplementary Figure B.6 c). AS2 controls proximal-distal patterning in *Arabidopsis* petals (Chalfun-Junior et al., 2005) and leaves (Ueno et al., 2007), adaxial/abaxial axis specification of leaves (Wu et al., 2008). The *as2* mutant presents leaves with defect phenotype. *scal-l as2* double mutant develops spines on the edge of the leaf (Mateo-Bonmatí et al., 2015). In rose, RC3G0419900 is especially highly expressed in NPI stage, and its expression is very low in stage PI, and no expression is detected in other stages (33b). Thus, AS2 homolog is a good negative candidate gene for prickle initiation.

RC3G0386900 (*RcAKR1*) belongs to NAD(P)-linked oxidoreductase superfamily protein. In OB, this gene has five duplicates with highly-similar (> 85%) sequence and, the five genes are present in cluster under the QTLs of chromosome 3 (Supplementary Figure B.6 d). Its orthologs, GmAKR1 inhibits nodule development in soybean (Hur et al., 2009). Interestingly, the sequences of RC3G0386900 and GmAKR1 are highly conserved in different species. RC3G0386900 were relatively highly expressed in early stage of glabrous stems. Therefore, it is a good candidate for repressing prickle initiation.

RC3G0394400 (*RcMMD1*) encodes a PHD-domain containing protein, its *A. thaliana* ortholog is MALE MEIOCYTE DEATH 1 (MMD1, AT1G66170) (Supplementary Figure B.6 e) which is required for male meiosis (Yang et al., 2003). RC3G0394400's expression is highest in PI and significantly decreases as prickles develop (it may be linked with the gradual pattern ability of cell to divide), its expression in PI is fourteen times more than in NPI (33a). These supported that RcMMD1 is a good candidate gene for prickle initiation and may promote the mitotic process of prickle cell differentiation and proliferation.

RC3G0416400 (*RcNAP1-like1*) encodes a nucleosome assembly homolog protein (Supplementary Figure B.6 f). Its homolog, NAP1, is involved in cell differentiation and cell population proliferation (Galichet and Gruissem, 2006), DNA repair and somatic homologous recombination (Zhou et al., 2016), as positive regulators in ABA signaling pathways (Liu et al., 2009). RcNAP1-like1 is expressed in both prickle and non-prickle samples. The expression is higher in prickle samples than in glabrous ones, its expression decreases progressively as prickles develop. In early stages (stages I and IIa), its transcript accumulation is three times higher in prickle stems than in glabrous ones (33b). Therefore, RcNAP1-like1 is a good candidate for the cell differentiation or proliferation required for prickle formation.

RC3G0350900 (*RcPKL*) encodes Chromodomain helicase DNA-binding (CHD) homolog protein (Supplementary Figure B.6 g). Its ortholog, AT2G25170 (PKL, CHD3, SSL2, SLR2, PICKLE, LWR1) negatively regulates auxin-mediated later root formation in *Arabidopsis* by chromatin remodeling (Fukaki et al., 2006). PKL also plays an important role in other organ development such as hypocotyl, leaf, and inflorescence stem elongation (Park et al., 2017), and activation of FLOWERING LOCUS T (FT) to promote flowering (Jing et al., 2019). Interestingly, in rose three RcPKL homologue genes were found in cluster on chromosome 3 and a fourth one located on chromosome 6. The transcript accumulation of RC3G0350900 in NP is two times higher than in P at stages I and IIa (Figure 31 b), suggested it may be a good negative candidate for prickle initiation.

RC3G0359600 (*RcAMI1*) encodes an amidase signature homolog protein (Supplementary Figure B.6 h). Its homolog, AT1G08980 (AMI1), is involved in auxin and indoleacetic acid biosynthetic process (Pollmann et al., 2003). RC3G0359600 relatively highly expressed in all the stages of prickle samples and lowly expresses in glabrous samples, this may indicate that auxin is positively regulating prickle initiation and development. Interestingly, in rose this gene is also duplicated with four genes in cluster on the chromosome 3.

4.4 Discussion

Just like other organs, the development of prickles undergoes a process of initiation, growth, maturation, and death. Prickle formation involves many cellular processes, including cell fate, cell proliferation, cell differentiation, cell cycle control, cell polarity, cell-cell communication, etc. To our knowledge, the molecular study in each process for prickle is still largely unknown. In this study, we reported the first transcriptomic analysis for prickle initiation by comparing glabrous and prickle sample at early stage of initiation and development (stage I and IIa, Figure 14 d-g). We also reported the first transcriptomic analysis for prickle development at the stage I, IIa, IIb, IIc and III (Figure 13 a, 14 d-l).

4.4.1 Material and sampling limitations and improvement solution

In this project, one of the challenges was the material limitations for RT-qPCR and RNA-seq: to our knowledge, no single line of prickless mutant in roses resources was found. Thus, we selected sisters in the OW population and used a mixing pool for prickless and prickles samples to reduces the variance of genetic background. Since there are only two individuals completely prickless and once-time flowering (to obtained vegetative branch), we chose the individuals for the prickle pool following the principle of being as close as possible to the prickless progeny on the other traits. Although we have tried to limit the differences as much as possible, it is impossible to completely avoid that a few genes' differential expression in prickle and prickless may cause by the slight difference of genetic background.

Another challenge is the technical limitation for sampling: the prickle initiation happened at a very early stage of stem development (just below the shoot apical meristem) (Figure 14), and it is impossible to isolate the prickle from the stem tip during sampling (a perspective can be to used microdissection). Therefore, in order to be consistent, we decide not to separate prickle from stem (leaves and buds were removed) as the strategy for the sampling of all the stages. This led to the stem development genes were mixed in the candidates of prickle development which brings more challenges for data analysis. We displayed a model method to obtain the 'specific' SDE genes involved in prickles development by comparing group NPIIavsNPI and PIIavsPI. We proposed that the specific SDE genes of PIIavsPI are more interesting for prickle development and the common SDE genes are more associated with stem development. It still needs to be reminded that the development of prickles and stems are probably sharing some genes. That means the 'common' SDE genes may also contain a number of genes that function in prickle development.

Due to the technical limitations for sampling the early stage of prickle initiation, we were unable to have the earliest stage (as initiation). Stage I samples included prickles initiation and development (grow out by cell proliferation) (see Chapter 2, Figure 14). In order to remove potential noise and obtain the most interesting candidates, I designed two unconventional processes in the analysis: 1) We removed the SDE genes of stage I that have been studied in the clusters 4, 5, 6, 7 and 8 (in the time-course study (Figure 30 c)). The reason is that these genes mainly expressed in the later stages (IIb, IIc, III (Figure 13 a)) of prickle development but expressed quite lowly in stage I. We have revealed the potential functions of these genes are not related to prickle initiation, and mainly involved in the cell wall modification, organization, biogenesis, macromolecule metabolic process, cell death and response to the different stimuli (Figure 30 d); 2) We compared the SDE genes involved in stage I and IIa between prickle and glabrous sample. This analysis is based on the histological study in Chapter 2, we proposed that the stages PI (Figure 14 d-f) and PIIa (Figure 14 g) are both including cell proliferation and cell division required for prickle growth. Fortunately, the 660 'specific' SDE genes of stage I included the most interesting GO enrichment processes for prickle initiation, thereby, they were considered as priority gene for further function prediction and the protein-protein network studies.

The best candidates for prickle initiation were selected by combining transcriptome with the genetic

approaches. Since some genes may be simultaneously involved in initiation and development, we used the total 2118 candidate genes discovered between PI and NPI in this analysis step.

4.4.2 Mechanisms underlying prickle development

For the first time, we present a detailed analysis of processes that may control prickle development in rose. By clustering the different expressed genes (DE) in different developmental stages (I, IIa, IIb, IIc, III) of prickle sample (Figure 30), we revealed these DE genes' expression pattern in development stages. Using GO enrichment for the genes of each cluster, we observed many interesting biological processes that are highly associated with the different stages of prickle morphogenesis. (Figure 30 d).

For the genes mainly expressed in early stages I or/and IIa (Figure 30 c, clusters 1 and 2) of prickle samples, we discovered genes that are enriched in biological processes such as cell fate commitment, differentiation, proliferation and cell division. Those genes were described to be involved in organ or tissue development (floral, shoot, leaf, meristem, post-embryonic plant morphogenesis). These early steps correspond to the prickle initiation with acquisition of a new fate for some cells from the ground meristem (below the protoderm, see Chapter 2). Then, through cell proliferation, the prickle develops. The DE genes are therefore good candidate to be involved in prickle initiation and first steps of prickle development.

For the genes mainly expressed in later stages: (1) in cluster 4 (mainly in PIIa, PIIb, PIIc) and 5 (mainly in IIc), we discovered genes have potential function involved in cell wall modification. These genes associated with cell wall modifications might be required for cell elongation that are observed in the stage IIa ,IIb and IIc of prickle development (Chapter 2, Figure 14); (2) in clusters 6 (mainly in PIIc), 7 (mainly in PIIc and PIII), and 8 (mainly in PIII), we observed genes have potential function involved in cell wall organization, biogenesis and macromolecule metabolic processes. These processes might be related to cell wall thickening and lignification in developing and maturing of prickle. In addition, among the genes specifically highly expressed in stage IIc (cluster 5), we also observed genes involved in ethylene, jasmonic acid and auxin response. It may be related to the prickle (or/and stem) growth. 'Cell death', 'secondary metabolic' and 'anion transport' processes were also enriched among the genes that are a specifically highly expression in stage III, that may be associated with the prickles maturing.

Future more, in stages IIc and III (corresponding mainly to cluster 5, 6, 7 and 8), we found many genes that present GO enrichment in responding to different stimuli (wounding, insect, bacterium, virus, oomycetes), organic cyclic compound and drug catabolic process. These results are quite interesting from the perspective of defense function. Prickles are usually covered with a lot of bacteria, viruses or fungus (microorganisms). Some microorganisms species may randomly scatter on prickles. Some species probably are inhabitants that multiply on the spinescences (hence they are present in large numbers) and not just landed on the spinescence accidentally (Halpern et al., 2007). Prickle as a defense structure plays an important role against insects and mammal herbivores and the aggregated bacteria strengthen the defense of its physical structure (as we introduced in Chapter 1). Our results showed that the microorganisms may start

to aggregating in stage IIc of prickle development. These results are highly consistent with the environment of prickles growth, because the prickles completely expose to the external environment when they are get in stage IIc.

4.4.3 Mechanisms underlying prickle initiation

We investigated in detail the genetic network that is controlling prickle initiation by comparing the transcriptome between prickle (P) and sample glabrous (NP) samples at the early stages of prickle initiation and development (or the corresponding stages in NP tissues). We provide a candidate gene pool contains 2118 genes (inhibitors and promoters) for prickle initiation and we recommended 660 priority genes by comparing the SDE gene in stage I and IIa. We explored these 660 specific genes of stage I included the most interesting GO enrichment processes for organ initiation, such as 'cell fate commitment', 'post-embryonic plant morphogenesis', 'anatomical structure formation involved in morphogenesis'. Among the genes involved in these seven SSE-GO terms, a large interaction network between these genes (25 out of 37 *Arabidopsis* protein) were detected. While most of these genes are highly co-expressed in stage I of prickless samples, and only few genes in prickle samples. This majority of genes are therefore putative inhibitors of prickle initiation that control cell fate, anatomical structure or post-embryonic plant morphogenesis (26 a). Moreover, many SDE genes expressed in PI (but not in NP) also highly expressed in other stages of P (Figure 31 b, d). That means some promotor genes may both involved in prickle initiation and development, and these genes are mostly presented in the 'common' SDE genes list of stage I and IIa (Figure 31 g). Therefore, there are probably a few interesting activators that exist in the common list.

Our final objective was to obtain the best candidate genes (inhibitors or promoters) for prickle initiation. We combined the transcriptomics and genetic approach with a functional prediction. It allows us to obtain more confidence and a limited number of candidate genes (Figure 27). We exported the SDE genes located under the confidence interval of the major prickle loci (QTL on LG3 and LG4, (see Zhou et al., 2020, Chapter 3)), and only 43 (out of 2118) genes meet these conditions.

Among them, we explored seven (*RcAS2, RcJAG, RcWOX-g1, RcWOX-g2, RcDOT5, RcAKR1*) that may positively regulate glabrous stem development (or inhibitor for prickle initiation). AS2 is a later organ boundaries protein as known to control proximal-distal patterning in *Arabidopsis* petals (Chalfun-Junior et al., 2005) and leaves (Ueno et al., 2007), adaxial/abaxial axis specification of leaves (Wu et al., 2008). *as2* mutant presents leaves with defect phenotype (Bumpy). *scal-l as2* double mutant develops spines on the edge of the leaf (Mateo-Bonmatí et al., 2015).

JAG is a C2H2 and C2HC zinc fingers superfamily protein, controls the morphogenesis of lateral organs. Functions with AS1 and AS2 in the sepal and petal primordia to repress boundary-specifying genes, thereby, define these organs from their boundaries(Xu et al., 2008). Loss JAG function causes organs to have serrated margins (Dinneny et al., 2004; Ohno et al., 2004).

WUSCHEL-related homeobox (WOX) family genes are known to be involved in different organ development.

WOX1 and WOX3 (or PRS) are important for lateral-specific blade outgrowth and margin-specific cell fate in *Arabidopsis,nakata2012*. A WUSCHEL-WOX 3B gene, *dep*, conditions the glabrous phenotype of rice leaves and glumes (Angeles-Shim et al., 2012). WUSHEL is known to maintain the identity of the undifferentiated cells in the shoot apical meristem(Laux et al., 1996; Ma et al., 2019). In roses, RcWOX-g1 and RcWOX-g2 are co-expressed with AS2 and JAG that may function in deciding the stem boundaries.

Interestingly, RcJAG, RcAS2, RcWOX-g1 and RcWOX-g2 were detected to be central in the protein--protein network (26c). They are co-regulating glabrous stem phenotype in roses with other important genes (as AFO, YAB2, YAB5, KNAT1, TCP4, NTT, ROXY1 homologue), indicating that lost function of these genes may cause out control of stem boundary, thereby, caused prickle initiation. Therefore, they are considered inhibitors for prickle formation. The expressed dose of these inhibitors may regulate the prickle density. That means more inhibitors lost function may cause more ground meristem cells to get the ability to out of stem boundary fate and driven into the first step of prickle (grow out).

We also explored two genes (*RcMMD1*, *RcNAP1-like1*) may be involved in the cell differentiation and division for prickle initiation and development, and an auxin gene (*RcAMI1*) may regulate prickle initiation and development.

RcMMD1 encodes a PHD (plant homeodomain) zinc finger protein. PHD fingers are Zn-coordinating domains that generally recognize unmodified or methylated lysines(Jain et al., 2020). They are central "readers" of histone post-translational modifications (PTMs) (Jain et al., 2020), and can modify chromatin as well as mediate molecular interactions in gene transcription (Sanchez and Zhou, 2011). 14 times expression of RcMMD1 in PI more than NPI, suggesting that RcMMD1 play an important role in prickle initiation.

RcAMI1 encodes an amidase signature homolog protein. In AT, AMI1 involves in auxin and indoleacetic acid biosynthetic process (Pollmann et al., 2003). Auxin signaling regulates lateral root (LR) initiation and subsequent LR primordium formation in Arabidopsis(Laskowski et al., 1995); mutants defective in auxin biosynthesis, homeostasis, transport and signaling caused increased or decreased numbers of LRs (Casimiro et al., 2003; Fukaki et al., 2007). Interestingly, *RcPKL* encodes a CHD homolog protein, and its ortholog AtPKL negatively regulates auxin-mediated LR formation by chromatin remodeling (Fukaki et al., 2006). In roses, RcAMI1 relatively highly expressed in all the stages of prickle (P) samples and lowly expressed in glabrous (NP) samples, while RcPKLis highly expressed in NP and lowly in P. These may suggest that: prickle formation is also regulated by auxin signaling; RcAMI1 is a positive regulator for prickle formation and RcPKL is a repressor.

Nucleosome assembly protein 1 (NAP-1) shuttles histones into the nucleus, assembles nucleosomes, and promotes chromatin fluidity, thereby affecting the transcription of many genes (Park and Luger, 2006). AtNAP1 is involved in cell differentiation and cell population proliferation (Galichet and Gruissem, 2006). RcNAP1-like1 is highly expressed in both prickles and non-prickle samples, and more than two times higher in stage I of the prickle sample than in the glabrous sample. This supported RcNAP-1 may play an important role in cell proliferation both in the meristem tissue of prickle.

In the gene pathway, AS2 was detected to be a center that linked with JAG, WOX1, WOX3 and MMD1. RcJAG and RcMMD1 are both zinc fingers genes and their expression are totally opposite expression, indicating that RcMMD1 may inhibit RcJAG expression, and there by, repress RcAS2 expression as well as RcWOX1-g1 and RcWOX-g2 expression. Therefore, we propose that RcMMD1 may activate prickle initiation by repressing the activity of the 'JAG-AS2-WOX' gene pathway.

Author's contributions

NN Zhou conceived the projects and obtained funding, planned and performed experiments, developed the workflow and bioinformatics scripts and performed data analyses, and wrote the manuscript. F. Foucher and L. Hibrand-Saint Oyant were responsible for piloting and supervising the project, and for revising the manuscript. KX Tang contributed to conceiving the projects and obtaining the fundings. J. Jeauffre participates in the discussion of experimental design and guides RNA extraction. T. Thouroude managed the cuttings of F1 individuals in the greenhouse.

Orcid-ID

Zhou NN: orcid.org/0000-0002-5208-6788

Tang KX: orcid.org/0000-0003-3807-784X

Jeauffre J: orcid.org/0000-0001-6770-0552

Thouroude T: orcid.org/0000-0001-7908-7353

Foucher F: orcid.org/0000-0002-3693-7183

Hibrand-Saint Oyant L: orcid.org/0000-0002-4451-8798

Acknowledgments

We thank the experimental unit (UE Horti) for their technical assistance in plant management, and the ImHorPhen team (D. Besnard, R. Gardet) of IRHS for taking care of the plant cuttings in the greenhouse. We thank S. Balzergue of VALEMA team for participates in the discussion of experimental design and data analysis. We thank J. Chameau of the GDO team for helping to obtain the different stages of the sample. Further, NN ZHOU thanks Prof. Hao Zhang and Dr. Ji-hua Wang of Yunnan Academy of Agricultural Sciences (YAAS) for accepting to be the recommenders for applying for the project funding. Thanks also HY Jian (FRI, YAAS) for revising the project manuscript.

Funding

This work was supported by funding from the National Natural Science Foundation of China (31760585), the China Scholarship Council ([2017]3109) and the Natural Science Foundation of Yunnan (2016FB061).

General discussion and perspectives

5 General Discussion and Perspectives

This thesis focused on filling the gaps in prickle knowledge using morphological, genetics, and genomic approaches. Our objective was to decipher the molecular and genetic control of the initiation and development of prickles on rose stems. Since the basic botanical terminologies (trichomes, prickles, thorns and spines) were frequently inaccurately cited in scientific reports, and these words were confusing for most researchers, we first described and compared them in the Introduction in Chapter 1. One of the most confusing points is the relationship between trichomes and prickles, which is important for the experimental design in our study. The current mainstream hypothesis is that prickles originate from the epidermis (Peitersen, 1921; Canli, 2003) and are considered to be modified glandular trichomes. In the late developmental stage, the prickles become cutinized as a hard-sharp appendage, like in roses (Kellogg et al., 2011), *Rubus* (Peitersen, 1921; Coyner et al., 2005; Kellogg et al., 2011; Khadgi and Weber, 2020a) and grapes (Ma et al., 2016b). In fact, the tissues from which the prickles originated are not clearly defined, since no anatomical evidence was ever provided to support the 'epidermis' hypothesis. To well understand the origin of prickles, their types, and their development, we investigated the prickle types in rose wild species, in parents and progeny of a F1 population (OW). We carried out a comprehensive anatomical study for two representative types of prickles (Chapter 2). In the OW progeny, we classified rose prickles into two major categories: non-glandular (NGPs) and glandular (GPs) prickles. We also discovered other types of prickles in wild roses and classified them into the sub-categories of NGPs and GPs. We found that NGPs and the major structure (stalk) of GPs come from the ground meristem (the underlayers of protoderm). GP and NGP initiation take place at an early stage of shoot development (just below the shoot apical meristem). The first layers of gland cells of GP originate from epidermal cells (or protoderm) of the bump (the first stage of GPs). These new insights constitute valuable information for further study. We adjusted the experimental design in the middle of the project and decided to study the NGPs and GPs separately.

For the genetic approach (Chapter 3), we performed QTL analysis for these two types of prickles. However, for the GPs, we were unable to detect any significant QTLs since the individuals presenting GPs were not numerous enough in the OW population. Thus, we focused on exploring genetic determinism and the gene network for the NGPs, the most common type of prickles on rose stems. We detected a major locus on LG3 that controls the absence/presence of prickles on rose stems and several other loci controlling prickle density. In addition, to identify the relationship between prickles and trichomes at the molecular level, we

used a candidate-gene approach to characterize rose gene homologues known in *Arabidopsis* to be involved in trichome initiation. Almost no difference of transcript accumulation for these candidate genes between prickle and prickless roses were detected, suggesting that prickle and trichome initiation is controlled by two different genetic pathways. This conclusion was also supported by results from the transcriptomic approach (Chapter 4).

In Chapter 4, by transcriptomic approach (RNA-Seq), using a mixed pool of F1 individuals with or without NGPs, respectively, we discovered many genes involved in prickle initiation and development. We developed unconventional methods to optimize the candidate gene discovery. By combining a genetic approach and gene function prediction, we mined the ten best candidate genes for prickle initiation. By combining the results obtained by the anatomical/histological (Chapter 2), genetic (Chapter 3) and transcriptomic (Chapter 4) approaches, we proposed a genetic and molecular mechanism for prickle initiation and development (see Discussion below).

During this project, we provided a general framework to study the genetics and genomics of prickles in woody plants. Our study significantly improved the knowledge of the genetic determinism and molecular mechanisms underlying prickle formation in rose. Here, we discuss the implication of such approaches for rose breeding.

5.1 Two types of prickles in roses, glandular and non-glandular, and two different gene networks

In Chapters 2 and 3, by studying the morphology and anatomy of prickles, from their initiation to their complete development, and their distribution in the OW population, we proposed that non-glandular prickles (NGPs) and glandular prickles (GPs) are different types of prickles with different genetic determinism.

The most common prickles observed in the OW population are the NGPs. They have no glandular structure at any point in their development. Another type of prickles appears in some F1 individuals (17.9%) but not in parents: these prickles have a gland head and were denominated by glandular prickles (GPs). So our results did not support the previous hypothesis that 'GP and NGP are the early and later stages of same prickle (Coyner et al., 2005; Kellogg et al., 2011; Ma et al., 2016b; Khadgi and Weber, 2020a).

For the first time, NGP and GP initiation and development were histologically characterized in-depth from the early to later stages. NGPs are initiated from the ground meristem below the protoderm.At the initiation stage, no essential difference was observed between GPs and NGPs. Both are initiated from the ground meristem below the protoderm. In GPs, the gland at the head of the prickle originates from the protoderm (or epidermis) cells of the newly formed prickle at the early stages of development. So our results did not support the previous hypothesis that 'Prickles originate from the epidermis' (Peitersen, 1921; Esau, 1960; Canli and Skirvin, 2003; Kellogg et al., 2011).

In Chapter 2, at the morphological level, we reported more different types of prickles in the *Rosa* genus. There are 'naked' and 'hairy' forms in NGPs and GPs. GPs can be unbranched and branched. Some GPs are present with a gland head, whereas some have several glands randomly distributed on their surface.

As in OW population, the most common type found in wild rose species or cultivars are the 'unbranched and naked' NGPs. The unbranched (naked or hairy) GPs are generally not present alone but always associated with NGPs. Moreover, the gland (a specific structure of GPs) was not produced at the prickle initiation but during the prickle's development (Chapter 2, Figure 14 m-r). Therefore, we supposed that GPs may be modified from NGPs.

A similar hypothesis was proposed for the trichomes: in an evolutionary perspective, the earliest glandular trichomes (GTs) are modified from the non-glandular trichomes (NGTs) (Krings et al., 2003; Lange, 2015). The NGTs and GTs evolve from protoderm (or epidermis) only, and different gene networks (Chapter 1) have been reported to control the initiation of NGTs (Folkers et al., 1997; Hülskamp, 2004; Balkunde et al., 2010) and GTs (Payne et al., 1999; Huchelmann et al., 2017; Chalvin et al., 2020). This difference can be explained by morphogenetic evidences: mother protoderm cell(s) produced different structures, NGTs and GTs, which are probably controlled by different regulators. However, we do not know if the developmental program is different at the first mother cell initiation (cell fate) or later in the developmental process. In Chapter 1, I gave examples to show the developmental stages of GTs and NGTs (Figure 3). They look similar in the beginning: one mother protoderm cell starts to enlarge. This enlarged cell continues to grow without cell cycle division and begins endoreplication (unicellular NGT, Figure 3 a1) (Hülskamp, 2004), or divides into two cells. The two cells then continue normal division (multicellular NGT, Figure 3 a2 and a3) (Kintzios, 2002), or one of the two cells becomes a clear gland cell (multicellular GT, Figure 3 b and c) (Bosabalidis and Tsekos, 1982; Karousou et al., 1992). In *Arabidopsis*, it has been shown that interruption of endoreplication can modify unicellular NGTs into multicellular NGTs (Schnittger et al., 2002b,a). Since the molecular mechanism of GT initiation is still unclear, we do not know how the genetic pathways interact between NGTs and GTs.

For glandular and non-glandular prickles on rose stems, the major difference is the presence/absence of a gland. This difference appears the early developmental stage of GPs and NGPs. In GP initiation, ground meristem cells first rise and become a bump. At this stage, GP initiation is similar to that of NGP. Then, gland cells evolve from the protoderm (or epidermis) cells of the newly initiated prickle (Chapter 2). We can hypothesize that two genetic pathways control the GP and gland initiation. One controls the cell fate of the ground meristem cells (a process that may be shared with NGPs), and another pathway controls the cell fate of the protoderm (or epidermis) cells (only in glandular trichomes and may be similar to the gland initiation in glandular trichomes). Another possibility is that GPs and NGPs have different genetic pathways that control the cell fate of the first mother cell. Further studies are necessary to clarify these hypotheses. However, as demonstrated by the genetic approach (Chapter 3), GP and NGP genetic determinism is different, suggesting that the genetic network controlling GP and NGP development is different in rose. Since GPs were rare in the OW progeny and we were unable to study their genetic determinism in OW progeny, our further analyses focus on NGPs, the most common prickles in rose.

These conclusions are different from the current mainstream hypothesis: prickles evolve from multiple cellular divisions of the epidermis (Peitersen, 1921; Canli, 2003) and prickles are modified glandular trichomes that later become cutinized as a hard-sharp appendage (Peitersen, 1921; Coyner et al., 2005; Kellogg et al., 2011; Ma et al., 2016b; Khadgi and Weber, 2020a), or induced by glandular trichome (Pandey et al., 2018). In the next section, we will compare the studies in *Rosa* and *Rubus* in detail.

5.2 Genetic determinism and molecular mechanisms underlying NGP formation

5.2.1 Prickle formation from initiation to late stages

For the first time, we present a detailed transcriptomic analysis of processes that may control prickle formation from initiation to late developmental stages, in rose (Chapter 4). We have combined anatomical and transcriptomic approaches to propose molecular mechanisms underlying prickle formation (Figure 34).

Just like other organs, prickle formation involves many cellular processes, including cell fate, cell differentiation, cell-to-cell communication, cell proliferation, cell cycle division, cell polarity, etc. For the genes mainly expressed in stages I or/and IIa (cluster 1 and 2), we discovered genes that are enriched in these processes. Stage I corresponds to prickle initiation with several cells from the ground meristem (below the protoderm) that acquire a new fate. These cells then grow to give the first stage of prickles (Figure 34, Chapter 2, Figure 14 a). Cluster 1 genes are specifically highly expressed in stage I, with genes described to be involved in organ or tissue development (floral, shoot, leaf, meristem, post-embryonic plant morphogenesis (Chapter 4, Figure 30)). This suggests that many genes in this cluster may be related to the cell fat and differentiation required for prickle initiation. Then, through cell proliferation, the prickle develops. Genes from cluster 2 are highly expressed in stages I and IIa, and their expression decreases as the prickle and stem develop. Numerous genes in this cluster are involved in cell proliferation and in the processes of cell cycle division. These results are highly consistent with the development of the prickle, i.e., prickle meristem cells gradually lose their meristematic activity as the prickle develops (Chapter 2, Figure 14 d-l). We therefore propose that cluster 2 genes may be highly associated with cell proliferation required for prickle and/or stem growth at the early stage. In stage II, some cells still maintain their cell division ability (IIa an IIb), some (from top to bottom) lose this ability and start to elongate and to gradually enlarge (Chapter 2, 14g-i). Many genes in Clusters 4 (mainly in stages PIIa, PIIb and PIIc) and 5 (mainly in stage IIc) are potentially involved in the cell wall modification process, which might be related to the cell elongation in stage II of prickle development (Figure14 g-l, Chapter 2). From stages IIc to III, prickles begin to lignify and gradually harden, forming a structure-like abscission layer. Genes of clusters 6, 7 (mainly in stages IIc and III) and 8 (mainly in stage III) are involved in cell wall organization, biogenesis and macromolecule metabolic processes. These processes may be related to cell wall thickening and lignification observed in late developmental stages of prickle (maturation). The cell death pro- cess is observed in cluster 9, whose

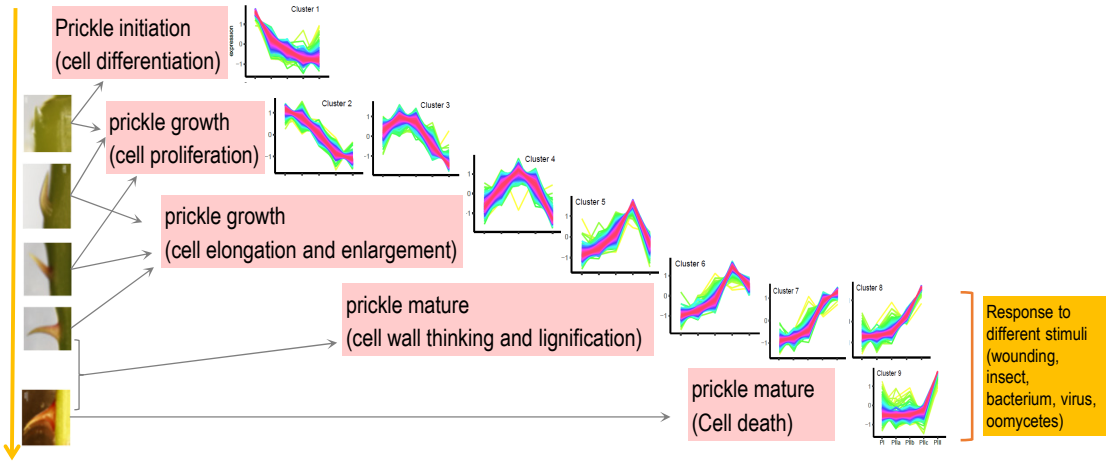

Figure 34: The molecular mechanisms of prickle formation from initiation to the developed stages

genes are specifically highly expressed in stage III. The genes in this cluster may be associated with the formation of the structure-like abscission layer.

Furthermore, in stages IIc and III (corresponding mainly to clusters 5, 6, 7 and 8), we found many genes that present GO enrichment in response to different stimuli (wounding, insects, bac- teria, viruses, oomycetes), organic cyclic compounds and drug catabolic processes. These results are quite interesting in terms of defense functions. Prickles are usually covered with many bacteria, viruses or fungi (Halpern et al., 2007, 2011; Lev-Yadun, 2016). Some microorganisms (bacteria, viruses or fungi) may randomly scatter on prickles, such as *Sporothrix*, a fungus taht causes sporotrichosis (also known as 'rose gardener's disease'). This fungus lives throughout the world in soil and on plant matter. The infection occurs when the fungus enters the skin through a small injury. The 'organic cyclic compound' and 'drug catabolic' processes may also be related to the defense function against certain microorganisms. Some species are probably to spinescences (hence, they are present and can multiply to reach large numbers) and not just present accidentally (Halpern et al., 2007). Prickle as a defense structure plays an important role against insects and mammal herbivores, and the aggregated microorganisms strengthen the defense of its physical structure (as reported in Chapter 1). Our results suggest that the microorganisms may start to aggregate in stage IIc of prickle development. These results are highly consistent with the prickles environment at this stage, since the prickle is completely exposed to the external environment (no longer protected by leaves).

Based on our knowledge, the genomic studies on prickle formation are rare. In *Solanum vivarium*, a prickle (wild type, WT) and prickless (mutant) individuals were used in a transcriptomic study. Pandey et al. (2018) sequenced the total RNA of the 'skin' that they peeled off from the later stage of stem development. Although the samples were described as epidermis in the article (the epidermis is the first cell layer of the organ), the 'skin' might be more complex and may correspond to the term 'bark' in woody plants. Both the WT and mutant (prickle and prickless) present many glandular trichomes. The larger prickles in the WT were considered to have induced from those glandular trichomes, but no prickle is induced in the mutant. Based on this hypothesis, they proposed a pathway that would govern prickle initiation from GTs, and that would

enhance secondary metabolism. However, this hypothesis is not supported by strong evidence: the larger prickles in *S. vivarium* look like glandular prickles, with or without branches (see from the macroscope graph, Pandey et al. (2018)). Thus, the wild type and mutant of *S. vivarium* are good materials to study glandular prickles. However, the sample (stem skin) was harvested when the stem and prickle were well developed. By comparing them with rose prickles, we consider that these samples may correspond to stages IIc and III (Chapter 2, Figure 14) in our study. To study prickle initiation, it is necessary to do so at the time of their initiation. Furthermore, the presence of trichomes and prickles at the same time (mix of structures) may complexify the interpretation of the results. By comparing the prickle and prickless samples, they found a higher percentage of DE genes that were enriched to responses to stimulus (both biotic and abiotic), responses to stress and responses to defense. If we consider that their material corresponds to stages IIc and III of the GPs, these processes were also found in stages IIc to III of the NGPs in our study. This may suggest that NGPs and GPs in the later stages both aggregate many microorganisms.

5.2.2 Zoon in prickle initiation

Through an anatomical study, we confirmed that prickle initiation does not happen in prickless individuals (Chapter 2, Figure 13 c and 15). That means: (1) prickless phenotype is caused by the absence of prickle initiation and not by an interruption during prickle development; (2) prickle density is related to prickle initiation that takes place in the ground meristem. Those facts allowed us to combine the genetic and transcriptomic approaches to raise the question of prickle initiation. We thus combined these two approaches to be discussed and, furthermore, proposed a detailed hypothesis for the genetic determinism and molecular mechanisms underlying prickle initiation (Figure 35).

5.2.2.1 A complex genetic determinism for prickles in rose

In Chapter 3, we revealed a complex genetic determinism of NGPs in rose stems with a major locus on LG3 that controls the absence/presence of prickles and several other loci controlling prickle density. We detected three QTLs on LG4, 3 and 1 which are involved in prickle density in the OW population.

We extended the description of the QTLs on LG3 that affect the presence/absence of prickles. We designated this locus as *PRICKLE*. On the basis of the phenotype-genotype relationship, we proposed that at this locus, the female OB and the male RW parents are both heterozygous (*np*/P), and that the presence of prickles is controlled by a dominant allele (*P*), and that the glabrous stem in the progeny is due to the combination of the two recessive alleles from both parents (*np/np*). Based on the genetic data, the presence of prickles seems to be controlled by activator(s) that is (are) present in prickle genotypes (*P*) and absent in glabrous genotypes (*np/np*). This *np* allele might be explained by a loss of function of the activator P (Figure 35 a). In addition, the *PRICKLE* locus is in the vicinity of other important loci for ornamental traits (continuous flowering, double flower and self-incompatibility (Hibrand-Saint Oyant et al., 2018)).

These results are important for breeders who need to combine recessive alleles to obtain glabrous roses.

However, since modern roses are tetraploid, a recessive allelic combination could be difficult to abtain in a tetraploid background. Furthermore, we do not know how the *np* and P alleles would behave in a tetraploid background. Development of specific molecular markers of the recessive allele may by useful for breeders. However, it should be mentioned that the two markers actually used (peak of the QTL) are not closely linked with the *PRICKLE* locus, and few recombinants are observed in the progeny.

Moreover, the phenotype of the individuals with the two recessive alleles is not stable and some of the hybrids regularly developed some prickles on parts of the stems, suggesting a leaky mutation. Indeed, this phenomenon is widespread in roses. Rose breeders have reported that glabrous mutants have either been unstable for the prickless trait (Nobbs, 1984; Rosu et al., 1995), or have reverted to the prickly character after a freezing winter or other environmental stresses (Nobbs, 1984; Oliver, 1986; Druitt and Shoup, 1991; Canli, 2003). These reversions may be explained by the chimeric nature of the prickless mutation in roses (Rosu et al., 1995; Canli, 2003). In our case, this hypothesis is unlikely as the mutation (*np*) is heritable. Another explanation is that the 'prickle state reversion' ability in rose could possibly be caused by unstable mutations involving transposable elements (Canli and Skirvin, 2008). Such an unstable and reverted phenotype has been already observed in rose for the continuous-flowering phenotype. This phenotype is due to the insertion of a retrotransposon in a floral repressor (Iwata et al., 2012). Recombination of the retrotransposon can occur and can restore a hypomorphic allele. Another explanation could be genetic redundancy or a phenotypic compensation mechanism. Previous studies have reported that many engineered mutants do not exhibit an obvious phenotype, and several studies have provided evidence on how the compensatory network is activated to buffer against deleterious mutations, such as in *Caenorhabditis* (Burga et al., 2011), *zebrafish* (Rossi et al., 2015) and *mouse* (El-Brolosy et al., 2019). This evidence supports the hypothesis that phenotypic outcome does not depend on the intrinsic properties of a mutation but on a range of compensatory mechanisms within the individual (Casci, 2012) instead and, of course, on the plant environment. Prickles, as a beneficial structure, have gone through a long evolutionary history to protect plants against herbivores. Consequently, prickles in roses may carry a second genetic compensation to pathway to maintain their genetic robustness, which can be triggered when the major function gene of prickle initiation is mutated and loses its function. This importance of prickle in rose co-evolution is also highlighted by the rareness of wild glabrous roses (see Chapter 2), suggesting an important role of prickles in rose adaptation.

5.2.2.2 The mechanisms underlying prickle initiation

Our final objective was to reveal genetic determinism of prickle and to obtain the best candidate genes (inhibitors or promoters) for prickle initiation. In the Chapter 3, and as discussed in the previous section, we detected a major locus on LG3 (*PRICKLE*) that controls the presence / absence of prickles (Zhou et al., 2020). We have proposed that *PRICKLE*(*P*) is an activator of prickle initiation. We also detected three QTLs on LG4, 3 and 1 (Y) that regulate prickle density in the OW population (Figure 36 a). By combining the transcriptomic and genetic approaches with a functional prediction, we mined ten best candidate-genes for prickle initiation. Seven are negatively associated with prickle initiation and three are positively associated: they were proposed as inhibitors and activators, respectively.

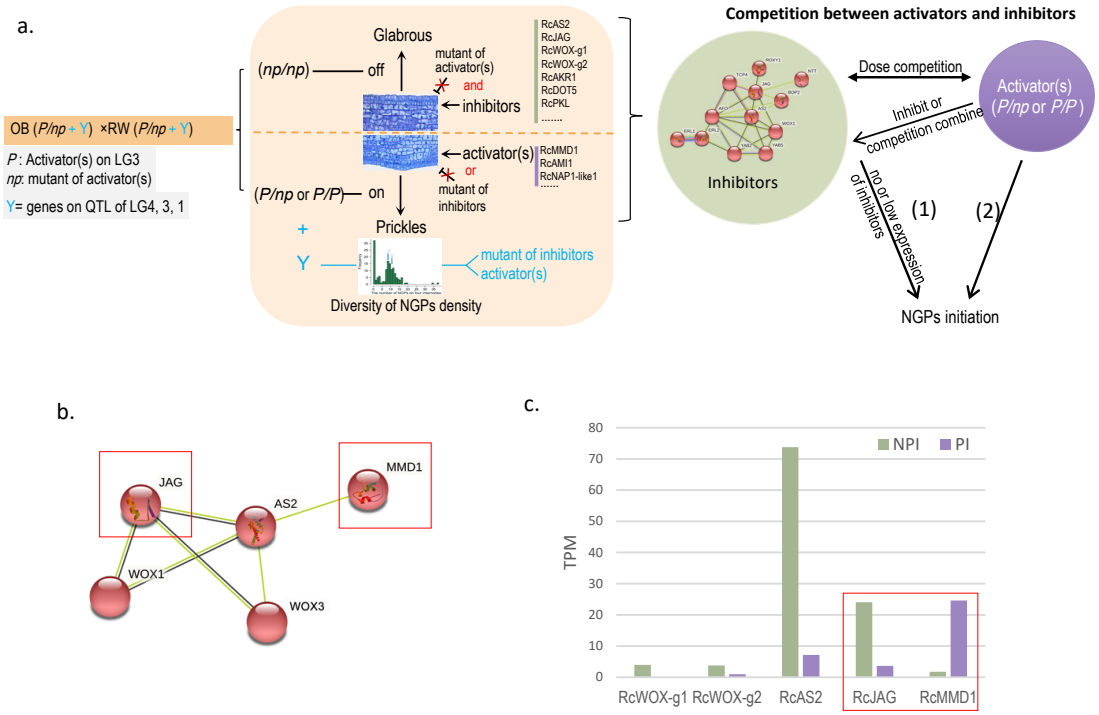

Figure 35: The molecular mechanisms of prickle initiation. (a) A general scheme for prickle initiation. *P* and *np* alleles were proposed to be an activator(s) and a mutant of activator(s) on LG3, respectively. Y means genes on QTL on LG4, 3, 1. (b) protein-protein interaction network between AS2, JAG, WOX1, WOX3, MMD1 in *A. thaliana*. (c) The best candidate gene expression pattern in stage I of prickle and glabrous samples.

Concerning the PRICKLE locus on LG3, the best candidates are potential activators. We detected three activators (RcMMD1, RcAMI1, RcNAP1-like1), whicha re located in the confident interval of the main QTL on LG3(Chapter 3). Among them, the most interesting gene is *RcMMD1*, which encodes a PHD (plant homeodomain) zinc finger protein. PHD fingers are Zn-coordinating domains that generally recognize unmodified or methylated lysines (Jain et al., 2020). They are central "readers" of histone post-translational modifications (PTMs) and can modify chromatin and mediate molecular interactions in gene transcription (Sanchez and Zhou, 2011). *RcMMD1* transcripts are accumulated fourteen times more in stage I of P than in NP tissues, supporting the hypothesis that *RcMMD1* plays an important role in prickle initiation. Interestingly, protein-protein network analysis showed that MMD1 was linked to an inhibitor protein network by interacting with AS2, JAG and WOX (Figure 35 b). *RcMMD1* and *RcJAG* are both zinc finger genes with an opposite pattern of expression in stage I of P and NP tissues (Figure 35 c). They both interact with AS2 in the protein network (Figure 35 b). *RcMMD1* might inhibit the expression of repressors such as RcJAG, RcAS2, RcWOX1-g1, or RcWOX-g2 (see below). Thus, we propose that RcMMD1 may activate prickle initiation by repressing the activity of the 'JAG-AS2-WOX' gene pathway.

RcAMI1 encodes an amidase signature homolog protein. In *A. thaliana*, AMI1 is involved in auxin and biosynthesis (Pollmann et al., 2003). Auxin signaling regulates lateral root (LR) initiation and subsequent LR primordium formation in *Arabidopsis*(Laskowski et al., 1995). Mutants, defective in auxin biosynthesis, homeostasis, transport or signaling, caused an increase or decrease in the numbers of LRs (Casimiro et al., 2003; Fukaki et al., 2007). Interestingly, *RcPKL* encodes a CHD homolog protein, and its ortholog ATPKL negatively regulates auxin-mediated LR formation by chromatin remodeling (Fukaki et al., 2006). In roses, RcAMI1 is relatively highly expressed in all the stages of prickle (P) samples and weakly expressed in glabrous (NP) samples, while RcPKL is highly expressed in NPs and poorly in P samples. We can hypothesize that: prickle formation might also be regulated by auxin signaling with; RcAMI1 as a positive regulator of prickle initiation and RcPKL as a repressor.

AtNAP1 is involved in cell differentiation and cell population proliferation (Galichet and Gruissem, 2006). *RcNAP1-like1* is highly expressed in both prickle and non-prickle samples, and its expression is twice as high in stage I of the prickle samples than in the glabrous ones. We can imagine that the speed of cell proliferation of the prickle precursor is faster than that of the surrounding meristem cells, and the mechanical force of the precursor cell proliferation pushes the formation of the early prickles. This supported the hypothesis that RcNAP-1 may play an important role in cell proliferation both in the meristem tissue of prickles and stems, and the dose of this gene expression may impact the speed or ability of the cell proliferation.

Surprisingly, we detected many SDE genes highly expressed in the glabrous samples, suggesting the importance of inhibitors that may block prickle initiation (Figure 31 d, 32 b and 33 a). Among the seven best inhibitors (RcAS2, RcJAG, RcWOX-g1, RcWOX-g2, RcDOT5, RcAKR1 and RcPKL), AS2, JAG and WOX are known to be positive regulators of the organ boundary in *Arabidopsis*. Indeed, AS2 is the LATERAL ORGAN BOUNDARIES (LOB) protein that are positively regulates lateral organ boundaries within the

shoot apex (Xu et al., 2016). Interestingly, the accurate regulation of AS2 expression may involve epigenetic regulation (Chen et al., 2013). As a putative repressor of AS2, RcMMD1 protein (see above) encodes a PHD zinc finger, which was proposed as a versatile epigenome reader (Sanchez and Zhou, 2011). In *Arabidopsis*, the *as2* mutant presents leaves with a defective phenotype (Bumpy). The *scal-l as2* double mutant develops spines on the edge of the leaf (Mateo-Bonmatí et al., 2015). JAG is a member of the C2H2 and C2HC zinc fingers superfamily protein, and controls the morphogenesis of lateral organs. In *Arabidopsis*, JAG, in interaction functions with AS1 and AS2, defines the boundaries between sepal and petal (Xu et al., 2008). Loss of JAG function causes organs to have serrated margins (Dinneny et al., 2004; Ohno et al., 2004).

WUSCHEL-related homeobox (*WOX*) family genes are known to be involved in different organ development. WUS, as an integrator of multiple signals plays a central role in the maintenance of the cell population in the shoot apical meristem. This maintenance is intimately balanced with cell recruitment into differentiating tissues through intercellular communication (Dodsworth, 2009). *WOX1* and *WOX3* (or *PRS*) are important for lateral-specific blade outgrowth and margin-specific cell fate in *Arabidopsis* (Nakata et al., 2012). A *WUSCHEL-WOX 3B* gene, *dep*, conditions the glabrous phenotype of rice leaves and glumes (Angeles-Shim et al., 2012). In roses, *RcWOX-g1* and *RcWOX-g2* are co-expressed with AS2 and JAG. They may play a role in determining te boundaries of the stem.

Interestingly, RcJAG, RcAS2, RcWOX-g1 and RcWOX-g2 were detected to be central in the protein - protein network (Figure 32 c). They might be co-regulators of glabrous stems in roses with other important genes (as *AFO, YAB2, YAB5, KNAT1, TCP4, NTT, ROXY1* homologues), indicating that a loss of function of these genes may cause a defect in cell fate, and thereby, may cause prickle initiation. As previously, RcMMD1 can be a negative regulator of this gene network. We proposed that *RcMMD1* is expressed at the early stage of prickle initiation and may control (by transcriptional repression) the inhibitory network. In the glabrous stems, where RcMMD1 is not expressed, and the repressive network is active and no prickle can be initiated.

In the OW population, we found that prickle density is controlled by QTLs on LG3, 4 and 1 (Chapter 3, Figure 25). As for trichomes in *Arabidopsis*, the density of prickles can be explained by a complex regulation with negative feedback loops and communication between neighboring cells. In *Arabidopsis*, trichome formation is promoted by a trimeric activator complex (MBW, see Figure 5 in Chapter 1). This complex is activated by R3MYB proteins such as TRY, which can move to neighboring cells and repress the formation of trichomes (Hülskamp, 2004). *try* mutants present a higher density of trichomes (nested trichome, Hülskamp et al. (1994)). A similar process can be suggested for prickles in rose. The negative regulators present below the QTL3 and 4 can be part of this negative regulatory network. A precise spatial and temporal expression analysis of these genes and their interaction is necessary to test this hypothesis. Combination of the different alleles at these different loci may contribute to the diversity of prickle density.

5.3 Prickles in *Rosa* and *Rubus*: comparison of the different studies

Prickles have been little studied in roses and *Rubus*. However, some publications so exist. We compared our results with the results of these publications (Figure 36).

Prickle morphology

Prickle types

In a previous study on *Rubus* and roses (Kellogg et al., 2011), glandular trichomes (GTs), non- glandular and glandular prickles (NGPs and GPs) were described as the different developmental stages for the same type of prickle. Their conclusions were based on the observations of late developmental stages on the stem. In the rose cultivar 'Radtko', NGPs and GPs were present at the same time and at the same location of the developed stem. NGPs were proposed for the later stage of GPs (or GTs) with the fall of the glandular head from the stalk. Then, following growth, the GPs (or GTs) are converted into NGPs. However, no morphological evidence was provided for the early stage since prickle initiation begins at the shoot tip. In our study, we carried out a comprehensive morphological study. We found that GPs had a glandular head or several glands positioned along the prickle. These glands are present throughout their lifetime. In contrast, NGPs did not present any glandular structure. NGPs and GPs have their own developmental process (Chapter 2, Figure 13 and 14), and clearly represent different types of prickles but not different stages of the same prickle. Thus, we classified them into two categories: NGPs and GPs. We also found several types of prickles in wild roses that were classified into the sub-categories of NGPs and GPs, depending on if the prickles are branched or unbranched and if their surface is naked or covered with hairs (hairy).

Prickle origin

In the previous studies, prickles were described as epidermal appendages that evolved from epidermis and modified glandular trichomes in raspberry and rose (Kellogg et al., 2011), in blackberry (Coyner et al., 2005) and in grapes (Ma et al., 2016b). However, this result was not supported by any anatomical evidence. In our study, we found that NGPs evolve from multiple cells of the ground meristem under the protoderm. For GPs, multiple cells of the ground meristem first give rise to a bump, and then the protoderm (or epidermis) of the bump differentiates into gland cells (Chapter 2, Figure 14m-r).

QTL analysis

We compared our results with previous genetic studies by associating genetic markers and the reference genome sequences. In the tetraploid K5 population, three QTLs on LG3, 4 and 6 were detected (Bourke et al., 2018a). Two SNP peak markers, K7826_576 and K5629_995 were reported. The first one is located within our Chr3 cQTL interval region (36,517,224 - 46,440,369 bp), and the second is very close to our Chr4

Results from previous studies

Prickle morphology:

- NGP and GP are the same type but present different development stages.

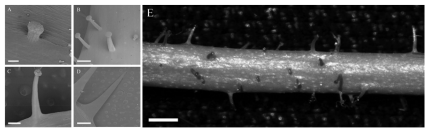

Developing prickles in *Rosa* hybrid (Kellogg et al. 2011).

Limitation: Lack of morphological evidence from early stage.

- Origin of prickles

Originated from epidermis (Peiterson 1921; Esau 1977; Coyner et al. 2005) and modified from GT (Kellogg et al. 2011; Ma et al. 2016; Khadgi, 2020a) or induced from GT (Pandey et al. 2018).

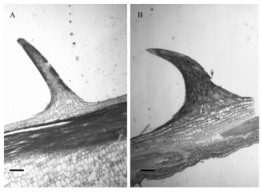

Raspberry (A) and blackberry (B) (Kellogg et al. 2011).

Limitation: no anatomical studies on the origin stages.

QTL

In raspberry (*Rubus idaeus*), a major QTL on LG4 and a minor QTL on LG6 were detected (Molina-Bravo et al. 2014). The QTL region on LG4 (position 0.101 Mb) is syntenic with the region on rose Chr4 (position 58,768 Mb), very close to the major QTL we detected on this chromosome. In another publication, Graham et al. (2006) detected a major QTL on LG2 (locus H) that controls cane pubescence. The locus is mapped on LG2, which is syntenic with the rose LG6 where one of the QTLs is detected in *R. x wichurana*.

Limitation:

1) Genetical study was conducted in a restricted genetic background.
2) Low density of genetic maps with SSR and AFLP makers
3) Prickle types was not considered as a factor in these studies.

RNA sequencing (Khadgi, 2020b):

Materials: Prickly 'Caroline', Prickless 'Joan J.' and their offspring. (*Rubus ideaus*). Morphology of three prickly and three prickless offspring are not clear.

Sampling: Sampled 'epidermal' tissues (the sampling method was not described).

Basic hypothesis:

NGPs, GTs or/and GPs on the stem of prickly 'Caroline' were considered as different stages of prickle. They were mixed in the sampling.

Workflow:

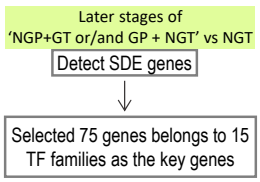

The limits of conclusions:

1) Used later stages of prickle development to answer the question of prickle initiation.
2) Based on an incorrect 'basic hypothesis' to propose the gene pathway is controversial.
3) The materials correspond to different stages of initiation and development of several structures (trichomes and prickles) making the results are difficult and distorted conclusions.

Results from our study

Prickle morphology (see Chapter 2):

- NGPs and GPs are different types of prickle and have their own developing process.

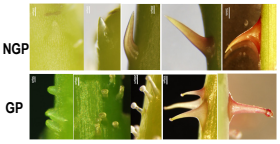

Developing process of NGP and GP in OW9106

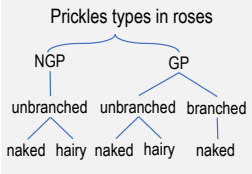

- Origin of prickles

NGP: Ground meristem under protoderm.

GP: multiple cells of the ground meristem first give rise to a bump, and then the protoderm (or epidermis) of the bump is differentiated into gland cells.

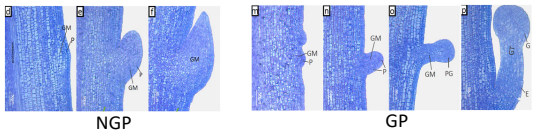

GM(ground meristem), P(protoderm), E(epidermis), PG(precursor gland), G(gland)

QTL (see Chapter 3)

The genetic determinism of prickle in rose is complex, with a major locus on LG3 that controls the absence/presence of prickles on the rose stem and several loci that control the prickle density. One major QTL on LG4 and two minor QTLs on LG1 and 3 were detected in the OW population (Zhou et al. 2020).

Limitation: Genetical study was conducted in a restricted genetic materials (a F1 population)

RNA sequencing (see Chapter 4):

Materials: Individuals of the F1 OW progenies (rose).

Sampling: Samples of stages I, IIa, IIb, IIc and III strictly according to the described stages of prickle (P) and glabrous stem (NP, stems at the same stages as P) (see Chapter 2; Zhou et al. 2020).

Workflow:

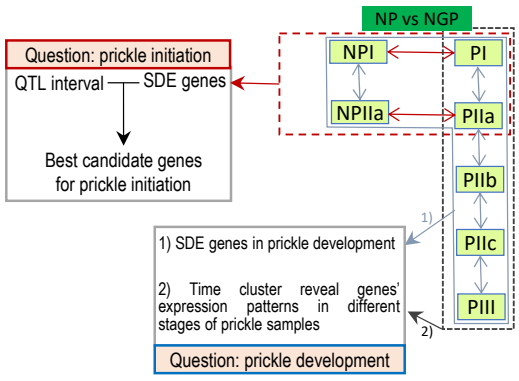

Materials and technical limitations :

1) Some differential expressed genes can be due to the different genetic background, even if we try to limit the differences by using individuals from the F1 progeny (brother/sister).
2) Due to technical limitations, the early stages of prickle initiation and development could not be separated from the stem. We, thus, took the prickle and stem together for all the stages (leaves and buds were removed). We could also not obtain the prickle initiation stage only; stage I represents initiation and the first growth of the prickle.

More details and Improvement solutions are presented in Chapter 4

Figure 36: Comparison of the different studies of prickles in *Rosa* and *Rubus*. NGP: non-glandular prickle, GP: glandular prickle, NGT: non-glandular trichome, GT: Glandular trichome, NP: no prickle

QTL interval region (46,189,407 - 56,107,784 bp). Thus we proposed that the QTLs on LG3 and 4 were detected in diploid OW (Zhou et al., 2020) and tetraploid K5 populations (Bourke et al., 2018) are probably the same QTL. A minor QTL was detected on LG1 in OW but not in K5. This is perhaps due to the different genetic background of the parents. In fact, one parent of K5 is prickly and the other one is glabrous, whereas both parents of OW have prickles.

In *Rosaceae*, a major QTL on LG4 and a minor QTL on LG6 were detected in raspberry (*Rubus idaeus*) (Molina-Bravo et al., 2014). We checked the synteny using synteny viewer tools (`https://www.rosaceae.org/synview/search;Jungetal.2014`). The QTL region, located on LG6 in *Rubus occidentalis* (position 6,028 Mb), is syntenic with a region on rose Chr2 (position 42,330 Mb), where no QTL was detected in our study. The major QTL region on LG4 (position 0.101 Mb) is syntenic with the region on rose Chr4 (position 58,768 Mb), that is very close to the major QTLs we detected on this chromosome (Table 2, Chapter 3). These results suggest that the two QTLs on LG4 in rose and raspberry might be syntenic and share a common evolutionary history. In another publication, Graham et al. (2006) identified the gene H that controls cane pubescence. The locus is mapped on LG2, which is syntenic with the rose LG6 where one QTL is detected in *R. x wichurana*. However, no precise location is available in *Rubus*, and no clear comparison can be made with rose, making it difficult to draw any conclusions concerning a possible common origin.

RNA sequencing

Only a few pieces of transcriptomic studies have been published. Unfortunately, as previously mentioned, these studies are based on potentially incorrect assumptions: GP and NGP are the different developmental stages of same type pf prickle, and prickles either develop directly from GTs (e.g., raspberry) or the signal coming from GTs induces the prickle development (Kellogg et al., 2011; Pandey et al., 2018; Khadgi and Weber, 2020a).

Khadgi and Weber (2020b) used two cultivars of red raspberry (*Rubus idaeus* L) to identify differentially expressed genes in the 'skin' tissue of 'Caroline' (a cultivar with prickle) and 'Joan J.' (a glabrous cultivar), and three prickly and prickless offspring. They sampled the 'epidermis' (the sampling method was not described) (Khadgi and Weber, 2020b), as prickles previously described as having originated from the epidermis (Khadgi and Weber, 2020a). As in Pandey et al. (2018), an imprecise term, epidermis, was used to describe the tissues. A more accurate description of the materials is needed. Another issue in this study the sampling of later stages of prickle development to decipher prickle initiation. Indeed, GP or GT were considered as the early stage of prickle development. It should also be mentioned that the prickly cultivar 'Caroline' presents NGPs, GPs or/and GTs and NGTs, while the prickless cutivar 'Joan J.' presented only NGTs. This means that in this study, the experimental design does not consider all the variable factors (NGP, GP, or/and GT). The six offspring were only described as prickly and prickless. Do they have NGPs, GPs, GTs or NGTs? This point is not clear. Furthermore, we do not know if the genetic background of the two cultivars is close or not. All these elements make it very difficult to interpret the results and to compare them with our results.

5.4 Old questions and new insight: prickles and trichomes

5.4.1 Homology

Several homologies and resemblances exist between prickles and trichomes. First, concerning their morphology, both trichomes and prickles are non-glandular or glandular, can be branched or unbranched, and neither have any vascular bundle. Second, considering their function and their co-evolution with herbivores, prickles and trichomes may have a certain homology. Non-glandular trichomes (NGTs) are normally thought to have evolved primarily as physiological barriers against extreme environmental conditions and herbivores (insects) (Kariyat et al., 2017). The earliest evidence of glandular trichomes (GTs) comes from the fossils of the late carboniferous (Stephanian stage, 290 Mya) where they are modified from NGTs in the process of their co-evolution with insects (Krings et al., 2003; Lange, 2015). Similarly, prickles are assumed to be an adaptation of rose against herbivores (insects and mammals) (Chaloner, 1970; Kariyat et al., 2017). A question therefore arises: are prickles or certain features of prickles inherited from trichomes? Combining morphological, ultrastructural, chemical and molecular evidence could help to answer this question. For example, from the morphology, NGPs and GPs are more closely related to NGTs and GTs, respectively.

5.4.2 Distinction

Trichomes, glandular or non-glandular, are epidermal appendages that originate from one or more protoderm (or epidermis) cell(s) only (Esau, 1953; Werker, 2000). Non-glandular prickles originate from the tissue under the protoderm, that we refer to as the ground meristem here (Figure 14). Glandular prickles also originate from the ground meristem, but their glands evolve from the protoderm of the stalk (or epidermis) during prickle development (Chapter 2). Usually, cells on the different positions perceive different signals, respond through intracellular signaling pathways and eventually adopt a specific cell fate, followed by the production of different organs or tissues. Thus, for trichomes and prickles, the tissue they evolve from is different (epidermis vs. sub-epidermis). Different gene networks may control prickle and trichome initiation and development. This hypothesis is supported by the results we obtained in the candidate genes (Chapter 3) and transcriptomic (Chapter 4) approaches. Since we proposed that the NGP may be more homologous to NGT than to GT, we identified in rose the homologues of genes involved in NGT initiation and development in *Arabidopsis*. In Chapter 3, we annotated 15 rose TFs that, based on similarity, can be involved in trichome development in rose: *RcGL1, RcMYB82, RcMYB61, RcCPC, RcTRY, RcGL3, RcTT8, RcMYC1, RcTTG1, RcTTG2, RcZFP5, RcGIS3, RcGIS2, RcZFP1* and *RcGL2* (Supplementary Table A.3). Among them, several were located in the confidence interval of the detected QTLs: *RcMYB61* and *RcTTG2* for the QTL on LG3; *RcGIS3* for the QTL on LG4; and *RcCPC*, *RcTRY* and *RcMYC1* for the QTL on LG1. *RcZFP5* (Chr04: 57,125,905 bp) is out of the QTL interval on LG4 in the OW progeny, but close to the LOD peak marker K5629_995 of a prickle QTL in the K5 population (Chr04: 57,791,999 bp) (Bourke et al., 2018a). These genes were considered as good candidates for the detected QTLs, but we cannot rule out the fact that these co-localizations may be just a coincidence. This coincidence is magnified,

especially when the morphological characteristics of trichomes and prickles are different, and when almost every chromosome has one or more candidate genes. Therefore, it is particularly important to gain further information by studying the transcript accumulation of these candidate-genes during prickle initiation and development. Consequently, we quantified the transcripts accumulation of 10 TF genes in glabrous and prickle F1 individuals at different developmental stages by RT-qPCR. Unfortunately, only minor differences were observed between glabrous and prickle samples. The main differences are between developmental stages but not between the type of stems (as demonstrated by the heatmap analysis). In Chapter 4, we compared the nine genes' whose expression was normalized by RNA sequencing and obtained quite similar expression patterns to those previously found by the RT-qPCR in Chapter 3. In addition, through Gene Ontology enrichment studies, we observed that some candidates for prickle initiation and development might be involved in organ development, including flowers, leaves, shoot, but not trichomes.

In conclusion, we suggest that NGPs and NGTs have different genetic pathways that control their initiation and development. This conclusion is different from the previous hypothesis: rose prickles and trichomes share a common genetic pathway (Khadgi and Weber, 2020b).

5.5 Beyond this study, what we can do next?

The genus *Rosa* is a very interesting model as it includes species at different ploidy levels, as well as rich phenotypes and a large genetic diversity. However, due to the highly heterozygosity character, the assembly of a rose genome is always a challenging task, which greatly limits the progress of related research in rose. The completion of two high-quality genomes is a starting point of genomic research in rose (Hibrand-Saint Oyant et al., 2018; Raymond et al., 2018). For genetic studies on prickles, we compared different genetic studies thanks to the positioning of the genetic markers on the sequence of the reference genomes. We easily combined genetics, candidate gene approaches and transcriptomic approaches. This integrative analysis has greatly enhanced our understanding of the genetic mechanism of prickle initiation and development. In this study, we provide a framework for studying the genetics and genomics of quantitative traits in a heterozygous woody species. Further studies that will combine GWAS, genomics (DNA sequencing) and functional validation can be done to go deeper into the analysis of the molecular mechanisms underlying the complexity of prickles in rose and to develop markers for breeding prickless roses.

5.5.1 Using genetic diversity to decipher prickle regulation and to develop markers for assisted breeding selection of prickless roses

5.5.1.1 GWAS study of different types of prickles (as a complex trait)

As a complement to QTLs analyses in F1 progeny, a genome-wide association study (GWAS) could be used on a rose core collection to study genetic determinism. QTL mapping is an efficient approach to study the genetic determinism in a target population and for a given trait. It provides high statistical power for

detecting QTLs. Despite the fact that QTL mapping has proved and remains a powerful method, it suffers from two fundamental limitations: the genetic basis is narrow in biparental approaches and the number of recombinations present in the F1 individuals limits the mapping resolution (especially if the population size is low). Consequently, we need larger populations to increase the resolution (Korte and Farlow, 2013). GWAS overcomes the limitations of QTL mapping but introduces other issues (Korte and Farlow, 2013). One of the main advantages of GWAS is to work on a larger genetic diversity, while the disadvantage is that the method is sensitive to the population structure that may lead to many false positives. GWAS can offer a very fine resolution (based on the LD decay). However, the power of QTL detection will be determined by the allele frequency. For instance, effects of rare alleles are difficult to detect. In GWAS, the genetic interaction between loci (epistasis), or the interaction between loci and the environment are not considered. Therefore, GWAS is often complementary to QTL mapping and, when performed together, they alleviate each other's limitations (Zhao et al., 2007; Brachi et al., 2010).

Since QTL mapping and GWAS are both based on the detection of correlations between phenotypes and molecular markers, the evaluation of the phenotype is an important issue when initiating genetic approaches. For example, as we discussed in the first section, we suggested that GPs and NGPs should be studied separately in F1 population ((Zhou et al., 2020), Chapter 3). Wild rose species or cultivated varieties have more diversified phenotypes than the F1 hybrids from the OW population. The scoring of the trait is then more complicated in GWAS. In Chapter 2, we proposed a rapid method to phenotype the different prickles in rose according to several characteristics. First, the presence of a glandular head (GPs vs. NGPs), then the presence of branched (unbranched vs. branched prickles) and, finally, the presence of hairs on the prickles ('naked' vs. 'hairy'). This method of phenotyping can be used by focusing on the different types of prickles and their anatomy. Different GWAS panels have recently been developed in roses (Schulz et al., 2016; Nguyen et al., 2017; Hibrand-Saint Oyant et al., 2018), and unpublished data from the GDO team) with a high-density genotyping using an AXIOM-ARRAY. These panels can be studied for different types of rose prickles (with the proposed method). It can help to identify new loci and to then validate other good candidates identified by the transcriptomic approach (Chapter 4).

5.5.1.2 Develpment of genetic markers for assisted breeding of prickless roses

Molecular markers remain essential for genomic research and for molecular breeding of any crop. The latest developments in rose genomics have led to the generation of a wide range of genomic tools and technologies for application in ornamental trait improvement. In Chapter 3, the peak markers of QTLs on LG3 are highly associated with the absence and present of prickles. However, few recombinants are observed in the progeny between the peak marker and the *PRICKLE* locus. Further studies are necessary to develop specific markers for assisted selection of prickleless roses. Combining QTL and GWAS results may help to develop markers that will be closer to the *PRICKLE* locus.

Single-nucleotide polymorphism (SNP) markers have now become the most popular markers due to advances in sequencing technologies. DNA sequencing (or whole genome sequencing) by Illumina technology

is now becoming cheaper and easier and could be used for genotyping in GWAS (Genotyping by Sequencing). Through mapping on the reference genome (Hibrand-Saint Oyant et al., 2018; Raymond et al., 2018), it was possible to detect SNPs and Indels everywhere on the genome. SNP and Indel effects can then be annotated as frameshift variants, new stop codons, splicing variants (splice donor or splice acceptor variant) or intron variants. Combined with the genetic knowledge from Chapter 3, a strategy can be developed to mine the SNP markers and associated SNP with prickless or prickle alleles. The preferred materials for DNA sequencing are the prickle and prickless genotype in another population, which was obtained in China from a cross between *R. chinensis* 'Old Blush' (OB) and *R. wichuraiana* 'Basyes' Thornless' (which may be a mutant or offspring of RW) (Zhou et al., 2017). The genetic information for prickle trait in this population will facilitate the data analysis in subsequent studies, and the sister genotype can reduce the uncertain genetic background factors.

5.5.1.3 Detecting the genetic diversity of the candidate genes discover in Chapter 4

Through the whole genome sequencing we mentioned above, a large number of genes can be assembled and annotated based on the reference genome. Presently, around 20 roses (prickly) genomes (short reads) have been released (Hibrand-Saint Oyant et al., 2018; Raymond et al., 2018). Rose comparative genomic strategies in prickle and prickless samples can be used to detect the genetic diversity of the candidate genes discovered in Chapter 4. However, the genome of prickless genotypes should be re-sequenced. The seven glabrous genotypes we presented in Chapter 2 are a material of choice to be re-sequenced. They are *R. multiflora* 'inermis', *R. wichurana* 'Bayses' Thornless', *R. pimpinellifolia* 'lutea', *R. banksiae* 'alba plena' and *R. banksiae* 'lutea', *R. banksiae* var. normalis, *R. fraxinifolia* Lindl.

5.5.2 RT-pPCR to identify if the inhibitors can impact NGP density

In Chapter 4, we mentioned many good candidate genes related to prickle initiation. Most of them are mainly expressed in prickless samples, and are considered to be inhibitors of prickle formation. We proposed that the inhibitors may be involved in a complex regulatory network that could impact prickle density. To test this hypothesis, we can use a RT-qPCR method to test if the transcript accumulation of those genes can be correlated with the density of NGPs. Different F1 individuals from the OW progenies with different density can be used. Materials should be sampled at an early developmental stage such as Stage I. We can expect to detect a correlation between the transcript level and prickle density. These inhibitors are RC3GO350900 (RcPKL), R3G0389900 (RcWOX-g1), RC4G0448500 (RcWOX-g2), RC3G0419900 (RcAS2), RC4G0393200 (RcJAG), RC4G0398800 (RcDOT5), RC3G0386900 (RcAKR1), RC1G0289800 (AFO), RC70233600 (AFO), RC4G0428600 (MYB16), RC1G0527600 (KCS6), RC7G0011600 (KNAT1), RC7G0049900 (MYB106), RC3G0071300 (MYB106), RC2G03132700 (BOP2), RC2G0036100 (YAB5), RC5G0428600 (YAB2) etc. The first seven can be studied in priority.

5.5.3 Functional validation

Through this project, we have explored ten good candidate genes for prickle initiation. Seven (*RcWOX-g1, RcWOX-g2, RcAS2, RcJAG, RcDOT5, RcAKR1*) were proposed to be positive regulators of glabrous stem development (or repressors of prickle initiation). Three (*RcMMD1, RcAMI1, RcNAP1-like1*) were suggested to be activators of prickle initiation and development. The candidate genes described in this study are highly associated with prickle formation since we combined transcriptomic and genetic approaches. However, it is still too early to say that they are the key regulators. Further research is necessary and, especially, functional validation.

For the seven potential repressors, we have suggested that using a RT-qPCR method to identify their relationship with prickle density as in the previous section. Another hypothesis is that they are the important regulators for the boundaries of glabrous stem development. To validate this argument, we can knock-down or silence these genes in individuals with glabrous stems to check if it will give a prickle phenotype or a defect stem (compare with glabrous).

For the three potential promotors (*RcMMD1, RcAMI1, RcNAP1-like1*), two approaches can be proposed for a functional validation: (1) An ectopic expression of these genes in glabrous individuals to check if the transgenic roses will have prickles; (2) A knock-down or silencing of the genes in individuals with prickles to check if transgenic roses will be prickless or will have a lower prickle density.

Since prickle and trichome development might not share a similar regulatory network (see previous discussion), functional validation in *A. thaliana* is not essential. Functional validation has to be done in rose where transient and stable transformation protocols exist (Firoozabady et al., 1994; Randoux et al., 2012). A recent review (Smulders et al., 2019) summarized rose genetic transformation. It should be observed that some candidates (*RcWOX-g1, RcWOX-g1, RcAKR1, RcMMD1, RcNPI1*) are duplicated and present paralogs. This may affect functional validation of single genes and may complicate the analysis. We should therefore pay more attention to this point for the experimental design and for the interpretation of the results.

Appendices

A Supplementary tables and figures associated with Chapter 3

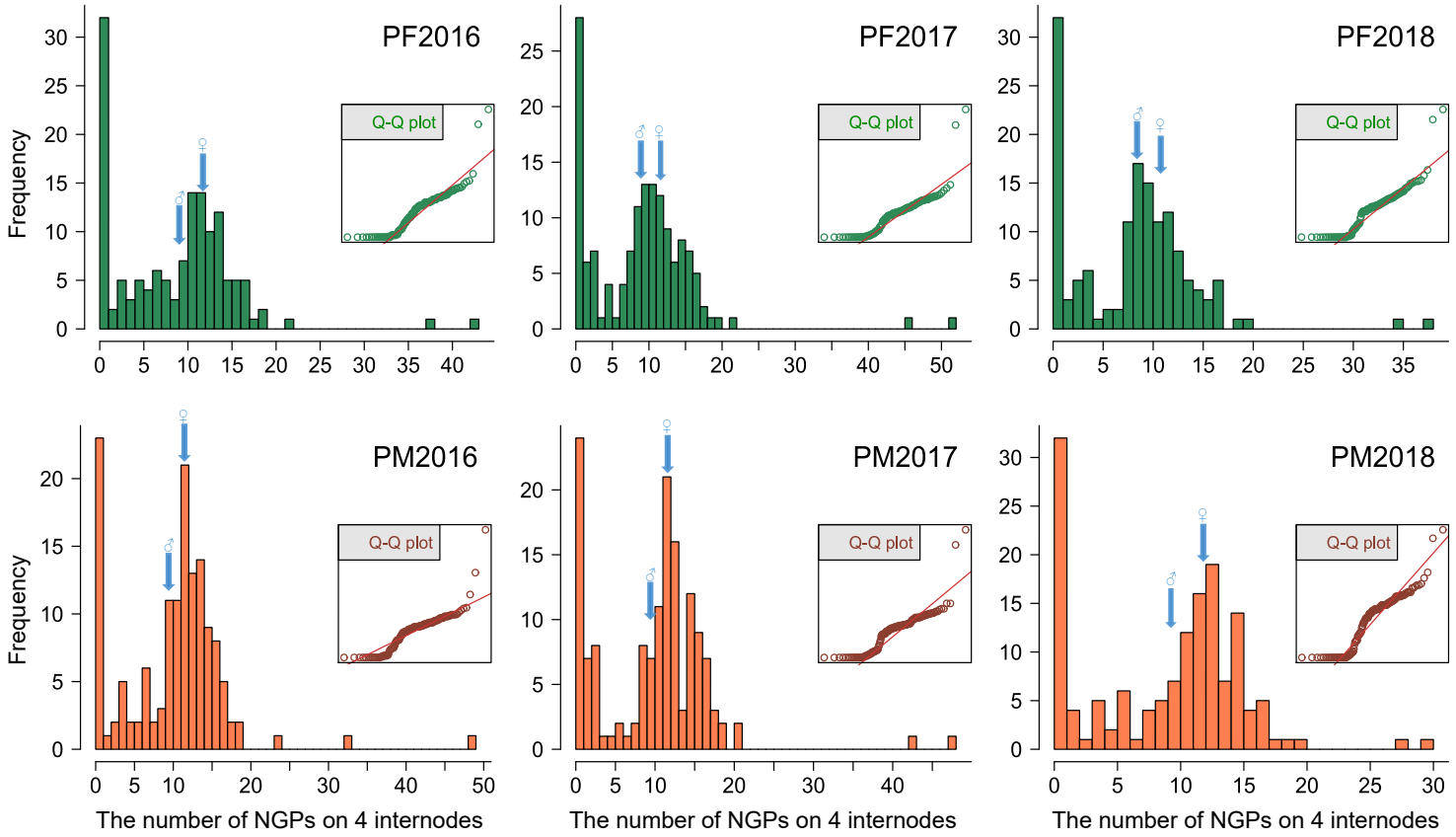

Supplementary Figure A.1: Frequency distribution and Q-Q plot of non-glandular prickles on four internodes in the OW population for floral stems (PF) and the main stem (PM) for the three years (2016, 2017 and 2018).

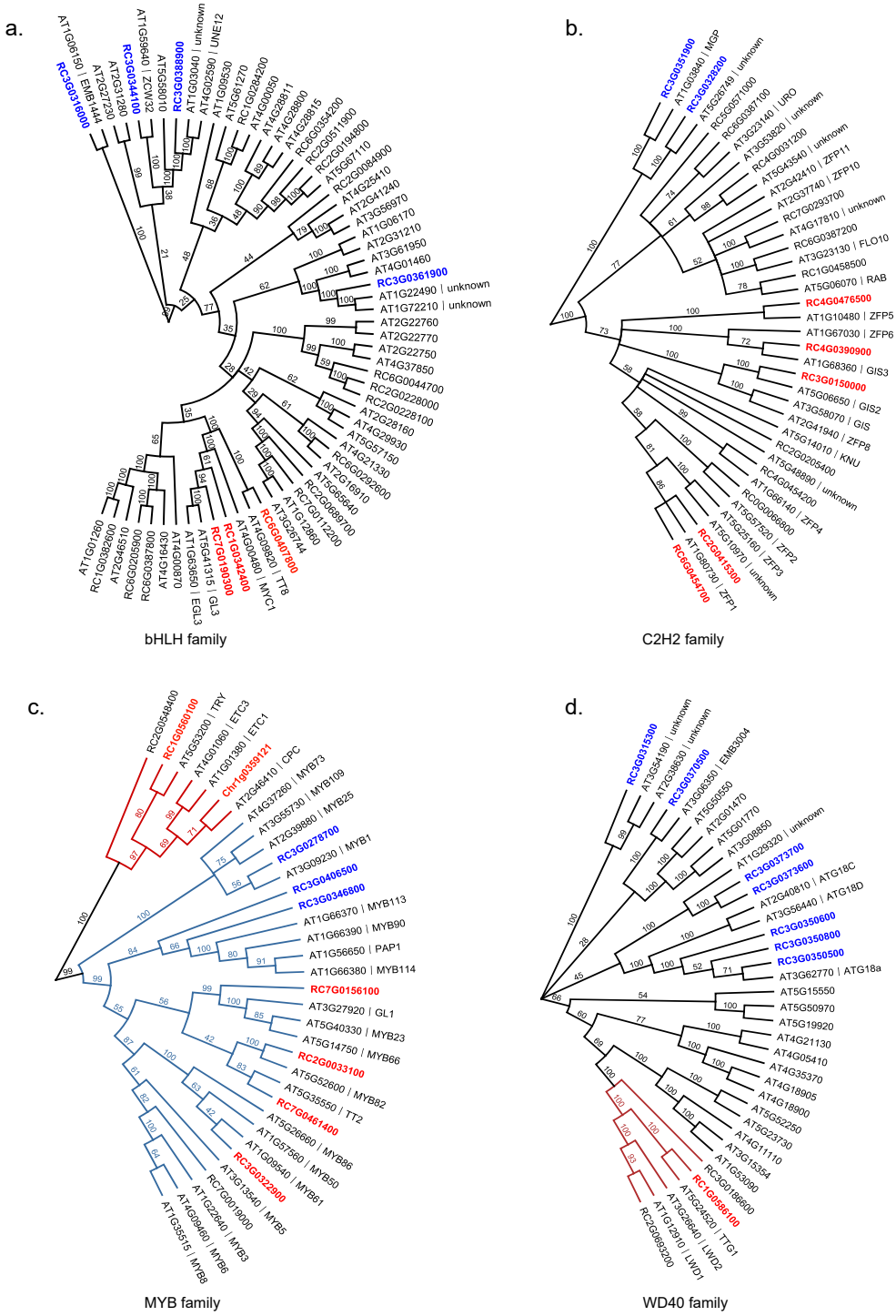

Supplementary Figure A.2: Phylogenetic analysis of the transcription factor family involved in trichome initiation and development: (a) bHLH, (b) C2H2 Zinc-Finger, (c) MYB: R3MYB (red sub-tree) and R2R3MYB (blue sub-tree), and (d) WD40. The rose genes homologues of genes involved in trichome initiation and development are in red. For *A. thaliana*, the protein name corresponds to the TAIR database (https://www.arabidopsis.org/), and for rose, to the reference genome of the haploid of 'Old Blush' (Hibrand-Saint Oyant et al. (2018)), except for Chr1g0359121 and Chr2g0138951 (Raymond et al. 2018)

Supplementary Table A.1: Primer sequences of candidate genes for qPCR.

Primer name	Sequence of primers
RcMYC1-1-F	5’ CCACCCTCAATGATGTTCTC 3’
RcMYC1-1-R	5’ TTCTGGCGTCTCAACACTTAC 3’
RcTT8-1-F	5’ AGAGAGCGATGGATTGTTGG 3’
RcTT8-1-R	5’ GCCCTCTTCACTTCTGTAATGG 3’
RcGIS2-1-F	5’ CTGGTGACTCCGTTGTTCG 3’
RcGIS2-1-R	5’ TCCCTAAGATGGATGGATTGA 3’
RcGIS3-1-F	5’ GGCCATCGTTGAGTAGGTTC 3’
RcGIS3-1-R	5’ GGAGTCAGAGGCTGAGTTGC 3’
RcTRY-1-F	5’ GGAAAGCAGAAGAAATAGAGAGG 3’
RcTRY-1-R	5’ CTACTACTGACAAGGAAAACCAATG 3’
RcTTG1-1-F	5’ TCCAATGTCAATGTACTCGGC 3’
RcTTG1-1-R	5’ CCTCCTCAAACCTTCAACAGC 3’
RcTTG2-1-F	5’ CCTCAAACCCAGGAGCATC 3’
RcTTG2-1-R	5’ CAACAGCTTGATCCCTGAGAG 3’
RcCPC-F	5’ GACATTGTGAGGTGTTTGCTGAG 3’
RcCPC-R	5’ AATCCGCTGAAAGTTCGACG 3’
RcMYB61-F	5’ GGATCTTCAGAGACTCGCTGTAGC 3’
RcMYB61-R	5’ CAAGCCCTCCTCTCACATTCAT 3’
RcZFP5-F	5’ CAGGAGAAAGCAGACCAGTGAT 3’
RcZFP5-R	5’ GGCAAGCCAATCCCTAACTG 3’

Supplementary Table A.2: Summary of QTLs for NGP with two-part QTL model in OW progeny.

			QTL Characteristics			
Trait	Phenotyping	PT[a]	$LG@positon$[b]	MM[c]	bd[d]	r(%)[e]
Binary(p)	PF2016	2.57	OB3@44.4	Rw35C24	40,215,502	15.93
	PF2017	2.53	OB3@44.4	Rw35C24	40,215,502	15.18
	PF2018	2.6	OB3@44.4	Rw35C24	40,215,502	16.12
	PM2016	2.47	OB3@44.4	Rw35C24	40,215,502	14.76
	PM2017	2.58	OB3@44.4	Rw35C24	40,215,502	13.38
	PM2018	2.51	OB3@44.4	Rw35C24	40,215,502	16.72
	PF2016	2.67	RW3@42.6	Rh12GR_52506_1218	42,317,122	29.31
	PF2017	2.59	RW3@42.6	Rh12GR_52506_1218	42,317,122	30.33
	PF2018	2.57	RW3@42.6	Rh12GR_52506_1218	42,317,122	28.72
	PM2016	2.54	RW3@42.6	Rh12GR_52506_1218	42,317,122	20.69
	PM2017	2.56	RW3@42.6	Rh12GR_52506_1218	42,317,122	26.84
	PM2018	2.59	RW3@42.6	Rh12GR_52506_1218	42,317,122	33.21
	PF2016	2.67	RW2@16.2	CTG356	1,674,220	1.80
	PM2016	2.47	RW6@22.3	RhMCRND_12897_444	17,698,816	2.70
Quntitative(μ)	PF2016	2.42	OB4@30.6	Rh12GR_60129_183	52,239,028	9.02
	PM2016	2.36	OB4@30.6	Rh12GR_60129_183	52,239,028	9.26
	PM2017	1.92	OB4@30.6	Rh12GR_60129_183	52,239,028	9.88
	PM2018	2.8	OB1@67.7	Rh12GR_62822_144	7,388,536	6.66
					7,633,108	
	PF2016	2.39	RW3@42.6	Rh12GR_52506_1218	42,317,122	20.98
	PM2016	2.26	RW3@28.3	Rh12GR_78941_279	36,727,828	14.23
	PM2017	1.88	RW3@32.3	Rh88_36897_190	38,554,327	12.61
	PM2018	2.52	RW3@42.6	Rh12GR_52506_1218	42,317,122	38.64
	PF2018	2.57	RW1@24.1	Rh88_6034_211	45,638,457	7.80

[a] PT Genome-wild LOD significance threshold was defined by a permutation test.
[b] LG@positon Chromosomal linkage group, using the separate map (OB and RW) numbering of (Hibrand-Saint Oyant et al., 2018) @ peak location in cM.
[c] MM Closest molecular marker (MM) associated.
[d] bp Location in base pair (bp) on the *Rosa chinensis* Genome v1.0 (Hibrand-Saint Oyant et al., 2018).
[e] r(%) Percentage of explanation.

Supplementary Table A.3: Summary the rose homologies genes know in *A. thaliana* to be involved in trichome initiation

Family	[a]AT genes	Function description	[b]Mutant vs WT	[c]Rose protein	[d]Rose geneID	[e]Genome location
R2R3MYB	AT3G27920/GL1	Interacts with JAZ and DELLA proteins to regulate trichome initiation	No trichome	RcGL1	RC7G0156100	Chr07:11958961..11961286 (2.33 Kb)
	AT5G52600/MYB82	MYB82 and GL1 can form homodimers and heterodimers at R2R3-MYB domains. At least one of the two introns in MYB82 is essential to the protein's trichome developmental function		RcMYB82	RC2G0033100	Chr02:2470719..2472719 (2 Kb)
	AT1G09540/MYB61	Affects trichome initiation, root development and stomatal aperture	Fewer trichome	RcMYB61	RC3G0322900	Chr03:39896892.. 39899077(2.18kb)
R3MYB	AT2G46410/CPC	Positive regulator of hair-cell differentiation. Preferentially transcribed in hairless cells.	Increase density	RcCPC	Chr1g0359121	Ch01: 47708266..47710558bp(2.32kb)
	AT5G53200/TRY	Involved in trichome branching	cluster phenotype	RcTRY	RC1G0560100	Chr01:62070383..62072848(2.47 Kb)
bHLH	AT5G41315/GL3	Encodes a basic helix loop helix domain protein that interacts with GL1 in trichome development. GL3 interacts with JAZ and DELLA proteins to regulate trichome initiation.	Fewer trichome	RcGL3	RC7G0190300	Chr07:15536877..15543259 (6.38 Kb)
	AT4G09820/TT8	TT8 is a regulation factor that acts in a concerted action with TT1, PAP1 and TTG1 on the regulation of flavonoid pathways, Also important for marginal trichome development.	Fewer trichome	RcTT8	RC6G0407800	Chr06:52002793..52009528 (6.74 Kb)
	AT4G00480/MYC1	MYC-related protein with a basic helix-loop-helix motif at the C-terminus and a region similar to the maize B/R family at the N-terminus	Fewer trichome	RcMYC1	RC1G0342400	Chr01:44468298..44473643 (5.35 Kb)
WD40	AT5G24520/TTG1	Involved in trichome and root hair development. Controls epidermal cell fate specification.	No trichome	RcTTG1	RC1G0586100	Chr01:63982095..63985616 (3.52 Kb)
WRKY	AT2G37260 /TTG2	Trichome development	Trichome clusters and a reduced trichome number	RcTTG2	RC3G0244800	Chr03:33397852..33403551 (5.7 Kb)
C2H2	AT1G10480/ZFP5	Acts downstream of ZFP6 in regulating trichome development by integrating GA and cytokinin signaling.		RcZFP5	RC4G0476500	Chr04:57125905..57127513 (1.61 Kb)
	AT1G68360/GIS3	GIS3 is involved in trichome initiation and development downstream of GA and cytokinin signaling.		RcGIS3	RC4G0390900	Chr04:50315805..50317009 (1.21 Kb)
	AT1G80730/ZFP1	Expressed at high levels in the shoot apex, including the apical meristem, developing leaves and the developing vascular system		RcZFP1-like1	RC2G0415300	Chr02:47908413..47909551 (1.14 Kb)
				RcZFP1-like2	RC6G0454700	Chr06:55856328..55858302 (1.98 Kb)
	AT5G06650/GIS2	Regulates trichome formation on inflorescence stems; is also influenced by cytokinins		RcGIS2	RC3G0150000	Chr03:23331984..23333173 (1.19 Kb)
HD-ZIP IV	AT1G79840/GL2	A homeodomain protein affects epidermal cell identity including trichomes, root hairs and seed coat		RcGL2	RC2G0467100	Chr02:54366345..54368366 (2.02 Kb)
					RC2G0467200	Chr02:54367536..54371324 (3.79 Kb)
					Chr2g0138951	Che02:54366345..54371324(5.81 Kb)

[a] AT *A. thaliana.*
[b] Mutant vs WT The trichome phenotype in mutant compare with wild type.
[c] Rose protein The rose protein were named according to gene name in *Arabidopsis*.
[d] Rose geneID The rose gene ID were named in *Rosa chinensis* Genome v1.0 (Hibrand-Saint Oyant et al., 2018).
[e] Genome location The gene Location on the *Rosa chinensis* Genome v1.0 (Hibrand-Saint Oyant et al., 2018).
Green The rose gene ID were named in *Rosa chinensis* 'Old Blush' homozygous Genome v2.0 (Raymond et al., 2018).

Supplementary Table A.4: Prickle number on four internodes of two types of stems for three years in OW progeny.

Indiciduals	PF2016	PF2017	PF2018	PM2016	PM2017	PM2018
Ow9001	0.67	5	2.67	10	12.67	10.33
Ow9003	0	0	0	14	12.33	8.33
Ow9004	2	3	0.33	3	3	0
Ow9005	10.67	12	11.67	10.67	12.33	11
Ow9006	3.67	4	9	3.67	4	0
Ow9007	3.67	4.67	8.33	10	4.67	5.67
Ow9008	6	0.67	0	6	2.67	1.33
Ow9009	7	4.33	2	7	5.33	12.33
Ow9010	11.67	11	7.67	11.67	15.67	12.67
Ow9011	11	11.67	9	11	11.67	11.67
Ow9012	11.67	14.67	11.67	15	17	14.33
Ow9013	1	2.67	4	2.67	2.67	4
Ow9014	2.33	10	0.67	9.67	10	2
Ow9016	NA	NA	NA	8.33	NA	NA
Ow9017	15.67	17	14.33	15.67	18.33	14.67
Ow9018	9.67	8.67	11.33	9.67	8.67	10
Ow9019	0	0	0	0	0	0
Ow9021	13.67	15.33	14.67	13.67	15.33	14.33
Ow9022	9.67	10	7.67	11.33	9.67	9.33
Ow9023	15.33	15.67	13.67	15.33	15.67	14.33
Ow9024	16	13	11.33	16	16.67	16.33
Ow9025	14	13	11.67	14	13	13.67
Ow9027	13	8.67	8.33	13	8.67	9
Ow9029	10	10	7.67	10	10	8.33
Ow9030	10.67	10.67	11.67	12	11	11.33
Ow9031	12.33	12.33	8.33	12.33	12.33	15.33
Ow9032	9.33	6.67	3.33	14.33	2	0.33
Ow9033	12.33	11	9	12.33	12	13.33
Ow9034	15.67	17.33	13.33	15.67	17.33	15
Ow9035	14	15	16.67	14	15	5
Ow9036	0	0	0	0	0	0
Ow9037	0	0.67	2	0.33	0.67	1
Ow9038	0	0	0	7.67	2.33	5.33
Ow9039	10.33	13	10.33	13.67	12	14.33
Ow9040	11.67	11.67	9	11.67	12	10.33
Ow9041	5.67	6.67	8.67	5.67	6.67	10.33
Ow9042	11.67	9.67	13	11.67	12.67	13.67
Ow9044	0.67	1	0.67	3.33	1	0
Ow9045	3.33	4.33	4.33	3.33	2.67	3.67
Ow9046	0	0.33	4	12.67	0.33	0.33
Ow9047	4.33	2	6	4.33	2	0
Ow9049	1	0	4	1	0	0
Ow9050	14	15.33	16	14	15.33	13.33
Ow9051	0.67	0.33	0	0.67	0.33	0.33
Ow9052	13.67	14.33	12.33	16.33	14.33	12.33
Ow9054	0	0	0	0	0	0
Ow9055	6.67	6.67	9.33	6.67	11	11.67
Ow9056	NA	0	0	0	0	0

Continued.....

Supplementary Table A.4–*Continued from previous page..*

Indiciduals	PF2016	PF2017	PF2018	PM2016	PM2017	PM2018
Ow9057	0	0	0	0	0	0
Ow9058	NA	0	0	0	0	0
Ow9059	0.33	1.33	0.33	0.33	1.33	0.67
Ow9060	1	1.33	2.67	1	1.33	1
Ow9061	12.67	12	9.33	11.33	12	12.33
Ow9062	12.67	9.67	7.67	14.67	14.33	14.67
Ow9065	2	1.67	0	3.67	8.67	4
Ow9066	2.33	6.33	3.67	10.67	10	11
Ow9067	0	0	0	0	0	0
Ow9068	0	0	0	0	0	0
Ow9069	14.33	14.67	11	14.33	14.67	13
Ow9071	14	21.33	12.67	18.67	16	13.67
Ow9072	16.67	16.67	13	16.67	16.67	12.33
Ow9074	11.67	11	10.33	11.67	11	5.67
Ow9075	11.67	14	9.33	11.67	14	12.67
Ow9076	2.67	3	1.67	11.67	3	0
Ow9077	10.67	9.67	10.33	10.67	15	14.33
Ow9078	0.67	0	0	0.67	0	0
Ow9079	11.67	8.67	7.67	11.67	12	12
Ow9080	12.67	10.33	9.67	13.33	16.33	12.33
Ow9081	13	13	12.33	13	15	15.33
Ow9082	9.33	12	11.33	9.33	12	11.33
Ow9083	12	9	9	12	9	12
Ow9084	14.33	14	13.67	15.67	20.33	17
Ow9085	12	3	10	12	12	13
Ow9087	14.33	15	12.67	14.33	15.33	14.67
Ow9088	10.33	11.33	10.33	12.33	11.33	11
Ow9089	13.33	13.67	13	13.33	15	15.33
Ow9091	0.67	1	0.67	0.67	1	0
Ow9092	8	7.33	8.33	15.67	12	6
Ow9095	11	11.33	7.33	11	11.33	12.33
Ow9096	5.67	10.67	9.33	9.67	10.67	11
Ow9098	2.67	10.67	9.33	9.33	11	11.33
Ow9099	13.33	12	14.67	13.33	12.67	9.33
Ow9100	6.67	8	8.33	6.67	8	9.33
Ow9101	15	16	11.33	15	15	17.33
Ow9103	15	8.67	11	15	15	14.33
Ow9104	10.67	12.33	9	13	11.67	13
Ow9105	12.67	12	8	12.67	12.33	12
Ow9106	43	45.67	38	48.67	48	30
Ow9107	38	52	35	32.33	42.33	29
Ow9109	12	10.67	9.67	12	10.67	11.33
Ow9111	6	2.67	0.33	16.33	2	10.33
Ow9113	15.67	14.33	13.33	15.67	18.33	13.33
Ow9115	6.67	0.33	0.33	6.67	6	1.33
Ow9116	12	12.67	12	12	12.67	11.33
Ow9117	13.33	14	15	15	16	14.33
Ow9119	0	0	0	0	0	0
Ow9120	8	10	9.33	8	10	7
Ow9121	4.67	5.33	5.67	11.67	10.33	9.67

Continued.....

Supplementary Table A.4–*Continued from previous page..*

Indiciduals	PF2016	PF2017	PF2018	PM2016	PM2017	PM2018
Ow9122	9	9.67	10.67	9	9.67	7.33
Ow9123	11.67	7.67	7.67	10	9	9
Ow9124	5	10	9.67	12.67	12.67	12.67
Ow9125	7.67	9	7	11.33	11.67	9.33
Ow9126	9.67	15	10	24	20.33	12.33
Ow9127	13.33	11.67	8.67	13.33	11.33	11
Ow9128	0	1.33	0	0	1.33	1.33
Ow9129	5	10.67	11.33	12	11	11.33
Ow9132	0	0	0	0	0	0
Ow9133	0.67	1.67	0	0.67	1.67	0
Ow9134	18	13.67	16.67	18	13.67	18.67
Ow9137	5	7.67	3.67	8.33	11	8
Ow9138	10.67	10	8	15	15.67	12.33
Ow9139	18.67	20	20	17.33	17.33	15
Ow9140	6.67	9	9	6.67	11.67	10.67
Ow9142	10.67	10.33	9.67	10.67	10.67	12.67
Ow9143	16.67	12	9.33	13	12.33	9.33
Ow9144	21.33	15	16	16	14.33	14.67
Ow9147	16.33	18	13.67	16.33	18	11.33
Ow9148	NA	16	16	NA	16	8
Ow9149	0	0	0	0	0	0
Ow9150	0	0	0	0	0	0
Ow9151	NA	12.33	12	NA	12.33	13.33
Ow9152	13.33	13.33	16.33	13.33	15	20
Ow9153	0	2.33	2.33	3.67	2.33	3
Ow9154	16.33	15.33	15.33	16.33	15	12.33
Ow9155	8	9	9	11.67	11.67	10.33
Ow9156	8.33	8	7.67	11.67	11.67	10.67
Ow9158	NA	9	3	NA	8.67	4
Ow9159	9.67	10	10.67	11	12.33	11.33
Ow9160	17	15.33	10	12	12.33	14.33
Ow9161	10.33	9.67	10	10.33	12	7.33
Ow9163	0.67	2.33	0	0.67	2.33	0.67
Ow9166	0	0	0	2	0	0
Ow9167	11	9.67	10	11	9.67	10
Ow9168	6.33	9	7	6.33	9	6
Ow9169	10.67	10.67	11	10.67	10.67	11.33
Ow9171	0	0.67	0	0	0.67	0
Ow9172	13.33	16.33	17	13.33	16.33	15.33
Ow9173	NA	16.67	16.67	NA	16.67	16.67
Ow9174	NA	8	8	13.33	8	5.33
Ow9175	11.67	9	8.33	13.33	14	12.33
Ow9178	0	0	0	0	0	0
Ow9179	12.67	13	12.33	12.67	12.67	16.33
Ow9180	11	10.33	10.67	11	11.33	12.33
Ow9181	0	0	0	0	0	0
Ow9182	7.67	NA	7.67	9.67	NA	3.67
Ow9185	12.67	11.33	11.67	12.67	11.33	11.67
Ow9186	0	NA	2.67	4.67	NA	2
Ow9190	11.67	16.33	10.67	11.67	13	13

Continued.....

Supplementary Table A.4–*Continued from previous page*..

Indiciduals	PF2016	PF2017	PF2018	PM2016	PM2017	PM2018
Ow9191	2.67	7.33	7.67	9.67	9	8.67
Ow9192	8.33	10.33	9	12.67	11.33	11.33
Ow9197	19	19	18.33	19	16.33	17

B Supplementary tables and figures associated with Chapter 4

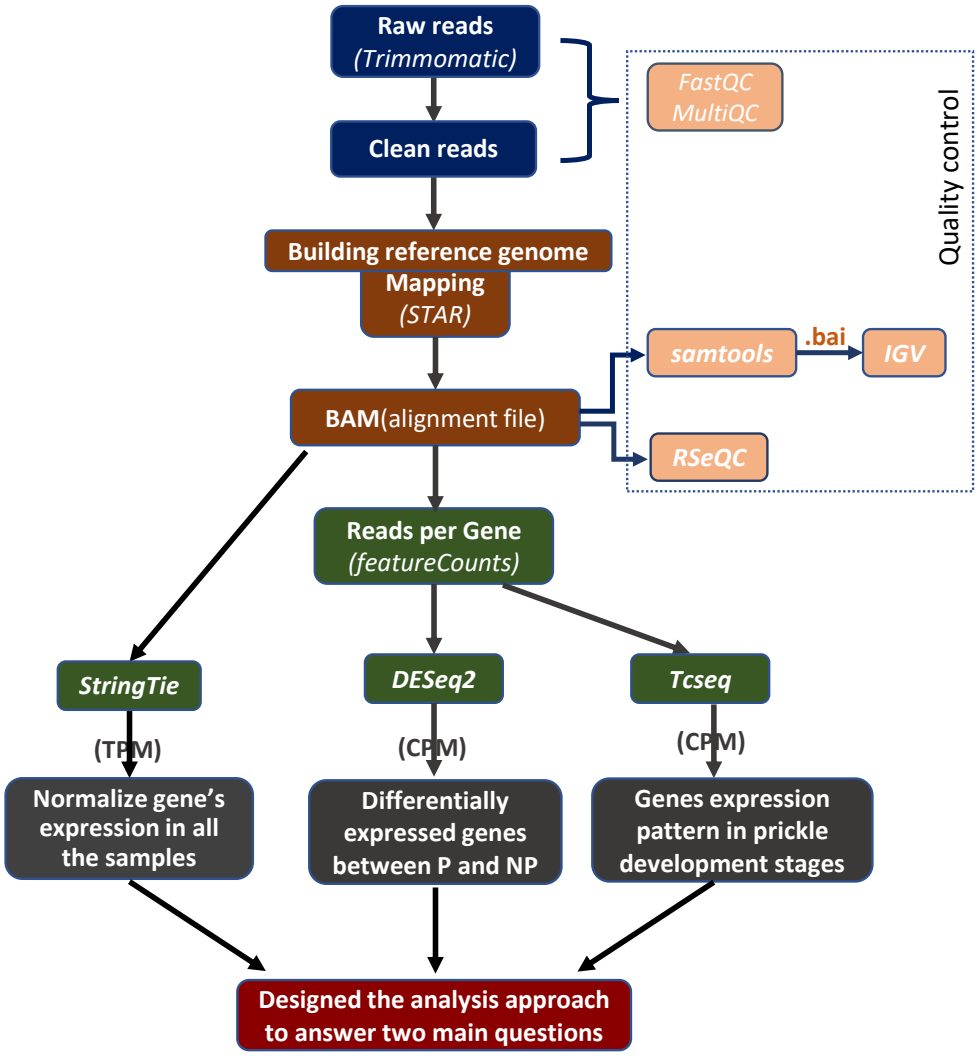

Supplementary Figure B.1: An overview of the pipeline for RNAseq Bioinformatics analysis. TPM: Transcripts Per Kilobase Million. CPM: Counts per million.

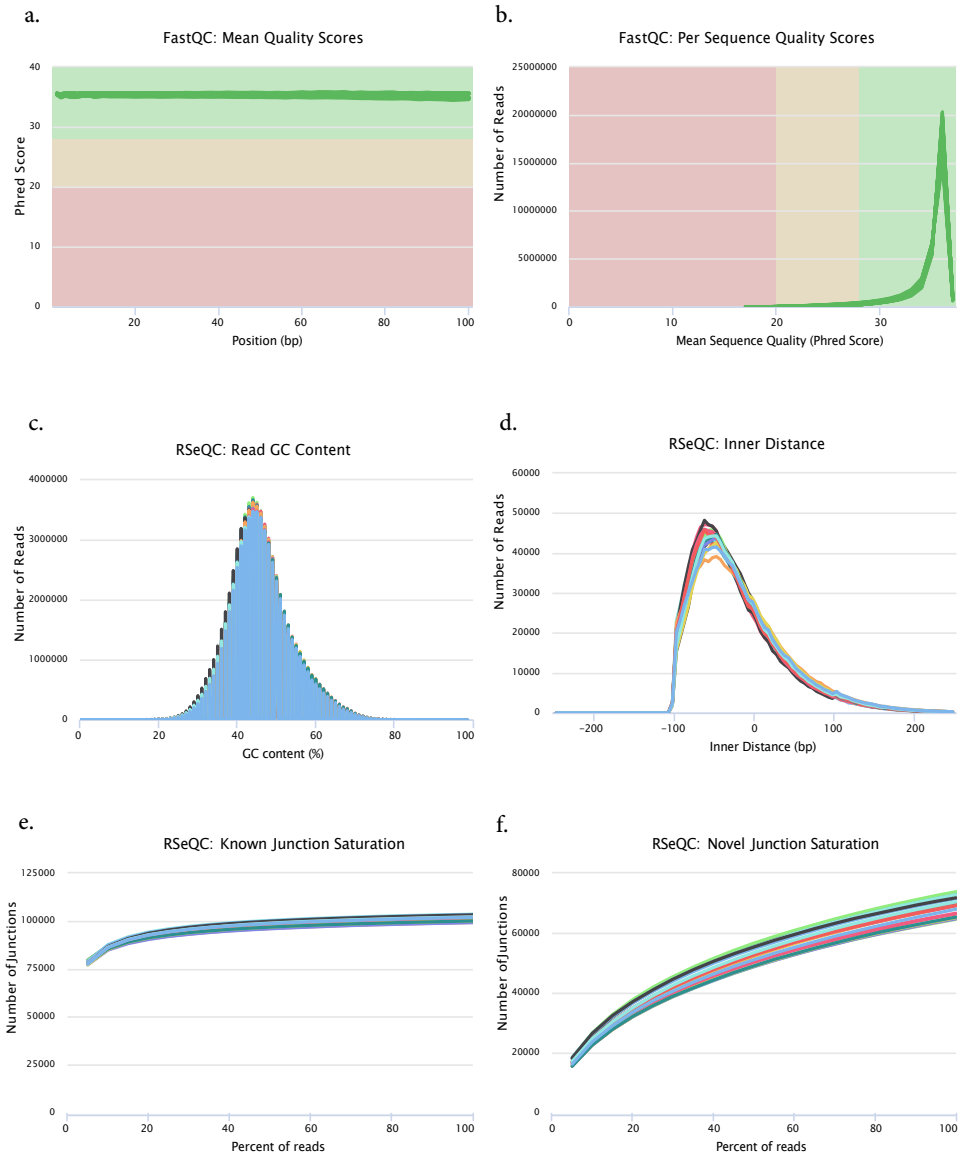

Supplementary Figure B.2: Quality control of clean reads in each dataset. (a) The mean quality value across each base position in the read. (b) The number of reads with average quality scores. Shows if a subset of reads has poor quality. (c) a histogram of read GC content. (d) Inner distance between two paired RNA reads.(e) The number of known splicing junctions that was observed. (f) the number of novel splicing junctions that was observed.

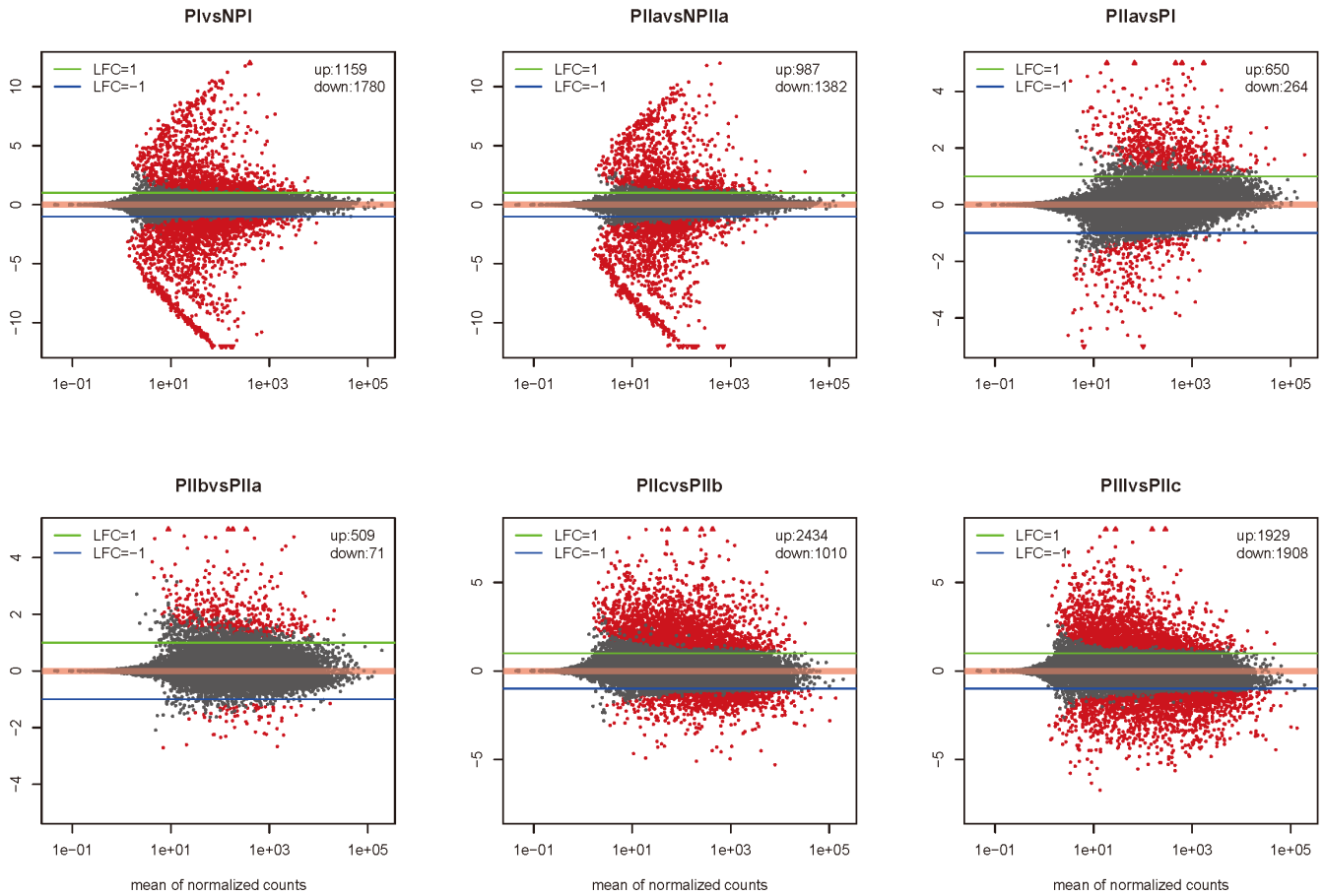

Supplementary Figure B.3: MA plot visualized the differences between expression taken in two compared samples, by transforming the data onto M (log fold changes) and A (mean of normalized counts) scales. Title names indicate ‘treatment’ vs ‘control’; LFC indicates shrunken log2 fold changes; ‘up:number’ and ‘down:number’ indicates the SDE genes number of up- and down-regulation expression respectively.

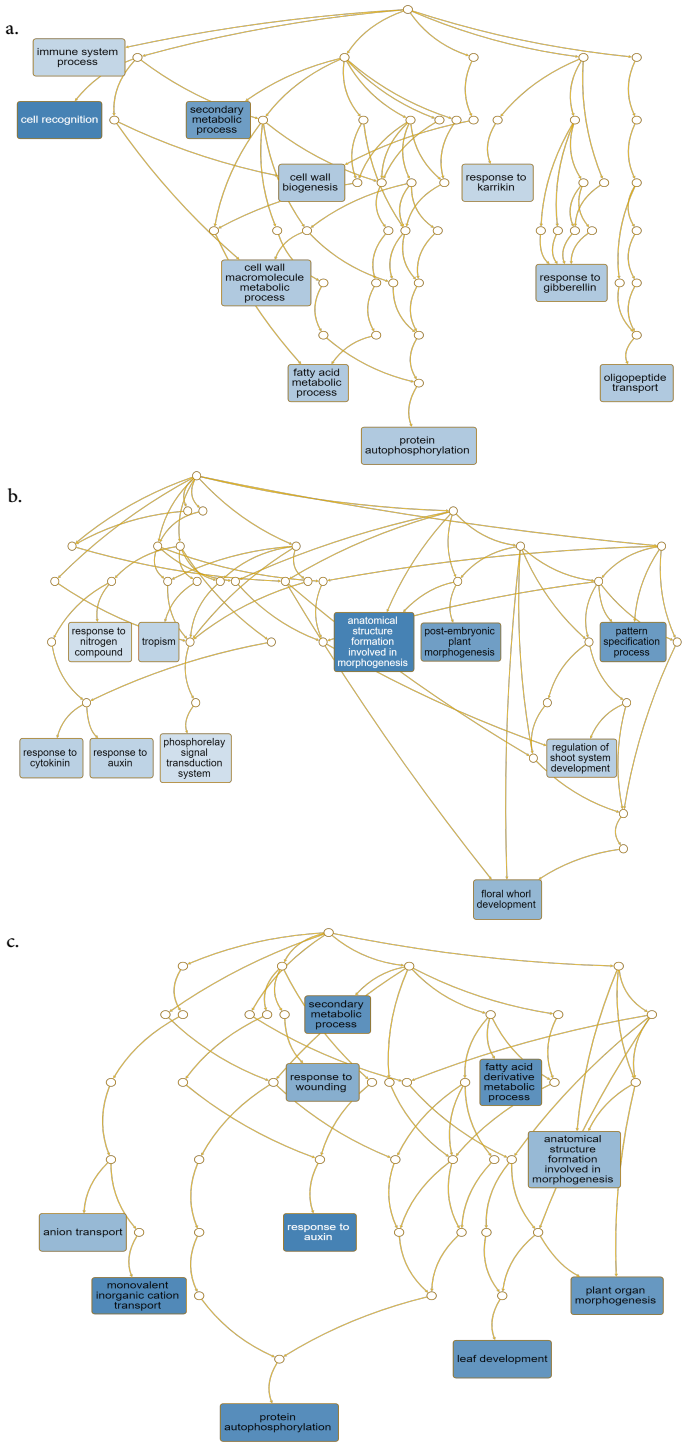

Supplementary Figure B.4: GO biological process tree for the specific, common SDE genes of each compared groups PIIavsPI and NPIIavsNPI. (a) 'specific' SDE genes of PIIavsPI, (b) 'common' SDE genes of PIIavsPI and NPIIavsNPI, (c) 'specific' SDE genes of NPIIavsNPI. The depth of blue indicates the level of significance, darker means more siginificant.

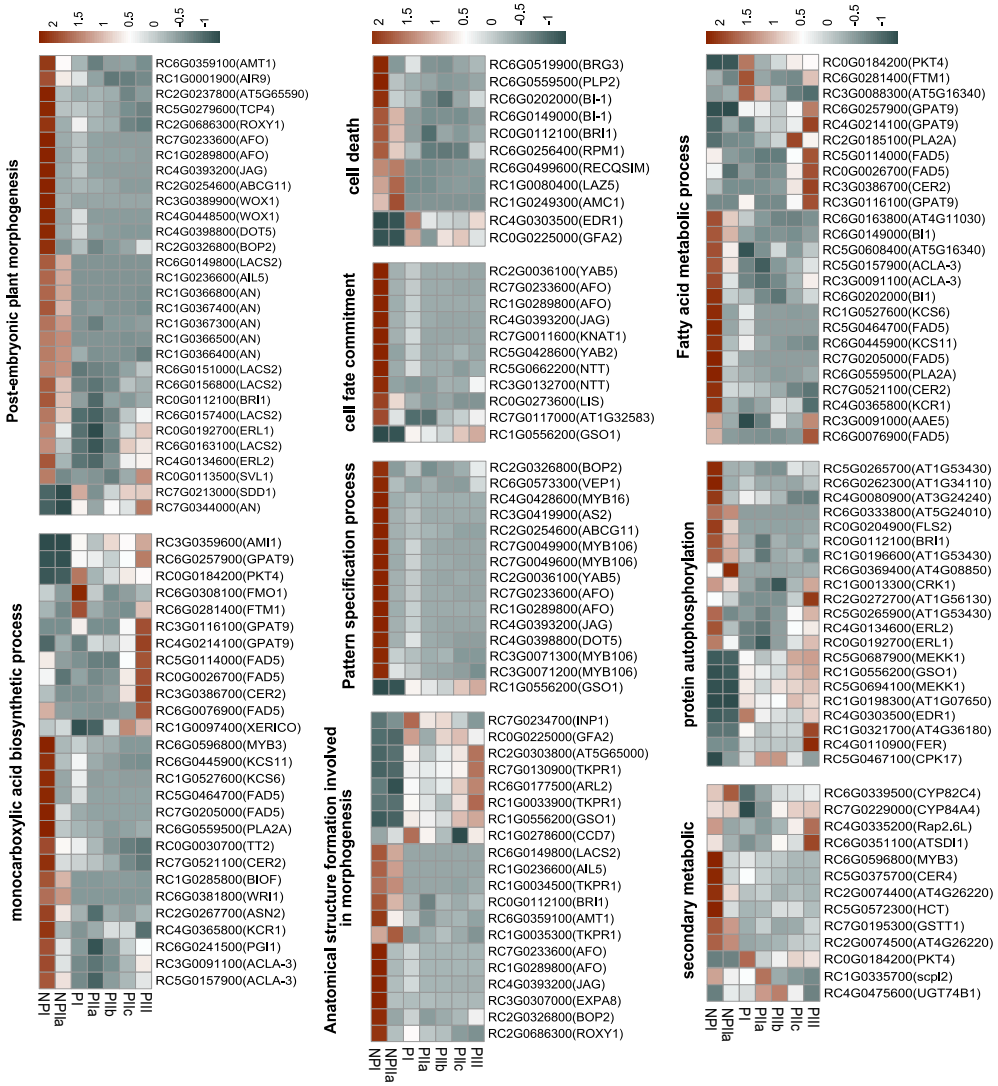

Supplementary Figure B.5: Heatmaps showed the 2118 SDE genes of PIvsNPI involved in the interesting GO enrichment and their co-expression pattern. *Arabidopsis* proteins inside brackets refers to the homologue of rose proteins, obtained from automatic annotation. A more precise annotation is needed to study by the phylogenetic family analysis.

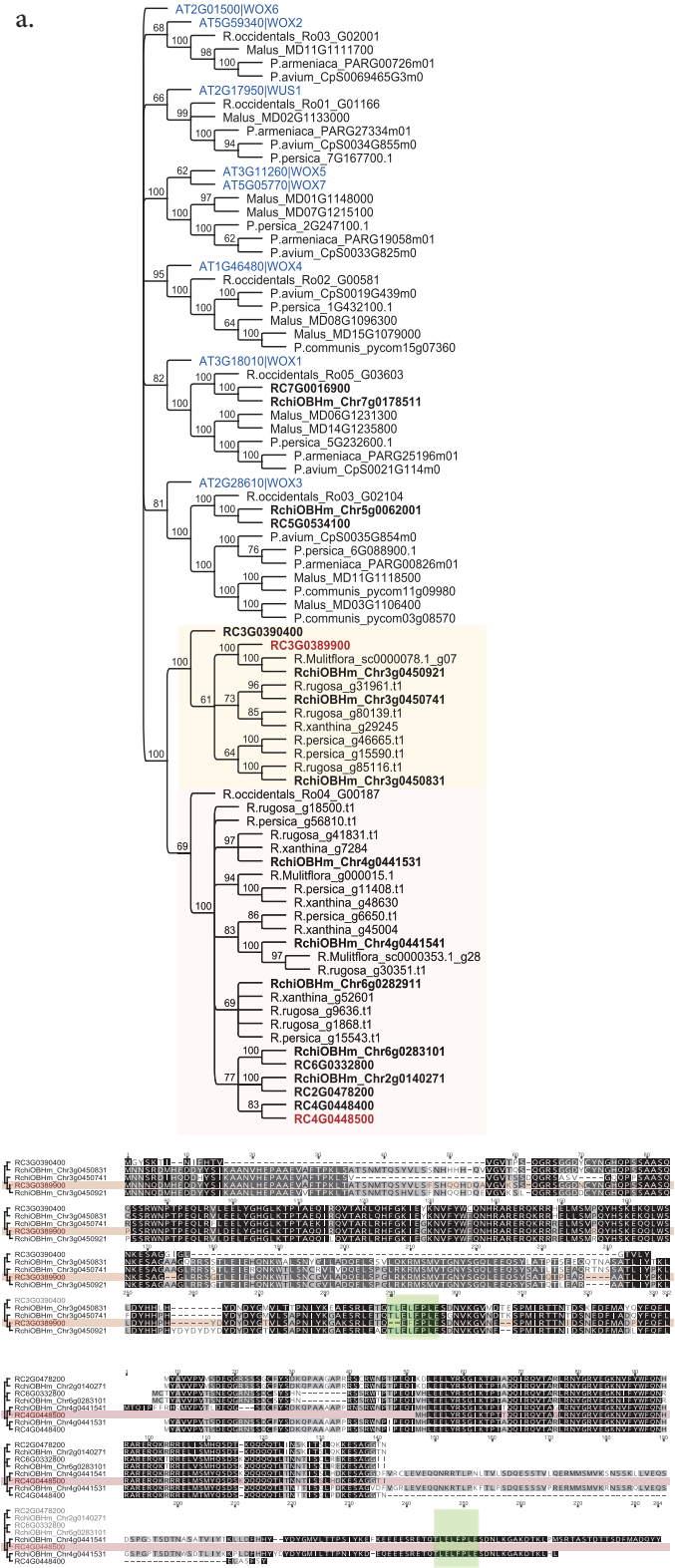

Supplementary Figure B.6: Continued on the next page....

b.

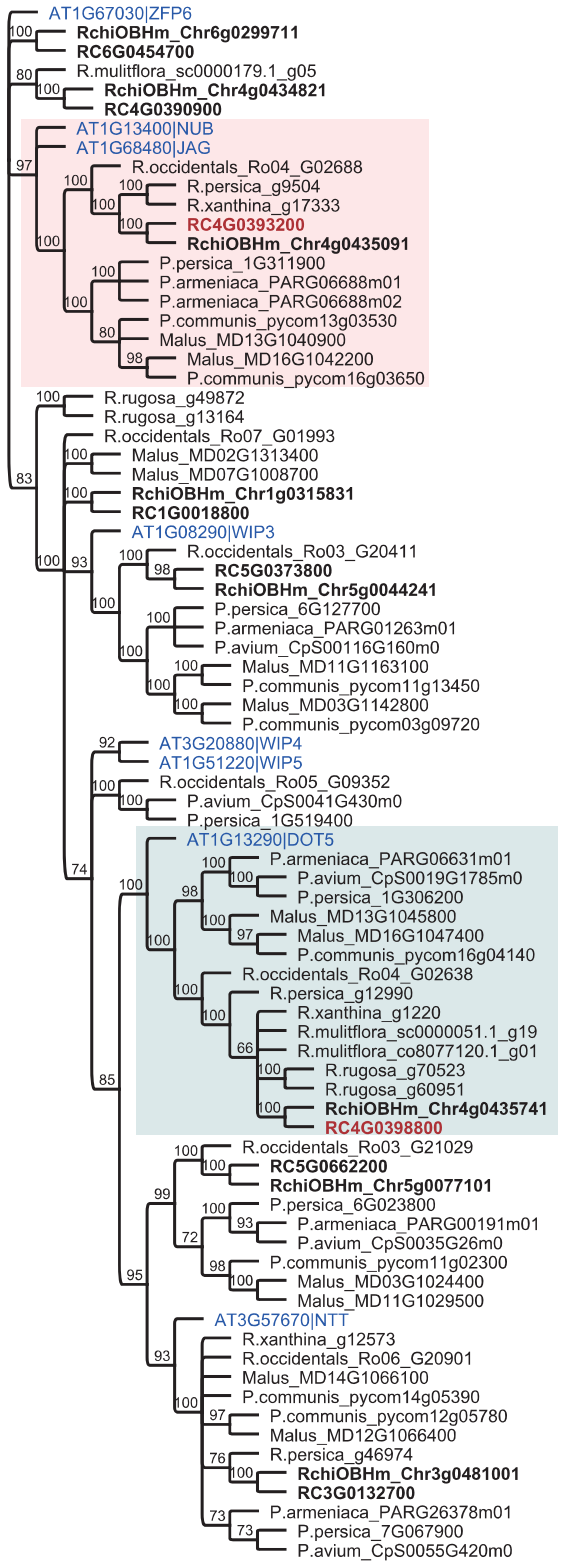

Supplementary Figure B.6: Continued on the next page....

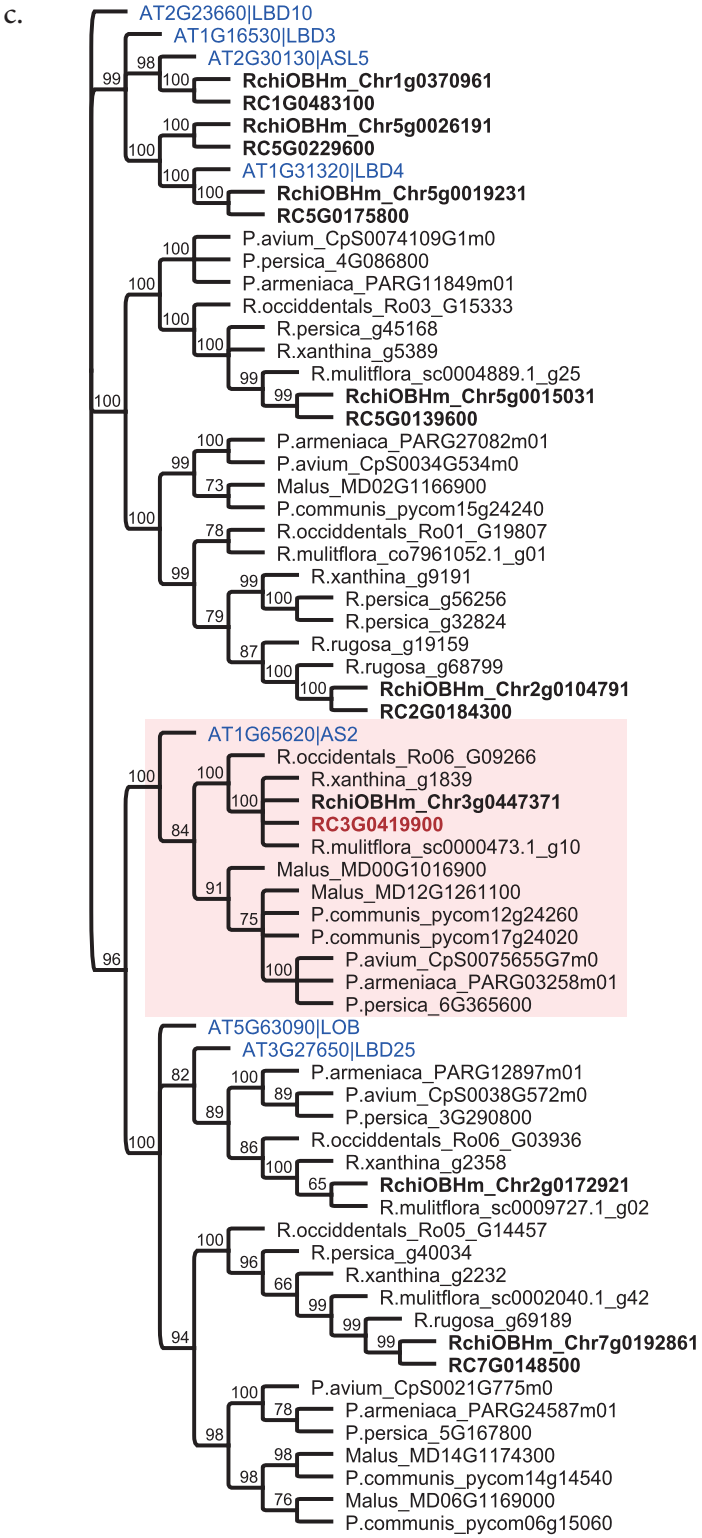

Supplementary Figure B.6: Continued on the next page....

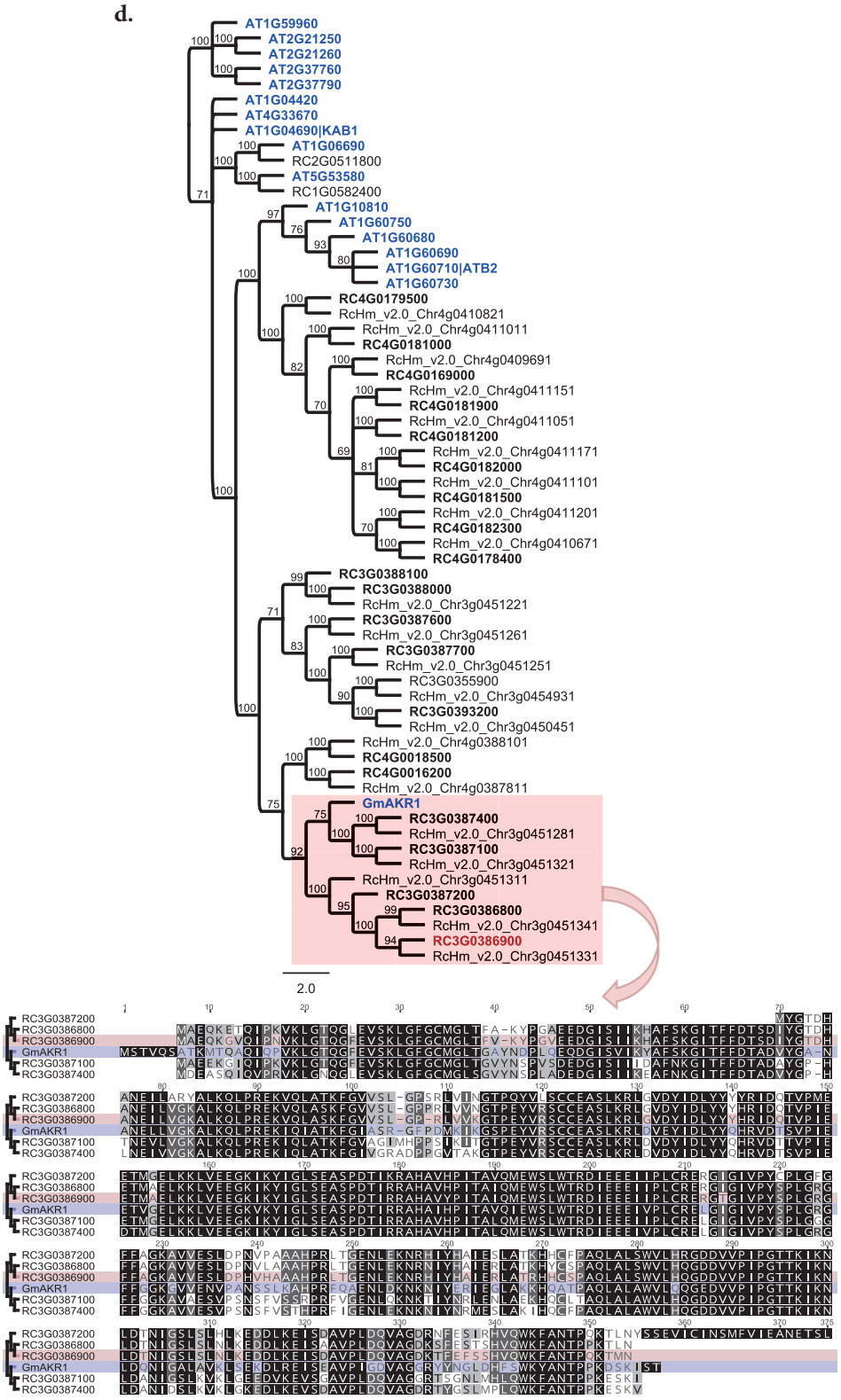

Supplementary Figure B.6: Continued on the next page....

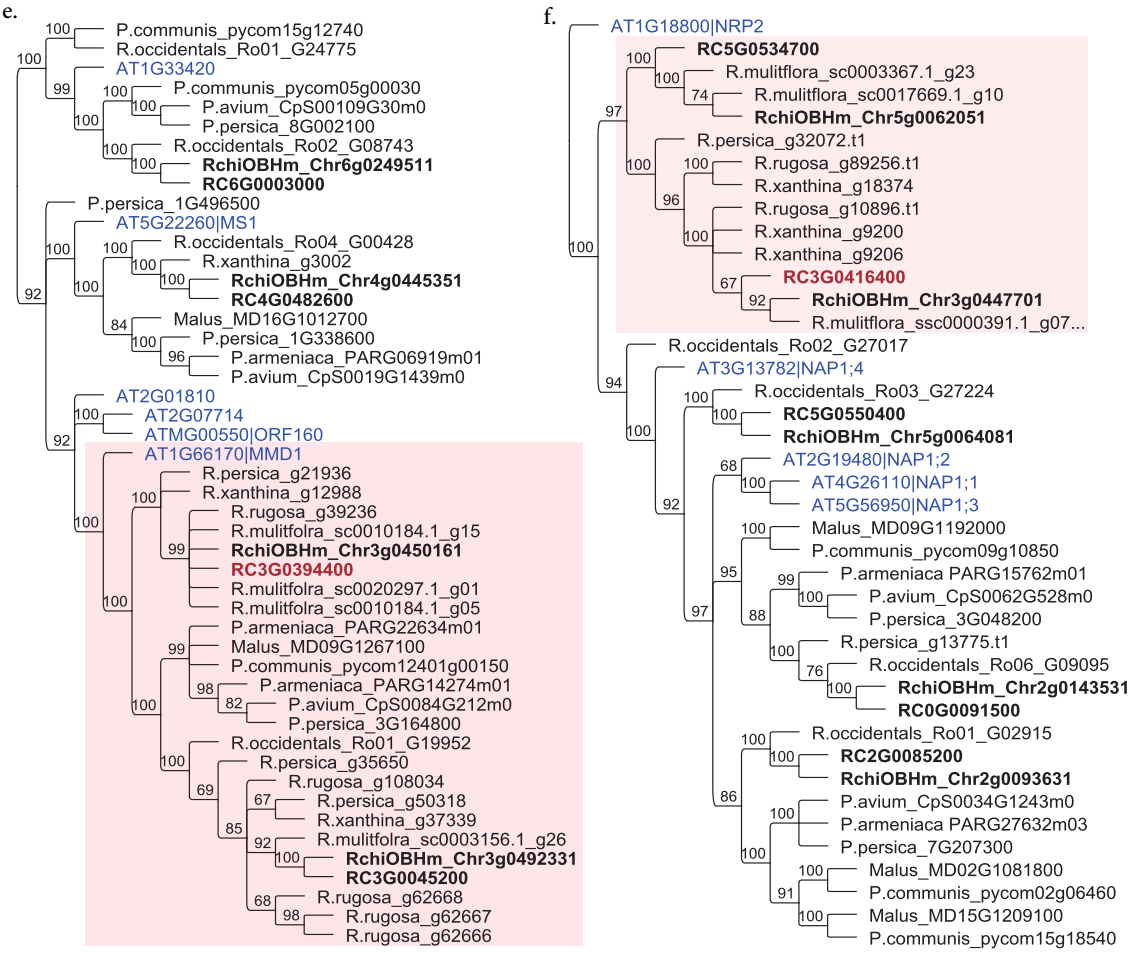

Supplementary Figure B.6: Continued on the next page....

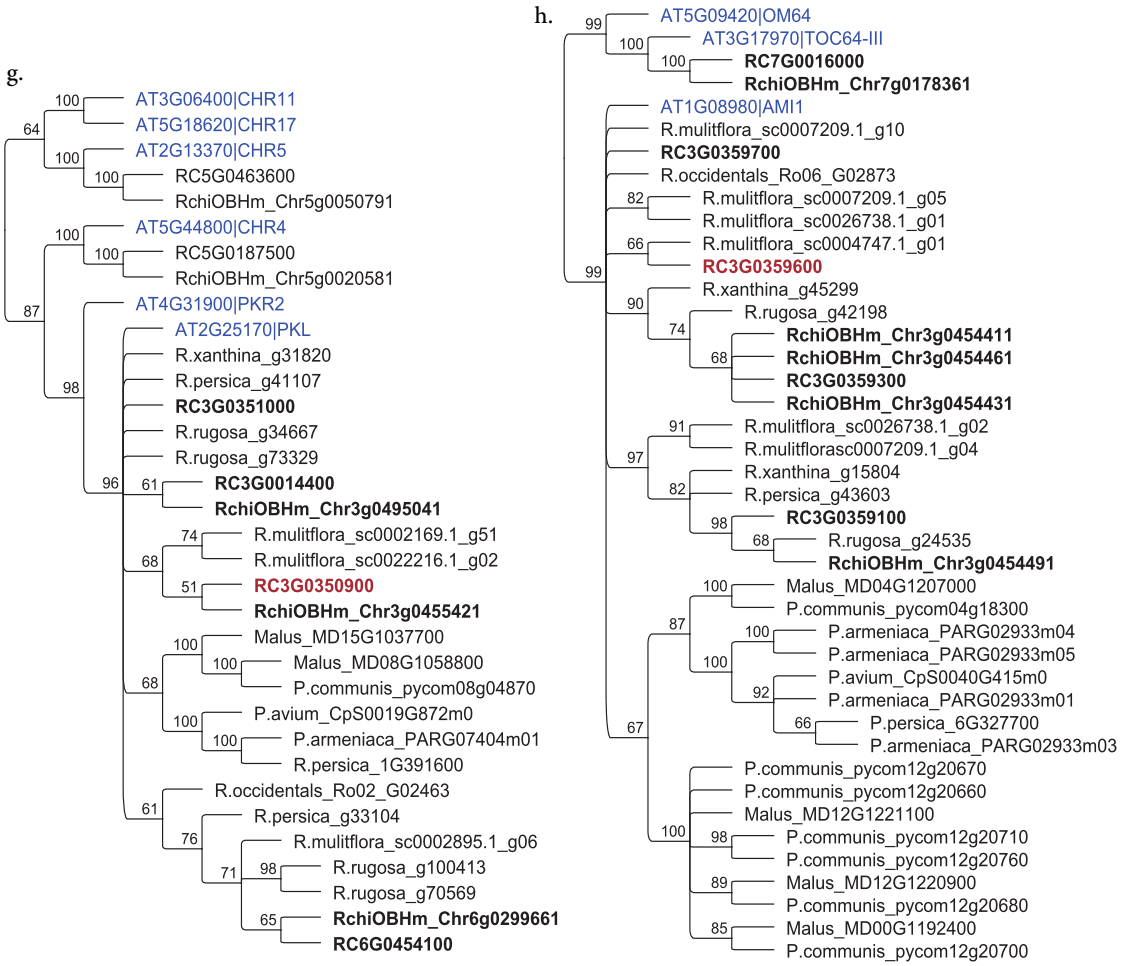

Supplementary Figure B.6: Phylogenetic family analysis for the best candidate genes based on their potential function in prickle initiation. (a) A phylogenetic tree for WOX protein family. (b) C2H2 zinc finger proteins. (c) LATERAL ORGAN BOUNDARIES (LOB) domain family proteins. (d) NAD(P)-linked oxidoreductase superfamily proteins. (e) PHD finger (C4HC3-type zinc finger -like) proteins. (f) Nucleosome assembly protein (NAP) family. (g) Chromodomain helicase DNA-binding (CHD) subfamily proteins. (h) Amidase signature family proteins. The 'Old Blush' candidate genes are in bold-red and their duplications are in bold-black. The *A. thaliana* homologs are in blue, the protein name corresponds to the TAIR database (https://www.arabidopsis.org/). For rose, 'RCxxxxxxxxx' protein corresponds to the reference genome of the haploid of 'Old blush' (Hibrand-Saint Oyant et al., 2018), 'RchiOBHm_Chrxxxxxxxxx' protein to the haploid genome of 'Old blush' (Raymond et al., 2018). The other rose genomes: *R. multiflora* (Nakamura et al., 2018), *R. xanthina, R. rugosa, R. persica* (Hibrand-Saint Oyant et al., 2018). The other *Rosaceae* species protein obtained from *R. occidentalis* genome (VanBuren et al., 2018), *M. domestica* Borkh genome (Daccord et al., 2017), *P. communis* genome (Linsmith et al., 2019), *P. armeniaca* genome (Jiang et al., 2019), *P. avium* 'Tieton' (Wang et al., 2020), *P. persica* genome (Verde et al., 2017).

Supplementary Table B.1: Quality control statistics per sample

Sample	Total Raw Reads(G)	Total Clean Bases(Gb)	Clean Reads Ratio(%)	Clean Reads Q20(%)	Clean Reads Q30(%)
NPI1	6.703	6.54	97.55	98.89	93.3
NPI2	6.623	6.46	97.56	98.96	93.58
NPI3	6.687	6.53	97.7	98.93	93.6
NPIIa1	6.596	6.43	97.47	98.93	93.54
NPIIa2	6.581	6.39	97.14	98.97	93.67
NPIIa3	6.61	6.45	97.55	98.93	93.53
PI1	6.73	6.55	97.4	98.96	93.69
PI2	6.734	6.56	97.38	98.96	93.66
PI3	6.626	6.44	97.23	98.97	93.56
PIIa1	6.635	6.45	97.17	98.93	93.43
PIIa2	6.67	6.43	96.34	98.92	93.39
PIIa3	6.613	6.4	96.84	98.87	93.23
PIIb1	6.689	6.52	97.47	98.91	93.62
PIIb2	6.589	6.42	97.42	98.91	93.43
PIIb3	6.609	6.4	96.89	98.96	93.53
PIIc1	6.557	6.39	97.49	99.01	93.88
PIIc2	6.625	6.45	97.32	98.91	93.5
PIIc3	6.647	6.44	96.82	98.91	93.37
PIII1	6.697	6.51	97.16	98.87	93.42
PIII2	6.64	6.46	97.34	98.95	93.65
PIII3	6.693	6.53	97.55	98.94	93.59
Average	6.65	6.46	97.28	98.93	93.53

Supplementary Table B.2: Mapped read statistics observed per sample

Samples	Unique mapped reads			Muti mapped reads		Unmapped reads
	Uniquely mapped read number	Uniquely mapped read %	Mismatch rate per base %	Reads mapped to multiple loci %	Reads mapped to too many loci %	Reads unmapped too short %
NPI1	30792634	94.01	0.67	2.21	0.04	3.73
NPI2	30562437	94.40	0.68	2.16	0.04	3.39
NPI3	30774402	94.01	0.67	2.24	0.04	3.69
NPIIa1	30387845	94.27	0.67	2.13	0.05	3.53
NPIIa2	30171264	94.06	0.69	2.15	0.07	3.68
NPIIa3	30515397	94.45	0.68	2.11	0.05	3.37
PI1	30700001	93.38	0.77	2.34	0.04	4.23
PI2	30692586	93.37	0.77	2.39	0.05	4.16
PI3	30237122	93.58	0.76	2.34	0.04	4.02
PIIa1	30355036	93.78	0.77	2.33	0.05	3.82
PIIa2	30180023	93.28	0.76	2.29	0.05	4.35
PIIa3	30112583	93.65	0.77	2.34	0.05	3.93
PIIb1	30435351	93.09	0.79	2.58	0.08	4.22
PIIb2	30092350	93.47	0.79	2.57	0.07	3.86
PIIb3	30020480	93.30	0.78	2.50	0.07	4.10
PIIc1	29676004	92.61	0.80	2.65	0.13	4.56
PIIc2	29927308	92.52	0.80	2.71	0.15	4.56
PIIc3	29953711	92.66	0.79	2.57	0.13	4.58
PIII1	29995551	91.91	0.80	2.69	0.13	5.25
PIII2	29948334	92.41	0.80	2.67	0.14	4.76
PIII3	30054770	91.89	0.81	2.74	0.19	5.16
Average	30265961	93.34	0.75	2.41	0.08	4.14

Supplementary Table B.3: Expression quantification statistics observed per sample

Samples	Uniquely mapped reads	[a]Assigned_Features		[b]Unassigned_NoFeature		[c]Unassigned_Ambiguity	
		Reads numbers	Ratio	Reads numbers	Ratio	Reads numbers	Ratio
NPI1	30792701	28953499	94.03%	1766548	5.74%	72653	0.24%
NPI2	30562520	28828692	94.33%	1661280	5.44%	72547	0.24%
NPI3	30774465	28941266	94.04%	1755029	5.70%	78169	0.25%
NPIIa1	30387941	28795262	94.76%	1522746	5.01%	69932	0.23%
NPIIa2	30171359	28494354	94.44%	1600052	5.30%	76952	0.26%
NPIIa3	30515461	28965769	94.92%	1473432	4.83%	76259	0.25%
PI1	30700095	28984939	94.41%	1641525	5.35%	73630	0.24%
PI2	30692655	28864523	94.04%	1748055	5.70%	80076	0.26%
PI3	30237205	28477838	94.18%	1685968	5.58%	73398	0.24%
PIIa1	30355124	28898519	95.20%	1380258	4.55%	76346	0.25%
PIIa2	30180124	28731063	95.20%	1363787	4.52%	85273	0.28%
PIIa3	30112682	28607136	95.00%	1427779	4.74%	77766	0.26%
PIIb1	30435425	28606734	93.99%	1746760	5.74%	81930	0.27%
PIIb2	30092435	28379088	94.31%	1634617	5.43%	78729	0.26%
PIIb3	30020580	28368243	94.50%	1579577	5.26%	72759	0.24%
PIIc1	29676062	27479562	92.60%	2120734	7.15%	75765	0.26%
PIIc2	29927383	27680212	92.49%	2169301	7.25%	77869	0.26%
PIIc3	29953780	27943061	93.29%	1935212	6.46%	75506	0.25%
PIII1	29995614	27575633	91.93%	2344783	7.82%	75197	0.25%
PIII2	29948419	27558971	92.02%	2315803	7.73%	73644	0.25%
PIII3	30054819	27465884	91.39%	2514763	8.37%	74171	0.25%
Average	30266040	28409536	93.86%	1780381	5.89%	76122	0.25%

[a] Assigned_Features The read (or fragment) was assigned to a gene feature in the annotation file.

[b] Unassigned_NoFeature The fragment mapped to a region that is not annotated in the annotation file.

[c] Unassigned_Ambiguity The fragment might originate from gene A or gene B, and it is not clear which gene it originated from.

Supplementary Table B.4: Summary of the annotated information for 43 SDE genes located on QTL-LG3,4.

Gene_ID	Gene_Position	TAIR		UNIPROT		Annotation	Annotation	Potential function
		AT Gene	e-value	SwissProt ID	e-value	name		
RC3G0350900	42174997..42181428	AT2G25170	0	Q9S775	0	PKL	CHD3-type chromatin-remodeling factor PICKLE	cell division: response to "auxin, gibberellin, water deprivation"
RC3G0373700	43671059..43678116	AT1G29320	4E-41	Q6RFH5	1E-10	WDR74	WD repeat-containing protein 74	cell fate: preimplantation development
RC3G0398600	45359094..45359645	AT5G28850	2E-25	Q5QIT3	4E-24	BETA	Serine/threonine protein phosphatase 2A regulatory subunit B"beta	others: Required for organ development
RC3G0408700	46043054..46044287	AT2G02230	2E-64	Q6NPT8	3E-63	PP2B1	F-box phloem protein PP2-B1	others: phloem protein
RC3G0380200	44011688..44014786	AT3G14470	1E-111	Q9LRR4	2E-110	RPPL1	Putative disease resistance RPP13-like protein 1	defense response: bacterial
RC3G0397000	45215053..45216638	na	na	na	na	na	na	na
RC3G0322100	39819975..39821329	na	na	na	na	na	na	na
RC3G0321700	39748324..39749807	na	na	na	na	na	na	na
RC3G0307000	38567684..38568951	AT2G40610	1E-136	O22874	2E-135	EXPA8	Expansin-A8	cell division: plant-type cell wall loosening, plant-type cell wall organization
RC3G0389900	44624768..44626218	AT3G18010	1E-29	Q6X7K0	2E-28	WOX1	WUSCHEL-related homeobox 1	cell fate: organ development
RC3G0351100	42192172..42192742	AT1G35910	2E-15	Q67XC9	3E-14	TPPD	Probable trehalose-phosphate phosphatase D	defense response: abiotix stess tolerance
RC3G0419900	46667066..46669290	AT1G65620	1E-79	O04479	2E-78	AS2	Lateral organ boundaries (LOB) domain family protein	cell fate: organ development
RC3G0285500	36789437..36792822	AT3G47570	0	C0LGP4	0	AT3G47570	Probable LRR receptor-like serine/threonine-protein kinase	others: Required for organ development
RC3G0307300	38580886..38581780	AT2G38530	1E-29	P83434	6E-33	AT2G38530	Non-specific lipid-transfer protein 1	cell development: cuticle-cell wall interface integrity
RC3G0390600	44685108..44688663	na	na	na	na	na	na	na
RC3G0386900	44426300..44430239	AT1G10810	4E-127	C6TBN2	8E-173	AKR1	Probable aldo-keto reductase 1	cell fate: organ development
RC3G0407300	45947848..45949114	na	na	na	na	na	na	na
RC3G0394400	45041606..45044025	AT1G66170	2E-134	Q7X6Y7	3E-133	MMD1	PHD finger protein MALE MEIOCYTE DEATH 1	cell division: mitosis
RC3G0416400	46439606..46443677	AT4G26110	7E-31	Q9SZI2	1E-29	NAP1	Nucleosome assembly protein 1;1	cell differentiation and proliferation
RC3G0379900	43996353..44002099	na	na	na	na	na	na	na
RC3G0297000	37583666..37587460	na	na	na	na	na	na	na
RC3G0399800	45435579..45437570	AT5G62970	7E-18	Q9FM55	1E-16	AT5G62970	Putative F-box/FBD/LRR-repeat protein	na
RC3G0385500	44348086..44348695	na	na	na	na	na	na	na
RC3G0359600	42723887..42724684	AT1G08980	2E-29	Q9FR37	4E-28	AMI1	Amidase 1	Auxin biosynthesis
RC3G0353900	42370775..42371639	AT1G55020	4E-41	Q43191	2E-43	LOX1	Probable linoleate 9S-lipoxygenase 5	defense response: bacterial

Continued.....

Supplementary Table B.4 –*Continued from previous page..*

Gene_ID	Gene_Position	TAIR		UNIPROT		Annotation	Annotation	Potential function
		AT Gene	e-value	SwissProt ID	e-value	name		
RC3G0384500	44273324..44274796	AT5G45060	1E-36	Q9XGM3	2E-34	RPS4	Disease resistance protein RPS4	defense response: guarding the plant against pathogens
RC3G0356400	42523016..42526787	AT3G47570	0	C0LGP4	0	AT3G47570	Probable LRR receptor-like serine/threonine-protein kinase	others: Required for organ development
RC3G0385400	44343641..44345479	AT4G19510	4E-40	Q9XGM3	4E-30	RPS4	Disease resistance protein RPS4	defense response: guarding the plant against pathogens
RC3G0402100	45588629..45590604	AT5G38260	1E-103	P93604	1E-137	LRK10	Rust resistance kinase Lr10	defense response: bacterial
RC4G0343600	46347068..46347836	AT4G15900	5E-74	Q42384	9E-73	PRL1	pleiotropic regulatory locus 1	cell development: cell elongation and stess responses
RC4G0344200	46402314..46404541	na	na	na	na	na	na	na
RC4G0347100	46567791..46573060	na	na	na	na	na	na	na
RC4G0359000	47552702..47553360	na	na	na	na	na	na	na
RC4G0365800	48216896..48219183	AT1G67730	5E-105	Q8L9C4	1.064E-147	KCR1	BETA-KETOACYL REDUCTASE 1	cell fate: embryo development
RC4G0366900	48308508..48309066	AT2G18980	2E-26	Q96518	4E-25	PER16		
RC4G0393200	50528968..50532271	AT1G68480	6E-35	Q6S591	1.45187E-51	JAG	C2HC zinc fingers superfamily protein	cell fate:Controls the morphogenesis of lateral organs
RC4G0398700	51013336..51015521	na	na	na	na	na	na	na
RC4G0398800	51048761..51050484	AT1G13290	4E-116	Q9FX68	4.6623E-126	WIP6, DOT5	C2HC zinc fingers superfamily protein	cell fate: organ development
RC4G0400600	51242442..51246144	na	na	na	na	na	na	na
RC4G0401600	51299705..51303048	AT3G25670	2E-158	Q5PP26	0	PII-2	Leucine-rich repeat (LRR) family protein	response to symbiotic fungus
RC4G0418500	52778042..52781021	AT1G13740	3E-43	Q9LMX5	5E-42	AFP2	ABI five binding protein 2	signal transduction: response to abscisic acid, water deprivation
RC4G0428600	53515878..53518069	AT5G15310	5E-110	Q9LXF1	9E-109	MYB16	R2R3 factor gene family	others: cell morphogenesis, cuticle pattern formation
RC4G0448500	55069906..55071397	AT2G28610	7E-24	Q9SIB4	6.52049E-18	WOX3	WUSCHEL-related homeobox 3	cell fate: Required to initiate organ founder cells in a lateral domain of shoot meristems

Bibiography

Bibliography

Agati, G., Azzarello, E., Pollastri, S., and Tattini, M. (2012). Flavonoids as antioxidants in plants: location and functional significance. *Plant science*, 196:67–76.

Allaby, M. (1999). *A dictionary of plant sciences*. Oxford University Press, second edition.

Andres, M. R. and Connor, E. F. (2003). The community-wide and guild-specific effects of pubescence on the folivorous insects of manzanitas *Arctostaphylos* spp. *Ecological Entomology*, 28(4):383–396.

Andrews, S. et al. (2010). Fastqc: a quality control tool for high throughput sequence data.

Angeles-Shim, R. B., Asano, K., Takashi, T., Shim, J., Kuroha, T., Ayano, M., and Ashikari, M. (2012). A WUSCHEL-related homeobox 3b gene, depilous (*dep*), confers glabrousness of rice leaves and glumes. *Rice*, 5(1):28.

Angyalossy, V., Pace, M., Evert, R., Marcati, C., Oskolski, A., Terrazas, T., Kotina, E., Lens, F., Cristina, M.-V., Angeles, G., Machado, S., Crivellaro, A., Rao, K., Junikka, L., Nikolaeva, N., and Baas, P. (2016). Iawa list of microscopic bark features. *IAWA journal*, 37:585–587.

Apothecary, A. (2020). Cultural & historical impact of rose oils. https://anandaessentialoils.com/science/rose/uses-of-rose/cultural-historical/.

Asano, G., Kubo, R., and Tanimoto, S. (2008). Growth, structure and lignin localization in rose prickle. *Bulletin of the Faculty of Agriculture*, 93:117–125.

Ascensão, L., Marques, N., and Pais, M. S. (1995). Glandular trichomes on vegetative and reproductive organs of *Leonotis leonurus* (*Lamiaceae*). *Annals of Botany*, 75(6):619–626.

Aubertot, M. (1910). Sur l'anatomie comparée des rameaux polymorphes chez quelques arbustes épineux de la famille des *Rosacées*. *Bulletin de la Société Botanique de France*, 57(8):615–619.

Bagella, S., Filigheddu, R., Benesperi, R., Giordani, P., Minuto, L., Viciani, D., Caria, M. C., Pisanu, S., and Casazza, G. (2019). Thorn, spine and prickle patterns in the Italian flora. *Plant Biosystems - An International Journal Dealing with all Aspects of Plant Biology*, 153(1):118–133.

Balkunde, R., Pesch, M., and Hülskamp, M. (2010). Chapter ten - trichome patterning in *Arabidopsis thaliana*: from genetic to molecular models. In Timmermans, M. C. P., editor, *Current Topics in Developmental Biology*, volume 91 of *Plant Development*, pages 299–321. Academic Press.

Barros, M. B. d. L., de Almeida Paes, R., and Schubach, A. O. (2011). *Sporothrix Schenckii* and *Sporotrichosis*. *Clinical Microbiology Reviews*, 24(4):633–654.

Beales, P. (2002). Klassische rosen classic roses in German. *DuMont*, page 423.

Becker, H. F. (1963). The fossil record of the genus *Rosa*. *Bulletin of the Torrey Botanical Club*, pages 99–110.

Bell, A. D. (1991). *Plant form: an illustrated guide to flowering plant morphology*. Oxford University Press, USA.

Belovsky, G. E., Schmitz, O. J., Slade, J. B., and Dawson, T. J. (1991). Effects of spines and thorns on Australian arid zone herbivores of different body masses. *Oecologia*, 88(4):521–528.

Billings, W. D. and Morris, R. J. (1951). Reflection of visible and infrared radiation from leaves of different ecological groups. *American Journal of Botany*, 38(5):327–331.

Blaser, H. W. (1956). Morphology of the determinate thorn-shoots of gleditsia. *American Journal of Botany*, 43(1):22–28.

Blechert, O. and Debener, T. (2005). Distribution of rose black spot (*Diplocarpon rosae*) genetic diversity in eastern north america using amplified fragment length polymorphism and implications for resistance screening. *Plant Pathology*, 54(1):82–90.

Boke, N. H. (1944). Histogenesis of the leaf and areole in *Opuntia Cylindrica*. *American Journal of Botany*, 31(6):299–316.

Boke, N. H. (1956). Developmental anatomy and the validity of the genus *Bartschella*. *American Journal of Botany*, 43(10):819–827.

Boke, N. H. (1980). Developmental morphology and anatomy in *Cactaceae*. *BioScience*, 30(9):605–610.

Bolger, A. M., Lohse, M., and Usadel, B. (2014). Trimmomatic: a flexible trimmer for illumina sequence data. *Bioinformatics*, 30(15):2114–2120.

Bombarely, A. (2018). Roses for darwin. *Nature Plants*, 4(7):406–407.

Bosabalidis, A. and Tsekos, I. (1982). Glandular scale development and essential oil secretion in *Origanum Dictamnus* l. *Planta*, 156(6):496–504.

Boudolf, V., Rombauts, S., Naudts, M., Inzé, D., and De Veylder, L. (2001). Identification of novel cyclin-dependent kinases interacting with the *CKS1* protein of *Arabidopsis*. *Journal of Experimental Botany*, 52(359):1381–1382.

Bourke, P. M., Arens, P., Voorrips, R. E., Esselink, G. D., Koning-Boucoiran, C. F. S., van't Westende, W. P. C., Leonardo, T. S., Wissink, P., Zheng, C., van Geest, G., Visser, R. G. F., Krens, F. A., Smulders, M. J. M., and Maliepaard, C. (2017). Partial preferential chromosome pairing is genotype dependent in tetraploid rose. *The Plant Journal*, 90(2):330–343.

Bourke, P. M., Gitonga, V. W., Voorrips, R. E., Visser, R. G. F., Krens, F. A., and Maliepaard, C. (2018a). Multi-environment QTL analysis of plant and flower morphological traits in tetraploid rose. *Theoretical and Applied Genetics*, 131(10):2055–2069.

Bourke, P. M., van Geest, G., Voorrips, R. E., Jansen, J., Kranenburg, T., Shahin, A., Visser, R. G. F., Arens, P., Smulders, M. J. M., and Maliepaard, C. (2018b). polymapr-linkage analysis and genetic map construction from f1 populations of outcrossing polyploids. *Bioinformatics (Oxford, England)*, 34(20):3496–3502.

Bourke, P. M., Voorrips, R. E., Visser, R. G. F., and Maliepaard, C. (2018c). Tools for genetic studies in experimental populations of polyploids. *Frontiers in Plant Science*, 9:513.

Bowling, S. A., Clarke, J. D., Liu, Y., Klessig, D. F., and Dong, X. (1997). The cpr5 mutant of *Arabidopsis* expresses both *NPR1*-dependent and *NPR1*-independent resistance. *The Plant Cell*, 9(9):1573–1584.

Boyartchuk, V. L., Broman, K. W., Mosher, R. E., D'Orazio, S. E. F., Starnbach, M. N., and Dietrich, W. F. (2001). Multigenic control of listeria monocytogenes susceptibility in rice. *Nature genetics*, 27(3):259–260.

Brachi, B., Faure, N., Horton, M., Flahauw, E., Vazquez, A., Nordborg, M., Bergelson, J., Cuguen, J., and Roux, F. (2010). Linkage and association mapping of *Arabidopsis thaliana* flowering time in nature. *PLoS Genet*, 6(5):e1000940.

Bramsiepe, J., Wester, K., Weinl, C., Roodbarkelari, F., Kasili, R., Larkin, J. C., Hülskamp, M., and Schnittger, A. (2010). Endoreplication controls cell fate maintenance. *PLOS Genetics*, 6(6):e1000996.

Breyne, P., Dreesen, R., Vandepoele, K., Veylder, L. D., Breusegem, F. V., Callewaert, L., Rombauts, S., Raes, J., Cannoot, B., Engler, G., Inzé, D., and Zabeau, M. (2002). Transcriptome analysis during cell division in plants. *Proceedings of the National Academy of Sciences*, 99(23):14825–14830.

Broman, K. W. (2003). Mapping quantitative trait loci in the case of a spike in the phenotype distribution. *Genetics*, 163(3):1169–1175.

Burga, A., Casanueva, M. O., and Lehner, B. (2011). Predicting mutation outcome from early stochastic variation in genetic interaction partners. *Nature*, 480(7376):250–253.

Burns, K. C. (2014). Are there general patterns in plant defence against megaherbivores? *Biological Journal of the Linnean Society*, 111(1):38–48.

Caissard, J.-C., Bergougnoux, V., Martin, M., Mauriat, M., and Baudino, S. (2006). Chemical and histochemical analysis of 'quatre saisons blanc mousseux', a moss rose of the *Rosa*× *damascena* group. *Annals of Botany*, 97(2):231–238.

Calo, L., García, I., Gotor, C., and Romero, L. C. (2006). Leaf hairs influence phytopathogenic fungus infection and confer an increased resistance when expressing a *Trichoderma* α-1,3-glucanase. *Journal of Experimental Botany*, 57(14):3911–3920.

Campbell, J. I., Yen, L. T. M., Loan, H. T., Diep, T. S., Nga, T. T. T., Hoang, N. V. M., Son, L. T., Chau, N. v. V., Parry, C., Farrar, J. J., Hien, T. T., and Baker, S. (2009). Microbiologic characterization and antimicrobial susceptibility of clostridium tetani isolated from wounds of patients with clinically diagnosed tetanus. *The American Journal of Tropical Medicine and Hygiene*, 80(5):827–831.

Canli, F. A. (2003). A review on thornless roses. *Pakistan Journal of Biological Sciences*, 6(19):1712–1719.

Canli, F. A. and Skirvin, R. M. (2003). Separation of thornless rose chimeras into their (*Rosa sp.*) consistent genotypes in vitro. *Pakistan Journal of Biological Sciences*, 6(19):1644–1648.

Canli, F. A. and Skirvin, R. M. (2008). In vitro separation of a rose chimera. *Plant Cell, Tissue and Organ Culture*, 95(3):353.

Casci, T. (2012). Genetic support network to the rescue. *Nature Reviews Genetics*, 13(2):74–74.

Casimiro, I., Beeckman, T., Graham, N., Bhalerao, R., Zhang, H., Casero, P., Sandberg, G., and Bennett, M. J. (2003). Dissecting arabidopsis lateral root development. *Trends in plant science*, 8(4):165–171.

Castro, P., Stafne, E. T., Clark, J. R., and Lewers, K. S. (2013). Genetic map of the primocane-fruiting and thornless traits of tetraploid blackberry. *Theoretical and Applied Genetics*, 126(10):2521–2532.

Chalfun-Junior, A., Franken, J., Mes, J. J., Marsch-Martinez, N., Pereira, A., and Angenent, G. C. (2005). ASYMMETRIC LEAVES2-LIKE1 gene, a member of the AS2/LOB family, controls proximal–distal patterning in *Arabidopsis* petals. *Plant molecular biology*, 57(4):559–575.

Chaloner, W. G. (1970). The rise of the first land plants. *Biological Reviews*, 45(3):353–377.

Chalvin, C., Drevensek, S., Dron, M., Bendahmane, A., and Boualem, A. (2020). Genetic control of glandular trichome development. *Trends in Plant Science*, 25(5):477–487.

Champagne, A. and Boutry, M. (2013). Proteomics of nonmodel plant species. *Proteomics*, 13(3-4):663–673.

Chang, J., Yu, T., Yang, Q., Li, C., Xiong, C., Gao, S., Xie, Q., Zheng, F., Li, H., Tian, Z., Yang, C., and Ye, Z. (2018). Hair, encoding a single c2h2 zinc-finger protein, regulates multicellular trichome formation in tomato. *The Plant Journal*, 96(1):90–102.

Chen, X. f., Wang, H., Li, J. q., Huang, H., and Xu, L. (2013). Quantitative control of asymmetric leaves2 expression is critical for leaf axial patterning in *Arabidopsis*. *Journal of experimental botany*, 64(16):4895–4905.

Chopra, D., Mapar, M., Stephan, L., Albani, M. C., Deneer, A., Coupland, G., Willing, E.-M., Schellmann, S., Schneeberger, K., Fleck, C., Schrader, A., and Hülskamp, M. (2019). Genetic and molecular analysis of trichome development in *Arabis alpina*. *Proceedings of the National Academy of Sciences*, 116(24):12078–12083.

Christ, H. (1873). *Die Rosen der Schweiz mit Berücksichtigung der umliegenden Gebiete Mittel-und Süd-Europas*. Ein monographischer Versuch, Georg.

Christenhusz, M. J. M. and Byng, J. W. (2016). The number of known plants species in the world and its annual increase. *Phytotaxa*, 261(3):201–217.

Churchman, M. L., Brown, M. L., Kato, N., Kirik, V., Hülskamp, M., Inzé, D., Veylder, L. D., Walker, J. D., Zheng, Z., Oppenheimer, D. G., Gwin, T., Churchman, J., and Larkin, J. C. (2006). Siamese, a plant-specific cell cycle regulator, controls endoreplication onset in *Arabidopsis thaliana*. *The Plant Cell*, 18(11):3145–3157.

Chwalkowski, F. (2016). *Symbols in arts, religion and culture: The soul of nature*. Cambridge Scholars Publishing, Newcastle upon Tyne, UK.

Cooper, S. M. and Owen-Smith, N. (1986). Effects of plant spinescence on large mammalian herbivores. *Oecologia*, 68(3):446–455.

Corellou, F., Camasses, A., Ligat, L., Peaucellier, G., and Bouget, F.-Y. (2005). Atypical regulation of a green lineage-specific B-type cyclin-dependent kinase. *Plant Physiology*, 138(3):1627–1636.

Corsi, G. and S., B. (1999). Glandular hairs of salvia officinalis: new data on morphology, localization and histochemistry in relation to function. *Annals of Botany*, 84(5):657 – 664.

Cott, H. B. (1940). *Adaptive coloration in animals*. Methuen, London, UK.

Coyner, M. A., Skirvin, R. M., Norton, M. A., and Otterbacher, A. G. (2005). Thornlessness in blackberries. *Small Fruits Review*, 4(2):83–106.

Crawley, M. J. (1983). Herbivory: The dynamics of animal-plant interactions. *Studies in Ecology*, 10:437.

Crépin, F. (1889). Sketch of a new classification of roses. *Journal of the Royal Horticultural Society,*, 11(3):217–228.

Crespel, L., Chirollet, M., Durel, C., Zhang, D., Meynet, J., and Gudin, S. (2002). Mapping of qualitative and quantitative phenotypic traits in *Rosa* using AFLP markers. *Theoretical and Applied Genetics*, 105(8):1207–1214.

Cruz, A. T., Cazacu, A. C., and Allen, C. H. (2007). Pantoea agglomerans, a plant pathogen causing human disease. *Journal of Clinical Microbiology*, 45(6):1989–1992.

Daccord, N., Celton, J.-M., Linsmith, G., Becker, C., Choisne, N., Schijlen, E., van de Geest, H., Bianco, L., Micheletti, D., Velasco, R., Di Pierro, E. A., Gouzy, J., Rees, D. J. G., Guérif, P., Muranty, H., Durel, C.-E., Laurens, F., Lespinasse, Y., Gaillard, S., Aubourg, S., Quesneville, H., Weigel, D., van de Weg, E., Troggio, M., and Bucher, E. (2017). High-quality de novo assembly of the apple genome and methylome dynamics of early fruit development. *Nature Genetics*, 49(7):1099–1106.

Dahal, S. (2013). Post harvest handling of cut-flower rose. *Department of Horticulture, Institute of Agriculture and Animal Sciences (IAAS),Rampur, Chitwan, Nepal*, page 23.

Dam, N. M. V. and Hare, D. J. (1998). Differences in distribution and performance of two sap-sucking herbivores on glandular and non-glandular Datura wrightii. *Ecological Entomology*, 23(1):22–32.

Debener, T. (1999). Genetic analysis of horticulturally important morphological and physiological characters in diploid roses. *Gartenbauwissenschaft*, 64(1):14–20.

Debener, T. and Mattiesch, L. (1999). Construction of a genetic linkage map for roses using RAPD and AFLP markers. *Theoretical and Applied Genetics*, 99(5):891–899.

Debray, K. (2020). *Phylogenomics of the genus* Rosa*: hybridization and polyploidy as factors for diversification*. PhD thesis, University of Angers, Angers, France. Doctor dissertation.

Delbrouck, C. (1875). *Die Pflanzen-Stacheln*. Botanische Abhandlungen aus dem Gebiet der Morphologie und Physiologie. Adolph Marcus.

Dickison, W. C. (2000). *Integrative plant anatomy*. Academic Press, California, USA, 1st edition.

Dinneny, J. R., Yadegari, R., Fischer, R. L., Yanofsky, M. F., and Weigel, D. (2004). The role of JAGGED in shaping lateral organs. *Development*, 131(5):1101–1110.

Dobin, A., Davis, C. A., Schlesinger, F., Drenkow, J., Zaleski, C., Jha, S., Batut, P., Chaisson, M., and Gingeras, T. R. (2013). Star: ultrafast universal RNA-seq aligner. *Bioinformatics*, 29(1):15–21.

Dodsworth, S. (2009). A diverse and intricate signalling network regulates stem cell fate in the shoot apical meristem. *Developmental biology*, 336(1):1–9.

Downes, B. P., Stupar, R. M., Gingerich, D. J., and Vierstra, R. D. (2003). The hect ubiquitin-protein ligase (upl) family in *Arabidopsis*: Upl3 has a specific role in trichome development. *The Plant Journal*, 35(6):729–742.

Druitt, L. and Shoup, M. (1991). Thornless roses. *Horticulture*, 69:78–82.

Dugo, M. L., Satovic, Z., Millán, T., Cubero, J. I., Rubiales, D., Cabrera, A., and Torres, A. M. (2005). Genetic mapping of QTLs controlling horticultural traits in diploid roses. *Theoretical and Applied Genetics*, 111(3):511–520.

Edelman, D. W. (1975). *The Eocene Germer Basin flora of south-central Idaho*. Master's thesis, University of Idaho, Moscow, Idaho, USA.

Edgar, B. A. and Orr-Weaver, T. L. (2001). Endoreplication cell cycles: more for less. *Cell*, 105(3):297–306.

Edmunds, M. (1974). *Defence in animals: a survey of anti-predator defences*. Longman Publishing Group.

Ehleringer, J. (1981). Leaf absorptances of mohave and sonoran desert plants. *Oecologia*, 49(3):366–370.

Ehleringer, J., Björkman, O., and Mooney, H. A. (1976). Leaf pubescence: effects on absorptance and photosynthesis in a desert shrub. *Science*, 192(4237):376–377.

Eisner, T., Eisner, M., and Hoebeke, E. R. (1998). When defense backfires: detrimental effect of a plant's protective trichomes on an insect beneficial to the plant. *Proceedings of the National Academy of Sciences*, 95(8):4410–4414.

El-Brolosy, M. A., Kontarakis, Z., Rossi, A., Kuenne, C., Günther, S., Fukuda, N., Kikhi, K., Boezio, G. L. M., Takacs, C. M., Lai, S.-L., Fukuda, R., Gerri, C., Giraldez, A. J., and Stainier, D. Y. R. (2019). Genetic compensation triggered by mutant mRNA degradation. *Nature*, 568(7751):193–197.

El Refy, A., Perazza, D., Zekraoui, L., Valay, J.-G., Bechtold, N., Brown, S., Hülskamp, M., Herzog, M., and Bonneville, J. M. (2004). The *Arabidopsis KAKTUS* gene encodes a HECT protein and controls the number of endoreduplication cycles. *Molecular Genetics and Genomics*, 270(5):403–414.

Ergonul, O., Erbay, A., Eren, S., and Dokuzoguz, B. (2003). Analysis of the case fatality rate of tetanus among adults in a tertiary hospital in Turkey. *European Journal of Clinical Microbiology and Infectious Diseases*, 22(3):188–190.

Esau, K. (1953). *Plant anatomy*, volume 75. Wiley.

Esau, K. (1960). Anatomy of seed plants. *Soil Science*, 90(2):149.

Esch, J. J., Chen, M., Sanders, M., Hillestad, M., Ndkium, S., Idelkope, B., Neizer, J., and Marks, M. D. (2003). A contradictory GLABRA3 allele helps define gene interactions controlling trichome development in *Arabidopsis*. *Development*, 130(24):5885–5894.

Escobar-Bravo, R., Klinkhamer, P. G., and Leiss, K. A. (2017). Interactive effects of UV-B light with abiotic factors on plant growth and chemistry, and their consequences for defense against arthropod herbivores. *Frontiers in Plant Science*, 8:278.

Evert, R. F. and Eichhorn, S. E. (2006). *Esau's plant anatomy: meristems, cells, and tissues of the plant body: their structure, function, and development*. John Wiley & Sons, 3rd edition.

Ewas, M., Gao, Y., Wang, S., Liu, X., Zhang, H., Nishawy, E. M. E., Ali, F., Shahzad, R., Ziaf, K., Subthain, H., Martin, C., and Luo, J. (2016). Manipulation of *SlMXl* for enhanced carotenoids accumulation and drought resistance in tomato. *Science Bulletin*, 61(18):1413–1418.

Ewels, P., Magnusson, M., Lundin, S., and Käller, M. (2016). MultiQC: summarize analysis results for multiple tools and samples in a single report. *Bioinformatics*, 32(19):3047–3048.

Fahal, A. H. (2004). Mycetoma: a thorn in the flesh. *Transactions of the royal society of tropical medicine and hygiene*, 98(1):3–11.

Fahn, A. (1979). *Secretory tissues in plants*. Academic Press, London, New York, San Francisco.

Fahn, A. (1986). Structural and functional properties of trichomes of *Xeromorphic leaves*. *Annals of Botany*, 57(5):631–637.

Fahn, A. and Shimony, C. (1996). Glandular trichomes of *Fagonia* l.(*Zygophyllaceae*) species: structure, development and secreted materials. *Annals of Botany*, 77(1):25–34.

Firoozabady, E., Moy, Y., Courtney-Gutterson, N., and Robinson, K. (1994). Regeneration of transgenic rose (hybrida) plants from embryogenic tissue. *Bio/technology*, 12(6):609–613.

Folkers, U., Berger, J., and Hulskamp, M. (1997). Cell morphogenesis of trichomes in *Arabidopsis*: differential control of primary and secondary branching by branch initiation regulators and cell growth. *Development*, 124(19):3779–3786.

Fougère-Danezan, M., Joly, S., Bruneau, A., Gao, X.-F., and Zhang, L.-B. (2015). Phylogeny and biogeography of wild roses with specific attention to polyploids. *Annals of Botany*, 115(2):275–291.

Frothingham, S. (2019). Rose thorns: a risk for bacterial and fungal infection. https://www.healthline.com/health/rose-thorns. Accessed: 2020-12-27.

Fukaki, H., Okushima, Y., and Tasaka, M. (2007). Auxin-mediated lateral root formation in higher plants. *International review of cytology*, 256:111–137.

Fukaki, H., Taniguchi, N., and Tasaka, M. (2006). PICKLE is required for SOLITARY-ROOT/IAA14-mediated repression of ARF7 and ARF19 activity during *Arabidopsis* lateral root initiation. *The Plant Journal*, 48(3):380–389.

Futuyma, D. J. and Agrawal, A. A. (2009). Macroevolution and the biological diversity of plants and herbivores. *Proceedings of the National Academy of Sciences*, 106(43):18054–18061.

Gachomo, E. W., Dehne, H. W., and Steiner, U. (2006). Microscopic evidence for the hemibiotrophic nature of *Diplocarpon Rosae*, cause of black spot disease of rose. *Physiological and Molecular Plant Pathology*, 69(1):86–92.

Gagliano, M., Renton, M., Depczynski, M., and Mancuso, S. (2014). Experience teaches plants to learn faster and forget slower in environments where it matters. *Oecologia*, 175(1):63–72.

Galichet, A. and Gruissem, W. (2006). Developmentally controlled farnesylation modulates AtNAP1; 1 function in cell proliferation and cell expansion during *Arabidopsis* leaf development. *Plant Physiology*, 142(4):1412–1426.

Gallenmüller, F., Feus, A., Fiedler, K., and Speck, T. (2015). Rose prickles and asparagus spines-different hook structures as attachment devices in climbing plants. *PLOS ONE*, 10(12):e0143850.

Gan, Y., Kumimoto, R., Liu, C., Ratcliffe, O., Yu, H., and Broun, P. (2006). GLABROUS INFLORESCENCE STEMS modulates the regulation by gibberellins of epidermal differentiation and shoot maturation in *Arabidopsis*. *The Plant Cell*, 18(6):1383–1395.

Gan, Y., Yu, H., Peng, J., and Broun, P. (2007). Genetic and molecular regulation by DELLA proteins of trichome development in *Arabidopsis*. *Plant Physiology*, 145(3):1031–1042.

Gao, S., Gao, Y., Xiong, C., Yu, G., Chang, J., Yang, Q., Yang, C., and Ye, Z. (2017). The tomato B-type cyclin gene, SlCycB2, plays key roles in reproductive organ development, trichome initiation, terpenoids biosynthesis and prodenia litura defense. *Plant Science*, 262:103–114.

Gausman, H. W. and Cardenas, R. (1973). Light reflectance by leaflets of pubescent, normal, and glabrous *Soybean Lines*. *Agronomy Journal*, 65(5):837–838.

Gibson, R. W. (1971). Glandular hairs providing resistance to aphids in certain wild potato species. *Annals of Applied Biology*, 68(2):113–119.

Gitonga, V. W., Koning-Boucoiran, C. F., Verlinden, K., Dolstra, O., Visser, R. G., Maliepaard, C., and Krens, F. A. (2014). Genetic variation, heritability and genotype by environment interaction of morphological traits in a tetraploid rose population. *BMC Genetics*, 15(1):146.

Givnish, T. J. (1990). Leaf mottling: relation to growth form and leaf phenology and possible role as camouflage. *Functional Ecology*, 4(4):463–474.

Glas, J. J., Schimmel, B. C. J., Alba, J. M., Escobar-Bravo, R., Schuurink, R. C., and Kant, M. R. (2012). Plant glandular trichomes as targets for breeding or engineering of resistance to herbivores. *International Journal of Molecular Sciences*, 13(12):17077–17103.

Gowda, J. H. (1996). Spines of *Acacia tortilis*: what do they defend and how? *Oikos*, 77(2):279–284.

Graham, J., Smith, K., Tierney, I., MacKenzie, K., and Hackett, C. A. (2006). Mapping gene H controlling cane pubescence in raspberry and its association with resistance to cane botrytis and spur blight, rust and cane spot. *Theoretical and Applied Genetics*, 112(5):818–831.

Gu, G. z., Li, C. l., Jiang, S. y., Alexander, C., Bartholomew, B., Brach, A. R., Boufford, D. E., Ikeda, H., Ohba, H., Robertson, K. R., and Spongberg, S. A. (2003). *Flora of China.* Rosaceae, volume 9. Science Press, Beijing.

Gu, G. z. and Robertson, K. R. (2003). *Flora of China* - Rosaceae*:* Rosa, volume 9. Science Press, Beijing.

Hackett, C. A., Boskamp, B., Vogogias, A., Preedy, K. F., and Milne, I. (2017). TetraploidSNPMap: software for linkage analysis and QTL mapping in autotetraploid populations using SNP dosage data. *Journal of Heredity*, 108(4):438–442.

Hall, H. K., Cohen, D., and Skirvin, R. M. (1986). The inheritance of thornlessness from tissue culture-derived 'thornless evergreen'blackberry. *Euphytica*, 35(3):891–898.

Halpern, M., Raats, D., and Lev-Yadun, S. (2007). Plant biological warfare: thorns inject pathogenic bacteria into herbivores. *Environmental Microbiology*, 9(3):584–592.

Halpern, M., Waissler, A., Dror, A., and Lev-Yadun, S. (2011). Chapter 4 - biological warfare of the spiny plant: introducing pathogenic microorganisms into herbivore's tissues. In Laskin, A. I., Sariaslani, S., and Gadd, G. M., editors, *Advances in applied microbiology*, volume 74, pages 97–116. Academic Press.

Handley, R., Ekbom, B., and Ågren, J. (2005). Variation in trichome density and resistance against a specialist insect herbivore in natural populations of *Arabidopsis thaliana*. *Ecological Entomology*, 30(3):284–292.

Hao, X., Zhong, Y., Nützmann, H.-W., Fu, X., Yan, T., Shen, Q., Chen, M., Ma, Y., Zhao, J., Osbourn, A., Li, L., and Tang, K. (2019). Light-induced artemisinin biosynthesis is regulated by the bZIP transcription factor AaHY5 in *Artemisia annua*. *Plant and Cell Physiology*, 60(8):1747–1760.

Hare, J. D. (2005). Biological activity of acyl glucose esters from *Datura wrightii* glandular trichomes against three native insect herbivores. *Journal of Chemical Ecology*, 31(7):1475–1491.

Hare, J. D. and Elle, E. (2002). Variable impact of diverse insect herbivores on dimorphic *Datura Wrightii*. *Ecology*, 83(10):2711–2720.

Hartmann, T. (2008). The lost origin of chemical ecology in the late 19th century. *Proceedings of the National Academy of Sciences*, 105(12):4541–4546.

Harvell, C. D. (1990). The ecology and evolution of inducible defenses. *The Quarterly Review of Biology*, 65(3):323–340.

Haudenschild, C. D. and Croteau, R. B. (1998). Molecular engineering of monoterpene production. In Setlow, J. K., editor, *Genetic engineering*, pages 267–280. Springer, Boston, MA.

Hibrand-Saint Oyant, L., Crespel, L., Rajapakse, S., Zhang, L., and Foucher, F. (2008). Genetic linkage maps of rose constructed with new microsatellite markers and locating QTL controlling flowering traits. *Tree Genetics & Genomes*, 4(1):11.

Hibrand-Saint Oyant, L., Ruttink, T., Hamama, L., Kirov, I., Lakhwani, D., Zhou, N. N., Bourke, P. M., Daccord, N., Leus, L., Schulz, D., de Geest, H. V., Hesselink, T., Laere, K. V., Debray, K., Balzergue, S., Thouroude, T., Chastellier, A., Jeauffre, J., Voisine, L., Gaillard, S., Borm, T. J. A., Arens, P., Voorrips, R. E., Maliepaard, C., Neu, E., Linde, M., Paslier, M. C. L., Bérard, A., Bounon, R., Clotault, J., Choisne, N., Quesneville, H., Kawamura, K., Aubourg, S., Sakr, S., Smulders, M. J. M., Schijlen, E., Bucher, E., Debener, T., Riek, J. D., and Foucher, F. (2018). A high-quality genome sequence of *Rosa chinensis* to elucidate ornamental traits. *Nature Plants*, 4(7):473.

Hodes, R. M. and B., T. (1990). Tetanus in ethiopia: analysis of 55 cases from addis ababa. *East African medical journal*, 67.

Howe, H. F. and Westley, L. C. (1988). *Ecological relationships of plants and animals*. Oxford University Press.

Huchelmann, A., Boutry, M., and Hachez, C. (2017). Plant glandular trichomes: natural cell factories of high biotechnological interest. *Plant Physiology*, 175(1):6–22.

Hülskamp, M. (2004). Plant trichomes: a model for cell differentiation. *Nature Reviews Molecular Cell Biology*, 5(6):471–480.

Hülskamp, M., Miséra, S., and Jürgens, G. (1994). Genetic dissection of trichome cell development in Arabidopsis. *Cell*, 76(3):555–566.

Hülskamp, M., Schnittger, A., and Folkers, U. (1998). Pattern formation and cell differentiation: trichomes in arabidopsis as a genetic model system. In *International review of cytology*, volume 186, pages 147–178. Academic Press.

Hur, Y.-S., Shin, K.-H., Kim, S., Nam, K. H., Lee, M.-S., Chun, J.-Y., and Cheon, C.-I. (2009). Overexpression of GmAKR1, a stress-induced aldo/keto reductase from soybean, retards nodule development. *Molecules and Cells*, 27(2):217–223.

Hurst, C. (1941). Notes on the origin and evolution of our garden roses. *Journal of the Royal Horticultural Society*, 66:282–289.

Hurst, C. C. (1925). Chromosomes and characters in *Rosa* and their significance in the origin of species. *Experiments in Genetics*, 37:534–550.

Đinh, S. T., Gális, I., and Baldwin, I. T. (2013). UV-B radiation and 17-hydroxygeranyllinalool diterpene glycosides provide durable resistance against mirid (*Tupiocoris notatus*) attack in field-grown *Nicotiana attenuata* plants. *Plant, Cell & Environment*, 36(3):590–606.

Inzé, D. and Veylder, D. L. (2006). Cell cycle regulation in plant development. *Annual Review of Genetics*, 40(1):77–105.

Ishida, T., Hattori, S., Sano, R., Inoue, K., Shirano, Y., Hayashi, H., Shibata, D., Sato, S., Kato, T., Tabata, S., Okada, K., and Wada, T. (2007). *Arabidopsis* TRANSPARENT TESTA GLABRA2 is directly regulated by R2R3 MYB transcription factors and is involved in regulation of GLABRA2 transcription in epidermal differentiation. *The Plant Cell*, 19(8):2531–2543.

Ishida, T., Kurata, T., Okada, K., and Wada, T. (2008). A genetic regulatory network in the development of trichomes and root hairs. *Annual Review of Plant Biology*, 59(1):365–386.

Iwata, H., Gaston, A., Remay, A., Thouroude, T., Jeauffre, J., Kawamura, K., Oyant, L. H.-S., Araki, T., Denoyes, B., and Foucher, F. (2012). The TFL1 homologue KSN is a regulator of continuous flowering in rose and strawberry. *The Plant Journal*, 69(1):116–125.

Jain, K., Fraser, C. S., Marunde, M. R., Parker, M. M., Sagum, C., Burg, J. M., Hall, N., Popova, I. K., Rodriguez, K. L., Vaidya, A., et al. (2020). Characterization of the plant homeodomain (PHD) reader family for their histone tail interactions. *Epigenetics & chromatin*, 13(1):1–11.

Janzen, D. H. (1976). Why bamboos wait so long to flower. *Annual Review of Ecology and Systematics*, 7(1):347–391.

Jenkins, G. I. (2009). Signal transduction in responses to UV-B radiation. *Annual Review of Plant Biology*, 60(1):407–431.

Jensen, G. B., Hansen, B. M., Eilenberg, J., and Mahillon, J. (2003). The hidden lifestyles of *Bacillus cereus* and relatives. *Environmental Microbiology*, 5(8):631–640.

Jeschke, V., Gershenzon, J., and Vassão, D. G. (2015). Metabolism of glucosinolates and their hydrolysis products in insect herbivores. In *The Formation, Structure and Activity of Phytochemicals*, pages 163–194. Springer.

Jian, H., Li, S., Guo, J., Li, S., Wang, Q., Yan, H., Qiu, X., Zhang, Y., Cai, Z., Volis, S., et al. (2018). High genetic diversity and differentiation of an extremely narrowly distributed and critically endangered decaploid rose (*Rosa praelucens*): implications for its conservation. *Conservation Genetics*, 19(4):761–776.

Jian, H., Zhang, H., Tang, K., Li, S., Wang, Q., Zhang, T., Qiu, X., and Yan, H. (2010a). Decaploidy in *Rosa praelucens* byhouwer (*Rosaceae*) endemic to zhongdian plateau, yunnan, china. *Caryologia*, 63(2):162–167.

Jian, H. Y., Zhang, H., Wang, Q. G., Tang, K. X., fa Li, S., Qiu, X. Q., Yan, H., and Zhang, T. (2010b). Karyological study of chinese old garden roses. *Acta Horticulturae Sinica*, 37(1):83–88.

Jiang, F., Zhang, J., Wang, S., Yang, L., Luo, Y., Gao, S., Zhang, M., Wu, S., Hu, S., Sun, H., and Wang, Y. (2019). The apricot (*Prunus armeniaca* l.) genome elucidates *Rosaceae* evolution and beta-carotenoid synthesis. *Horticulture Research*, 6(1):1–12.

Jing, Y., Guo, Q., and Lin, R. (2019). The chromatin-remodeling factor pickle antagonizes polycomb repression of FT to promote flowering. *Plant Physiology*, 181(2):656–668.

Johnson, H. B. (1975). Plant pubescence: an ecological perspective. *The Botanical Review*, 41(3):233–258.

Jolivet, P. (1998). *Interrelationship between insects and plants*. CRC Press.

Joret, C. (1892). *La rose dans l'antiquité et au Moyen âge: histoire, légendes et symbolisme*. Emile Bouillon, Paris, France.

Joubès, J., Chevalier, C., Dudits, D., Heberle-Bors, E., Inzé, D., Umeda, M., and Renaudin, J.-P. (2000). Cdk-related protein kinases in plants. In Inzé, D., editor, *The plant cell cycle*, pages 63–76. Springer Netherlands, Dordrecht.

Joyaux, F. (2015). *Nouvelle encyclopédie des roses anciennes*. Eugen Ulmer, Paris, France.

Jung, S., Ficklin, S. P., Lee, T., Cheng, C.-H., Blenda, A., Zheng, P., Yu, J., Bombarely, A., Cho, I., Ru, S., Evans, K., Peace, C., Abbott, A. G., Mueller, L. A., Olmstead, M. A., and Main, D. (2014). The genome database for *Rosaceae* (GDR): year 10 update. *Nucleic Acids Research*, 42(D1):D1237–D1244.

Jung, S., Lee, T., Cheng, C.-H., Buble, K., Zheng, P., Yu, J., Humann, J., Ficklin, S. P., Gasic, K., Scott, K., Frank, M., Ru, S., Hough, H., Evans, K., Peace, C., Olmstead, M., DeVetter, L. W., McFerson, J., Coe, M., Wegrzyn, J. L., Staton, M. E., Abbott, A. G., and Main, D. (2019). 15 years of GDR: new data and functionality in the genome database for *Rosaceae*. *Nucleic Acids Research*, 47(D1):D1137–D1145.

Kant, M. R., Jonckheere, W., Knegt, B., Lemos, F., Liu, J., Schimmel, B. C. J., Villarroel, C. A., Ataide, L. M. S., Dermauw, W., Glas, J. J., Egas, M., Janssen, A., Van Leeuwen, T., Schuurink, R. C., Sabelis, M. W., and Alba, J. M. (2015). Mechanisms and ecological consequences of plant defence induction and suppression in herbivore communities. *Annals of Botany*, 115(7):1015–1051.

Karabourniotis, G. and Fasseas, C. (1996). The dense indumentum with its polyphenol content may replace the protective role of the epidermis in some young xeromorphic leaves. *Canadian Journal of Botany*, 74(3):347–351.

Karabourniotis, G., Liakopoulos, G., Nikolopoulos, D., and Bresta, P. (2020). Protective and defensive roles of non-glandular trichomes against multiple stresses: Structure-function coordination. *Journal of Forestry Research*, 31(1):1–12.

Karban, R. (2015). *Plant sensing and communication*. University of Chicago Press.

Karban, R. and Baldwin, I. (1997). *Induced responses to herbivory*. University of Chicago Press, Chicago.

Kariyat, R. R., Hardison, S. B., De Moraes, C. M., and Mescher, M. C. (2017). Plant spines deter herbivory by restricting caterpillar movement. *Biology letters*, 13(5):20170176.

Karousou, R., Bosabalidis, A. M., and Kokkini, S. (1992). *Sideritis syriaca ssp. syriaca*: Glandular trichome structure and development in relation to systematics. *Nordic Journal of Botany*, 12(1):31–37.

Kasili, R., Walker, J. D., Simmons, L. A., Zhou, J., De Veylder, L., and Larkin, J. C. (2010). SIAMESE cooperates with the CDH1-like protein CCS52A1 to establish endoreplication in *Arabidopsis thaliana* trichomes. *Genetics*, 185(1):257–268.

Kawamura, K., Oyant, L. H.-S., Crespel, L., Thouroude, T., Lalanne, D., and Foucher, F. (2011). Quantitative trait loci for flowering time and inflorescence architecture in rose. *Theoretical and Applied Genetics*, 122(4):661–675.

Kellogg, A. A., Branaman, T. J., Jones, N. M., Little, C. Z., and Swanson, J.-D. (2011). Morphological studies of developing rubus prickles suggest that they are modified glandular trichomes. *Botany*, 89(4):217–226.

Kessler, A. and Baldwin, I. T. (2001). Defensive function of herbivore-induced plant volatile emissions in nature. *Science*, 291(5511):2141–2144.

Khadgi, A. and Weber, C. A. (2020a). Morphological characterization of prickled and prickle-free *Rubus* using scanning electron microscopy. *HortScience*, 55(5):676–683.

Khadgi, A. and Weber, C. A. (2020b). RNA-Seq analysis of prickled and prickle-free epidermis provides insight into the genetics of prickle development in red raspberry (*Rubus ideaus* l.). *Agronomy*, 10(12):1904.

Khan, I. A. and Abourashed, E. A. (2011). *Leung's encyclopedia of common natural ingredients: used in food, drugs and cosmetics*. John Wiley & Sons.

Kieffer, M., Stern, Y., Cook, H., Clerici, E., Maulbetsch, C., Laux, T., and Davies, B. (2006). Analysis of the transcription factor wuschel and its functional homologue in Antirrhinum reveals a potential mechanism for their roles in meristem maintenance. *The Plant Cell*, 18(3):560–573.

Kieselova, K., Santiago, F., and Henrique, M. (2017). Rose thorn injury. *BMJ Case Reports*, 2017.

Kim, S. Y., Hyoung, S., So, W. M., and Shin, J. S. (2018). The novel transcription factor TRP interacts with ZFP5, a trichome initiation-related transcription factor, and negatively regulates trichome initiation through gibberellic acid signaling. *Plant molecular biology*, 96(3):315–326.

Kintzios, S. E. (2002). *Oregano: the Genera Origanum and Lippia*. CRC Press.

Kirik, V., Bouyer, D., Schöbinger, U., Bechtold, N., Herzog, M., Bonneville, J. M., and Hülskamp, M. (2001). Cpr5 is involved in cell proliferation and cell death control and encodes a novel transmembrane protein. *Current Biology*, 11(23):1891–1895.

Kirik, V., Lee, M. M., Wester, K., Herrmann, U., Zheng, Z., Oppenheimer, D., Schiefelbein, J., and Hulskamp, M. (2005). Functional diversification of MYB23 and GL1 genes in trichome morphogenesis and initiation. *Development*, 132(7):1477–1485.

Koning-Boucoiran, C., Dolstra, O., van der Linden, C., van der Schoot, J., Gitonga, V., Verlinden, K., Maliepaard, C., and Krens, F. (2009). Specific mapping of disease resistance genes in tetraploid cut roses. *Acta Horticulturae*, 836:137–142.

Koning-Boucoiran, C. F. S., Gitonga, V. W., Yan, Z., Dolstra, O., van der Linden, C. G., van der Schoot, J., Uenk, G. E., Verlinden, K., Smulders, M. J. M., Krens, F. A., and Maliepaard, C. (2012). The mode of inheritance in tetraploid cut roses. *Theoretical and Applied Genetics*, 125(3):591–607.

Koornneeff, M. (1981). The complex syndrome of *ttg* mutants. *Arabidopsis Information Service*, 18:45–51.

Koornneeff, M., Dellaert, L. W. M., and van der Veen, J. H. (1982). EMS-and relation-induced mutation frequencies at individual loci in *Arabidopsis thaliana* l. heynh. *Mutation Research/Fundamental and Molecular Mechanisms of Mutagenesis*, 93(1):109–123.

Körner, C. (2003). *Alpine plant life: functional plant ecology of high mountain ecosystems*. Springer, second edition.

Korte, A. and Farlow, A. (2013). The advantages and limitations of trait analysis with GWAS: a review. *Plant methods*, 9(1):1–9.

Krings, M., Kellogg, D. W., Kerp, H., and Taylor, T. N. (2003). Trichomes of the seed fern blanzyopteris praedentata: implications for plant-insect interactions in the late carboniferous. *Botanical Journal of the Linnean Society*, 141(2):133–149.

Lange, B. M. (2015). The evolution of plant secretory structures and emergence of terpenoid chemical diversity. *Annual Review of Plant Biology*, 66(1):139–159.

Lange, B. M. and Turner, G. W. (2013). Terpenoid biosynthesis in trichomes - current status and future opportunities. *Plant Biotechnology Journal*, 11(1):2–22.

Larkin, J. C., Brown, M. L., and Schiefelbein, J. (2003). How do cells know what they want to be when they grow up? lessons from epidermal patterning in Arabidopsis. *Annual Review of Plant Biology*, 54(1):403–430.

Laskowski, M. J., Williams, M. E., Nusbaum, H. C., and Sussex, I. M. (1995). Formation of lateral root meristems is a two-stage process. *Development*, 121(10):3303–3310.

Laux, T., Mayer, K., Berger, J., and Jurgens, G. (1996). The WUSCHEl gene is required for shoot and floral meristem integrity in *Arabidopsis*. *Development*, 122(1):87–96.

Leelavathi, P. and Ramayya, N. (1983). Structure, distribution and classification of plant trichomes in relation to taxonomy iii. *Papilionoideae*. *Proceedings: Plant Sciences*, 92(5):421–441.

Leffingwell, J. C. (1999). Aroma from carotenoids - rose. http://www.leffingwell.com/rose.htm.

Leus, L., Van Laere, K., De Riek, J., and Van Huylenbroeck, J. (2018). Rose. In Van Huylenbroeck, J., editor, *Ornamental crops*, Handbook of plant breeding, pages 719–767. Springer International Publishing, Cham.

Lev-Yadun, S. (2003). Weapon thorn automimicry and mimicry of aposematic colorful thorns in plants. *Journal of Theoretical Biology*, 224(2):183–188.

Lev-Yadun, S. (2009). Aposematic warning coloration in plants. In *Plant-environment interactions: from sensory plant biology to active plant behavior*, pages 167–202. Springer, Berlin, Heidelberg.

Lev-Yadun, S. (2016). Color changes in old aposematic thorns, spines, and prickles. In *Defensive (anti-herbivory) coloration in land plants*, pages 139–148. Springer, Cham.

Levin, D. A. (1973). The role of trichomes in plant defense. *The Quarterly Review of Biology*, 48(1):3–15.

Li, H., Liu, F. L., Xi, L., Gao, B., Yan, S., Wang, L., Ma, N., Zhao, L., and Yang, C. (2012). Studies on anatomical structure and chemical composition in prickles of *Rosa* hybrida. *Acta Horticulturae Sinica*, 39(7):1321–1329.

Liakoura, V., Stefanou, M., Manetas, Y., Cholevas, C., and Karabourniotis, G. (1997). Trichome density and its UV-B protective potential are affected by shading and leaf position on the canopy. *Environmental and Experimental Botany*, 38(3):223–229.

Liao, Y., Wang, J., Jaehnig, E. J., Shi, Z., and Zhang, B. (2019). Webgestalt 2019: Gene set analysis toolkit with revamped uis and apis. *Nucleic Acids Research*, 47(W1):W199–W205.

Linde, M., Hattendorf, A., Kaufmann, H., and Debener, T. (2006). Powdery mildew resistance in roses: QTL mapping in different environments using selective genotyping. *Theoretical and Applied Genetics*, 113(6):1081–1092.

Linsmith, G., Rombauts, S., Montanari, S., Deng, C. H., Celton, J.-M., Guérif, P., Liu, C., Lohaus, R., Zurn, J. D., Cestaro, A., et al. (2019). Pseudo-chromosome-length genome assembly of a double haploid "bartlett" pear (*Pyrus communis* l.). *GigaScience*, 8(12):138.

Liorzou, M., Pernet, A., Li, S., Chastellier, A., Thouroude, T., Michel, G., Malécot, V., Gaillard, S., Briée, C., Foucher, F., Oghina-Pavie, C., Clotault, J., and Grapin, A. (2016). Nineteenth century french rose (*Rosa* sp.) germplasm shows a shift over time from a european to an asian genetic background. *Journal of Experimental Botany*, 67(15):4711–4725.

Liu, Z.-Q., Gao, J., Dong, A.-W., and Shen, W.-H. (2009). A truncated *Arabidopsis* NUCLEOSOME ASSEMBLY PROTEIN 1, AtNAP1; 3T, alters plant growth responses to abscisic acid and salt in the Atnap1; 3-2 mutant. *Molecular Plant*, 2(4):688–699.

Longhi, S., Giongo, L., Buti, M., Surbanovski, N., Viola, R., Velasco, R., Ward, J. A., and Sargent, D. J. (2014). Molecular genetics and genomics of the *Rosoideae*: State of the art and future perspectives. *Horticulture Research*, 1(1):1–18.

Lopez-Arias, D., Chastellier, A., Thouroude, T., Bradeen, J., Van Eck, L., De Oliveira, Y., Paillard, S., Foucher, F., Hibrand-Saint Oyant, L., and Soufflet-Freslon, V. (2020). Characterization of black spot resistance in diploid roses with QTL detection, meta-analysis and candidate-gene identification. *Theoretical and Applied Genetics*, 133(12):3299–3321.

LoPresti, E. F. and Karban, R. (2016). Chewing sandpaper: Grit, plant apparency, and plant defense in sand-entrapping plants. *Ecology*, 97(4):826–833.

Love, M. I., Huber, W., and Anders, S. (2014). Moderated estimation of fold change and dispersion for RNA-seq data with DESeq2. *Genome Biology*, 15(12):550.

Lubbe, A. and Verpoorte, R. (2011). Cultivation of medicinal and aromatic plants for specialty industrial materials. *Industrial crops and products*, 34(1):785–801.

Lucas, P. W., Turner, I. M., Dominy, N. J., and Yamashita, N. (2000). Mechanical defences to herbivory. *Annals of Botany*, 86(5):913–920.

Ma, D., Hu, Y., Yang, C., Liu, B., Fang, L., Wan, Q., Liang, W., Mei, G., Wang, L., Wang, H., Ding, L., Dong, C., Pan, M., Chen, J., Wang, S., Chen, S., Cai, C., Zhu, X., Guan, X., Zhou, B., Zhu, S., Wang, J., Guo, W., Chen, X., and Zhang, T. (2016a). Genetic basis for glandular trichome formation in cotton. *Nature Communications*, 7(1):1–9.

Ma, Y., Miotk, A., Šutiković, Z., Ermakova, O., Wenzl, C., Medzihradszky, A., Gaillochet, C., Forner, J., Utan, G., Brackmann, K., et al. (2019). WUSCHEL acts as an auxin response rheostat to maintain apical stem cells in *Arabidopsis*. *Nature communications*, 10(1):1–11.

Ma, Z.-Y., Wen, J., Ickert-Bond, S. M., Chen, L.-Q., and Liu, X.-Q. (2016b). Morphology, structure, and ontogeny of trichomes of the grape genus (*Vitis, Vitaceae*). *Frontiers in Plant Science*, 7:704.

MacFarlane, W. V. (1963). The stinging properties of *Laportea*. *Economic Botany*, 17(4):303–311.

Maes, L., Inzé, D., and Goossens, A. (2008). Functional specialization of the TRANSPARENT TESTA GLABRA1 network allows differential hormonal control of laminal and marginal trichome initiation in *Arabidopsis* rosette leaves. *Plant Physiology*, 148(3):1453–1464.

Mahajan, V. K. (2014). Sporotrichosis: an overview and therapeutic options. *Dermatology Research and Practice*, 2014:13.

Marissen, N. (1999). Effects of pre-harvest light intensity and temperature on carbohydrate levels and vase life of cut roses. In *VII International Symposium on Postharvest Physiology of Ornamental Plants 543*, pages 331–336.

Marks, M. D. (1997). Molecular genetic analysis of trichome development in Arabidopsis. *Annual Review of Plant Physiology and Plant Molecular Biology*, 48(1):137–163.

Masure, P. (2013). *Guide Des Rosiers Sauvages: 500 Espèces, Variétés et Hybrides Du Monde*. Delachaux et Niestlé, Paris, France.

Mateo-Bonmatí, E., Casanova-Sáez, R., Quesada, V., Hricová, A., Candela, H., and Micol, J. L. (2015). Plastid control of abaxial-adaxial patterning. *Scientific Reports*, 5(1):15975.

Matías-Hernández, L., Jiang, W., Yang, K., Tang, K., Brodelius, P. E., and Pelaz, S. (2017). AaMYB1 and its orthologue AtMYB61 affect terpene metabolism and trichome development in *Artemisia annua* and *Arabidopsis thaliana*. *The Plant Journal*, 90(3):520–534.

Mazza, C. A., Giménez, P. I., Kantolic, A. G., and Ballaré, C. L. (2013). Beneficial effects of solar UV-B radiation on soybean yield mediated by reduced insect herbivory under field conditionss. *Physiologia Plantarum*, 147(3):307–315.

Mazza, C. A., Zavala, J., Scopel, A. L., and Ballaré, C. L. (1999). Perception of solar UV-B radiation by phytophagous insects: behavioral responses and ecosystem implications. *Proceedings of the National Academy of Sciences*, 96(3):980–985.

McPheeters, K. and Skirvin, R. M. (1983). Histogenic layer manipulation in chimeral thornless evergreen trailing blackberry. *Euphytica*, 32(2):351–360.

Melaragno, J. E., Mehrotra, B., and Coleman, A. W. (1993). Relationship between endopolyploidy and cell size in epidermal tissue of *Arabidopsis*. *The Plant Cell*, 5(11):1661–1668.

Mershon, J. P., Becker, M., and Bickford, C. P. (2015). Linkage between trichome morphology and leaf optical properties in New Zealand alpine Pachycladon (Brassicaceae). *New Zealand Journal of Botany*, 53(3):175–182.

Metcalfe, C. R. and Chalk, L. (1957). *Anatomy of The Dicotyledons Vol I.* Oxford At The Clarendon Press., reprint edition.

Metcalfe, C. R. and Chalk, L. (1965). *Anatomy of the Dicotyledons: Volume II: Wood Structure and Conclusion of the General Introduction*. Oxford University Press, USA, first edition.

Mewis, I., Schreiner, M., Nguyen, C. N., Krumbein, A., Ulrichs, C., Lohse, M., and Zrenner, R. (2012). UV-B irradiation changes specifically the secondary metabolite profile in broccoli sprouts: induced signaling overlaps with defense response to biotic stressors. *Plant and Cell Physiology*, 53(9):1546–1560.

Michael G., S. (2010). *Plant Systematics*. Academic Press, second edition.

Ministry of Culture and Sports (2007). Blue bird fresco. Heraklion Archaeological Museum.

Molina-Bravo, R., Fernandez, G. E., and Sosinski, B. R. (2014). Quantitative trait locus analysis of tolerance to temperature fluctuations in winter, fruit characteristics, flower color, and prickle-free canes in raspberry. *Molecular Breeding*, 33(2):267–280.

Morgan, D. O. (1997). CYCLIN-DEPENDENT KINASES: Engines, clocks, and microprocessors. *Annual Review of Cell and Developmental Biology*, 13(1):261–291.

Morohashi, K. and Grotewold, E. (2009). A systems approach reveals regulatory circuitry for Arabidopsis trichome initiation by the gl3 and gl1 selectors. *PLOS Genetics*, 5(2):e1000396.

Mortensen, L. M. and Fjeld, T. (1998). Effects of air humidity, lighting period and lamp type on growth and vase life of roses. *Scientia Horticulturae*, 73(4):229–237.

Nadakuduti, S. S., Pollard, M., Kosma, D. K., Allen, C., Ohlrogge, J. B., and Barry, C. S. (2012). Pleiotropic phenotypes of the sticky peel mutant provide new insight into the tole of CUTIN DEFICIENT2 in epidermal cell function in tomato. *Plant Physiology*, 159(3):945–960.

Nakamura, N., Hirakawa, H., Sato, S., Otagaki, S., Matsumoto, S., Tabata, S., and Tanaka, Y. (2018). Genome structure of *Rosa multiflora*, a wild ancestor of cultivated roses. *DNA Research*, 25(2):113–121.

Nakata, M., Matsumoto, N., Tsugeki, R., Rikirsch, E., Laux, T., and Okada, K. (2012). Roles of the middle domain–specific wuschel-related homeobox genes in early development of leaves in Arabidopsis. *The Plant Cell*, 24(2):519–535.

Nédelec, P.-Y. (2018). *Roses grandeur nature: la collection des roses loubert*. Delachaux et Niestlé.

Netolitzky, F. and Uphof, J. C. T. (1962). *Plant Hairs*, volume 4. Borntraeger.

Nguyen, T. H. N., Schulz, D., Winkelmann, T., and Debener, T. (2017). Genetic dissection of adventitious shoot regeneration in roses by employing genome-wide association studies. *Plant Cell Reports*, 36(9):1493–1505.

Nguyen, T. H. N., Tänzer, S., Rudeck, J., Winkelmann, T., and Debener, T. (2020a). Genetic analysis of adventitious root formation in vivo and in vitro in a diversity panel of roses. *Scientia Horticulturae*, 266:109277.

Nguyen, T. H. N., Winkelmann, T., and Debener, T. (2020b). Genetic analysis of callus formation in a diversity panel of 96 rose genotypes. *Plant Cell, Tissue and Organ Culture (PCTOC)*, 142(3):505–517.

Nobbs, K. J. (1984). American rose annual. In Shreveport, editor, *Breeding Thornless Roses*, pages 37–43. The American Rose Society.

Nobel, P. (1988). *Environmental Biology of Agaves and Cacti*. Cambridge: Cambridge University Press.

Nobel, P. S. (2002). *Cacti: Biology and Uses*. University of California Press, first edition edition.

Ntefidou, M. and Manetas, Y. (1996). Optical properties of hairs during the early stages of leaf development in *Platanus orientalis*. *Functional Plant Biology*, 23(4):535–538.

O'Brien, T. P., Feder, N., and McCully, M. E. (1964). Polychromatic staining of plant cell walls by toluidine blue o. *Protoplasma*, 59(2):368–373.

Ohno, C. K., Reddy, G. V., Heisler, M. G., and Meyerowitz, E. M. (2004). The *Arabidopsis* jagged gene encodes a zinc finger protein that promotes leaf tissue development. *Development*, 131(5):1111–1122.

Oliver, W. G. (1986). A prçcis of thornless development. *The rose. The Royal National Rose Society*, 80(3):61–66.

Osman, A. K. (2012). Trichome micromorphology of *Egyptian Ballota* (*Lamiaceae*) with emphasis on its systematic implication. *Pakistan Journal of Botany*, 44(1):33–46.

Pandey, S., Goel, R., Bhardwaj, A., Asif, M. H., Sawant, S. V., and Misra, P. (2018). Transcriptome analysis provides insight into prickle development and its link to defense and secondary metabolism in *Solanum viarum* dunal. *Scientific Reports*, 8(1):1–12.

Park, J., Oh, D.-H., Dassanayake, M., Nguyen, K. T., Ogas, J., Choi, G., and Sun, T.-p. (2017). Gibberellin signaling requires chromatin remodeler PICKLE to promote vegetative growth and phase transitions. *Plant Physiology*, 173(2):1463–1474.

Park, Y.-J. and Luger, K. (2006). The structure of nucleosome assembly protein 1. *Proceedings of the National Academy of Sciences*, 103(5):1248–1253.

Pascual, F., McGinley, E., Zanardi, L., Cortese, M., and Murphy, T. (2003). Tetanus surveillance-united states, 1998-2000. *Morbidity and Mortality Weekly Peport CDC Surveillance Summaries*, 52(3).

Patra, B., Pattanaik, S., and Yuan, L. (2013). Ubiquitin protein ligase 3 mediates the proteasomal degradation of GLABROUS 3 and ENHANCER OF GLABROUS 3, regulators of trichome development and flavonoid biosynthesis in Arabidopsis. *The Plant Journal*, 74(3):435–447.

Pattanaik, S., Patra, B., Singh, S. K., and Yuan, L. (2014). An overview of the gene regulatory network controlling trichome development in the model plant, Arabidopsis. *Frontiers in Plant Science*, 5:259.

Payne, T., Clement, J., Arnold, D., and Lloyd, A. (1999). Heterologous *myb* genes distinct from *GL1* enhance trichome production when overexpressed in *Nicotiana tabacum*. *Development*, 126(4):671–682.

Payne, W. W. (1978). A glossary of plant hair terminology. *Brittonia*, 30(2):239.

Peiffer, M., Tooker, J. F., Luthe, D. S., and Felton, G. W. (2009). Plants on early alert: Glandular trichomes as sensors for insect herbivores. *New Phytologist*, 184(3):644–656.

Peitersen, A. K. (1921). *Blackberries of New England–genetic status of the plants*. Vermont Agricultural Experiment Station.

Pertea, M., Pertea, G. M., Antonescu, C. M., Chang, T.-C., Mendell, J. T., and Salzberg, S. L. (2015). StringTie enables improved reconstruction of a transcriptome from RNA-seq reads. *Nature biotechnology*, 33(3):290–295.

Pesch, M., Dartan, B., Birkenbihl, R., Somssich, I. E., and Hülskamp, M. (2014). Arabidopsis TTG2 regulates TRY expression through enhancement of activator complex-triggered activation. *The Plant Cell*, 26(10):4067–4083.

Pesch, M. and Hülskamp, M. (2004). Creating a two-dimensional pattern *de Novo* during *Arabidopsis* trichome and root hair initiation. *Current Opinion in Genetics & Development*, 14(4):422–427.

Pesch, M. and Hülskamp, M. (2011). Role of TRIPTYCHON in trichome patterning in *Arabidopsis*. *BMC Plant Biology*, 11(1):130.

Petit, L., Gibert, M., and Popoff, M. R. (1999). Clostridium perfringens: Toxinotype and genotype. *Trends in Microbiology*, 7(3):104–110.

Petricka, J. J., Clay, N. K., and Nelson, T. M. (2008). Vein patterning screens and the defectively organized tributaries mutants in Arabidopsis thaliana. *The Plant Journal*, 56(2):251–263.

Pierce, S. (2007). The jeweled armor of tillandsia - multifaceted or elongated trichomes provide photoprotection. *Aliso: A Journal of Systematic and Evolutionary Botany*, 23(1):44–52.

Pollmann, S., Neu, D., and Weiler, E. W. (2003). Molecular cloning and characterization of an amidase from Arabidopsis thaliana capable of converting indole-3-acetamide into the plant growth hormone, indole-3-acetic acid. *Phytochemistry*, 62(3):293–300.

Porceddu, A., Stals, H., Reichheld, J.-P., Segers, G., Veylder, L. D., Barrôco, R. d. P., Casteels, P., Montagu, M. V., Inzé, D., and Mironov, V. (2001). A plant-specific cyclin-dependent kinase is involved in the control of G2/M progression in plants. *Journal of Biological Chemistry*, 276(39):36354–36360.

Pradhan, K. and Maradi, R. M. (2020). Plant glandular trichomes: the natural pesticide factories. *Biotica Research Today*, 2(8):713–716.

Pullin, A. S. and Gilbert, J. E. (1989). The stinging nettle, *Urtica Dioica*, increases trichome density after herbivore and mechanical damage. *Oikos*, 54(3):275–280.

Qi, T., Song, S., Ren, Q., Wu, D., Huang, H., Chen, Y., Fan, M., Peng, W., Ren, C., and Xie, D. (2011). The Jasmonate-ZIM-domain proteins interact with the WD-Repeat/bHLH/MYB complexes to regulate Jasmonate-mediated anthocyanin accumulation and trichome initiation in *Arabidopsis thaliana*. *The Plant Cell*, 23(5):1795–1814.

Randoux, M., Jeauffre, J., Thouroude, T., Vasseur, F., Hamama, L., Juchaux, M., Sakr, S., and Foucher, F. (2012). Gibberellins regulate the transcription of the continuous flowering regulator, RoKSN, a rose TFL1 homologue. *Journal of Experimental Botany*, 63(18):6543–6554.

Ranger, C. M., Backus, E. A., Winter, R. E. K., Rottinghaus, G. E., Ellersieck, M. R., and Johnson, D. W. (2004). Glandular trichome extracts from *Medicago sativa* deter settling by the potato leafhopper empoasca fabae. *Journal of Chemical Ecology*, 30(5):927–943.

Raymond, O., Gouzy, J., Just, J., Badouin, H., Verdenaud, M., Lemainque, A., Vergne, P., Moja, S., Choisne, N., Pont, C., Carrère, S., Caissard, J.-C., Couloux, A., Cottret, L., Aury, J.-M., Szécsi, J., Latrasse, D., Madoui, M.-A., François, L., Fu, X., Yang, S.-H., Dubois, A., Piola, F., Larrieu, A., Perez, M., Labadie, K., Perrier, L., Govetto, B., Labrousse, Y., Villand, P., Bardoux, C., Boltz, V., Lopez-Roques, C., Heitzler, P., Vernoux, T., Vandenbussche, M., Quesneville, H., Boualem, A., Bendahmane, A., Liu, C., Le Bris, M., Salse, J., Baudino, S., Benhamed, M., Wincker, P., and Bendahmane, M. (2018). The *Rosa* genome provides new insights into the domestication of modern roses. *Nature Genetics*, 50(6):772–777.

Rehder, A. (1940). Manual of cultivated trees and shrubs hardy in North America. *Manual of cultivated trees and shrubs hardy in North America.*

Remay, A., Lalanne, D., Thouroude, T., Le Couviour, F., Hibrand-Saint Oyant, L., and Foucher, F. (2009). A survey of flowering genes reveals the role of gibberellins in floral control in rose. *Theoretical and Applied Genetics*, 119(5):767–781.

Renfrew, J. M. (1973). The prehistoric food plants of the near east and europe. *Proceedings of the Prehistoric Society*, 48:248.

ReportLinker (2020). *Cut flowers market forecast to 2027 - COVID-19 impact and global analysis by flower type and application, and geography*. Global Cut Flowers Market Analysis: Rose. Research and Markets Publishers.

Rerie, W. G., Feldmann, K. A., and Marks, M. D. (1994). The GLABRA2 gene encodes a homeo domain protein required for normal trichome development in *Arabidopsis*. *Genes & Development*, 8(12):1388–1399.

Ribeiro, S. P., Pimenta, H. R., and Fernandes, G. W. (1994). Herbivory by chewing and sucking insects on *Tabebuia ochracea*. *Biotropica*, 26(3):302–307.

Ro, D.-K., Paradise, E. M., Ouellet, M., Fisher, K. J., Newman, K. L., Ndungu, J. M., Ho, K. A., Eachus, R. A., Ham, T. S., Kirby, J., Chang, M. C. Y., Withers, S. T., Shiba, Y., Sarpong, R., and Keasling, J. D. (2006). Production of the antimalarial drug precursor artemisinic acid in engineered yeast. *Nature*, 440(7086):940–943.

Roberts, A. V., Gladis, T., and Brumme, H. (2009). DNA amounts of roses (*Rosa* l.) and their use in attributing ploidy levels. *Plant Cell Reports*, 28(1):61–71.

Robinson, J. T., Thorvaldsdóttir, H., Winckler, W., Guttman, M., Lander, E. S., Getz, G., and Mesirov, J. P. (2011). Integrative genomics viewer. *Nature biotechnology*, 29(1):24–26.

Robson, T. M., Klem, K., Urban, O., and Jansen, M. a. K. (2015). Re-interpreting plant morphological responses to UV-B radiation. *Plant, Cell & Environment*, 38(5):856–866.

Roda, A. L., Oldham, N. J., Svatos, A., and Baldwin, I. T. (2003). Allometric analysis of the induced flavonols on the leaf surface of wild tobacco (Nicotiana attenuata). *Phytochemistry*, 62(3):527–536.

Roman, H., Rapicault, M., Miclot, A. S., Larenaudie, M., Kawamura, K., Thouroude, T., Chastellier, A., Lemarquand, A., Dupuis, F., Foucher, F., Loustau, S., and Oyant, L. H.-S. (2015). Genetic analysis of the flowering date and number of petals in rose. *Tree Genetics & Genomes*, 11(4):85.

Ronel, M. and Lev-Yadun, S. (2012). The spiny, thorny and prickly plants in the flora of Israel. *Botanical Journal of the Linnean Society*, 168(3):344–352.

Rossi, A., Kontarakis, Z., Gerri, C., Nolte, H., Hölper, S., Krüger, M., and Stainier, D. Y. R. (2015). Genetic compensation induced by deleterious mutations but not gene knockdowns. *Nature*, 524(7564):230–233.

Rosu, A., Skirvin, R. M., Bein, A., Norton, M. A., Kushad, M., and Otterbacher, A. G. (1995). The development of putative adventitious shoots from a chimeral thornless rose (*Rosa multiflora* Thunb. ex J. Murr.) in vitro. *Journal of Horticultural Science*, 70(6):901–907.

Royal Botanic Gardens and Kew and Missouri Botanic Garden (2013). The plant list - *Rosaceae*. http://www.theplantlist.org/browse/A/Rosaceae/. Accessed: 2020.

Ruxton, G. D., Allen, W. L., Sherratt, T. N., and Speed, M. P. (2004). *Avoiding Attack: The Evolutionary Ecology of Crypsis, Aposematism, and Mimicry*. Oxford University Press.

Sanchez, R. and Zhou, M.-M. (2011). The PHD finger: a versatile epigenome reader. *Trends in biochemical sciences*, 36(7):364–372.

Sarkar, A. K., Luijten, M., Miyashima, S., Lenhard, M., Hashimoto, T., Nakajima, K., Scheres, B., Heidstra, R., and Laux, T. (2007). Conserved factors regulate signalling in Arabidopsis thaliana shoot and root stem cell organizers. *Nature*, 446(7137):811–814.

Scheres, B. (2002). Plant patterning: TRY to inhibit your neighbors. *Current Biology*, 12(23):R804–R806.

Schiefelbein, J. (2003). Cell-fate specification in the epidermis: A common patterning mechanism in the root and shoot. *Current Opinion in Plant Biology*, 6(1):74–78.

Schnittger, A., Folkers, U., Schwab, B., Jürgens, G., and Hülskamp, M. (1999). Generation of a spacing pattern: The role of TRIPTYCHON in trichome patterning in *Arabidopsis*. *The Plant Cell*, 11(6):1105–1116.

Schnittger, A., Schöbinger, U., Bouyer, D., Weinl, C., Stierhof, Y.-D., and Hülskamp, M. (2002a). Ectopic d-type cyclin expression induces not only dna replication but also cell division in *Arabidopsis* trichomes. *Proceedings of the National Academy of Sciences*, 99(9):6410–6415.

Schnittger, A., Schöbinger, U., Stierhof, Y.-D., and Hülskamp, M. (2002b). Ectopic B-Type cyclin expression induces mitotic cycles in endoreduplicating *Arabidopsis* trichomes. *Current Biology*, 12(5):415–420.

Schnittger, A., Weinl, C., Bouyer, D., Schöbinger, U., and Hülskamp, M. (2003). Misexpression of the cyclin-dependent kinase inhibitor ick1/krp1 in single-celled *Arabidopsis* trichomes reduces endoreduplication and cell size and induces cell death. *The Plant Cell*, 15(2):303–315.

Schulz, D. F., Schott, R. T., Voorrips, R. E., Smulders, M. J. M., Linde, M., and Debener, T. (2016). Genome-wide association analysis of the anthocyanin and carotenoid contents of rose petals. *Frontiers in Plant Science*, 7.

Segers, G., Gadisseur, I., Bergounioux, C., Engler, J. d. A., Jacqmard, A., Montagu, M. V., and Inzé, D. (1996). The *Arabidopsis* cyclin-dependent kinase gene cdc2bAt is preferentially expressed during S and G2 phases of the cell cycle. *The Plant Journal*, 10(4):601–612.

Shi, P., Fu, X., Shen, Q., Liu, M., Pan, Q., Tang, Y., Jiang, W., Lv, Z., Yan, T., Ma, Y., et al. (2018). The roles of aa mixta 1 in regulating the initiation of glandular trichomes and cuticle biosynthesis in *Artemisia annua*. *New Phytologist*, 217(1):261–276.

Shmida, A. (1981). Mediterranean vegetation in California and Israel: Similarities and differences. *Israel Journal of Botany*, 30(3):105–123.

Shull, C. A. (1929). A spectrophotometric study of reflection of light from leaf surfaces. *Botanical Gazette*, 87(5):583–607.

Shupert, D., Byrne, D., and Brent Pemberton, H. (2007). Inheritance of flower traits, leaflet number and prickles in roses. *Acta Horticulturae*, 751:331–335.

Simmons, A. T. and Gurr, G. M. (2006). Trichomes of *Lycopersicon* species and their hybrids: effects on pests and natural enemies. *Agricultural and Forest Entomology*, 8(1):1–11.

Simmons, A. T., Gurr, G. M., McGrath, D., Martin, P. M., and Nicol, H. I. (2004). Entrapment of helicoverpa armigera (hübner) (lepidoptera: Noctuidae) on glandular trichomes of *Lycopersicon* species. *Australian Journal of Entomology*, 43(2):196–200.

Simmons, A. T., Nicol, H. I., and Gurr, G. M. (2006). Resistance of wild *Lycopersicon* species to the potato moth, *Phthorimaea operculella* (Zeller) (Lepidoptera: Gelechiidae). *Australian Journal of Entomology*, 45(1):81–86.

Skaltsa, H., Verykokidou, E., Harvala, C., Karabourniotis, G., and Manetasi, Y. (1994). UV-B protective potential and flavonoid content of leaf hairs of *Quercus ilex*. *Phytochemistry*, 37(4):987–990.

Smith, C. M. (1999). Plant resistance to insects. *Biological and biotechnological control of insects'.(Eds J Rechcigl, N Rechcigl) pp*, pages 171–207.

Smulders, M. J. M., Arens, P., Bourke, P. M., Debener, T., Linde, M., Riek, J. D., Leus, L., Ruttink, T., Baudino, S., Saint-Oyant, L. H., Clotault, J., and Foucher, F. (2019). In the name of the rose: A roadmap for rose research in the genome era. *Horticulture Research*, 6(1):1–27.

Speed, M. P. and Ruxton, G. D. (2005). Warning displays in spiny animals: One (more) evolutionary route to *Aposematism*. *Evolution*, 59(12):2499–2508.

Spiller, M., Linde, M., Hibrand-Saint Oyant, L., Tsai, C.-J., Byrne, D. H., Smulders, M. J. M., Foucher, F., and Debener, T. (2011). Towards a unified genetic map for diploid roses. *Theoretical and Applied Genetics*, 122(3):489–500.

Stuurman, J., Jäggi, F., and Kuhlemeier, C. (2002). Shoot meristem maintenance is controlled by a GRAS-gene mediated signal from differentiating cells. *Genes & Development*, 16(17):2213–2218.

Su, T., Huang, Y.-J., Meng, J., Zhang, S.-T., Huang, J., and Zhou, Z.-K. (2016). A miocene leaf fossil record of *Rosa* (*R. Fortuita* n. sp.) from its modern diversity center in SW China. *Palaeoworld*, 25(1):104–115.

Sun, W., Gao, D., Xiong, Y., Tang, X., Xiao, X., Wang, C., and Yu, S. (2017). Hairy leaf 6, an AP2/ERF transcription factor, interacts with OsWOX3B and regulates trichome formation in rice. *Molecular Plant*, 10(11):1417–1433.

Symonds, V. V., Hatlestad, G., and Lloyd, A. M. (2011). Natural allelic variation defines a role for ATMYC1: Trichome cell fate determination. *PLOS Genetics*, 7(6):e1002069.

Täckholm, G. (1920). *On the Cytology of the Genus* Rosa. Svensk Botanisk Tidskrift.

Tadele, H. (2017). Clinical profile and outcome of pediatrics tetanus: The experience of a tertiary hospital in Ethiopia. *Ethiopian Journal of Health Sciences*, 27(5):559–564.

Terefe, D. and Debener, T. (2011). An SSR from the leucine-rich repeat region of the rose *Rdr1* gene family is a useful resistance gene analogue marker for roses and other *Rosaceae*. *Plant Breeding*, 130(2):291–293.

Thorvaldsdóttir, H., Robinson, J. T., and Mesirov, J. P. (2013). Integrative genomics viewer (IGV): High-performance genomics data visualization and exploration. *Briefings in Bioinformatics*, 14(2):178–192.

Thurston, E. L. and Lersten, N. R. (1969). The morphology and toxicology of plant stinging hairs. *The Botanical Review*, 35(4):393–412.

Tian, D., Tooker, J., Peiffer, M., Chung, S. H., and Felton, G. W. (2012). Role of trichomes in defense against herbivores: Comparison of herbivore response to woolly and hairless trichome mutants in tomato (*Solanum Lycopersicum*). *Planta*, 236(4):1053–1066.

Tingey, W. M. (1991). Potato glandular trichomes. In *Naturally Occurring Pest Bioregulators*, volume 449 of *ACS Symposium Series*, pages 126–135. American Chemical Society.

Tomljenovic, N. and Pejić, I. (2018). Taxonomic review of the genus *Rosa*. *Agriculturae Conspectus Scientificus*, 83(2):139–147.

Touw, M. (1982). Roses in the middle ages. *Economic Botany*, 36(1):71–83.

Traw, B. M. and Dawson, T. E. (2002). Differential induction of trichomes by three herbivores of black mustard. *Oecologia*, 131(4):526–532.

Traw, M. B. and Bergelson, J. (2003). Interactive effects of jasmonic acid, salicylic acid, and gibberellin on induction of trichomes in *Arabidopsis*. *Plant Physiology*, 133(3):1367–1375.

Tsukaya, H., Fujikawa, K., and Wu, S.-G. (2002). Thermal insulation and accumulation of heat in the downy inflorescences of *Saussurea Medusa* (*Asteraceae*) at high elevation in yunnan, china. *Journal of Plant Research*, 115(4):263–268.

Tucker, A. O. (2004). Identification of the rose, sage, iris, and lily in the "blue bird fresco" from knossos, crete (ca. 1450 bce). *Economic Botany*, 58(4):733–736.

Turner, G. W., Gershenzon, J., and Croteau, R. B. (2000). Distribution of peltate glandular trichomes on developing leaves of *Peppermint*. *Plant Physiology*, 124(2):655–664. [object Object].

Ueno, Y., Ishikawa, T., Watanabe, K., Terakura, S., Iwakawa, H., Okada, K., Machida, C., and Machida, Y. (2007). Histone deacetylases and ASYMMETRIC LEAVES2 are involved in the establishment of polarity in leaves of *Arabidopsis*. *The Plant Cell*, 19(2):445–457.

Valverde, P. L., Fornoni, J., and NÚÑez-Farfán, J. (2001). Defensive role of leaf trichomes in resistance to herbivorous insects in *Datura Stramonium*. *Journal of Evolutionary Biology*, 14(3):424–432.

van de Wilhelmina, T. G., LeVesque, C. S., Perring, T. M., and Walling, L. L. (2000). Local and systemic changes in squash gene expression in response to silverleaf whitefly feeding. *The Plant Cell*, 12(8):1409–1423.

van der Graaff, E., Laux, T., and Rensing, S. A. (2009). The WUS Homeobox-containing (WOX) protein family. *Genome Biology*, 10(12):248.

Van Labeke, M.-C. and Dambre, P. (1998). Effect of supplementary lighting and CO2 enrichment on yield and flower stem quality of *Alstroemeria* cultivars. *Scientia Horticulturae*, 74(4):269–278.

Van loon, L. C., Kader, J.-c., and Delseny, M., editors (2009). *Plant innate immunity*. Academic press is an imprint of Elsevier.

VanBuren, R., Wai, C. M., Colle, M., Wang, J., Sullivan, S., Bushakra, J. M., Liachko, I., Vining, K. J., Dossett, M., Finn, C. E., Jibran, R., Chagné, D., Childs, K., Edger, P. P., Mockler, T. C., and Bassil, N. V. (2018). A near complete, chromosome-scale assembly of the black raspberry (*Rubus Occidentalis*) genome. *GigaScience*, 7(8).

Vandenbussche, M., Horstman, A., Zethof, J., Koes, R., Rijpkema, A. S., and Gerats, T. (2009). Differential recruitment of WOX transcription factors for lateral development and organ fusion in petunia and Arabidopsis. *The Plant Cell*, 21(8):2269–2283.

Vásquez-del-Mercado, E., Arenas, R., and Carmen, P.-D. (2012). *Sporotrichosis*. *Clinics in Dermatology*, 30(14):437–443.

Vendemiatti, E., Zsögön, A., e Silva, G. F. F., de Jesus, F. A., Cutri, L., Figueiredo, C. R. F., Tanaka, F. A. O., Nogueira, F. T. S., and Peres, L. E. P. (2017). Loss of Type-IV glandular trichomes is a heterochronic trait in tomato and can be reverted by promoting juvenility. *Plant Science*, 259:35–47.

Verde, I., Jenkins, J., Dondini, L., Micali, S., Pagliarani, G., Vendramin, E., Paris, R., Aramini, V., Gazza, L., Rossini, L., Bassi, D., Troggio, M., Shu, S., Grimwood, J., Tartarini, S., Dettori, M. T., and Schmutz, J. (2017). The peach v2.0 release: High-resolution linkage mapping and deep resequencing improve chromosome-scale assembly and contiguity. *BMC Genomics*, 18(1):225.

Vermeij, G. J. (2015). Plants that lead: Do some surface features direct enemy traffic on leaves and stems? *Biological Journal of the Linnean Society*, 116(2):288–294.

Vincent, K. and Szabo, R. M. (1988). Enterobacter agglomerans osteomyelitis of the hand from a rose thorn: A case report. *Orthopedics*, 11(3):465–467.

Vukosavljev, M., Arens, P., Voorrips, R. E., van 't Westende, W. P., Esselink, G. D., Bourke, P. M., Cox, P., van de Weg, W. E., Visser, R. G., Maliepaard, C., and Smulders, M. J. (2016). High-density SNP-based genetic maps for the parents of an outcrossed and a selfed tetraploid garden rose cross, inferred from admixed progeny using the 68k rose SNP array. *Horticulture Research*, 3(1):1–8.

Wagner, G. J. (1991). Secreting glandular trichomes: more than just hairs. *Plant Physiology*, 96(3):675–679.

Wang, E., Hall, J. T., and Wagner, G. J. (2004). Transgenic *Nicotiana tabacumL.* with enhanced trichome exudate cembratrieneols has reduced aphid infestation in the field. *Molecular Breeding*, 13(1):49–57.

Wang, G. (2005). A study on the history of chinese roses from ancient works and images. In *IV International Symposium on Rose Research and Cultivation 751*, pages 347–356.

Wang, G., Tian, L., Aziz, N., Broun, P., Dai, X., He, J., King, A., Zhao, P. X., and Dixon, R. A. (2008). Terpene biosynthesis in glandular trichomes of hop. *Plant Physiology*, 148(3):1254–1266.

Wang, J., Liu, W., Zhu, D., Zhou, X., Hong, P., Zhao, H., Tan, Y., Chen, X., Zong, X., Xu, L., Zhang, L., Wei, H., and Liu, Q. (2020). A de novo assembly of the sweet cherry (*Prunus avium* cv. tieton) genome using linked-read sequencing technology. *PeerJ*, 8:e9114.

Wang, L., Wang, S., and Li, W. (2012). RSeQC: quality control of RNA-seq experiments. *Bioinformatics*, 28(16):2184–2185.

Wang, S. and Chen, J.-G. (2014). Regulation of cell fate determination by single-repeat R3 MYB transcription factors in *Arabidopsis*. *Frontiers in Plant Science*, 05:133.

Wargent, J. J. and Jordan, B. R. (2013). From ozone depletion to agriculture: understanding the role of UV radiation in sustainable crop production. *New Phytologist*, 197(4):1058–1076.

Webster, J., Inayatullah, C., Hamissou, M., and Mirkes, K. (1994). Leaf pubescence effects in wheat on yellow sugarcane aphids and greenbugs (homoptera: Aphididae). *Journal of Economic Entomology*, 87(1):231–240.

Werker, E. (2000). Trichome diversity and development. In *Advances in Botanical Research*, volume 31, pages 1–35. Academic Press.

Werker, E., Putievsky, E., and Ravid, U. (1985). The essential oils and glandular hairs in different chemotypes of *Origanum vulgare* l. *Annals of Botany*, 55(6):793–801.

Wester, K., Digiuni, S., Geier, F., Timmer, J., Fleck, C., and Hülskamp, M. (2009). Functional diversity of R3 single-repeat genes in trichome development. *Development*, 136(9):1487–1496.

Widrlechner, M. P. (1981). History and utilization of *Rosa damascena*. *Economic Botany*, 35(1):42–58.

Wilcox, C. (2017). The thorny truth about spine evolution. https://www.quantamagazine.org/the-thorny-truth-about-spine-evolution-20170614/. Accessed: 2020.

Willey, J. M., Sherwood, L., and Woolverton, C. J. (2008). *Prescott, Harley, and Klein's microbiology*. McGraw-Hill Higher Education, seventh edition.

Wissemann, V. (2003). *Conventional taxonomy (wild roses)*. Elsevier edition, Oxford.

Wu, G., Lin, W.-c., Huang, T., Poethig, R. S., Springer, P. S., and Kerstetter, R. A. (2008). KANADI1 regulates adaxial-abaxial polarity in *Arabidopsis* by directly repressing the transcription of ASYMMETRIC LEAVES2. *Proceedings of the National Academy of Sciences*, 105(42):16392–16397.

Xu, B., Li, Z., Zhu, Y., Wang, H., Ma, H., Dong, A., and Huang, H. (2008). Arabidopsis genes as1, as2, and jag negatively regulate boundary-specifying genes to promote sepal and petal development. *Plant Physiology*, 146(2):566–575.

Xu, C. z., Luo, F., and Hochholdinger, F. (2016). Lob domain proteins: beyond lateral organ boundaries. *Trends in plant science*, 21(2):159–167.

Xu, J., van Herwijnen, Z. O., Dräger, D. B., Sui, C., Haring, M. A., and Schuurink, R. C. (2018). SlMYC1 regulates type VI glandular trichome formation and terpene biosynthesis in tomato glandular cells. *The Plant Cell*, 30(12):2988–3005.

Xu, X. C. and Wu, S. (2019). China's Kunming remains one of world's top flower markets. https://news.cgtn.com/news/3d3d414d7955544d34457a6333566d54/index.html. Accessed: 2020.

Yan, A., Pan, J., An, L., Gan, Y., and Feng, H. (2012). The responses of trichome mutants to enhanced ultraviolet-B radiation in *Arabidopsis Thaliana*. *Journal of Photochemistry and Photobiology B: Biology*, 113:29–35.

Yan, T., Chen, M., Shen, Q., Li, L., Fu, X., Pan, Q., Tang, Y., Shi, P., Lv, Z., Jiang, W., Ma, Y.-n., Hao, X., Sun, X., and Tang, K. (2017). HOMEODOMAIN PROTEIN 1 is required for jasmonate-mediated glandular trichome initiation in *Artemisia Annua*. *New Phytologist*, 213(3):1145–1155.

Yan, T., Li, L., Xie, L., Chen, M., Shen, Q., Pan, Q., Fu, X., Shi, P., Tang, Y., Huang, H., Huang, Y., Huang, Y., and Tang, K. (2018). A novel HD-ZIP IV/MIXTA complex promotes glandular trichome initiation and cuticle development in *Artemisia annua*. *New Phytologist*, 218(2):567–578.

Yan, Z., Denneboom, C., Hattendorf, A., Dolstra, O., Debener, T., Stam, P., and Visser, P. B. (2005). Construction of an integrated map of rose with AFLP, SSR, PK, RGA, RFLP, SCAR and morphological markers. *TAG. Theoretical and applied genetics*, 110(4):766–777.

Yang, C., Li, H., Zhang, J., Luo, Z., Gong, P., Zhang, C., Li, J., Wang, T., Zhang, Y., Lu, Y., and Ye, Z. (2011). A regulatory gene induces trichome formation and embryo lethality in tomato. *Proceedings of the National Academy of Sciences*, 108(29):11836–11841.

Yang, C. and Ye, Z. (2013). Trichomes as models for studying plant cell differentiation. *Cellular and molecular life sciences*, 70(11):1937–1948.

Yang, X., Makaroff, C. A., and Ma, H. (2003). The *Arabidopsis* MALE MEIOCYTE DEATH1 gene encodes a phd-finger protein that is required for male meiosis. *The Plant Cell*, 15(6):1281–1295.

Yoo, S.-C., Cho, S.-H., and Paek, N.-C. (2013). Rice WUSCHEL-related homeobox 3a (OsWOX3A) modulates auxin-transport gene expression in lateral root and root hair development. *Plant Signaling & Behavior*, 8(10):e25929.

Yoshida, Y., Sano, R., Wada, T., Takabayashi, J., and Okada, K. (2009). Jasmonic acid control of GLABRA3 links inducible defense and trichome patterning in *Arabidopsis*. *Development*, 136(6):1039–1048.

Young, M., Schorr, P., and Baer, R. (2007). Modern roses–12: The comprehensive list of roses in cultivation or of historical or botanical importance. *Shreveport: The American Rose Society*.

Yu, D. J. (1974). *Flora of China*, volume 36. Science Press, Beijing.

Zavala, J. A., Mazza, C. A., Dillon, F. M., Chludil, H. D., and Ballaré, C. L. (2015). Soybean resistance to stink bugs (*Nezara Viridula* and *Piezodorus Guildinii*) increases with exposure to solar UV-B radiation and correlates with isoflavonoid content in pods under field conditions. *Plant, Cell & Environment*, 38(5):920–928.

Zeist, W. and Palfenier-Vegter, R. M. (1981). Seeds and fruits from the swifterbant s3 site. final reports on swifterbant iv. *Palaeohistoria*, pages 105–168.

Zhang, F. (2003). A network of redundant bHLH proteins functions in all TTG1-dependent pathways of *Arabidopsis*. *Development*, 130(20):4859–4869.

Zhao, H., Wang, X., Zhu, D., Cui, S., Li, X., Cao, Y., and Ma, L. (2012). A single amino acid substitution in IIIf subfamily of basic Helix-Loop-Helix transcription factor AtMYC1 leads to trichome and root hair patterning defects by abolishing its interaction with partner proteins in *Arabidopsis*. *Journal of Biological Chemistry*, 287(17):14109–14121.

Zhao, K., Aranzana, M. J., Kim, S., Lister, C., Shindo, C., Tang, C., Toomajian, C., Zheng, H., Dean, C., Marjoram, P., et al. (2007). An *Arabidopsis* example of association mapping in structured samples. *PLoS Genet*, 3(1):e4.

Zhou, N. N., Li, S. B., Li, Y. B., Jian, H. Y., Yan, H. J., Wang, Q. G., Chen, M., Qiu, X. Q., Zhang, H., and Tang, K. X. (2017). Hybrids identification and genetic analysis in diploid roses population (f1) using ssr markers. *Acta Horticulturae Sinica*, 44(1):151–160.

Zhou, N. N., Tang, K. X., Jeauffre, J., Thouroude, T., Lopez Arias, D. C., Foucher, F., and Hibrand-Saint Oyant, L. (2020). Genetic determinism of prickles in rose. *Theoretical and Applied Genetics*, 133(11):3017–3035.

Zhou, W., Gao, J., Ma, J., Cao, L., Zhang, C., Zhu, Y., Dong, A., and Shen, W.-H. (2016). Distinct roles of the histone chaperones NAP1 and NRP and the chromatin-remodeling factor INO80 in somatic homologous recombination in *Arabidopsis Thaliana*. *The Plant Journal*, 88(3):397–410.

Zhou, Z., An, L., Sun, L., Zhu, S., Xi, W., Broun, P., Yu, H., and Gan, Y. (2011). ZINC FINGER PROTEIN 5 is required for the control of trichome initiation by acting upstream of ZINC FINGER PROTEIN 8 in *Arabidopsis*. *Plant Physiology*, 157(2):673–682.

Zhou, Z., Sun, L., Zhao, Y., An, L., Yan, A., Meng, X., and Gan, Y. (2013). ZINC FINGER PROTEIN 6 (ZFP6) regulates trichome initiation by integrating gibberellin and cytokinin signaling in *Arabidopsis thaliana*. *New Phytologist*, 198(3):699–708.

Zhu, A., Ibrahim, J. G., and Love, M. I. (2019). Heavy-tailed prior distributions for sequence count data: Removing the noise and preserving large differences. *Bioinformatics*, 35(12):2084–2092.

UNIVERSITE ECOLOGIE
BRETAGNE GEOSCIENCES
LOIRE AGRONOMIE ALIMENTATION

université angers

Titre : Génétique et génomique des aiguillons de la tige du rosier

Mots clés : Structure glandulaire et non glandulaire, Trichome, Anatomie de l'aiguillon, QTL, Séquençage d'ARN, Transcriptomique

Résumé : Les aiguillons sont un caractère indésirable. Leur présence rend difficile la culture et la récolte et provoque des blessures sur les producteurs. Le rosier est la plante ornementale la plus importante économiquement. Du fait de la présence d'aiguillons chez de nombreuses roses, la demande des obtenteurs et producteurs est forte pour des rosiers inermes. Les mécanismes génétiques et moléculaires de l'initiation et du développement des aiguillons sont peu connus. Les objectifs sont d'identifier les réseaux génétiques et moléculaires de l'initiation et du développement des aiguillons par des approches anatomique, génétique et génomique. Une analyse anatomique au sein du genre *Rosa* a mis en évidence 2 types d'aiguillons : glandulaires et non-glandulaires. Ces derniers sont les plus courants et ont une origine sous-épidermique. Par une approche génétique, nous avons identifié 4 QTLs responsables de la présence et de la densité des aiguillons sur la tige. L'analyse d'homologues, connus pour contrôler les trichomes chez *Arabidopsis*, n'a pas montré de différence d'expression entre rosiers épineux et glabres, suggérant peu de lien entre trichomes et aiguillons. Les bases moléculaires de l'initiation et du développement des aiguillons ont été étudiées par RNA-Seq en comparant le transcriptome de tiges (i) avec et sans aiguillons et (ii) à différents stades de développement des aiguillons. Nous avons identifié des réseaux de régulation contrôlant l'initiation et le développement des aiguillons, avec des gènes intéressants sous les QTLs. Par cette étude, nous avons construit un modèle génétique pour l'étude des aiguillons et ouvert des perspectives de recherche de ces structures.

Title : Genetics and genomics of prickles on rose stem

Keywords : Glandular and non-glandular structure, Trichome, Prickle anatomy, QTL, RNA sequencing, Transcriptomics

Abstract : Prickle is an undesirable trait in many crops as it makes crops difficult to handle, harvest, and can injure workers. Roses are among the most important ornamental plants, and most roses present prickles on their stems. There is a strong demand from producers and breeders for glabrous rose cultivars, particularly in cut roses. The genetic and molecular mechanisms underlying prickle initiation and development remain still largely unknown. Our objectives are to decipher the genetic and molecular control of prickle initiation and development in rose using anatomic, genetic and genomic approaches. By a survey of the different types of prickle within the genus *Rosa*, we classified them in two types: non-glandular (NGP) and glandular prickles (GP), with the NGP being the most common. We demonstrated that NGP are originated from a cell layer below the protoderm contrary to what was previously described. Using a F1 progeny, we detected four QTLs controlling the presence and density of stem prickle. We characterized rose gene homologues known in *Arabidopsis* that involved in trichome initiation. Minor different expression of the homologues in P and NP, suggesting different gene pathway between prickles and trichomes. Molecular bases of prickle initiation and development were explored using an RNA-Seq strategy by comparing the transcriptome (i) of glabrous and prickle shoots and (ii) during prickle development. We have identified key genes and regulatory networks controlling prickle initiation and development, with interesting genes below the QTLs. Through this project, we have built a genetic model system for studying prickles and open new research areas in the plant sciences.